ProQuest LLC.
789 East Eisenhower Parkway
P.O. Box 1346
Ann Arbor, MI 48106 – 1346

Characterisation of Novel Antimicrobial Peptides from Egyptian Scorpion and Snake Venoms

Mohamed Tawfik Elzayat

A thesis submitted in partial fulfillment of the requirements of Sheffield Hallam University for the degree of Doctor of Philosophy

March 2017

Dedication

This thesis is dedicated to both my parents. My father, without you I would not be who I am today. I hope if I can succeed, it may be a cause for your recovery. My mother has been a source of motivation and strength during moments of despair and discouragement.

This thesis is also dedicated to my lovely wife and kids who have been a great source of patience, support, motivation, and inspiration all the way since the beginning of my study.

Acknowledgments

Firstly, I would like to thank my supervisors, Dr Keith Miller and Prof. Peter Strong, for the patient guidance, encouragement, and advice they have provided throughout my time at the Biomolecular Sciences Research Centre (BMRC), Sheffield Hallam University. I sincerely acknowledge the continuous help and support of Dr Mohamed Abdel Rahman since the beginning of the studies. Thanks to Dr Patrick Harrison for helping me with the lab work.

Thank you also to both Dr Paul Heath for his kind help in Microarray experiments and Mr Christopher Hill for helping me with electron microscopy imaging at the University of Sheffield, your help is acknowledged and appreciated.

It is important for all the facilities to have been offered by BMRC to be acknowledged. I would also like to thank all the members of staff at BMRC, particularly microbiology research group. I gratefully acknowledge National BioResource Project Japan (NBRP) for providing me with the Keio mutant strains.

I would like to extend thanks to many friends especially Meriam Sheilabi, Peter Kanengoni, Mootaz Salman, Hasan Aldewachi, Abdurrrahman Eswayah, Yasin Al-luaiby, Ranwa Elrayess and Amal Arhoma who so generously contributed to the work presented in this thesis and for their friendship and support and for making my time in the BMRC enjoyable and memorable.

I gratefully acknowledge the funding of the Egyptian cultural office at London through an Egyptian Government scholarship awarded to me.

Publications, presented work and conferences attended

Publications

Manuscript published:

Patrick L. Harrison, Mohamed A. Abdel-Rahman, Peter N. Strong, **Mohamed M. Tawfik**, Keith Miller (2016). Characterisation of three alpha-helical antimicrobial peptides from the venom of *Scorpio maurus palmatus*. TOXICON (30-36 Volume 117).

Abstract:

Mohamed M. Tawfik, Ranwa A. Elrayess, Patrick L. Harrison, Mohamed A. Abdel-Rahman, Peter N. Strong, Keith Miller (2015, September).Cytotoxic properties of Smp24 and Smp43, alpha-helical antimicrobial peptides from the Egyptian scorpion, *Scorpio maurus palmatus.* TOXICON Vol. 103S (2015), proceedings of the 18th world congress of the international society on toxinology, Oxford, UK.

Presented work

Mohamed M. Tawfik, Patrick L. Harrison, Mohamed A. Abdel-Rahman, Keith Miller, Peter N. Strong. (2013, September). Purification of an antibacterial protein from the venom of the Egyptian cobra *Naja haje*. Poster presented at The 2nd Oxford World Symposium on Venoms, Venoms 2013 Making Sense of Venoms in Health and Disease, Oxford, UK.

Mohamed M. Tawfik, Mohamed A. Abdel-Rahman, Patrick L. Harrison, Peter N. Strong, Keith Miller (2014, October, November).Characterisation of Antimicrobial Peptides from Egyptian Elapids Snake Venoms. Poster presented at the 9thNorth East

Postgraduate Conference (NEPG), New Castle, United Kingdom, and the 9th Antibiotic Resistance Mechanisms Workshop for Researchers, Birmingham, UK.

Mohamed M. Tawfik, Ranwa A. Elrayess, Patrick L. Harrison, Mohamed A. Abdel-Rahman, Peter N. Strong, Keith Miller (2015, September).Cytotoxic properties of Smp24 and Smp43, alpha-helical antimicrobial peptides from the Egyptian scorpion, *Scorpio maurus palmatus*. TOXICON Vol. 103S (2015), proceedings of the 18th world congress of the international society on toxinology, Oxford, UK.

Ranwa A. Elrayess, **Mohamed M. Tawfik**, Mohamed Abdel-Rahman, Sarah Haywood-Small, Mahmoud E. Mohallal, Yomn M. Mobarak, Hala M. Ebaid, Peter N. Strong and Keith Miller. (2015, October). Cytotoxic effects of a novel antimicrobial peptide, Smp43 on acute leukaemia cell lines. 10thNorth East Postgraduate Conference (NEPG), New Castle, UK.

Mohamed M. Tawfik , Patrick L. Harrison, Mohamed A. Abdel-Rahman, Peter N Strong, Keith Miller. (2015, November). Smp24 and Smp43: novel antimicrobial peptides from the Egyptian scorpion *Scorpio maurus palmatus*. 10th Antibiotic Resistance Mechanisms Workshop for Researchers, Birmingham, UK.

Mohamed M. Tawfik, Paul R. Heath, Mohamed A. Abdel-Rahman, Peter N. Strong, Keith Miller (2016, June). Microarray analysis of *E.coli* transcriptomic responses to antimicrobial peptides characterised from scorpion venom gland. ASM Microbe 2016 Boston, USA.

Abstract

Scorpion and snake venoms consist of diverse mixtures of peptides and proteins with varying biological activities and offer an attractive source for the development of novel therapeutics. Smp24 (24 aa) and Smp43 (43 aa) are antimicrobial peptides (AMPs) that were identified from the venom gland of the Egyptian scorpion *Scorpio maurus palmatus*. These alpha-helical peptides showed potent activity against both Gram positive and Gram negative bacteria with MICs ranging from 4 to 128 µg/ml. Four anti-bacterial peptides were purified using HPLC chromatography from the venom of three different species of Egyptian snakes. The molecular masses of the purified proteins were identified by MALDI-TOF/MS and N-terminal sequences suggest that they are members of the three-finger toxin superfamily. Both SEM and TEM were employed to visualise morphological changes and membrane damage of *E. coli* and *S. aureus* in response to different concentrations of Smp peptides at different time intervals. Using DNA microarray, we examined the transcriptomic responses of *E. coli* to sub-inhibitory doses of Smp24 and Smp43 peptides following 5 hours of incubation. Differentially expressed genes in the presence of peptides or a control antibiotic (Polymyxin B) compared with the absence of peptides were predominantly related to siderophore biosynthesis and transport, as well as more generalised cation transport and oxidative stress responses. The antibacterial effects of Smp peptides were inhibited in the presence of calcium and magnesium ions, but not other cations. Smp peptides offer a promising starting point for the development of new antimicrobial agents and transcriptomic analysis can help identify metabolic processes affected by scorpion venom AMPs which may be beneficial in understanding their mechanism of action.

Table of contents

List of Figures

List of Tables

Abbreviations

3FTxs	Three-finger toxins
A230	Absorbance at 230 nm
A260	Absorbance at 260 nm
A280	Absorbance at 280 nm
ABC	ATP-binding cassette
AFM	Atomic force microscopy
AMPs	Antimicrobial peptides
APD	Antimicrobial Peptide Database
BG	Background
BLAST	Basic local alignment search tool
blastp	Protein-protein BLAST
BSAC	British Society for Antimicrobial Chemotherapy
CD	Circular Dichroism
cDNA	Complementary DNA
CL	Cardiolipin
Conc	concentration
cRNA	Complementary RNA
CTX	Chlorotoxins
CV	Column volume
Cy3	Cyanine 3-CTP
DAVID	Database for Annotation, Visualisation and Integrated Discovery
DBPs	Disulfide-bridged peptides
DMEM	Dulbecco's modified Eagle's medium
EM	Electron microscopy

EPP	Epoxypropane
ES	Enrichment score
FAC	Functional annotation clustering
FBS	Fetal Bovine Serum
FDA	Food and Drug Administration
FITC	Fluorescein isothiocyanate
FU	Fluorescence units FU
G-	Gram negative
G+	Gram positive
GO	Gene Ontology
HPLC	High Performance Liquid Chromatography
LAAO	L-amino acid oxidases
LPS	lipopolysaccharide
m/z	mass-to-charge ratio
MALDI-TOF	Mass-assisted laser desorption ionization time of flight
mAU	milli absorption units
MIC	Minimum inhibitory concentration
MMP2	Matrix metalloproteinase 2
MRSA	Methicillin-resistant *Staphylococcus aureus*
NDBPs	Non disulfide-bridged peptides
NFQ-MGB	Non-fluorescent quencher with minor groove binder
NMR	Nuclear magnetic resonance
OD_{600}	Optical density at 600 nm
PBS	Phosphate-buffered saline
PC	Phosphatidylcholine
PE	Phosphatidylethanolamine

PG	Phosphatidylglycerol
PI	Phosphatidylinositol
Pin1	Pandinin 1
Pin2	Pandinin 2
PLA_2	Phospholipases A2
PS	Phosphatidylserine
QC	Quality control
QCM-D	quartz crystal microbalance-dissipation
RIN	RNA Integrity Number
ROS	Reactive oxygen species
RT-PCR	Reverse transcription polymerase chain reaction
SDS	Sodium dodecyl sulfate
SEM	Scanning Electron Microscopy
SHU	Sheffield Hallam University
SM	Sphingomyelin
Smp	*Scorpio maurus palmatus*
SPLMU	Special Populations Limited Medical Use
TEM	Transmission Electron Microscope
TFA	Trifluoroacetic acid
TFE	trifluoroethanol
UV	Ultraviolet detector for HPLC
WHO	World Health Organization
XPS	X-ray photoelectron spectroscopy
ΔCt	Difference of expression between 2 genes

1 Introduction

1.1 Antimicrobial resistance

Antimicrobial resistance is an increasingly serious worldwide threat associated with millions of illnesses and deaths annually over the world. Antimicrobial resistance is predicted to cause ten million deaths in 2050 (O'Neil 2014). The emergence of resistant strains is endangering the efficacy of a wide range of antibiotics. Resistance is an old phenomenon, when sulphonamide and penicillin were marketed in the first half of the 20th century; researchers reported that resistance patterns started to appear only a few years after their introduction (Rammelkamp, Maxon 1942, Damrosch 1946).

Antimicrobial resistance is a major cause of morbidity and high healthcare spending worldwide. Massive epidemics as a consequence of microbial resistance to antibiotics emerge after their widespread clinical use, misuse and overuse, resulting in selective pressure by allowing survival of the resistant bacteria (Yanling, Zhiyuan *et al*. 2013, Fonkwo 2008). Sub-inhibitory and sub-therapeutic antibiotic doses can promote changes in gene expression and mutagenesis, leading to antibiotic resistance (Viswanathan 2014, Ventola 2015). Resistance to a range of antibiotics is one the common key factors that drive Methicillin-resistant *Staphylococcus aureus* epidemics (MRSA). MRSA was reported in the United Kingdom hospitals in 1960. Thereafter, MRSA have spread globally and were multiply resistant to non-β-lactam antibiotics recognized as epidemic MRSA (EMRSA) associated with serious infections in hospitals (Barber 1961, Devons 1961, Enright, Robinson et al. 2002, Stapleton, Taylor 2002, Udo, Boswihi et al. 2016).

Until 2003, carbapenem-resistant strains were extremely rare in both the UK and Europe. However, some carbapenem-resistant clinical isolates have been recently

identified within the UK. The UK has launched ambitious programs to limit and control the development and spread of antimicrobial resistance. The major components of these programs include increasing the understanding of this threat among the public such as hand and environmental hygiene, patient isolation and patient/staff screening besides reducing the prescribing of antibiotics among human and animals. Accordingly, a significant reduction in the incidence of Methicillin-resistant *Staphylococcus aureus* (MRSA) has been achieved within hospitals in the UK and proportions of isolates of some resistant species has stabliblized. Nevertheless, a significant increase has occurred in some infections such as bacteremia which require novel antibiotics to control it (Shallcross, Howard *et al.* 2015, Hopkins 2016).

The threat of antimicrobial resistance requires an understanding of the antibiotic targets as well as the biochemical and genetic aspects of antibiotic resistance mechanisms in order to develop antimicrobial agents that are more effective against bacterial resistance (Figure 1.1). Bacteria have developed various mechanisms to resist novel chemotherapeutics (Rodríguez-Rojas, Rodríguez-Beltrán *et al.* 2013). Although the intrinsic genes that could produce resistance to certain antibiotics in bacterial genomes or transfer among species, bacteria can also acquire resistance via mutations in existing genes (Blair, Jessica MA, *et al.*2015). Bacterial resistance can be achieved biochemically in different general ways such as efflux pumps (Poole 2005), modification of bacterial target sites (Lambert 2005) and enzymatic degradation (Figure 1.1) (Vranakis, Goniotakis *et al.* 2014).

Resistant pathogens require novel antibiotic classes or new generations of marketed antibiotics and the crisis of antibiotic resistance has increased with the decline in new antibiotic drugs entering the clinical development pipeline (Conly, Johnston 2005).

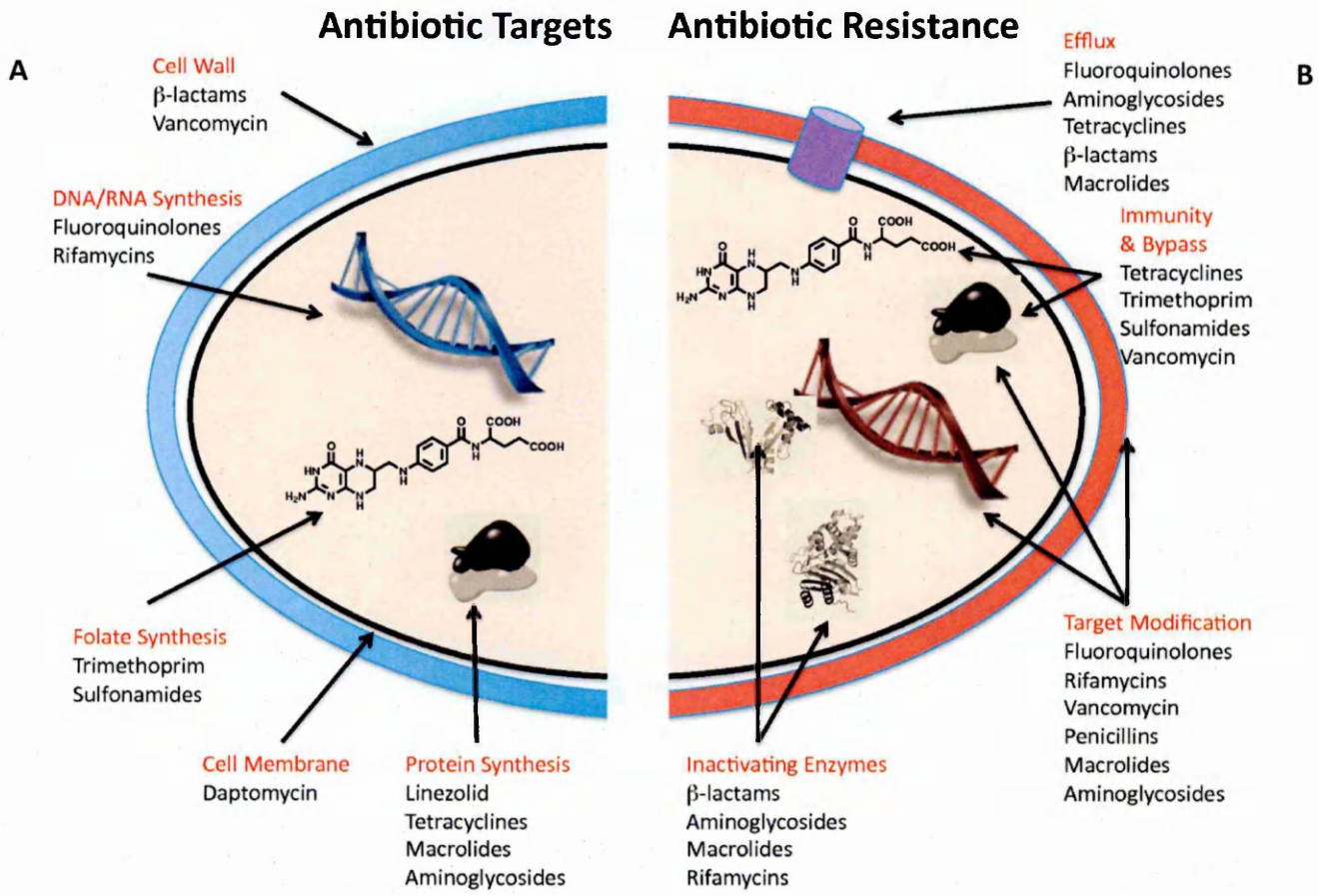

Figure 1.1 Common mechanism of action of antibiotics and mechanisms of bacterial resistance. A. Antibiotic targets with examples include cell wall biosynthesis inhibitors, DNA/RNA biosynthesis inhibitors, Folate synthesis, protein synthesis inhibitors and cell membrane targets. B. Examples of some antibiotic resistance mechanisms such as efflux pumps, target modification and inactivating enzymes (Wright 2010).

1.2 Antimicrobial drug discovery

Different ancient cultures have used natural products to treat bacterial infections. Many observations have revealed the antagonism effect of *Penicillium* on microbial growth (Burdon-Sanderson 1871, Lister 1875). However, the main breakthrough in antimicrobial drug research was observation by Fleming in 1921 of the susceptibility of *Micrococcus lysodeikticus* to lysozyme. This observation led to Fleming's discovery of the specific mold species (P*enicillium notatum*) that inhibited the growth of *Staphylococcus* bacteria (Fleming 1922). Following this discovery penicillin was eventually purified and charcterised by Florey and Chain in the 1940s (Abraham, Chain 1942). Penicillin was the first antimicrobial agent isolated from a natural source. Many other antibiotics were released later following penicillin's development, although the sulfonamide drug Prontosil was marketed as the first synthetic antibiotic in the 1930s (Domagk 1935).

Natural products are the main source for the isolation of novel antimicrobial drugs. At the beginning of the antibiotic era, actinomycetes and fungi were the major sources for antibiotics such as penicillin derived from *Penicillium* sp and fusidic acid, from the fungi *Fusidium griseum.* Approximately 65% of current antimicrobials are produced from *Streptomyces* species including vancomycin, fosfomycin, tetracycline, chloramphenicol, and gentamycin (Pelaez 2006, Abdulkadir, Waliyu 2012). Streptomycin was isolated from *Streptomyces griseus* by the American scientist Stanley Waksman. Streptomycin was the first successful antibiotic against tuberculosis (Schatz, Bugle *et al.* 1944), and Waksman was awarded the Nobel Prize in 1952. Many other antibiotics were isolated from bacteria that have evolved a biosynthetic process to protect themselves. This is a particular trend for soil bacteria (e.g. *Bacillus* sp.) in order

to increase dominance in their own ecological niche. For examples, antibiotics such as bacitracin and gramicidin were identified from *Bacillus licheniformis* and *Bacillus brevis* respectively (Abdulkadir, Waliyu 2012).

The golden age of antibiotic discovery was from 1943 to 1960, and in this period more than twenty classes of antibiotics were released into global markets. The majority of current antibiotic classes today were developed from this earlier era (Coates, Halls *et al*. 2011, Lewis 2013). Based on the penicillin structure, antimicrobial researchers have succeeded in producing semi-synthetic beta-lactam antibiotics such as cephradine, cephalexin and cefadroxil (Elander 2003, Thakuria, Lahon 2013). Analysis of global antibiotic consumption from the 71 countries during the period of 2000 to 2010 revealed that beta-lactam antibiotics led the field (**Error! Reference source not found.**) (Van Boeckel, Gandra *et al*. 2014).

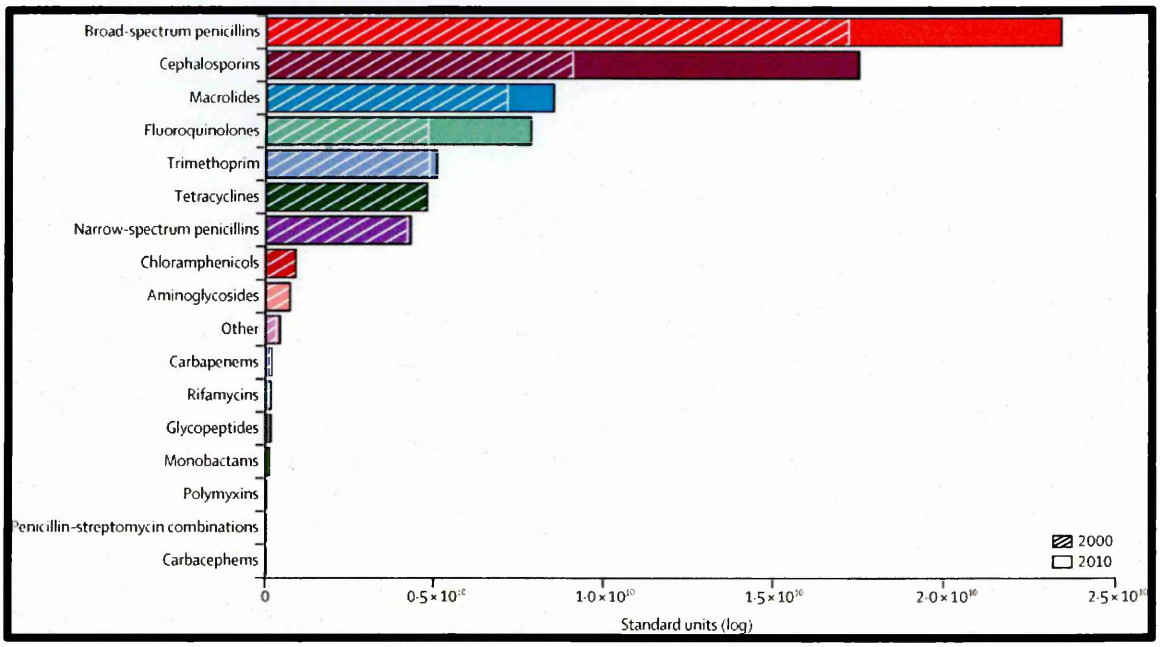

Figure 1.2 Global antibiotic consumption in from 2000-2010 (Van Boeckel et al., 2014).

1.3 Antibiotic innovation gap

Between the mid- sixties until the turn of the millennium, no new classes of antibiotics have been commercially approved, although there are some antibiotics that have been found in the different phases of clinical trials (Figure 1.3). Only two new classes have been marketed in the last fifteen years daptomycin and linezolid (Coates, Halls *et al.* 2011, Gostelow, Gonzalez *et al.* 2014). Daptomycin (Cubicin) is a lipopeptide-based antibiotic produced by *Streptomyces roseosporus,* discovered in the 1980s and approved for use (Shoemaker, Simou *et al.* 2006, Humphries, Pollett *et al.* 2013, Kelesidis 2014). Daptomycin has a broad spectrum activity against Gram positive bacteria including MRSA strains and no activity against Gram negative bacteria (Streit, Jones *et al.* 2004). The most recently discovered antibiotic class is that of oxazolidinones, such as Linezolid. Linezolid is used to treat pneumonia, skin infection and bacteremia caused by vancomycin-resistant strains (Livermore 2003, Wilcox 2005).

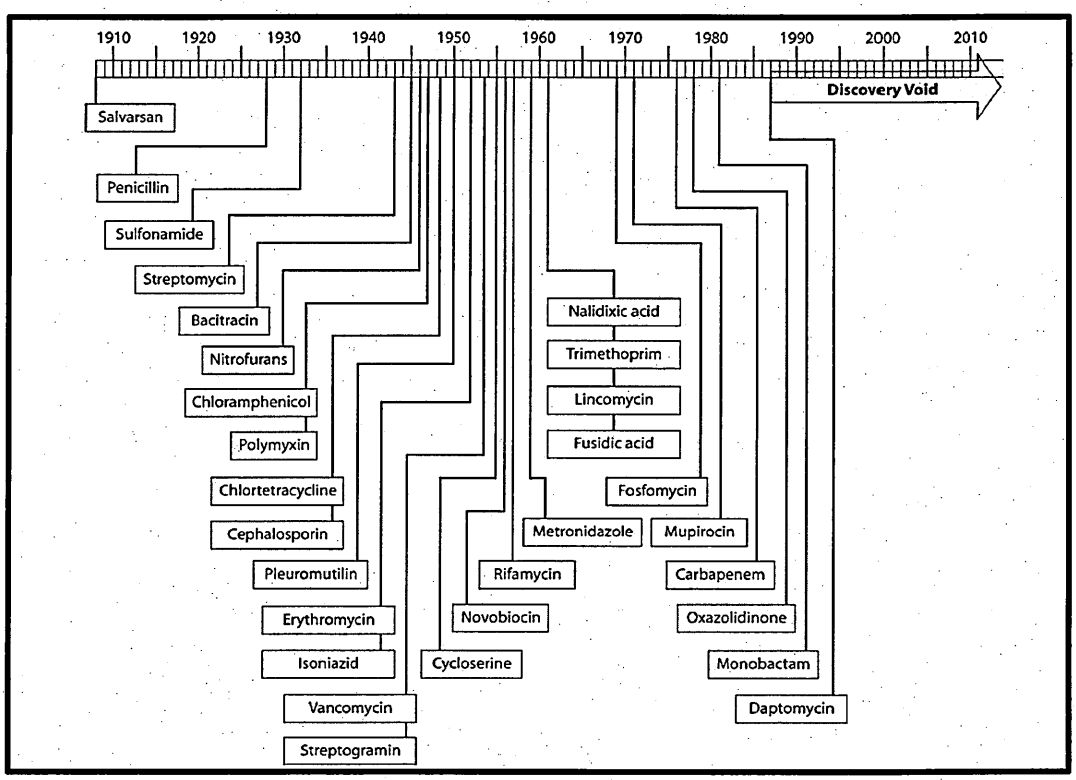

Figure 1.3 Illustration of the "discovery innovation gap." (Silver 2011).

The antibiotic drug discovery innovation gap has been caused by a combination of several factors (Bérdy 2012) and the development of drug safety regulations has had a great impact on the antibiotic pipeline. These regulations have raised the cost and timeline of antibiotic development, resulting in a shortage of novel antibiotics in production. Currently, many new antibiotics are in late-stage clinical development but few of them belong to novel classes (Butler, Blaskovich *et al.* 2016, Fernandes, Martens 2016). More recently, the FDA has, however, announced a new, shorter and more feasible procedure called Special Populations Limited Medical Use (SPLMU), to approve some critically needed drugs to treat life-threatening diseases like resistant infections, allowing patients earlier access to promising new antibiotics (Spellberg 2012). Under this new program, a quinoline-based antibiotic (Sirturo ™) has been approved to treat multi-drug resistant tuberculosis (Dowling, O'Dwyer *et al.* 2013).

From a pharmaceutical industry perspective, antibiotic drug research and development is unattractive economically. Most pharmaceutical companies have diminished investment into the discovery and development of new antibiotics due to the rapid increase of drug resistance caused by resistant bacteria. Pharmaceutical companies can gain twenty times more profit if they develop new drugs to treat chronic disease such as diabetes and epilepsy than generating a novel antibiotic (Figure 1.4) (Fernandes, Martens 2016). According to the Regional Drug and Therapeutics Centre at Newcastle in 2016, the cost of a 5-day treatment of antibiotics was from £0.5 to £114, as compared with £150 to £2500 spent on the cost of insulins for 1 year. Many novel antibiotic classes are urgently needed in the next fifty years to treat bacterial infection caused by resistant species (Coates, Halls *et al.* 2011).

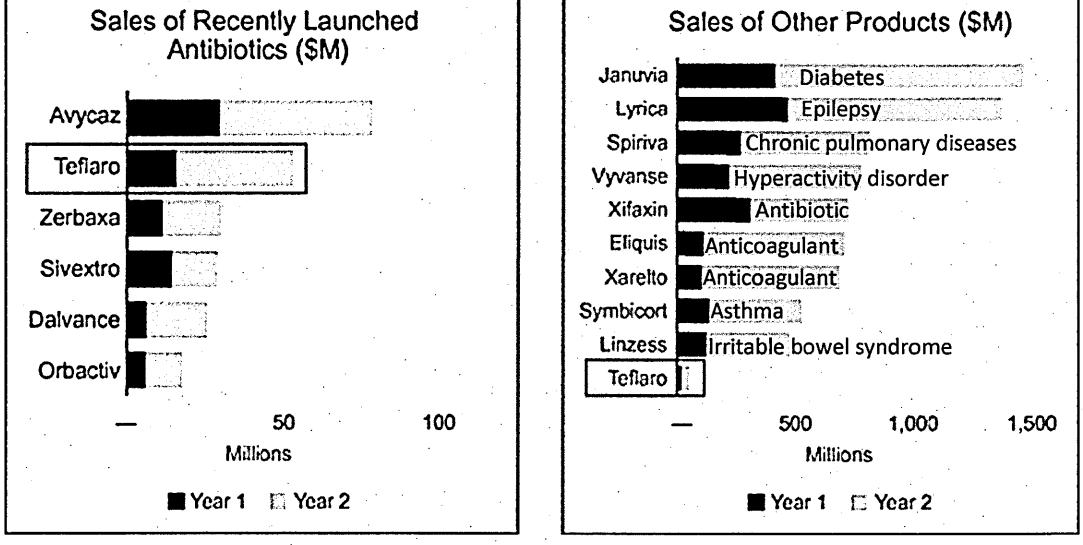

Figure 1.4 Drug expenditures in USA of recently launched antibiotics versus other brands according to the IMS Health National Sales Perspectives (NSP) database in 2016 with focus on Teflaro sales over two years (Fernandes and Martens, 2016).

The decline in the antibiotic drug discovery and production pipeline may be attributed to the limitation of some methodologies which were used previously to identify new antibiotics such as screening soil-derived actinomycetes (Lewis 2013). Recent advances in high throughput screening techniques may decrease costs and the time to generate novel antibiotics, for example, isolation chip which was used to identify a new class of lipid II binding antibiotics (teixobactin) (Ling, Schneider *et al.* 2015). Such techniques may encourage antimicrobial researchers and pharmaceutical companies to reinvest again in antibiotic drug discovery (Chan, Macarron *et al.* 2002, Dougherty, Barrett *et al.* 2002). There is an urgent need to discover novel antimicrobial agents with different mechanisms of action for overcoming the life-threatening resistance of pathogenic microorganisms to classic antibiotics (Hancock 2001). Transcriptomic and bioinformatic approaches such as cDNA microarray and other sequence-based technologies may offer an opportunity to identify new molecular pathways, beneficial in understanding the mechanism of killing action of bacteria, in order to develop new antibiotic (Brazas, Hancock 2005, Scanlon, Dostal *et al.* 2014).

1.4 Antimicrobial peptides

Most living organisms are continuously exposed to a large number of pathogens and therefore have evolved two main defence mechanisms against infection; the innate immune system which constitutes the first line of non-specific host defence mechanism and the adaptive immune system which includes a specific recognition to a particular pathogen acting as a second line through generation of specific antibodies. The innate immune system provides a broad range of different immediate defensive mechanisms against the invasion by other organisms such as phagocytes, macrophages and natural killer cells as well as the activation and/or release of some antimicrobial molecules ranging from small inorganic molecules to large proteins (Ganz 2003, Oppenheim, Biragyn *et al.* 2003, Diamond, Beckloff *et al.* 2009).

Antimicrobial peptides (AMPs; also called host defence peptides) play a critical role in the innate immune defence system of all living organisms ranging from bacteria and other single celled organisms to plants and multicellular animals (Zasloff 2002, Zasloff 2007, Guilhelmelli, Vilela *et al.* 2014). However, in organisms that have no adaptive immunity, AMPs represent the principal constituent of their defence mechanisms (Meister, Lemaitre *et al.* 1997). AMPs are found and secreted in varied tissues and cells such as epithelial surfaces, granules of phagocytic cells, haemolymph and glandular structures (Rosa, Barracco 2010).

Most AMPs have hydrolytic activities to kill pathogenic organisms such as bacteria, parasites, and viruses as well as cancer cells. They have been used as food preservatives and in biological control of plant pathogens and they are considered to be promising templates for the design of novel antibiotics. A small number of these

peptides have been commercially developed into therapeutics such as daptomycin, polymyxin B and Locilex™ (an analogue of magainin 2) (Brahmachary, Krishnan *et al.* 2004, Jenssen, Hamill *et al.* 2006, Giuliani, Pirri *et al.* 2007, Laverty, Gorman *et al.* 2011, Hintz, Matthews *et al.* 2015).

1.5 Antimicrobial peptide diversity, classification and structure

According to the Antimicrobial Peptide Database (APD) more than 2500 peptides have been discovered as of December 2015. About 75% of AMPs have been isolated from animal sources (Wang, Wang 2004, Wang, Li *et al.* 2016). In 1939 the first AMP, gramicidin, was discovered from the bacterium *Bacillus brevis* with antimicrobial activity on both Gram negative and Gram positive bacteria (Yamada, Shinoda *et al.* 2006, Phoenix, Dennison *et al.* 2013).

Antimicrobial peptide research has expanded with the discovery of AMPs from multi cellular organisms; among the first were cecropins (Hultmark, ENGSTRÖM *et al.* 1982). Cecropins were initially identified in silk moth (*Hyalophora cecropia*) haemolymph, with broad spectrum activity against both Gram positive and Gram negative bacteria and little or no haemolytic effects (Moore, Beazley *et al.* 1996). Cecropins and their derivatives were also isolated from other insects and nematodes (Pillai, Ueno *et al.* 2005, Castillo, Reynolds *et al.* 2011).

Defensins were the first mammalian AMPs, isolated from rabbit macrophages in 1980 (Kaiser, Diamond 2000). Defensins and defensin-like peptides were also isolated from a wide variety of organisms such as fungi (Mygind, Fischer *et al.* 2005), platypus venom (Torres, Dantas *et al.* 2010), and dung beetles (Hwang, Lee *et al.* 2009). Defensins have also been reported in plants. However, plant defensins differ from other defensins as

they are mainly active on fungi and yeast rather than bacteria (Stotz, Thomson *et al.* 2009, de Oliveira Carvalho, Moreira Gomes 2011).

AMPs can be classified on the basis of their biological activities, biochemical properties or on the biological source from which have been isolated from. However, they are categorized based mainly on their secondary structure, into two groups namely α-helical structures and those with β-sheet structures. However, some AMPs have mixed structures and others have non- α- or β- structures (extended) (Figure 1.5) (Vizioli, Salzet 2002, Bahar, Ren 2013).

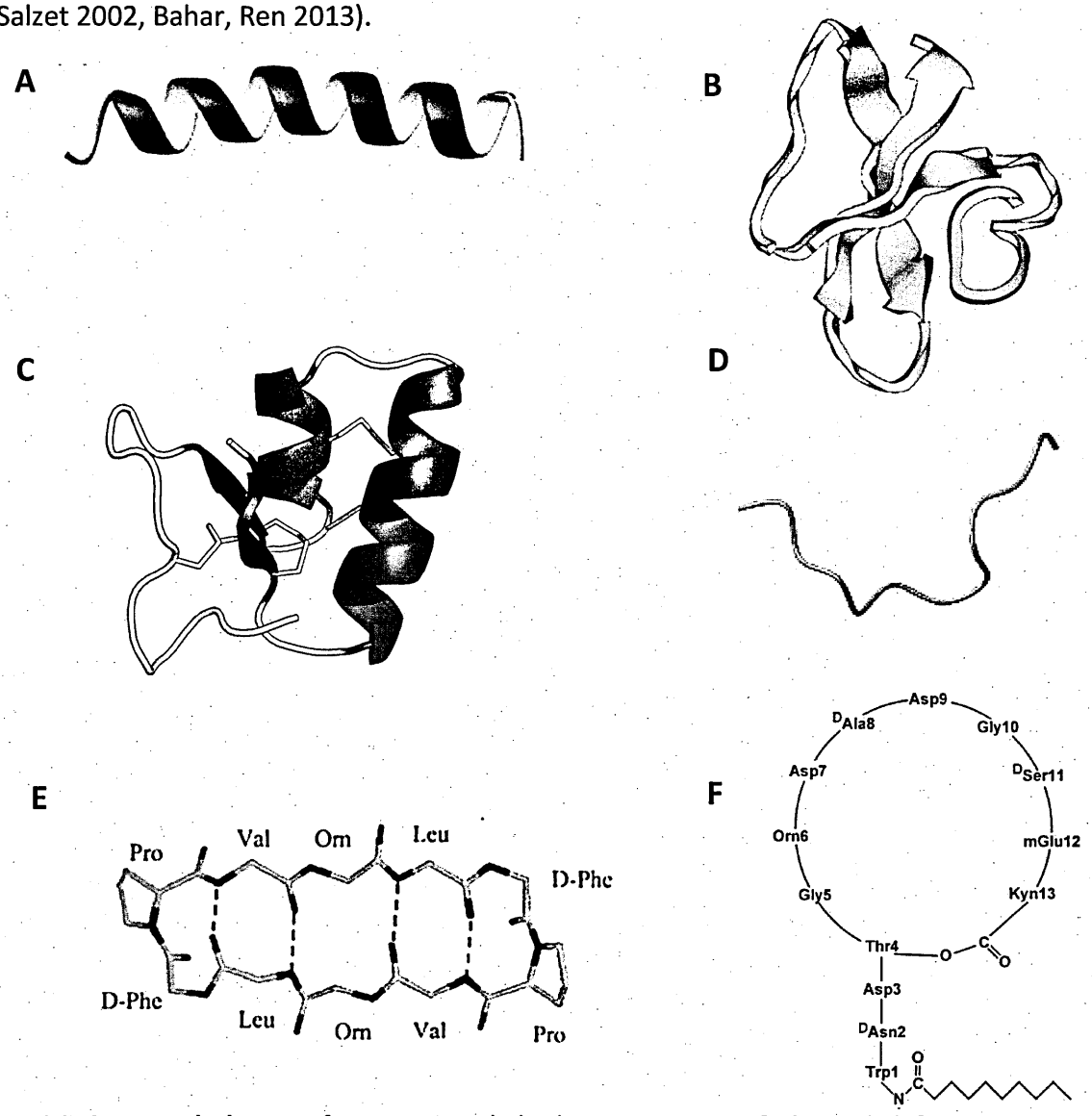

Figure 1.5 Structural classes of AMPs. A: α-helical magainin-2, B: β-sheeted defensin, C: mixed structure of thionins, D: extended indolicidin, E: cyclic structure of gramicidin S and F: Lipopeptide (Daptomycin) (modified from (Ganz 2003, Lee, Hodges 2003, Jenssen, Hamill et al. 2006).

I-α-helical AMPs

The best-studied AMPs are the α-helix peptides such as cecropins, magainins, and mellitin (Epand, Vogel 1999, Bahar, Ren 2013). Several spectroscopic studies have revealed that α-helix peptides are usually unstructured in aqueous solution and form helices in the presence of membrane-like models (Bechinger, Zasloff *et al.* 1998). The α-helical structure of magainin 2 and its analogues have been abundant reported using circular dichroism (CD) spectroscopy and nuclear magnetic resonance (NMR) analysis (Ludtke, He *et al.* 1994, Mecke, Lee *et al.* 2005) in the presence of membrane-mimicking environments such as solvents like trifluoroethanol (TFE) (Gesell, Zasloff *et al.* 1997) (Figure 1.5A). The secondary structure analysis of melittin and cecropin B1 by CD and NMR revealed two helical segments (Bazzo, Tappin *et al.* 1988, Srisailam, Arunkumar *et al.* 2000).

II- β-sheet AMPs

Defensins are one of the most common β-sheet AMPs, they are cationic peptides having six (vertebrates) to eight (plants) conserved cysteine residues (Tu, Li *et al.* 2015). Defensins are classified into two subfamilies α- and β -defensins based on cysteine linking pattern (Ganz 2003). Secondary structure analysis of human β-defensins by NMR revealed 3-stranded antiparallel β-sheets with a single helical turn (Bauer, Schweimer *et al.* 2001, Qi, Xu *et al.* 2016) (Figure 1.5B).

III- Mixed structure AMPs

Some peptides have α-helix and β sheet mixed structures. For instance, thionins are cationic plant AMPs which includes two α-helices and double-stranded β-sheet with three or four disulfide bonds (Figure 1.5C). For example, NMR analysis of hordothionin-α revealed two α-helical regions running in opposite directions and two short

antiparallel β-sheets (Nawrot, Barylski *et al.* 2014, Tam, Wang *et al.* 2015).

IV- Extended AMPs

Indolicidin is an AMP that belongs to the cathelicidins family isolated from bovine neutrophils. CD spectra of indolicidin in 0-50% TFE, on neutral and negatively charged liposomes showed no distinct conformational change suggesting unordered peptide (Rozek, Friedrich *et al.* 2000, Friedrich, Rozek *et al.* 2001, Hsu, Chen *et al.* 2005, Chan, Prenner *et al.* 2006a) (Figure 1.5D).

V- Cyclic AMPs

Gramicidin S is a cyclic broad spectrum AMP isolated firstly from the bacterium *Bacillus brevis*. It is synthesised by gramicidin S synthetase enzymes by forming thioester bonds to join two identical pentapeptides head to tail (Figure 1.5E) (Bredesen, Berg *et al.* 1968, Abraham, Prenner *et al.* 2014). Other cyclic AMPs have a fatty acid chain attached to the peptide moiety (lipopeptides); the lipid tail facilitates peptide insertion into bacterial membranes which enhance their antimicrobial activities (Pirri, Giuliani *et al.* 2009, Meena, Kanwar 2015). For example, daptomycin is a cyclic anionic (−3 net charge) lipopeptide isolated from actinobacteria *Streptomyces roseosporus* made up of 13 amino acids connected to a fatty acid side chain (Jung, Rozek *et al.* 2004, Steenbergen, Alder *et al.* 2005) (Figure 1.5F).

1.6 Important Properties of AMPs

I- Net charge

Most AMPs are cationic peptides with a positive net charge from +1 to +10 that are rich in arginine and/or lysine amino acids (Vizioli, Salzet 2002, Jenssen, Hamill *et al.* 2006, Zasloff 2007). They are amphipathic molecules as hydrophobic and positively

charged amino acids are arranged in opposite regions of the structure (Melo, Ferre *et al.* 2009, Seo, Won *et al.* 2012). Binding of AMPs to pathogen membranes is crucial in order to disrupt lipid bilayer integrity and to permeabilise the membrane leading to cell death. The cationic amphipathic nature is essential for AMPs killing activity as it helps AMPs to interact electrostatically and hydrophobically with the bacterial membrane, which has an anionic surface and is rich in hydrophobic components (Wimley 2010, Midura-Nowaczek, Markowska 2014). A small number of aspartate-rich AMPs are anionic (charges -1 to -7), for example Dermcidin (-2 net charge) which is secreted by human sweat glands (Schittek, Hipfel *et al.* 2001, Fales-Williams, Brogden *et al.* 2002, Harris, Dennison *et al.* 2009, Paulmann, Arnold *et al.* 2012). Anionic AMPs interact with the membrane of the pathogen by forming cationic bridges with metal ions such as zinc (Fales-Williams, Brogden *et al.* 2002, Harris, Dennison *et al.* 2009, Becucci, Valensin *et al.* 2014).

II- Hydrophobicity

Previous studies on structure activity relationships of AMPs revealed that the hydrophobic face of AMPs enhances their affinity with target membrane lipid bilayers, which results in antimicrobial effects and leads additionally to cytotoxicity (Kim, Jang *et al.* 2014, Lee, Lee 2015). The hydrophobic face of peptides enhances their penetration into the hydrophobic core of membrane (Chen, Guarnieri *et al.* 2007, Bahar, Ren 2013). Thus, the replacement of hydrophobic residues with more hydrophilic ones or removal of hydrophobic C- or N-terminals of some cytotoxic peptides improve their selectivity toward prokaryotic membranes and reduces their toxicity toward eukaryotes (Skerlavaj, Gennaro *et al.* 1996, Lee, Park *et al.* 1997, Ciornei, Sigurdardottir *et al.* 2005).However, there is an optimal threshold of hydrophobicity for any AMP,

beyond which its antimicrobial activity decreases or is abolished (Chen, Guarnieri *et al.* 2007, Bahar, Ren 2013).

III- Helicity

The helicity of α-helical AMPs plays an important role in peptide specificity toward prokaryotic membranes (Matsuzaki 2009). Several studies have investigated the relationship of peptide helicity and hydrophobicity (Chen, Mant *et al.* 2005, Huang, He *et al.* 2014, Zhang, Song *et al.* 2016). Minimising the hydrophobicity of peptides to improve their therapeutic indices resulted in a remarkable decrease in α-helical content, due to the change in continuity of the hydrophobic/hydrophilic face of the helical structure.

1.7 Selectivity of antimicrobial peptides

Phospholipids are the main target of cationic AMPs. The antibacterial activity of several AMPs was found to depend upon the binding affinity of the phospholipid constituents of bacterial membranes (Ntwasa 2012, Park, Kang *et al.* 2013). The phospholipid composition of bacterial membranes plays a key role in the mechanism of membrane disruption of AMPs, determining the susceptibility of bacteria and driving the specificity of AMPs.

Bacterial membranes contain varying amounts and composition of negatively charged phospholipids such as phosphatidylglycerol (PG) and cardiolipin (CL) as well as zwitterionic phospholipids such as phosphatidylethanolamine (PE). Gram positive bacterial membranes contain no or lower amounts of PE and higher amounts of negatively charged phospholipids when compared with Gram negative membranes (Table 1.1) (Epand, Savage *et al.* 2007, Epand, Epand 2009). Most cationic AMPs have

less affinity for eukaryotic cell membranes which have mainly neutral lipids such as PE and phosphatidylcholine (PC). Also the presence of a large amount of cholesterol in a eukaryotic cell membrane inhibits membrane disruption by rigidifying the lipid bilayer structure compared with the lack of cholesterol in bacterial cell membranes which makes the membrane disruption by an AMP easier (Figure 1.6) (Sanderson 2005, Brender, McHenry *et al*. 2012, Seo, Won *et al*. 2012, Sani, Separovic 2016).

Table 1.1 Percentages of major phospholipid components of bacterial membranes

Bacterial species		% Total membrane phospholipid			References
		PE	PG	CL	
Gram positive	*S. aureus*	0	58	42	(Epand *et al*., 2007, Epand and Epand, 2009)
	B. subtilis	12	70	4	(Clejan, Krulwich *et al*. 1986)
Gram negative	*E. coli*	80	10-15	0-10	(Shokri, Larsson 2004, Epand, Epand 2009)

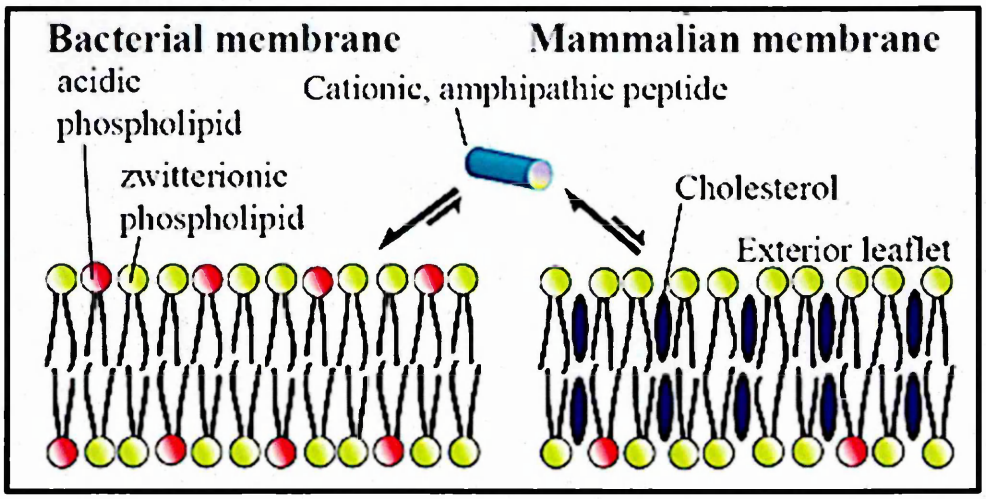

Figure 1.6 Lipid bilayers mimicking bacterial and eukaryotic cell membranes (Brender et al., 2012).

Another significant factor driving the binding affinity of bacterial membranes is the asymmetric distribution of phospholipids in membrane leaflets. The outer leaflet of bacterial membrane consists mainly of PG, while CL is found in both membrane leaflets (Barsukov, Kulikov *et al.* 1976, Marquardt, Geier *et al.* 2015). Negatively charged phospholipids such as phosphatidylinositol (PI) and phosphatidylserine (PS) are located in the inner monolayer of eukaryotic membranes (Zwaal, R. F. A. 1991). PS is exposed externally in mammalian cells as an apoptotic signal and the presence of PS in the outer monolayer of cancer cell membranes play a major role in the disruption of these membranes by AMPs (Hoskin, Ramamoorthy 2008, Riedl, Rinner *et al.* 2011). Such asymmetry promoting electrostatic interactions of cationic peptides with negatively charged phospholipids in bacterial and cancer cell membranes provides another explanation for AMP specificity (Sato, Feix 2006).

A large number of studies have investigated AMP selectivity toward model membranes of various compositions, mimicking different prokaryotic and eukaryotic membranes. For instance, it has been found that the ability of cathelicidin AMP (LL-37) to induce membrane disruption is dependent on negatively charged phospholipids, as the peptide showed no disruptive action toward zwitterionic membranes (Zhang, Oglęcka *et al.* 2010). Such preferential activity toward anionic phospholipids is typical for abundant AMPs such as melittin (Kleinschmidt, Mahaney *et al.* 1997) and novicidin (Dorosz, Gofman *et al.* 2010), which showed membrane selectivity to enriched negative phospholipid model membranes rather than zwitterionic membranes.

Consistent with other species, several cationic AMPs from scorpion venom have been shown to target the anionic phospholipid components in prokaryotic mimetic membranes. For example, UyCT peptides identified from Australian scorpion venom

Urodacus yaschenkoi induced more efficient fluorescent dye release from membrane bilayers mimicking *E. coli* and *S. aureus*, rather than phospholipids mimicking human red blood cells (Luna-Ramírez, Quintero-Hernández *et al.* 2013). From these studies, a strategy of how to develop these AMPs as novel antibiotics have begun to emerge, as the phospholipid selectivity of AMPs is used to increase their therapeutic index (Matsuzaki 2009, Aoki, Ueda 2013).

Some AMPs, however, are not cell-selective; they can lyse both prokaryotic and normal eukaryotic membranes (Shai 1999) and this represents one of the biggest barriers to the use of AMPs as therapeutic agents. For instance, the lytic activity of Aurein 1.2, an AMP isolated from the skin of the Australian tree frog is not a charge dependent as it has the ability to induce membrane disruption to both negative and zwitterionic bilayers (Shahmiri, Enciso *et al.* 2015). Recent studies have revealed that the substitution of some non-polar residues with basic and hydrophobic residues of both AR-23 (a melittin-related peptide) (Zhang, Song *et al.* 2016) and snake venom cathelicidin-BF (Jin, Bai *et al.* 2016) have resulted in a series of analogues with high specificity toward prokaryotic cells.

1.8 Proposed models of membrane disruption mechanisms of AMPs

The interactions of AMPs with phospholipid bilayers indicate different mechanisms for pore formation and lysis of model membranes. The general mechanism proposed is that the peptides (i) interact with membranes, (ii) concentrate to reach a threshold concentration to (iii) permeabilise or rearrange membranes by a variety of different mechanisms dependent on the specific AMP (Glaser, Sachse *et al.* 2005, Matsuzaki 2009, Yu, Guo *et al.* 2009).

Several spectroscopic techniques such as CD spectroscopy and NMR, and microscopic techniques such as atomic force microscopy (AFM), have been used to analyse membrane disruption and pore formation mechanisms by AMPs into lipid bilayer models (Oliynyk, Kaatze *et al*. 2007, Fernandez, Sani *et al*. 2013). Three main mechanisms for artificial membrane disruption or pore formation have been suggested depending on the peptide structure, membrane lipid composition and peptide concentration; these are the carpet, barrel-stave, and toroidal models (Figure 1.7) (Sengupta, Leontiadou *et al*. 2008, Wimley 2010).

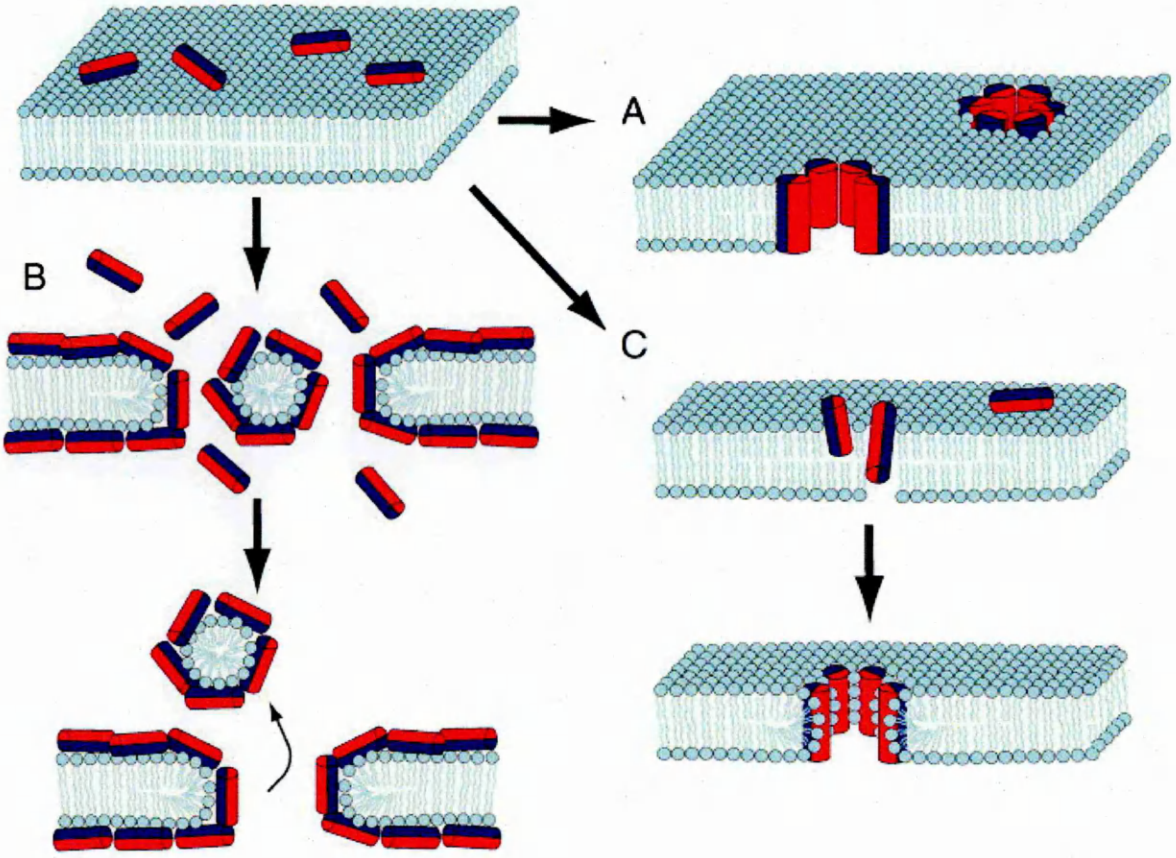

Figure 1.7 Classical models of pore forming antimicrobial peptide. (A) Barrel-stave pore: peptides form a bundle with a central lumen, the hydrophobic surfaces interact with the lipid core. (B) Carpet mechanism: a detergent-like action forming micelles which disrupt the membrane structure. (C) Toroidal pore: the hydrophilic portion of the peptide interacts with the phospholipid head groups while the hydrophobic regions associate with the lipid core. The red part of the peptide represents a hydrophilic surface, while blue is hydrophobic (modified from Chan, David I.,2006).

The carpet model is characterised by covering the membrane with the peptide parallel to the membrane surface via electrostatic interactions until a threshold concentration is reached. This is followed by a detergent-like action forming micelles, as the polar residues facing the hydrophilic head groups of the phospholipids lead to the disruption of the membrane structure (Figure 1.7) (Shai 1999, Li, Xiang *et al.* 2012, Teixeira, Feio *et al.* 2012). Specific peptide–peptide interactions are not included in this model (Melo, Ferre *et al.* 2009). Multiple studies have proposed the carpet mechanism to explain the activity of several α-helical cationic AMPs such as cecropin P1 (Gazit, Miller *et al.* 1996) and aurein 1.2 (Fernandez, Le Brun *et al.* 2012, Sani, Gagne *et al.* 2014). The findings of NMR and other spectroscopic experiments revealed that AMPs which are proposed to act with the carpet model were incorporated parallel to the lipid bilayer liposome and didn't penetrate deeper into the bilayer interior (Gazit, Miller *et al.* 1996, Yamaguchi, Huster *et al.* 2001). The interaction of aurein 1.2 with eukaryotic-like bilayers was analysed using NMR and CD spectroscopy and revealed that the fatty acyl chains of the outer bilayer were the most affected and not the bilayer interior, following peptide incorporation (Fernandez, Sani *et al.* 2013). Liposome leakage assays with fluorescent markers of varying sizes on PC/PG liposomes at different lipid/peptide ratios have been carried out to examine the effects of aurein 1.2. Markers were released in an uncontrolled manner following treatment with the peptide, indicating a carpet mechanism for membrane breakdown (Fernandez *et al.*, 2012).

The barrel-stave model proposes that the peptide firstly binds to the membrane as a monomer, and then oligomerizes to form a bundle with a central aqueous pore; the hydrophobic surfaces interact with the lipid core, while the hydrophilic surfaces orient

inwardly to line the pore (Figure 1.7). This arrangement creates an aqueous channel resulting in disturbance of membrane function which leads to the discharge of cytoplasmic contents and subsequent death of the cell (Jenssen, Hamill *et al.* 2006, Li, Xiang *et al.* 2012, Schmidtchen, Pasupuleti *et al.* 2014). The Barrel stave pore model has been proposed firstly for alamethicin (Baumann, Mueller 1974) describing the channel forming properties of the peptide. Subsequently, many studies have been published on alamethicin pore formation using a varied composition of phospholipid bilayers and a variety of techniques. Such studies revealed that alamethicin induced pores consisting of 6 to 11 monomers, with varied outside and inside diameters from 18 - 26 and 40 -50 Å respectively (Constantin, Brotons *et al.* 2007, Qian, Wang *et al.* 2008, Ye, Li *et al.* 2012, Rahaman, Lazaridis 2014).

Other peptides, such as the magainins and melittins, insert into in the phospholipid bilayer forming toroidal-shaped pores (toroidal or wormhole model). In this model a wider ranging peptides firstly aggregate, then initiate binding of the hydrophilic portion of the peptide with the phospholipid head groups while the hydrophobic regions associate with the lipid core. The peptide insertion induces inward membrane bending to form a pore, lined by the head groups of the bilayer together with the charged and polar side chains of the peptide molecules, while the peptide hydrophobic side chains are oriented toward the inside of the bend (Figure 1.7) (Jenssen, Hamill *et al.* 2006, Sengupta, Leontiadou *et al.* 2008, Li, Xiang *et al.* 2012, Lee, Sun *et al.* 2013, Schmidtchen, Pasupuleti *et al.* 2014).

Both toroidal and barrel stave models are functionally similar but differ in the suggested structure of the pore and membrane interactions (Gee, Burton *et al.* 2013). The barrel-stave model was the prototype before the introduction of the toroidal

model in the mid of 1990s to describe the pore forming mechanism of magainin (Yang, Harroun *et al.* 2001, Matsuzaki, Murase *et al.* 1996).

The toroidal pore is a lipid-dependent pore as lipids play a key role in the membrane bending (Sengupta, Leontiadou *et al.* 2008, Gilbert, Dalla Serra *et al.* 2014, Sychev, Balandin *et al.* 2015). The NMR data of LL-37 in PC lipid bilayers reflected conformational changes of lipid headgroups, as they become bent in the presence of LL-37 in a concentration-dependent manner suggesting a toroidal pore mechanism for the peptide (Henzler Wildman, Lee *et al.* 2003). According to biophysical studies, it is suggested that AMP binding to some lipid bilayer models generates membrane curvature depending on the lipid composition; curved membranes facilitate AMP insertion. These suggestions are consistent with the formation of toroidal pores (Hallock, Lee *et al.* 2003, Sato, Feix 2006, Chen, Mark 2011). The same observations were seen in a study of Smp24 against prokaryotic-like membranes using AFM (Harrison, Heath *et al.* 2016). Toroidal pores of varying size are observed, dependent on the AMP; for example, the magainin-1 pores (assembled by 4 to 10 monomers) have diameters ranging from 0.5 - 3 nm in mammalian and bacterial membranes (Watanabe, Kawano 2016), while Smp 24 induced pores in PC/PG bilayers have diameters averaging 80 nm (Harrison, Heath *et al.* 2016).

Recent models have provided minor modifications for these original prototypes models. For instance, a variant model with irregular arrangements of peptide and lipid molecules (disordered toroidal pore model) has been revealed through the analysis of the interaction of magainin MG-H2 with PC phospholipid bilayers. Only one molecule of the MG-H2 peptide is found near the centre of the pore, while other peptide molecules line the pore (Leontiadou, Mark *et al.* 2006). Only one or two melittin

molecules were found inserted into a pore-induced PC bilayer, also suggesting the disordered toroidal pore as a mechanism of melittin. This pore (diameter 1.5 nm) contains 8–10 lipid head-groups (Sengupta, Leontiadou *et al.* 2008).

The aggregate channel model is another variant that was proposed to explain increasing on membrane permeability without causing cell death. Cationic peptides destabilise areas and gain access to both outer and inner membranes by the removal or displacement of lipopolysaccharide (LPS)-associated cations (Mg2+ and Ca2+) (Giuliani, Pirri *et al.* 2007, Li, Xiang *et al.* 2012).

1.9 Other targets of AMPs in bacteria

The previous models propose that AMPs induce an increase in membrane permeability leading to cell death (Carnicelli, Lizzi *et al.* 2013). AMPs may have multiple modes of action causing lethal cell damage including additional or alternative non-membrane permeabilising mechanisms, such as targeting specific intracellular molecules and resulting in inhibition of the biosynthesis of DNA, RNA, protein and the cell wall (Bahar, Ren 2013, Guilhelmelli, Vilela *et al.* 2014, Scocchi, Mardirossian *et al.* 2016).

Several studies have suggested DNA and RNA as targets for the antibacterial activity of some AMPs. For example, fluorescein isothiocyanate (FITC)-labelled buforin II was observed to penetrate the cell membrane of *E. coli* at subinhibitory concentrations; the peptide also inhibited the migration of DNA and RNA in a concentration-dependent manner (Park, Kim *et al.* 1998). Similarly, gel retardation assays have revealed the specific interaction of indolicidin with DNA (Hsu, Chen *et al.* 2005).

Some AMPs can interfere with cell wall biosynthesis. For instance, bacteriocins inhibit

septum formation in *Lactococcus lactis* as a primary target of their killing activity. Lactococcin 972 did not show any immediate decrease in cell viability indicating that no membrane lysis occurred upon addition of the bacteriocin (Martínez, Suárez *et al.* 1996). Newer studies have found that bacteriocins like nisin and lactococcin 972 bind to Lipid II, the main component in peptidoglycan biosynthesis which leads to cell wall synthesis inhibition (Breukink, de Kruijff 2006, Martinez, Bottiger *et al.* 2008).

1.10 Bacterial resistance to AMPs

Understanding bacterial resistance mechanisms to AMPs is crucial in the development and use of AMPs as anti-infective agents. Although AMPs are non-specifically targeted antimicrobial agents and there is a relatively low potential of bacterial resistance emerging to AMPs , however bacterial resistance to AMPs should also be highlighted in order to develop and use AMPs as novel antimicrobials (Gruenheid, Le Moual 2012, Nawrocki, Crispell *et al.* 2014).

One of the common resistance strategies is AMP hydrolysis by bacterial proteases. For example, extracellular metalloproteases are secreted by *Bacillus anthracis* to catalyse the hydrolysis of peptide bonds of some AMPs such as cathelicidin-derived peptide LL-37. The addition of metalloprotease inhibitors significantly increases the sensitivity of *B. anthracis* to LL-37, which reveals the key role of proteolytic activity in inducing *B. anthracis* resistance (Thwaite, Hibbs *et al.* 2006). Also, a number of proteases secreted by Gram negative bacteria such as *Pseudomonas aeruginosa* and *Proteus mirabilis* have been reported that they inactivate and cleave LL-37 (Gruenheid, Le Moual 2012).

Some bacteria produce extracellular polymeric substances such as exopolysaccharides which are involved in biofilm and exopolysaccharide capsule formation. These

structures protect bacteria by binding or repulsing AMPs, to reduce their access to the cell (Gruenheid, Le Moual 2012, Schurr 2013). *S. epidermidis* produces the polysaccharide adhesion, as an intercellular resistance mechanism against some AMPs such as LL-37, and dermcidin (Costa, Henriques *et al*. 2009, Nawrocki, Crispell *et al*. 2014). Also, *Neisseria meningitidis and Klebsiella pneumoniae* shield their cell surfaces by using capsule polysaccharides to reduce the amount of AMPs reaching the bacterial membrane such as polymyxin B, defensins and LL-37 (Gruenheid, Le Moual 2012).

Other resistance mechanisms may be implicated such as the use of efflux pumps. For instance, *E. coli* and *Klebsiella pneumoniae* strains lacking the AcrAB efflux pump were more sensitive to polymyxin B, LL-37 and human β-defensin-1 peptides than the parental strain (Padilla, Llobet *et al*. 2010, Warner, Levy 2010). ATP-binding cassette (ABC) transporters are one of the most efficient resistance mechanisms involved in AMP export by using the energy of ATP hydrolysis (Gebhard 2012). DNA microarray analysis of *S. aureus* following exposure to Ovispirin-1 and dermaseptin K4-S4(1-16) revealed a significant upregulation of *vraDE* (encoding an ABC transporter). The deletion of genes that encode ABC transporters such as *yejABEF* (*Brucella melitensis)* and *vraDE* (*S. aureus*) resulted in significant increase in the MIC of bacitracin and polymyxin B respectively compared with values on the parent strains (Pietiäinen, François *et al*. 2009, Wang, Bie *et al*. 2016).

Additionally, some bacterial species alter their membrane permeability to lower their sensitivity to AMPs. This mechanism includes modifications to their membrane structure such as reducing or neutralising surface negative charges and increasing the concentration of the fatty acids in order to decrease the affinity of AMPs. For example, examination of the outer membrane of a nisin-resistant strain of *Listeria*

monocytogenes revealed a higher proportion of lipids on its surface. Some bacteria such as *Proteus mirabilis* synthesise a LPS with reduced negative net charge; this induces resistance to the cationic polymyxin B (Gutsmann, Hagge *et al.* 2005, Gruenheid, Le Moual 2012). Moreover, the specific aminoacylation of the polar head group of phospholipids in the bacterial membrane have been also used to resist AMPs, for examples addition of alanine or lysine to PG to neutralise its net negative charge of in *Pseudomonas aeruginosa* or *Staphylococcus aureus* respectively. This aminoacylation is mediated by aminoacyl-phosphatidylglycerol synthases results in conferring several resistance phenotypes in the presence of some AMPs such as protamine (Roy, Dare et al. 2009, Arendt, Hebecker et al. 2012, Joo, Fu et al. 2016).

Nevertheless, most bacterial resistance to AMPs has limitations. Bacteria have not yet developed effective resistance to a broad range of AMPs in the way that they have succeeded against some classical antibiotic classes (Kraus, Peschel 2006, Greber, Dawgul 2017). However, the clinical use of AMPs is still limited (Section 1.11).

1.11 Antimicrobial peptides as potential antibiotics in clinical pipeline

Gramicidin, bacitracin, polymyxin B, colistin and daptomycin are examples of licensed and commercially available peptide-based antibiotics. They have achieved widespread usage as successful antibiotics to treat a broad range of infections, pointing to the clinical potential of other similar antimicrobials in the future.

Several new AMPs are being currently investigated and developed in different clinical phases, suggesting promise as future antibiotic therapies. For instance, Novexatin is a novel cationic peptide based on human α- and β-defensins structures. Novexatin has antifungal activity, particularly against *Candida* and *Cryptococcus* species. Phase II

clinical trials established the safety and efficacy of novexatinis as topical dermal therapy for fungal nail infection (onychomycosis) (Fox 2013). Also, phase II clinical trial data has been revealed the safety and effectivity of LL-37 as a topical treatment for hronic leg ulcers in patient population (Grönberg, Mahlapuu et al. 2014). Further larger clinical studies are required to support the use of these promising AMPs as marketed treatments.

Although AMPs represent promising antimicrobial therapeutic agents, their clinical and commercial development have some challenges due to high manufacturing costs associated with the chemical synthesis of peptides, in comparison with conventional small molecule antibiotic production (Bommarius, Jenssen *et al.* 2010). Gastrointestinal enzymatic degradation (Fosgerau, Hoffmann 2015), salt and serum inactivation (Mohanram, Bhattacharjya 2016), as well as short half-lives and rapid elimination (Kovalainen, Mönkäre *et al.* 2015), are other challenges that need to be overcome.

Some AMPs have failed to obtain regulatory approval as they were not able to demonstrate improvement over current therapies. For instance, omiganan (an indolicidin analogue) didn't show any significant anti-infective activity compared with positive controls like povidone iodinein phase III trials (Sader, Fedler *et al.* 2004, Gordon, Romanowski *et al.* 2005). XMP.629 peptide derived from human bactericidal/permeability-increasing protein (BPI) failed Phase II clinical trials as a topical use for acne because the peptide offered no significant clinical benefit over a vehicle-gel control treatment (Lim, Ammons *et al.* 2001, Gordon, Romanowski *et al.* 2005).

1.12 Snake and scorpion venoms

Both snakes and scorpions use their venoms to immobilise the prey, defend against predators and help in the digestion process by solubilizing food (Kuhn-Nentwig 2003). Snake venom is a salivary secretion, stored in the venom gland and injected through specialised fangs which connect to the gland via venom ducts (Mackessy 2016). In contrast, the scorpion venom apparatus consists of a pair venom glands found in the telson at the end of the abdomen (metasoma) which deliver venom through sharp stinger (Torres-Larios, Gurrola *et al.* 2000). Snake venom is composed mainly of mixtures of large proteins/enzymes. However, scorpion venom is primarily characterised by having smaller peptides and mucopolysaccharides. Venom composition can vary inter - or intraspecifically according to age, diet, and sex as well as the environmental habitat of the snake or scorpion (Blaylock 2000, Newton, Clench *et al.* 2007, Ruiming, Yibao *et al.* 2010).

Most snake venoms are nonlethal, while a proportion causes significant mortality. Scorpion venoms contain some of the most lethal toxins derived from animals. Scorpion venom includes a wide variety of peptides which are categorised based on their structure into two main groups; the majority are disulfide-bridged peptides (DBPs) which usually target membrane-bound ion channels. A few non disulfide-bridged peptides (NDBPs) comprise a smaller group within scorpion venom that exhibit multifunctional activities. DBPs are further sub-grouped according to their ion channel targets (Na^+, K^+, $Ca^{2+}$and Cl^-) which play key roles in many essential cellular processes, such as nerve conduction or muscle contraction. Scorpion venoms also contain toxic enzymes such as hyaluronidase and phospholipases A2 (PLA_2) (Venancio, Portaro *et al.* 2013, Díaz-García, Ruiz-Fuentes *et al.* 2015, Nabi, Ahmad *et al.* 2015, Shanbhag 2015).

1.13 Therapeutic uses of snake and scorpion venoms

Early Egyptian and Chinese civilisations have used bee, scorpion and snake venoms for various medicinal purposes, including analgesic and anti-inflammatory agents (Utkin 2015). Snake and scorpion venoms contain a variety of biologically active molecules with diverse potential therapeutic applications such as anticancer agents, insecticides, antimicrobials, anticoagulants, and painkillers (Hmed, Serria *et al.* 2013, Vyas, Brahmbhatt *et al.* 2013).

Some snake venoms have hypotensive properties through the combined actions of bradykinin-potentiating peptides, Ca^{2+}-channel blockers and natriuretic peptides. These antihypertensive molecules induce the dilation of blood vessels resulting in lowering blood pressure (Koh, Kini 2012, Vyas, Brahmbhatt *et al.* 2013). Capoten, one of the most widely prescribed drugs used in the treatment of hypertension since 1981, it has been developed based on the structure of teprotide, isolated from the snake *Bothrops jararaca*. Teprotide is angiotensin converting enzyme (ACE) inhibitor which inhibits the breakdown of angiotensin and therefore prevents vasoconstriction (Komajda, Wimart 2000).

Numerous anticoagulant drugs have been designed based on snake venom components such as three-finger toxins, phospholipases A2, metalloproteinases and disintegrins. For instance, Tirofiban and Eptifibatide are antiplatelet drugs based on peptides and proteins isolated from *Echis carinatus* and *Sistrurus miliarius barbouri* respectively. They inhibit platelet aggregation by interfering with the binding of the major platelet surface receptor to integrins. Ancrod and batroxobin are procoagulant serine proteases isolated from the venoms of *Agkistrodon rhodostoma* and *Bothrops*

atrox respectively, which convert fibrinogen to fibrin. Defibrase a currently licensed defibrinogenating drug based on the structure of batroxobin, while Viprinex is approved for patients with acute ischemic stroke and is based on the structure of ancord (Calvete, Marcinkiewicz *et al.* 2005, Koh, Kini 2012, Marcinkiewicz 2013).

Some snake venom peptides of the family of three finger toxins exhibited distinct *in vivo* analgesic activities that could lead to the development of new potent pain reliever agents. For instance, hannalgesin, isolated from the venom of king cobra (*Ophiophagus hannah*), has been found to show significant analgesia without any neurotoxic effects (Pu, Wong *et al.* 1995, Alewood, Allerton *et al.* 2013).

Generally, licensed snake venom-based medicines are more numerous than those medicines based from scorpion venoms; this might refer to difficulties in the characterisation of low abundance peptides generally found in scorpion venom (Hmed, Serria *et al.* 2013). A wide range of scorpion venoms peptides have potential therapeutic effects but these have yet to be developed into licensed drugs. Anti-hypertensive peptides have been isolated from scorpion venoms, for example bradykinin-potentiating peptides, first purified from *Tityus serrulatus* venom (Ferreira, Alves *et al.* 1993). A variety of scorpion venom peptides could lead to the development of novel analgesic agents. For example, several peptides with analgesic activities were isolated from the venom of Chinese scorpion *Buthus martensii*. Such peptides might be potential templates for new painkillers as most of them are insect neurotoxins with no cytotoxic effects against human cells (Guan, Wang *et al.* 2001, Shao, Kang *et al.* 2007, Shao, Cui *et al.* 2014).

Chlorotoxins (CTX) isolated from *Leiurus quinquestriatus* are playing key roles in the

diagnosis and development of treatment for several cancers. CTX specifically binds to matrix metalloproteinase 2 (MMP-2) which is overexpressed in many tumor cells and is involved in cancer progression (Dong, Li *et al.* 2011). CTX - anticancer conjugates enhance the delivery of some anticancer agents such as platinum-based anticancer drugs (Wang, Wang *et al.* 2015). Fluorescently-labelled chlorotoxin can be used in imaging diagnostics and I-radiolabelled toxin is in clinical trials to target gliomas (Veiseh, Gabikian *et al.* 2007).

1.14 Antimicrobial activities of scorpion and snake venoms

Snake and scorpion food is frequently contaminated with a variety of potential prey-borne pathogens (Bastos 2012). The main areas of infection for snakes are the mouth and fang, while the telson of scorpions is the most accessible to a wide range of pathogenic microbes (Gao, Tian *et al.* 2007). *Salmonella* and *Bacillus* sp are the most frequently isolated bacteria from snakes (Garcia-Lima, Laure 1987, Shek, Tsui *et al.* 2009) There are a few reports of the prevalence of pathogenic infections in snakes such as mouth rot infections caused *Pasteurella and Proteus* sp and ulcerative dermatitis which may lead to snake death (Talan, Citron *et al.* 1991, Garcia-Lima, Laure 1987). The presence of potent antimicrobial constituents in snake and scorpion venoms might contribute to antimicrobial protection as a host defence mechanism when attacking prey. For example, a significant upregulation of the AMP BmKb1 in the venom gland of *Buthus martensii* has been detected when infected by *E. coli* and *Micrococcus luteus*. Interestingly, the milked crude venom of the challenged individuals showed greater antibacterial activity against Gram positive bacteria than uninfected individuals. It has also been observed that *B. martensii* use their venoms as antimicrobial sprays to protect their bodies against pathogens (Gao, Tian *et al.* 2007,

Torres-Larios, Gurrola *et al.* 2000).

The crude venoms of numerous scorpion species have been shown to inhibit the growth of diverse pathogens such as Gram negative, Gram positive bacteria, fungi and viruses (Erdeş, Doğan *et al.* 2014). Varied bactericidal and viricidal activities have been reported from crude venoms of different species such as the Chinese *Buthus martensii* (Gao, Tian *et al.* 2007) and Egyptian species such as *Leiurus quinquestriatus* (Salama, Geasa 2014), *Scorpio maurus palmatus* and *Androctonus australis* (El-Bitar, Sarhan *et al.* 2015).

Three viperid venoms (*Agkistrodon rhodostoma*, *Bothrops jararaca* and *B. atrox*) have been shown to have potent antimicrobial activity against resistant bacteria strains such as *Staphylococcus epidermidis* and *Enterococcus faecalis* (Ferreira, Santos *et al.* 2011). Venoms of *Bothrops alternatus* (Argentina) (Bustillo, Leiva *et al.* 2008), *Echis carinatus* (Iran) (Fathi, Jamshidi *et al.* 2011), Egyptian snakes venoms (*Pseudechis australis*, *Naja naja* and *Naja nigricollis*) (Shebl, Mohamed *et al.* 2012) and *Bothrops jararaca* (Brazil) (Cendron, Bertol *et al.* 2014, Lucas Henrique Cendron, 2014) all have significant antimicrobial activities against wide range of bacteria and fungi. These studies encourage further investigation to detect and identify other novel active antimicrobial peptides in snake and scorpion venoms using highly developed proteomic and genomic techniques.

1.15 Enzymes of scorpion and snake venoms with antimicrobial activities

The antimicrobial potential of snake venom enzymes is widely investigated. PLA_2 and L-amino acid oxidases (LAAO1 and LAAO2) are among the best studied enzymes associated with antibacterial properties (Samy, Pachiappan *et al.* 2006). Both PLA_2 and

LAAO are usually responsible for the major toxic effects during snake envenomation. The phospholipid of the bacterial membranes is the main target of PLA_2, as they hydrolyse the phospholipid by releasing the fatty acids from the second carbon group of the glycerol backbone of the membrane phospholipid (Toyama, Rodrigues *et al.* 2012). Some PLA_{2es} derived from snake venoms have displayed a variety of potent antibacterial activities. For example, PLA_2 from *Daboia russelii pulchella* venom exerts antibacterial activity against both Gram positive and Gram negative bacteria (Sudharshan, Dhananjaya 2015); similar antibacterial activities have been reported for PLA_{2es} from the venom of *Naja naja* (Sudarshan, Dhananjaya 2016).

LAAO is widely found in snake venoms in high concentrations. Several snake venom LAAOs have shown potential antibacterial activity. For example, Balt-LAAO-I, an acidic LAAO isolated from *Bothrops alternatus* venom inhibits *S. aureus* and *E. coli* growth in a dose-dependent manner (Stábeli, Marcussi *et al.* 2004). Several reports have suggested that the antibacterial action of LAAO might be caused by the generation of H_2O_2 during the deamination of L- amino acids which have induced the oxidative stress leading to membrane damage and consequently, bacterial cell death (Torres, Dantas *et al.* 2010, Lee, Tan *et al.* 2011).

1.16 Antimicrobial peptides from scorpion and snake venoms

Scorpion venoms have an abundant supply of AMPs; although less than 1% (≈ 50 AMPs) of all described AMPS from living organisms were isolated from scorpion venoms (Harrison, Abdel-Rahman *et al.* 2014, Tarazi 2016). Scorpion venom AMPs are classified based on the presence of disulfide bonds in their structure into two main groups: the majority are NDBPs and DBPs (Table 1.2) (Luna-Ramírez, Jiménez-Vargas *et*

al. 2016). NDBPs are further sub-grouped according to their sequence length into long (>35 amino acids), intermediate (20-35 amino acids) and short (< 20 amino acids) chain peptides (Zeng, Corzo *et al*. 2005, Almaaytah, Tarazi *et al*. 2014, Harrison, Abdel-Rahman *et al*. 2014).

Table 1.2 List of selected antimicrobial peptides with corresponding scorpion species and length as a number of amino acids with MIC values for pathogens.

Peptide			Scorpion	Length (residues)	Activity	MIC (μM)	Cytotoxicity	References
DBPs		Opiscorpine-1	*Opistophthalmus carinatus*	76	G- , G+ and malaria	(IC50=8.8-10)	Not determined	(Zhu, Tytgat 2004)
		HgeScplp1	*Hadrurus gertschi*	76	*B. subtilis*	2	Haemolytic	(Diego-García, Schwartz *et al.* 2007).
NDBPs	Long	Hadrurin	*hadrurus aztecus*	41	G- and G+	10-50	Haemolytic	(Zeng *et al.*, 2005
		Pandinin 1	*Pandinus imperator*	44	G- , G+ and fungi	1-20	Less or no Haemolytic	(Corzo, Escoubas *et al.* 2001)
		Opistoporin 1	*Opistophthalmus carinatus*	44	G- , G+ and fungi	1-50	Low haemolytic	(Harrison *et al.*, 2014,Tarazi, 2016)
	Intermediate	Pandinin 2	*Pandinus imperator*	24	G- , G+ and fungi	2-38	Haemolytic	(Corzo, Escoubas *et al.* 2001)
		HsAp	*Heterometrus spinifer*	29	G- , G+ and fungi	11.8-51.2	Haemolytic	(Nie, Zeng *et al.* 2012)
		Heterin-2	*Heterometrus spinifer*	24	G- and G+	5->45	Haemolytic	(Wu, Nie *et al.* 2014)
	Short	IsCT	*Opisthacanthus madagascariensis*	13	G- and G+	0.7-150	Low haemolytic	(Dai, Yasuda *et al.* 2001)
		Pantinin-1	*Pandinus imperator*	13	G- , G+ and fungi	8-87	Low haemolytic	(Zeng, Zhou *et al.* 2013)
		Hp1404	*Heterometrus petersii*	14	G- and G+	4-100	Low haemolytic	(Li, Xu *et al.* 2014)

Scorpine is considered as the first antimicrobial DBPs was isolated from scorpion (*Pandinus imperator*) venom. The amino-terminal sequence of scorpine shares some similarities with insect cecropins (Possani, Corona *et al.* 2002).Other scorpine-like peptides have subsequently identified such as HgeScplp1 (*Hadrurus gertschi*) (Diego-García, Schwartz *et al.* 2007) and Heteroscorpine-1 (*Heterometrus laoticus*) (Uawonggul, Thammasirirak *et al.* 2007).

To date approximately 34 antimicrobial NDBPs have been identified and functionally characterised from scorpions (Table 1.2). One of the most basic peptides among this subfamily is hadrurin (+5 net charge) (Zeng, Corzo *et al.* 2005). It was purified from the venom of the Mexican scorpion *Hadrurus aztectu* (Torres-Larios, Gurrola *et al.* 2000). CD spectra of pandinin 1 isolated from *P. imperator* showed the peptide adopts an α helical structure in different membrane mimicking solvents, it was predicted that Pin1 should have two α helical regions separated by a random coil region (Corzo, Escoubas *et al.* 2001).

Pandinin 2 (Pin 2) was the first intermediate chain AMPs charcterised were, has been purified from the venom of the scorpion *P. imperator*. Pin2 shares 60 to 70% homology with some AMPS from frog skin such as brevinin 1, pipinins and magainins (Corzo, Escoubas *et al.* 2001). HsAp considered as novel class intermediate chain peptides showed no significant homology to any other class of scorpion AMPs (Nie, Zeng *et al.* 2012).

The first short chain AMPs were isolated from the African scorpion *Opisthacanthus madagascarienis*; IsCT and IsCT2 differ only in 3 positions (Dai, Yasuda *et al.* 2001). Pantinin-1, -2 and -3 are homologous peptides (61–81%) have been identified from the

venom gland of *P. imperator* showed considerable sequence identities (50-64%) with IsCT and IsCT2 (Zeng, Zhou *et al*. 2013). Interestingly the emergence of Hp1404 resistance was evaluated in *S. aureus*; no significant resistance for was seen until 15 passages (Li, Xu *et al*. 2014).

Few small and moderate sized non-enzymatic peptides with potent antimicrobial effects against a wide range of bacteria and fungi have been reported from snake venoms (Table 1.3). Most characterised AMPs from snake venoms belong to cathelicidins (Wang *et al*., 2008, Zhao *et al*., 2008, Zhang *et al*., 2010).

Table 1.3 List of selected antimicrobial peptides with corresponding snake species and length as a number of amino acids with MIC values for pathogens.

Family	Peptide	Snake	Length (residues)	Activity	MIC (μg/ml)	Cytotoxicity	References
Novel	NAP	*Naja naja*	21	G- and G+	100-300	No haemolytic activity	(Sachidananda, Murari *et al.* 2007)
Cathelicidins	OH-CATH	*Naja atra*	34	G- and G+	1–20	Weak or no haemolytic or cytotoxic activities against endothelial and cancer cell lines	(Zhao, Gan *et al.* 2008, Zhang, Zhao *et al.* 2010)
	cathelicidin-BF	*Bungarus fasciatus*	30	G-, G+ and fungi	0.15-400	No haemolytic or cytotoxic activities against mouse macrophage and human liver tumor cell	(Wang, Hong *et al.* 2008)
	Hc-CATH	*Hydrophis cyanocinctus*	30	G-, G+ and fungi	0.5-200	Low haemolytic and cytotoxic effects	(Wei, Gao *et al.* 2015)
Myotoxins	crotamine	*Crotalus durissus terrificus*	42	G-, G+ and fungi	50-200	No haemolytic activity, while have cytotoxic effect toward cancer cells	(Oguiura, Boni-Mitake *et al.* 2011, Yamane, Bizerra *et al.* 2013, Pereira, Kerkis *et al.* 2011)
Waprins	omwaprin	*Oxyuranus microlepidotus*	50	G+	2–10	No haemolytic activity	(Nair, Fry *et al.* 2007)

Three-finger toxins (3FTxs) are a family of cytotoxic proteins abundantly present in elapid and colubrid venoms. They are relatively small proteins (6-7 KDa) in contrast to the other families of snake venom proteins. 3FTxs have three β-stranded loops in their structure (Figure 1.8), these loops fixed to central core by four or five conserved disulphide bridges (Girish, Kumar *et al.* 2012, Dubovskii, Utkin 2014). 3FTxs include two subfamilies short-chain (four disulfides, 60–62 residues) and long-chain (five disulfides, 66–75 residues) (Tsetlin 1999). They can be structurally classified into two divisions as P-type (have Pro30 residue at the tip of the second loop) and S-type (presence of a serine residue at position 29) (Chien, Chiang *et al.* 1994, Menez 2002, Dubovskii, Utkin 2014).

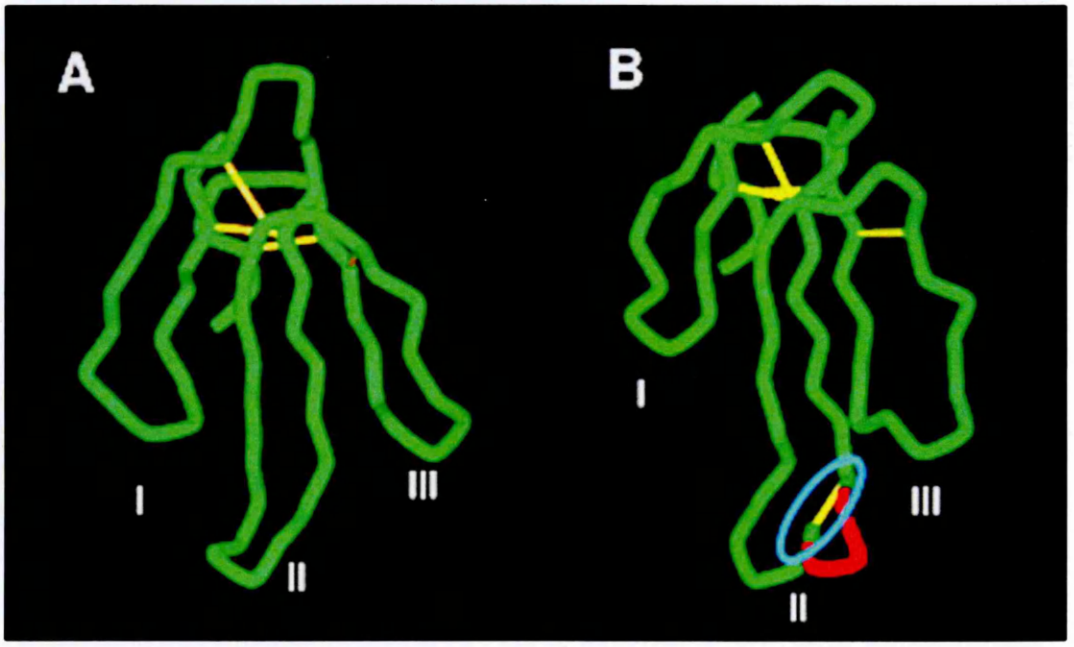

Figure 1.8 Three-dimensional structures of three-finger toxins (3FTx) showing loops and disulphide bridges. A) Short-chain (Erabutoxin) and B) Long-chain (κ-bungarotoxin). The loops ('fingers') are marked with Roman numbers I–III. The extension of second loop in long-chain 3FTx due to fifth disulphide bridge and is shown in red color (Kini, Doley 2010).

3FTxs are multi-target proteins with a wide variety of biological activities including neurotoxic (Jiang, Li *et al.* 2011), anticoagulant (Barnwal, Jobichen *et al.* 2016)) and antiplatelet (Chanda, Sarkar *et al.* 2013) effects. This family is also one of the most cytotoxic, believed to contribute to the antibacterial and cytolytic properties of snake venom (Dubovskii, Utkin 2014, Florea, Andrei *et al.* 2016).

Most 3FTxs such as short-chain cardiotoxins can induce structural and functional effects of the heart, rich in basic residues (mainly lysine) that flank the tips of the loops which are otherwise dominated by hydrophobic residues (Anbazhagan, Reddy *et al.* 2007, Dubovskii, Utkin 2014). Depending on their amphipathic characteristics, 3FTxs can bind and insert into anionic or neutral lipid bilayers (Kini, Evans 1989, Efremov, Volynsky *et al.* 2002, Bechinger, Lohner 2006). The mode of action of 3FTxs against prokaryotic and eukaryotic model membranes has been studied using several spectroscopic techniques revealing that they have a higher affinity for negatively charged model membranes than zwitterionic surfaces. Studies also suggest that loop I play a key role in cardiotoxin binding to membranes (Carbone, Macdonald 1996, Efremov, Volynsky *et al.* 2002).

1.17 Scope of the present study

This present study aims to explore several Egyptian scorpion and snake venoms as a source for novel antimicrobial peptides. It also aims to improve our understanding the mechanism of action of some synthetic AMP identified previously from Egyptian scorpion *Scorpio maurus palmatus*. These findings will be useful in elucidating AMP mechanism of action and using these peptides templates to develop therapeutically useful drugs.

The objectives were to:

- Evaluate the antimicrobial and cytotoxic activities of the purified peptides from snake venoms and three synthetic alpha-helical (Smp) peptides identified previously through the genomic analysis of the Egyptian scorpion *Scorpio maurus palmatus*.
- Identify and characterise novel AMPs from Egyptian snake venoms.
- Examine the morphological changes of bacterial cells in response to different concentrations of Smp peptides treatment at different time intervals.
- Identify the differentially expressed genes following to exposure of Smp24 and Smp43 in *E. coli* as a model for pathogenic Gram negative bacteria.
- Investigate the antibacterial activity of Smp24 in presence of different concentrations of various cations.

2 Materials and Methods

2.1 Materials

All strains used in this study were provided by SHU culture collection except the Keio collection and the parental *E. coli* BW25113 were provided by the National BioResource Project (NBRP), National Institute of Genetics (NIG), Japan. All chemicals used in this study were purchased from Sigma-Aldrich, UK.

2.2 Collection of scorpion and snake venoms.

Venoms were collected from scorpions and snakes originating from Egypt's deserts. Scorpion venom was collected by electrical stimulation of the telson (Ozkan, Filazi 2004, Oukkache, Chgoury *et al.* 2013). Venom droplets were collected in an Eppendorf tube lyophilised and stored at -20 °C. Venoms were extracted in 1% acetic acid and centrifuged (15,000 x g) to remove insoluble matter. Snake venoms were collected by manual milking, lyophilized and stored at -20 °C. Snake venom was extracted in water and centrifuged as scorpion venoms for 15,000 x g.

2.3 Peptide synthesis

Smp13, Smp24 and Smp43 (10-20 mg each) were synthesised by solid phase FMOC synthesis (ProImmune Limited, Oxford, UK). Peptide purity was > 90% (C18 reverse phase HPLC and mass spectroscopy). The sequences of the three peptides are given in Table 2.1.

Table 2.1 Amino acid sequences of *Scorpio maurus palmatus* venom gland AMPs used for this study

Peptide	Amino acids sequence
Smp13	ILQDIWNGIKNLF
Smp24	IWSFLIKAATKLLPSLFGGGKKDS
Smp43	GVWDWIKKTAGKIWNSEPVKALKSQALNAAKNFVAEKIGATPS

2.4 Antimicrobial activity assay and determination of minimum inhibitory concentrations

The minimum inhibitory concentrations (MICs) of the active peptides against a variety of organisms were determined using the BSAC broth micro-dilution method described by Andrews (2001) and performed on a Tecan CENios Plus (Tecan, Männedorf, Switzerland). Thermo Scientific™ Nunc™ 96-Well Polypropylene MicroWell™ plates were used.

Serial dilutions of synthetic AMPs and purified snake venom peptides were assayed. Cultures without peptides were used as positive controls. Fresh uninoculated Mueller-Hinton broth was used as a negative control. The MIC was determined as the concentration of the peptides in the last well in which no growth was observed. All samples were tested in duplicate on two separate occasions for a total of four replicates. Test strains used in this project included three Gram negative bacteria, seven Gram positive bacteria, and one fungus and were obtained from the BMRC (Table 2.2).

Table 2.2 Microorganisms used for micro-broth dilution minimum inhibitory concentration tests and their sources

	Microorganism	Source
Gram-negative bacteria	*Escherichia coli* JM109	**SHU culture collection**
	Klebsiella pneumoniae NCTC 13439	
	Pseudomonas aeruginosa NCIMB 8295	
Gram positive bacteria	*Staphylococcus aureus* SH1000	
	Staphylococcus epidermidis	
	Bacillus cereus NCTC 2599	
	Bacillus cereus UM20.1.	
	Bacillus subtilis NCIMB 8054	
	Bacillus subtilis NCIMB 8056	
	Bacillus subtilis NCIMB 3610	
Fungus	*Candida albicans*	

2.5 Haemolytic activity assay

The haemolytic activity of a peptide was tested using sheep erythrocytes as described by Corzo *et al.*, (2001). Briefly, a 10% (v/v) suspension of washed erythrocytes in Phosphate-buffered saline (PBS) was incubated with the purified protein in a 96-well plate for 1 h with intermittent shaking. The absorbance in the supernatant was measured at 570 nm. PBS and 10% (v/v) Triton X-100 were used as 0% and 100% controls respectively. The percent hemolysis was calculated using the following formula: Percent Haemolysis = 100 x [(Absorbance of sample – Absorbance of negative control) / (Absorbance of positive control – Absorbance of negative control)].

2.6 Cytotoxicity assay

Cellular proliferation was determined by measuring the amount of ATP generated by viable cells using the CellTiter-Glo luminescent cell viability assay (Promega, Madison, USA) as per manufacturer's instructions. Peptides were assayed at different

concentrations against a human kidney cell line (HEK293) and a human keratinocyte (HaCat) cell line to determine the potential toxic effects *in vitro.* All cell lines were tested routinely for mycoplasma. Cells were grown in Dulbecco's modified Eagle's medium (DMEM) with 5 % of fetal bovine serum (FBS), 1% penicillin/streptomycin, and 1% glutamine. All cells were incubated at 37°C in a 5% CO_2 atmosphere. The medium was changed twice a week. Briefly, HEK293 and HaCat cells were seeded at a density of 2.5×10^4 per well in a 96-well plate in 100 µl DMEM media and incubated with peptide for 24 hours. Untreated cells were used as a negative control. 10% triton (v/v) was used as a positive control. All treatments were performed in triplicate, in three independent experiments. Before cell viability was determined, plates were equilibrated at room temperature for 30 minutes, thereafter 100 µl CellTiter-Glo Reagent® was added to each well. The plate was shaken for 2 minutes to induce cell lysis and incubated for 10 minutes at room temperature to stabilise the luminescent signal. The luminescence was recorded using CLARIOstar® microplate reader and MARS data analysis software (BMG LABTECH, Ortenberg, Germany).

2.7 Fluorescence microscopy

Following treatment with Smp24 and Smp43 as in the previous section, HEK293 and HaCat cell lines were examined using Hoechst 33342 and Propidium Iodide (PI) staining (Sigma-Aldrich, Dorset, UK). Cells were stained with 10 µg/ml Hoechst 33342 and 10 µg/ml PI for 30 min at 37°C and examined using a fluorescence microscope (Olympus, IX81, UK) and images were captured using Cell-F software.

2.8 Purification of crude snake venoms

Individual venoms were initially fractionated by size-exclusion chromatography. Lyophilised crude venoms (35-60 mg) were dissolved in water and applied to a HiLoad 26/600 Superdex 200 pg column (60 x2.6 cm diameter) connected to an ÄKTA Prime system (GE Healthcare) and equilibrated with 10 mM sodium chloride/50mM sodium acetate buffer pH 4.3. Fractions (3 ml) were monitored at 280/220 nm and collected at a flow rate of 0.5 ml/min. Fractions were collected, dialysed (MW Cut off 500 Da) against distilled water at 4°C using PUR-A-Lyzer™ dialysis kit (Sigma-Aldrich, USA) and then freeze dried. The protein concentrations were measured (NanoDrop™ 1000, Thermo Scientific, USA) and screened for antibacterial activity against different species of bacteria.

Active fractions were resuspended in 1 ml of water and further purified by cation exchange chromatography with a SP Sepharose column (100×16 mm diameter). Prior to this purification process, the column was equilibrated in buffer (A) 10 mM sodium chloride/50 mM sodium acetate buffer pH 4.3. The column washed with buffer A to remove any unbound proteins. Samples were eluted with a linear gradient (20 CV) of buffer (B) 1 M sodium chloride/50 mM sodium acetate buffer pH 4.3 at a flow rate of 0.5 ml/min. The chromatography was carried out at 4˚C using an ÄKTA Prime system as before.

2.9 Analysis of molecular mass by mass spectrometry

The molecular mass of purified peptides was determined by mass-assisted laser desorption ionization time of flight (MALDI-TOF) mass spectrometry of the fraction obtained after separation through cation exchange chromatography. 5 µL of fraction

was mixed with 5 µL of matrix solution (α-cyano-4-hydroxy-cinnamic acid in 0.1% Trifluoroacetic acid (TFA) /acetonitrile 1:2). 0.5 – 1 µL of this mixture was transferred to a MALDI sample plate and allowed to dry. The molecular mass was determined using MALDI-TOF mass spectrometry (Voyager Spec # 1 MC) in positive ionization mode.

2.10 Identification of N-terminal residues

N-terminal sequencing using the Edman degradation technique was used to identify the first five amino acids (Alta Bioscience Ltd, University of Birmingham, Birmingham, UK of purified snake proteins.

2.11 Peptide homology analysis

Online bioinformatics tools were used to characterise the purified active peptides by comparing the N-terminal sequence to the database of published sequences of peptides and proteins. EXPASY BLAST software, Protein-protein BLAST (blastp) (http://blast.ncbi.nlm.nih.gov/Blast.cgi), was used to subject the obtained N-terminal sequence to a similarity search.

2.12 Preparation of cells for scanning electron microscopy

Overnight cultures of *E. coli* JM109 and *S. aureus* SH1000 were diluted into fresh MH Broth to a cell density $1x10^6$ CFU/ml then incubated at 37°C until an $OD_{600\ nm}$ of 0.3 was reached (mid-exponential growth phase). Bacterial cells were treated with different concentrations of Smp peptides for different time intervals (10 minutes, 1 hour, and 24 hours) at 37°C . Untreated controls were prepared in free MH medium.

The cells were harvested by centrifugation (10,000 × g, 10 mins) re-suspended in wash buffer (0.1 M sodium phosphate buffer, pH 7.4), and then collected by centrifugation (10,000 × g, 10 mins).Cells were fixed with 2% glutaraldehyde in 0.1 M sodium phosphate at 4°C for 24 hours. Cells were washed twice with 0.1 M phosphate buffer for 15 minutes intervals at room temperature. To post fix the cells, 1% aqueous osmium tetroxide was added and the samples were left at room temperature for one hour and then washed twice with 0.1 M phosphate buffer. The samples were dehydrated with graded ethanol solutions (75% ethanol for 15 minutes, 95% for 15 minutes, 100% ethanol for 15 minutes, 100% ethanol for 15 minutes). Samples were then exposed to 100% ethanol: hexamethyldisilazane (1:1) for 30 minutes followed by 30 minutes in hexamethyldisilazane. All dehydration steps were carried out at room temperature. Specimens were allowed to air dry overnight in a fume hood and mounted onto a pin-stub using a Leit-C sticky tab (Agar Scientific Ltd, Essex, UK) and gold coated using an Edwards S150B sputter coater (BOC Edwards, UK) and examined in a Philips XL-20 SEM (Philips, Eindhoven, The Netherlands) at 15kV.

2.13 Preparation of cells for transmission electron microscopy

TEM was used to investigate the morphology of bacterial cells induced only by subinhibitory concentrations of Smp peptides for different time intervals (10 minutes, 1 hour, and 24 hours) at 37°C. Samples were prepared in the same manner as for the SEM experiments, except that after dehydration in ethanol, samples were cleared in epoxypropane (EPP) and infiltrated in 50/50 araldite resin: EPP mixture overnight on a rotor. This mixture was changed twice, over 8 hours, with fresh araldite resin mixture before being embedded and cured in a 60 °C oven for 48-72 hours.Ultrathin sections, approximately 85nm thick, were cut on a Leica UC 6 ultramicrotome (Leica, Wetzlar,

Germany) onto 200 mesh copper grids, stained for 30 mins with saturated aqueous Uranyl Acetate followed by Reynold's Lead Citrate for 5 mins. Sections were examined using a FEI Tecnai Transmission Electron Microscope (FEI Tecnai™, Oregon, USA) at an accelerating voltage of 80Kv. Electron micrographs were recorded using a Gatan Orius 1000 digital camera and Digital Micrograph software (Gatan, Pleasanton, USA).

2.14 Determination of killing curves

Four independent cultures of the *E. coli* strain JM109 were exposed to different concentrations (zero to MIC) of each peptide. A culture of *E. coli* JM109 was grown overnight in Mueller-Hinton broth, then diluted into fresh Mueller-Hinton broth ($2x10^7$ CFU/ml) 2.7 ml of this suspension was then added to 0.3 ml of peptide, and incubated at 37°C with shaking and grown to the exponential growth phase of an optical density at 600 nm (OD_{600}) of 0.6. At specific time points, OD was measured at 600 nm wavelength by a Jenway 6715 (UV/Vis) spectrophotometer (Jenway, Staffordshire, UK). Untreated bacteria were used as negative controls. The assay was repeated three times and the average was reported.

2.15 Isolation of total cellular RNA

Total RNA was extracted by using a SV Total RNA Isolation System (Promega Corporation, Madison, WI, USA). The cells were harvested by centrifugation for 2 minutes at 14,000 × g. Pellets were resuspended and incubated for five minutes in 100µl of freshly prepared TE containing 0.4mg/ml lysozyme. Cells were lysed with 75 µl SV RNA Lysis buffer, then incubated at 70°C in SV RNA dilution buffer for 3 minutes, followed by centrifugation at 14,000 × g at room temperature for 10 minutes. 200 µl of 95% ethanol was added to the cleared lysate. The lysate was passed through a SV Total

RNA Isolation System spin column. From this point on the manufacturer's recommendations were followed. The extracted RNA was assessed for its concentration, purity and integrity using the NanoDrop Spectrophotometer and the Agilent 2100 Bioanalyzer instrument (Agilent, Wokingham, UK) in order to reduce biases in microarray analysis caused by poor RNA quality. For RNA judged suitable for microarray analysis, the following criteria were met (Table 2.3) (Bhagwat, Ying *et al.* 2013).

Table 2.3 Recommended parameters for RNA used for microarray analysis

Parameters	Range
RNA concentration	10 - 200 ng/μL
260/280 nm	≥ 1.9
260/230 nm	≥ 1.9
RNA Integrity Number (RIN)	8-9
23S rRNA / 16S rRNA	≥ 1.5

2.16 Gene expression microarray analysis

Gene Expression Analysis protocol (version 6.5, May 2010) was performed using a one-Colour Microarray technique (Agilent, Wokingham, UK). Unless indicated, all microarray reagents, data analysis software were ordered from Agilent.

2.16.1 Sample labelling and hybridisation

For each tested sample, serial dilutions of Agilent One-Colour Spike-In Mix which contains 10 pre-designed positive control transcripts were mixed with a total RNA input amount of 100 ng/dilution. Sample RNA, together with the internal control transcripts, were labelled with Cyanine 3-CTP (Cy3) dye during an amplification reaction using the Agilent Low Input Quick Amp Kit. The generated fluorescent complementary RNA (cRNA) products were then purified (RNeasy Mini Kit, Qiagen). The yield of the linearly amplified cRNA and the Cy3 specific activity were quantified by absorbance at 260 nm. To reduce its structural complexity, 600 ng cRNA of each sample was fragmented to reduce the size of the cRNA to approximately 50-200 bases with a median of around 85 bases. The fragmentation step took place at 60°C for 30 min using a Fragmentation Mix for 8- pack microarray format. Such fragmentation would improve cRNA specificity and binding efficiency to the oligo arrays which have 60mers as the target probes. 25 µL of the fragmentation reaction were combined with 25 µL hybridisation buffer and immediately loaded onto the gasket slide. The 8 x 15K whole *E. coli* K12 oligo array slide was placed on top of the gasket slide loaded with hybridisation mixture and the microarray slide chamber was prepared. Assembled slide chambers were placed in a hybridisation rotator (10 rpm, 65°C) hybridization oven. After 17 hours, hybridised slides were disassembled, washed and then scanned at 3 µm resolution using Agilent C Microarray Scanner (Agilent, Wokingham, UK) pre-set with the default settings for a 8 x 15K Microarray Format. All samples were tested in duplicate on each of two separate arrays.

2.16.2 Data analysis

After detecting the fluorescence signals of the hybridised slides, the Agilent Feature Extraction (FE) Software (version 10.7) was used to process the generated image. A pre-defined protocol (GE1_107_Sep09) that matches the slide type was initiated to import a set of parameter values and settings, which allow the software to align the default grid to the image. Following identification of the image spots, the software automatically performs a background correction and dye normalisation by subtracting the background intensities from the foreground intensities and scale average signal intensity for each sample to the average signal intensity for all samples in order to flag and reject the outliers and low quality probes. This was followed by an automatic computing of feature log ratios (Agilent's Processed Signal value) and their p-values. The FE preliminary processing ends with producing a quality control (QC) report for each array image, which includes statistical results with thresholds useful for evaluating the reproducibility and reliability of the microarray, and an exportable raw data file in a "txt" format, which contains all the parameters, statistical calculations and the annotation information associated with the Agilent microarray used in the experiment.

Raw "txt" data files were then analysed using Agilent GeneSpring GX software (version 13.1) (http://www.genomics.agilent.com/article.jsp?pageId=2141). Briefly, intensity values were subjected to a log2 transformation and normalisation to the 75th percentile-shift normalisation. The imported data files were then grouped and assigned to the experiment parameters and conditions. For instance, data files of cells treated with peptide were assigned to the condition "treated", while the control cells were assigned to the condition "untreated". To identify differentially expressed genes,

statistical analysis was performed by using unpaired T-test and applying a Benjamini-Hochberg multiple testing correction method to correct the computed *p*-values. Finally, the list of the identified genes was filtered to include only genes with a ≥ 2 fold change using the built-in fold change function before exporting the list into an Excel file.

2.17 Gene cluster and pathway enrichment analysis

Database for Annotation, Visualisation and Integrated Discovery (DAVID) software tools was used for gene and molecular pathways analysis (https://david.ncifcrf.gov/home.jsp). In our work, the significant biological process terms and pathways enrichment analyses of the differentially expressed genes were performed using DAVID 6.7 with the thresholds of *p*-value <0.05 and enrichment gene count >2. Functional annotation clustering (FAC) allows clustering of Gene Ontology (GO) categories sharing a significant number of genes.

2.18 Reverse transcriptase-polymerase chain reaction (RT-PCR)

RT-PCR was performed to confirm the microarray expression data obtained by bioinformatics analysis. Total RNA was isolated from cell samples as described previously. RNA was reverse transcribed into cDNA with a QuantiTect Reverse Transcription Kit (QiagenInc., Chatsworth, CA, USA). Manufacturer's instructions were followed and briefly as follows. Sample RNA was mixed with water in the presence of RNase and incubated at 42°C for 3 minutes, this was followed by the addition of polymerase and nucleotide mix plus Quantiscript RT buffer. The cocktail was incubated for a further 30 min at 42°C, then Incubated at 95°C for 3 minutes to inactivate the

reverse transcriptase. Once DNA has been synthesised, a Nanodrop measurement was taken to determine the concentration of DNA.

The RT-PCR reactions were then performed on a StepOnePlusTM Real-Time PCR System (Applied Biosystems, California, USA) using DNA samples in order to investigate gene expression levels of investigated genes. *cysG*, *idnT*, and *hcaT* were used as housekeeping genes. These housekeeping genes have been strongly recommended by (Zhou, Zhou *et al.* 2011) as novel reference genes for quantifying gene expressions of *E. coli* by RT-PCR and they were stably expressed under all the conditions investigated in this study. Probes for real-time PCR were purchased from Applied Biosystems, conjugated at the 5' end to the fluorochrome FAM, and at the 3' end to the non-fluorescent quencher with minor groove binder NFQ-MGB. Two µl aliquots containing 25 ng of the investigated samples were used in the preparation of the total ten-microlitre reactions using the TaqMan Universal PCR Master Mix (Applied Biosystems). Samples were run for 40 cycles and results were analysed using the $2^{-\Delta\Delta Ct}$ method and presented as relative gene expression normalised to the average cycle threshold for the three housekeeping genes. Each sample was run in triplicate for each biological replicate. To test the primers for specificity and quality, efficiency curves were performed.

2.19 Screening of Keio collection

In order to identify the essential genes whose products are involved in the response of *E. coli* when treated by Smp peptides, the susceptibility of 79 *E. coli* single knockout mutant strains was assayed. The Keio collection and the parental *E. coli* BW25113 were provided by the National BioResource Project (NBRP), National Institute of Genetics

(NIG), Japan. The pre-selection of the mutants for the assay was based on the differentially expressed genes produced from microarray analysis compared with that of the *E. coli* BW25113 parent strain. Also, eight strains with genes not identified as significant were selected from the Keio collection, having a single deletion of either *ihfB*, *uxuR*, *hacT*, *cysG*, *ugpQ*, *idnT*, *yghB* or *pbpC* genes and these were assayed as experimental controls. This assay was performed on a TecanCENios Plus (Tecan, Switzerland). Thermo Scientific™ Nunc™ 96-Well Polypropylene MicroWell™ plates were used and carried out as described in section 2.4.

2.20 Effect of cations on the antibacterial activity of Smp24

The effect of cation concentration on the antimicrobial activity of Smp24 was tested by determining the MICs of the peptides against *E. coli* in the presence of titrated cations. MICs were determined by the same method as described in Section 2.4 for determining the effect of the salt concentration on the activity of Smp24. The monovalent cation, Na^+ and four divalent cations, Fe^{2+}, Mn^{2+}, Ca^{2+}, and Mg^{2+} were added as chloride salts with Smp24. The concentrations of cations in the assay ranged from 0 to 20 mM.

2.21 Analysis of cell surface composition of *E. coli* treated with Smp24 using X-ray photoelectron spectroscopy (XPS)

A culture of *E. coli* JM109 was grown overnight in Mueller-Hinton broth, then diluted into fresh Mueller-Hinton broth ($2x10^7$ CFU/ml), and incubated at 37°C with shaking and grown to the exponential growth phase represented by an optical density at 600 nm (OD_{600}) of 0.4. 0.9 ml of this suspension was then added to 0.1 ml of peptide and then incubated for 10 minutes. The cells were harvested by centrifugation (10.000 xg,

10 minutes). Each cell sample (cells + any retained liquid) was placed as 1 µl on the sample holder at room temperature and atmospheric pressure. The sample holder was then placed in the preparatory chamber of the XPS and the atmosphere reduced to a pressure of 5 x 10^{-7} Torr. Once the sample was under vacuum the sample holder was cooled to -100 °C. The samples were then transferred to the analysis chamber. The temperature at the beginning of the analysis was -70˚C but had increased to -39 °C once the data had been collected. The analyses were carried out using a Kratos Supra XPS with the monochromated aluminum source (Kratos Analytical Ltd, UK). Survey scans were collected between 1200 to 0 eV binding energy, at 160 eV pass energy and at 1 eV intervals. The analysis area was 300 to 700 µm. The data was quantified using theoretical Scofield relative sensitivity factors with small angular distribution and kinetic energy corrections. The data was calibrated for binding energy by making the main carbon peak C 1s at 285.0, and correcting all data for each sample analysis accordingly.

3 Characterisation of novel antimicrobial peptides from Egyptian scorpion and snake venoms

3.1 Introduction

Snake and scorpion venoms have attracted some interest as a source of novel AMPs. However, they have been largely unexplored for identification of such agents in contrast to other organisms (de Lima, Alvarez Abreu *et al.* 2005, Samy, Stiles *et al.* 2015). Thus, a wider range of undiscovered peptides with potential antimicrobial activities are likely to be found in unexplored snake and scorpion venoms.

The majority of antimicrobial molecules that have been purified from snake venoms are enzymes such as LAAO and PLA_2 which constitutes the major component of snake venom (Torres, Dantas *et al.* 2010, Vargas, Londoño *et al.* 2012, Sudharshan, Dhananjaya 2015). These have been purified by conventional chromatographic techniques such as gel filtration, ion-exchange, reverse phase HPLC.

The identification and development of therapeutic molecules from snakes and scorpion venom as prototype drugs have been revolutionised by the rapid advancement of new methodologies in the last twenty years. Proteomic and genomic analyses have been widely used to determine the distribution of protein families in a variety of snake and scorpion venoms in order to expand our understanding regarding the venom complexity.

Further insights into venom compositions have been achieved by gene cloning by PCR-based methods conducted with cDNA libraries of venom gland tissue. Interestingly, most of the AMPs identified from scorpion and snake venoms have been cloned from the venom glands cDNA libraries combined with some proteomic analyses. A huge number of antimicrobial like sequences have been recorded from the transcriptome

analyses of several snake and scorpion venom glands (Ma, Zhao *et al*. 2009, Almeida, Scortecci *et al*. 2012).

The current study has evaluated the antimicrobial and cytotoxic activities of three synthetic alpha-helical peptides (Smp13, Smp24 and Smp24), previously identified from Egyptian scorpion *Scorpio maurus palmatus* as putative AMPs using a combination of proteomics and transcriptome sequencing approaches (Abdel-Rahman, Quintero-Hernandez *et al*. 2013). Some of these data have been published recently by our group (Harrison, Abdel-Rahman *et al*. 2016).

Although many different species of snakes are found in Egypt, no AMPs have been characterised from Egyptian snake venoms. To the best of our knowledge, this study is the first to isolate such antibacterial peptides. This chapter examines a number of different venoms of Egyptian elapids and vipersin order to both purify and investigate the potential of some purified peptides as antibacterial agents as well as to assess some of their cytotoxic effects in order to increase the prospects of developing novel AMPs.

3.2 Method Summary

Antimicrobial activity of Smp peptides (0-512μg/ml) was determined against Gram positive and Gram negative bacteria and fungi by the micro dilution method as described in section 2.4. The haemolytic potential was assayed against sheep erythrocytes and cytotoxic effects by CellTiter-Glo® assays using kidney and keratinocyte cell lines. Snake venoms were purified by size-exclusion and cation-exchange liquid chromatography. Antimicrobial activity was determined as above. Active fractions were characterised by MALDI-TOF mass spectrometry. N-terminal amino acid sequences were determined by Edman degradation. Fractions that displayed antimicrobial activity were assayed for their haemolytic and cytotoxic effects as above.

3.3 Results

3.3.1 Antimicrobial activity of synthetic scorpion venom antimicrobial peptides

The minimum inhibitory concentrations (MICs) of Smp13, Smp24 and Smp43 were determined using the broth microdilution method described in section 3.2. The test organisms included three Gram negative and three Gram positive bacteria as well as one fungi strain. The MICs are reported in Table 3.1.

No antimicrobial activities were found in Smp13. However, Smp24 and Smp43 showed potent broad-spectrum activity against all organisms tested. Both peptides exhibited highest activity against Gram positive bacteria with MICs ranging from 4 to 64 μg/ml. Smp43 showed a higher activity against Gram negative bacteria (MICs 32-64 μg/ml) than Smp24 (MICs 32-256 μg/ml). Both Smp24 and Smp43 showed antifungal activity toward the yeast, *C. albicans* with MIC values of 32 and 128 μg/ml respectively.

Table 3.1 Minimum inhibitory concentrations (MICs of μg/ml) of synthetic *Scorpio maurus palmatus* venom antimicrobial peptides against various organisms

Microorganism		Smp13	Smp24	Smp43
Gram-negative bacteria	*Escherichia coli* JM109	-	32	32
	Klebsiella pneumoniae NCTC 13439	-	128	64
	Pseudomonas aeruginosa NCIMB 8295	-	256	64
Gram positive bacteria	*Staphylococcus aureus* SH1000	-	8	16
	Staphylococcus epidermidis	-	8	64
	Bacillus subtilis NCIMB 8054	-	4	4
Fungus	*Candida albicans*	-	32	128

NC* Negative control was Fresh Muller-Hinton broth without peptides. – no inhibition.

3.3.2 Haemolytic activities of scorpion venom peptides

Smp43 showed very low haemolytic activity at the highest concentration of 512µg/ml. Smp24 exhibited high haemolytic effects at the same concentration. Smp43 showed very low toxicity at the maximum concentration tested (2.25 ± 0.2%) lysis at 512 µg/ml). In comparison, Smp24 caused significant erythrocyte disruption (88.4 ± 0.8%) at the same concentration. Indeed, a significant disruption was observed between 64 µg/ml (15.6 ± 0.5%) and 128 µg/ml (52 ± 1.7%) with an increase in lysis of 36.4% (Figure 3.1).

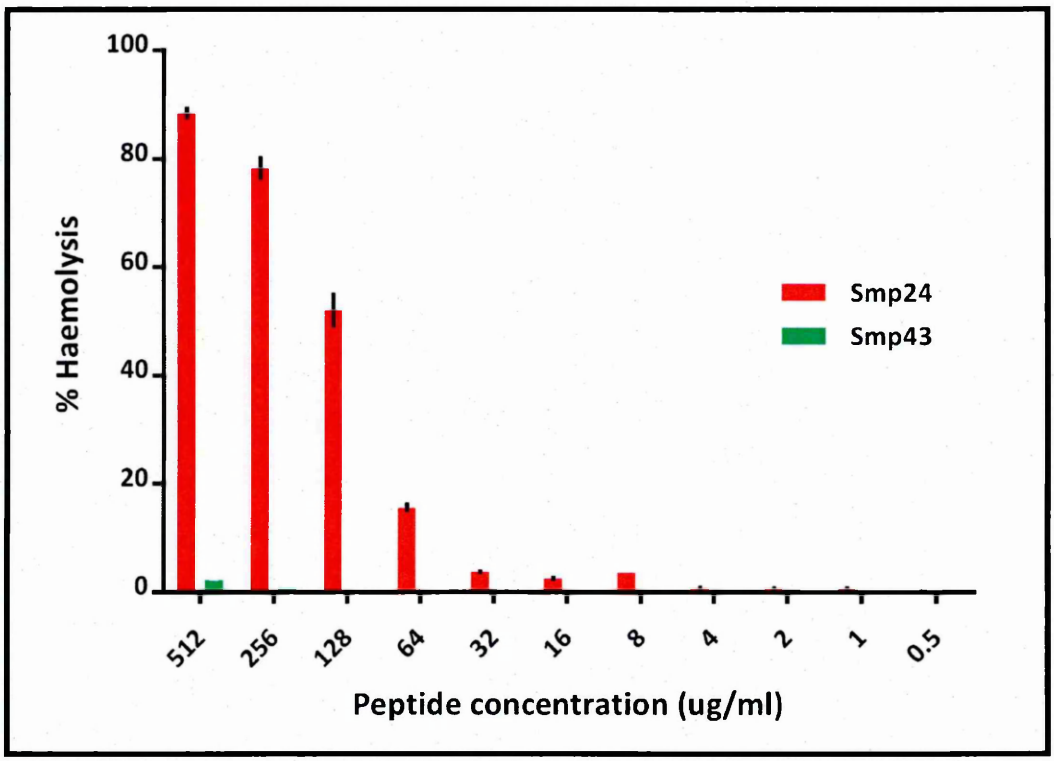

Figure 3.1 Haemolytic activities of Smp24 and Smp43. A 10% (v/v) suspension of washed erythrocytes in PBS was incubated with serial dilution peptides 1 h with intermittent shaking. The absorbance in the supernatant was measured at 570 nm. PBS and 10% (v/v) Triton X-100 were used as 0 and 100% controls respectively. Error bars indicate SD.

3.3.3 Cytotoxic activities of scorpion venom peptides

Smp24 caused increased damage to HaCaT cells but only at higher concentrations (128 and 256 μg/ml), in comparison to Smp43 which was inactive at all concentrations (Figure 3.2). At 16 μg/ml no peptide caused more than 15± 1.7% HEK293 cell damage; however, a doubling of the concentration caused 56 ± 6.6% cell damage with Smp43 and Smp24 showed a similar decrease in cell viability 67.3 ± 3.9% (Figure 3.3). Low cytotoxic activity was detected for Smp24 against HEK293 at concentrations higher than MICs for Gram positive strains (4-8 μg/ml).

Both tested cell lines were examined by fluorescence microscopy to assess the cell death pathway after incubation with Smp24 and Smp43. After 24 h, untreated cells showed normal structure without any signs of apoptosis or necrosis, whereas dead cells appeared red due to staining with PI which cannot cross intact cell membranes. Neither cell lines showed any morphological hallmarks of apoptosis such as nuclear fragmentation after incubation with Smp24 (Figure 3.4 and Figure 3.6). Only the highest concentration of Smp43 (256 μg/ml) induced apoptosis in a few human keratinocytes as indicated by the green arrows (Figure 3.5). Our results indicated that exposure to increasing doses of either Smp24 or Smp43 over a period of 24 hours decreased the viability of HEK293 cells in a dose-dependent fashion as the number of PI-stained cells increased (Figure 3.6 and Figure 3.7). The highest concentration of Smp43 (256 μg/ml) did not affect the viability of HaCaT cells as evidenced by Hoechst staining (Figure 3.5), although the numbers of dead cell treated with Smp24 increased at 128 μg/ml (Figure 3.4).

Both Smp peptides decreased the viability of HEK293 cells in a concentration-dependent manner with a noted effect seen at 32 μg/ml with both peptides.

Interestingly, HaCaT skin cell lines were not affected by Smp43 at 4x MIC 128 µg/ml for 24 hours of incubation, while Smp24 showed a noted decrease in cell viability at the same concentration.

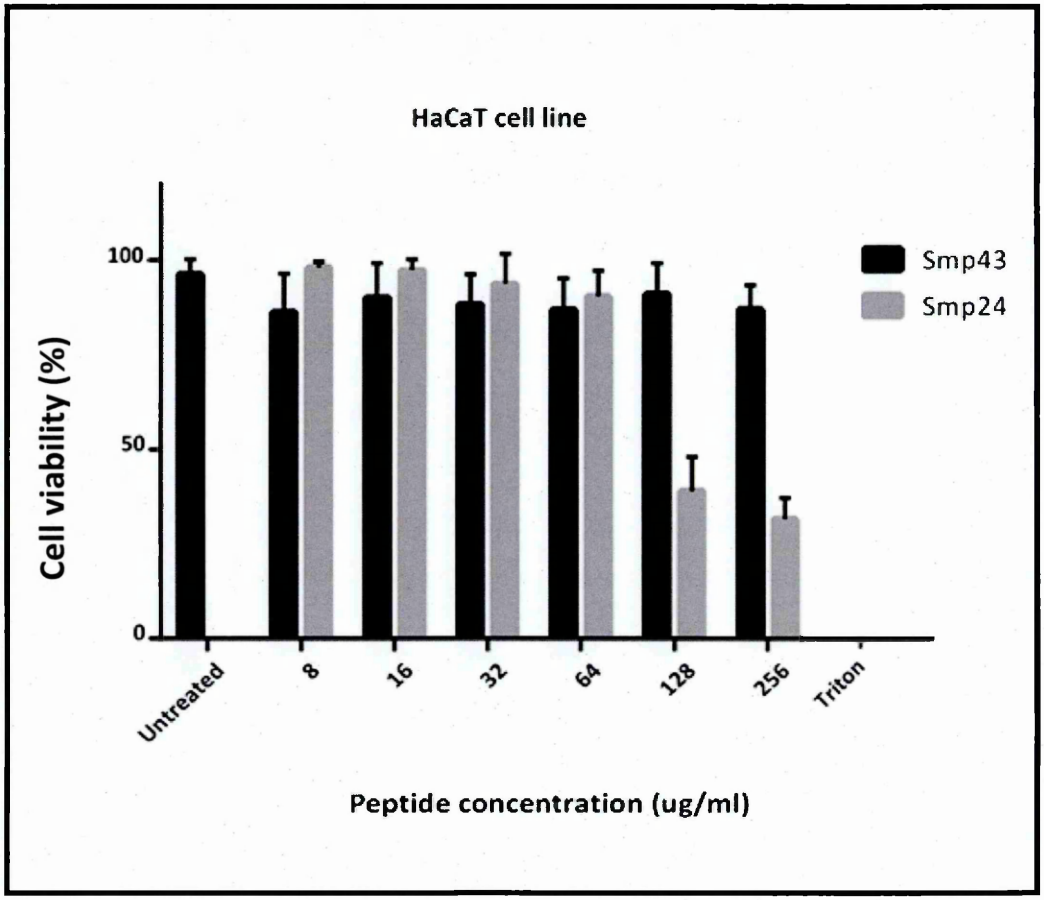

Figure 3.2 Evaluation of ATP-based cytotoxicity of human keratinocytes (HaCat) incubated with Smp peptides at various concentrations after 24 h of incubation. Control (HaCat) cells without treatment used as a control. HaCat cells were incubated with the different concentrations (8-256 µg/ml) of Smp24 and Smp43. 10% (v/v) Triton X-100 was used as positive control. Error bars indicate SD.

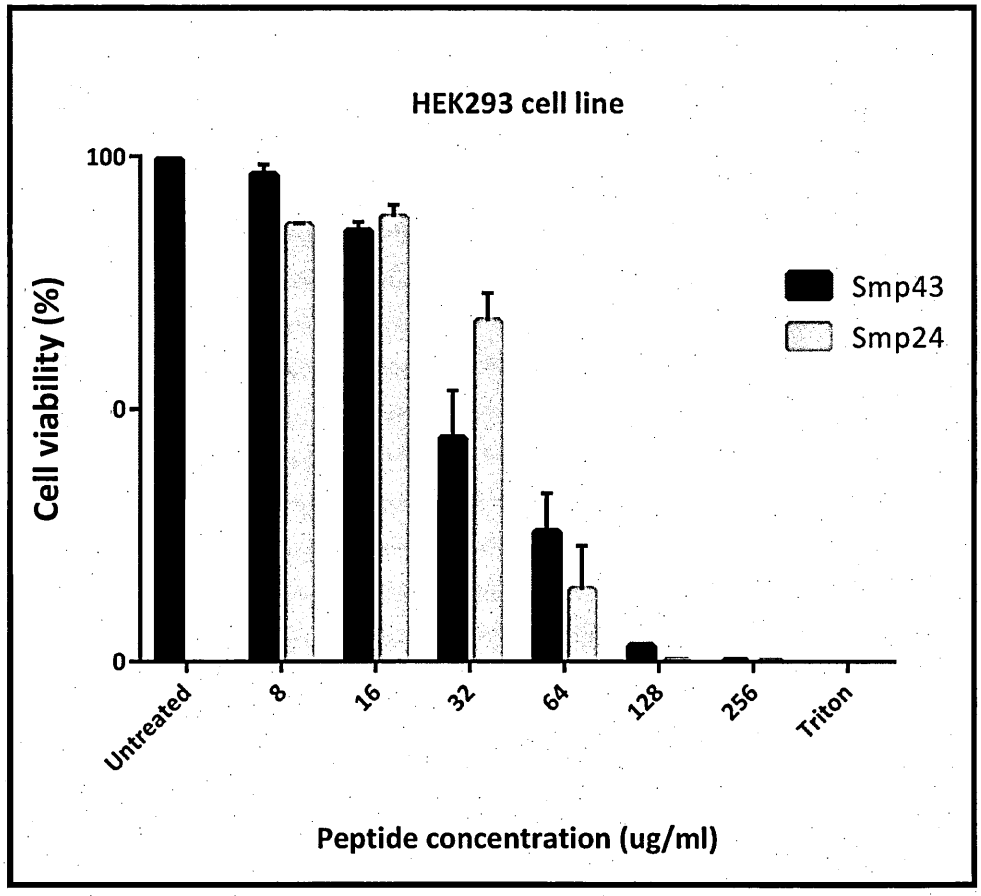

Figure 3.3 Evaluation of ATP-based cytotoxicity of human kidney cells (HEK293) incubated with Smp peptides at various concentrations after 24 h of incubation. Control (HEK293) cells without treatment used as a control. HEK293 cells were incubated with the different concentrations (8-256 µg/ml) of Smp24 and Smp43. 10% (v/v) Triton X-100 was used as positive control. Error bars indicate SD.

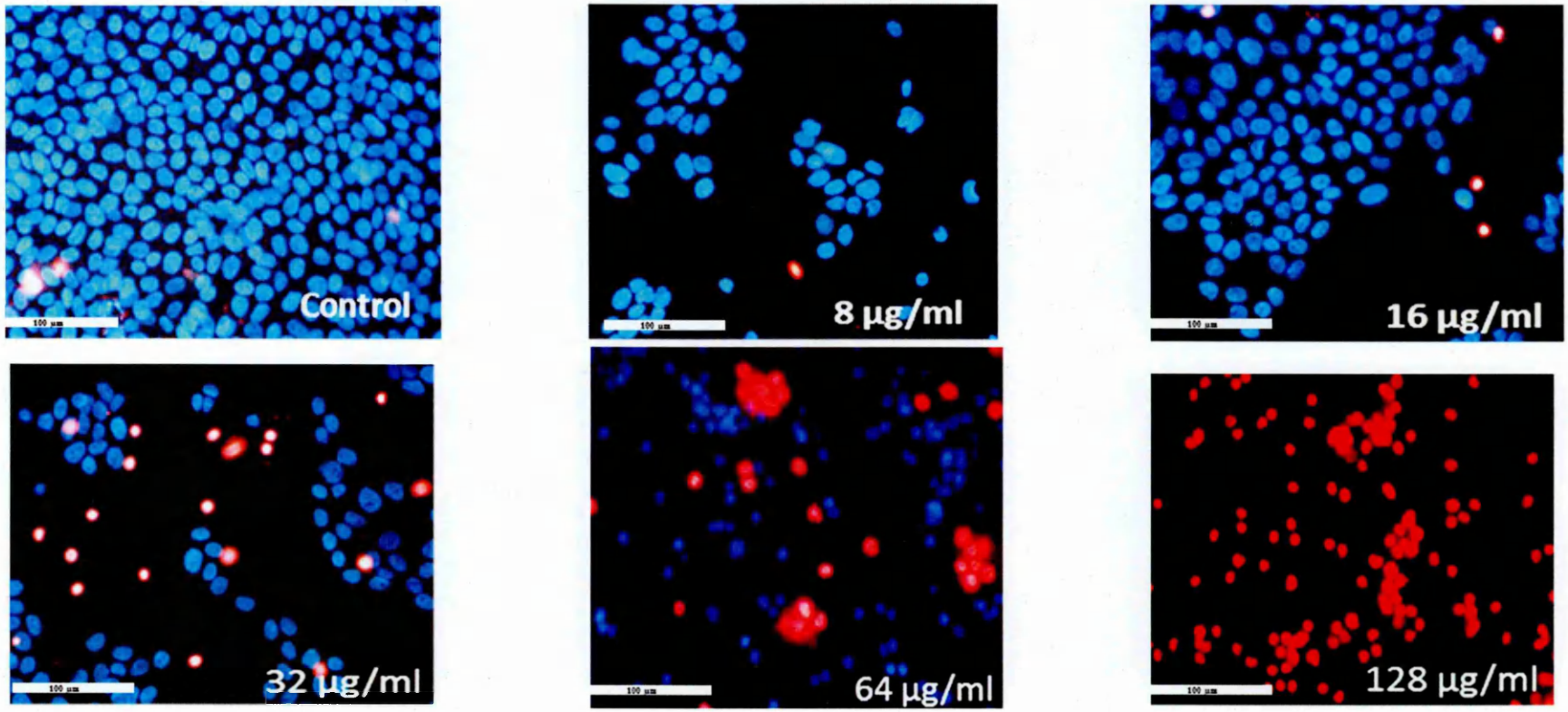

Figure 3.4 Cytotoxic effects of Smp24 on HaCat cells. Fluorescence microscopy of HaCat cells incubated with Smp24 at various concentrations after 24 h of incubation. Cells were stained with Hoechst 33342 (blue) and Propidium Iodide (PI) (red).

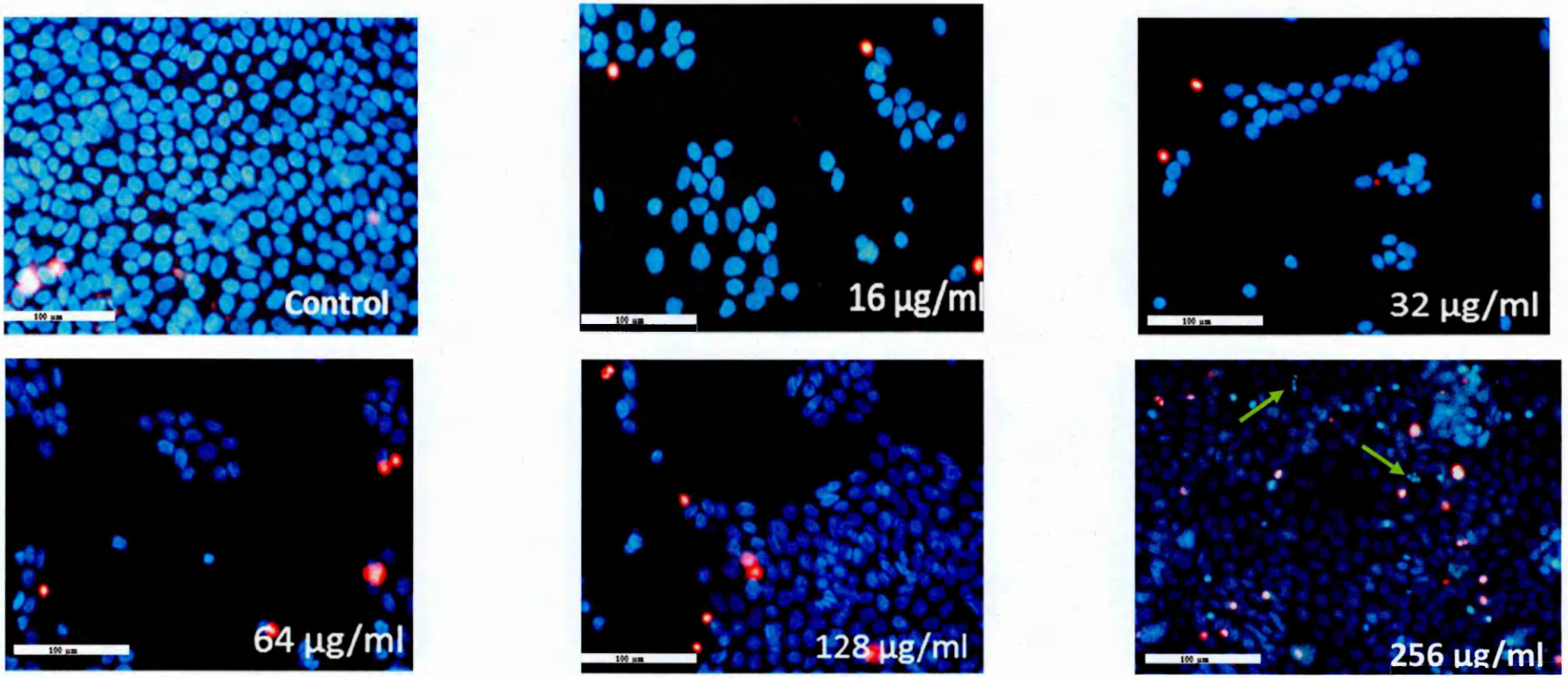

Figure 3.5 Cytotoxic effects of Smp43 on HaCat cells. Fluorescence microscopy of HaCat cells incubated with Smp43 at various concentrations after 24 h of incubation. Cells were stained with Hoechst 33342 (blue) and Propidium Iodide (PI) (red). Apoptotic cells are indicated by green arrows.

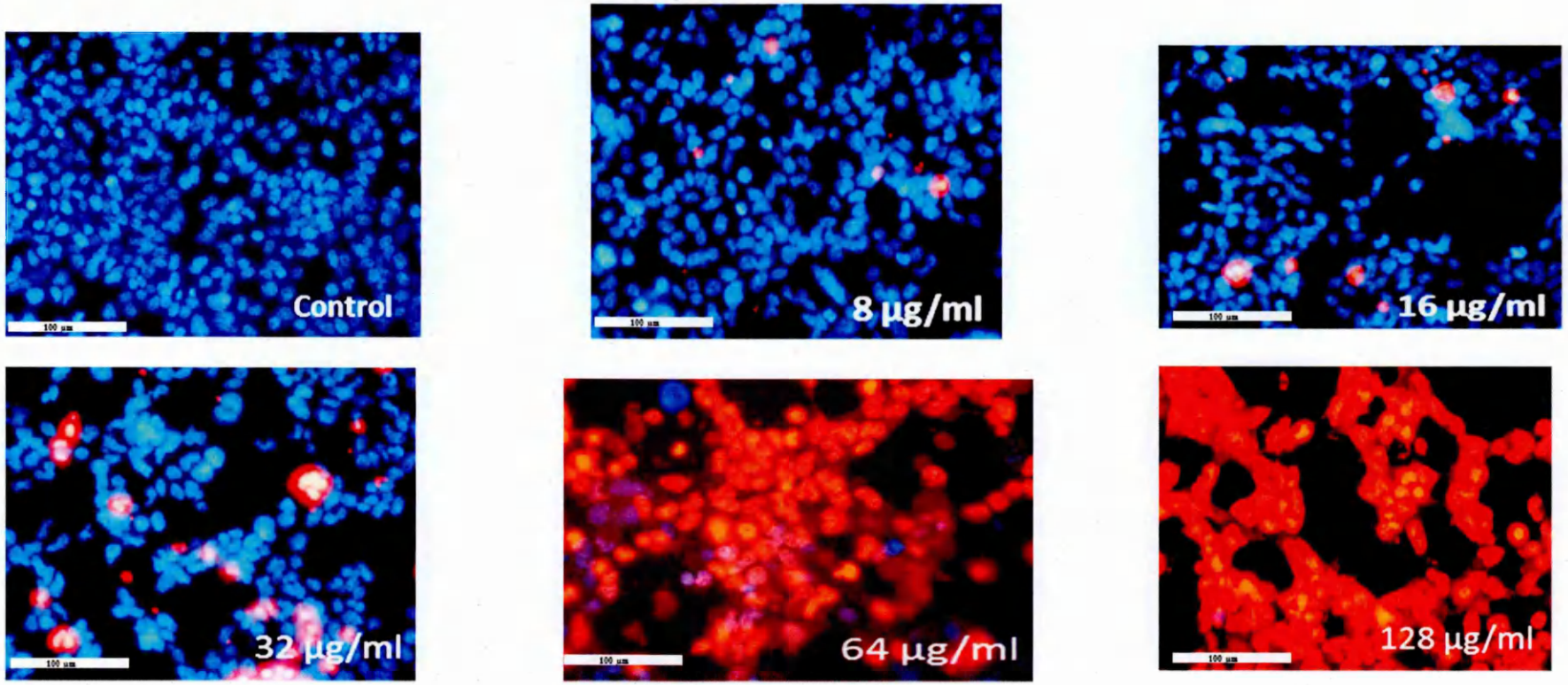

Figure 3.6 Cytotoxic effects of Smp24 on HEK293 cells. Fluorescence microscopy of HEK293 cells incubated with Smp24 at various concentrations after 24 h of incubation. Cells were stained with Hoechst 33342 (blue) and Propidium Iodide (PI) (red).

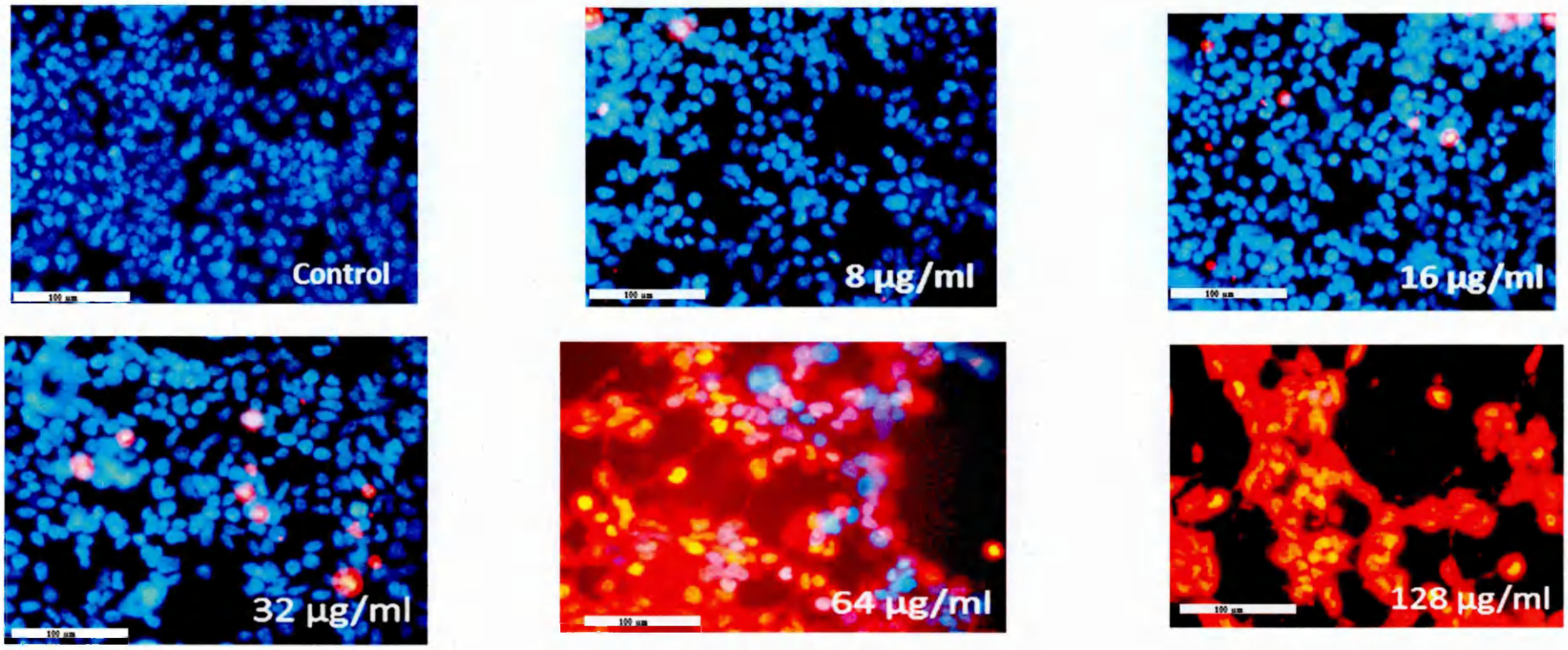

Figure 3.7 Cytotoxic effects of Smp43 on HEK293 cells. Fluorescence microscopy of HEK293 cells incubated with Smp43 at various concentrations after 24 h of incubation. Cells were stained with Hoechst 33342 (blue) and Propidium Iodide (PI) (red).

Smp24 and Smp43 are broad spectrum AMPs have been characterised from the venom gland of the Egyptian scorpion *Scorpio maurus palmatus*. They have potent activity against both Gram positive and Gram negative bacteria (MICs 4 to 128 µg/ml). The *in vitro* cytotoxicity assay indicated that HEK293 cells were more vulnerable to the Smp peptides-induced cytotoxicity than HaCaT cells.

In the following sections, crude snake venoms will be separated through HPLC chromatography to purify AMPs from snake venoms as follow:

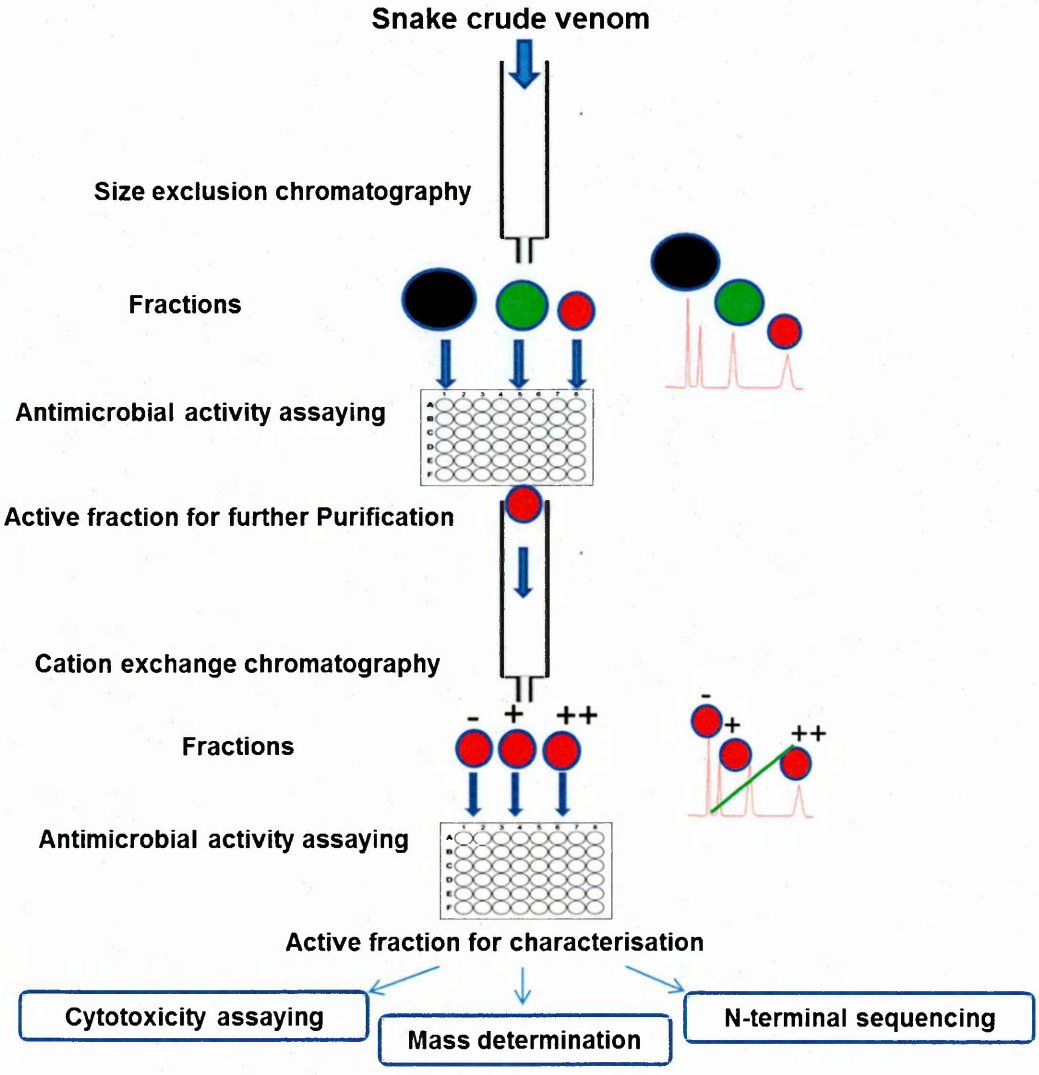

3.3.4 Purification of *Naja haje* venom peptides by size exclusion chromatography and cation exchange chromatography

60 mg of the elapid snake *Naja haje* crude venom extract was separated by Superdex 200 gel filtration. Chromatography resulted in 6 fractions designated NH1 to NH6 (Figure 3.8). Each fraction was dialysed against ultrapure water, freeze-dried and dissolved in 1 ml of water. Fractions were assayed against Gram negative bacteria (*Escherichia coli*) and Gram positive bacteria (*Staphylococcus aureus* and *Bacillus subtilis*) (Table 3.2). Three fractions (NH2, NH3 and NH4) showed antimicrobial activity. NHF2 exhibited full growth inhibition on all tested bacteria, whereas NH3 and NH4 showed full inhibitory activity against only *Bacillus subtilis,* with partial inhibitory activity against *Escherichia coli* compared with negative controls.

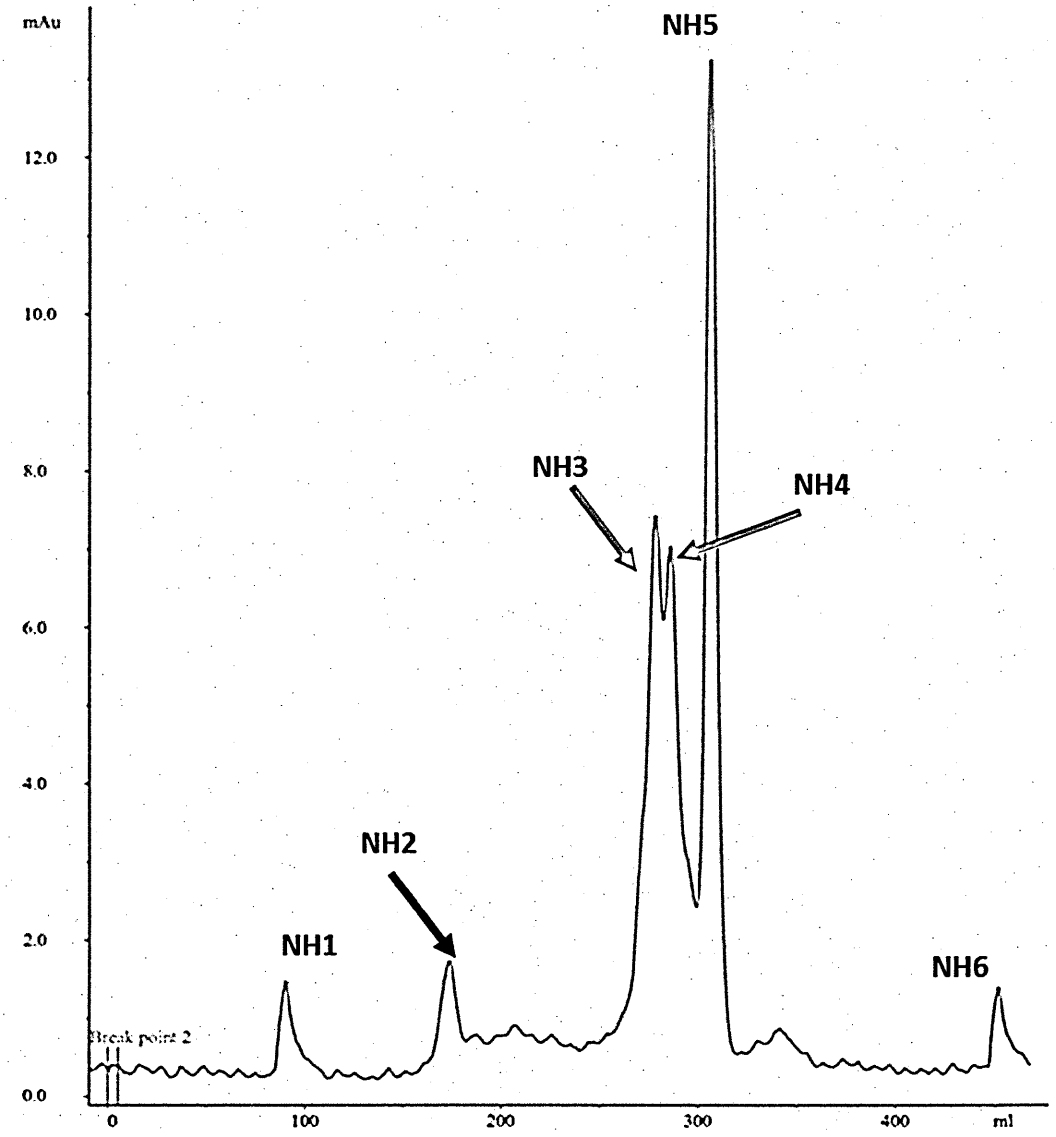

Figure 3.8 Fractionation of crude *Naja haje* venom by size-exclusion chromatography. Six peaks were obtained from the chromatography of 60 mg *Naja haje* crude venom on a HiLoad 26/600 (60 x2.6 cm diameter) Superdex 200 pg column at pH 4.3. Sample was eluted at 0.5 ml/min flow rate via 1.5 column volume of buffer A. Protein concentration was monitored at 280 nm and the collected fractions (3 mL/tube) were numbered from NH1 to NH6. Peak NH3 and NH4 were pooled together (NH3/4). The peak labelled with a black arrow exhibited inhibitory antibacterial activity against *Escherichia coli, Staphylococcus aureus*, and *Bacillus subtilis*. Peaks labelled with red arrow have an inhibitory activity against *Bacillus subtilis.*

Table 3.2 Antimicrobial activity of *Naja haje* fractions after gel filtration chromatography

Peak	Protein concentration (mg/ml)	Growth inhibition		
		Gram negative	Gram positive	
		E. coli	*S. aureus*	*B. subtilis*
NH1	0.01	-	-	-
NH2	0.5	++	++	++
NH3	3.2	+	-	++
NH4	6.2	+	-	++
NH5	0.5	-	-	-
NH6	0.02	-	-	-

Negative control was Fresh Muller-Hinton broth without peptides. – no inhibition, + partial inhibition and ++ Full inhibition.

Growth inhibition was determined using the broth microdilution method. Fractions were incubated with $1X10^6$ CFU/ml of overnight culture for 15 hours at 37°c. The optical density (OD) at a wavelength of 600 nm was read every 10 mins. Full inhibition was determined when OD =0.

NH2 was eluted mid-way through the run when one column volume of buffer had passed through the column (Vt 320ml, separation range 10 - 60 kDa) suggesting that the protein had a MW > 10 kDa. NH3 and NH4, with elution characteristics of low molecular weight peptides, were pooled (NH3/4) and further purified on a cationic SP Sepharose column. A NaCl gradient (0.1–1 M) was run and four peaks were collected (NH3/4-1 to NH3/4-4) (Figure 3.9). Each fraction was dialysed against ultrapure water, freeze-dried and then dissolved in 1 ml of water. Antibacterial activities were assayed against a range of Gram positive and Gram negative organisms (Table 3.3). Only peak NH3/4-4 (0.5 mg/ml) exhibited potent antibacterial activity, but, surprisingly, only against *B. subtilis*.

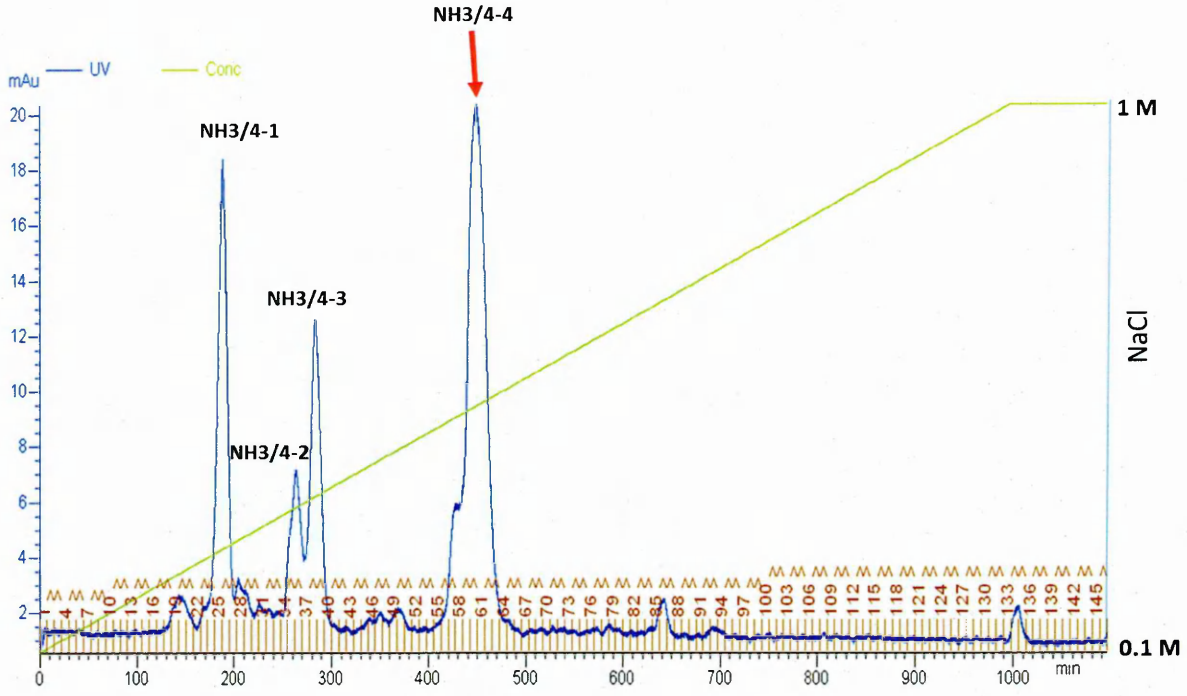

Figure 3.9 SP Sepharose cation exchange elution profile of NH3/4 from size exclusion fractionation of *Naja haje* (Figure 3.8). The column (100×16 mm diameter) was washed with buffer A (50 mM Sodium acetate pH 4.3) to remove any unbound proteins, and the bound proteins were eluted with a linear gradient of 20 column volumes of NaCl (0.1–1 M) in the same buffer. Sample was eluted at 0.5 ml/min flow rate. Protein concentration was monitored at 280 nm and collected fractions (3 mL/tube) were numbered from NH3/4-1 to NH3/4-4. The peak labelled with a black arrow fully inhibited the growth of *Bacillus subtilis*. NaCl gradient is shown by green line.

Table 3.3 Antimicrobial activity of *Naja haje* fractions after SP Sepharose cation exchange chromatography

Microorganism		Growth inhibition			
		NH3/4-1	NH3/4-2	NH3/4-3	NH3/4-4
Gram-negative bacteria	*E. coli* JM109	-	-	-	-
	Klebsiella pneumoniae NCTC 13439	-	-	-	-
	Pseudomonas aeruginosa NCIMB 8295	-	-	-	-
Gram positive bacteria	*S. aureus* SH1000	-	-	-	-
	S. epidermidis	-	-	-	-
	Bacillus cereus NCTC 2599	-	-	-	-
	Bacillus cereus UM20.1.	-	-	-	-
	B. subtilis NCIMB 8054	-	-	-	++
	B. subtilis NCIMB 8056	-	-	-	++
	B. subtilis NCIMB 3610	-	-	-	++

Negative control was Fresh Muller-Hinton broth without peptides. – no inhibition. ++ Full inhibition

Growth inhibition was determined using the broth microdilution method. Fractions were incubated with $1X10^6$ CFU/ml of overnight culture for 15 hours at 37°c. The optical density (OD) at a wavelength of 600 nm was read every 10 mins. Full inhibition was determined when OD =0.

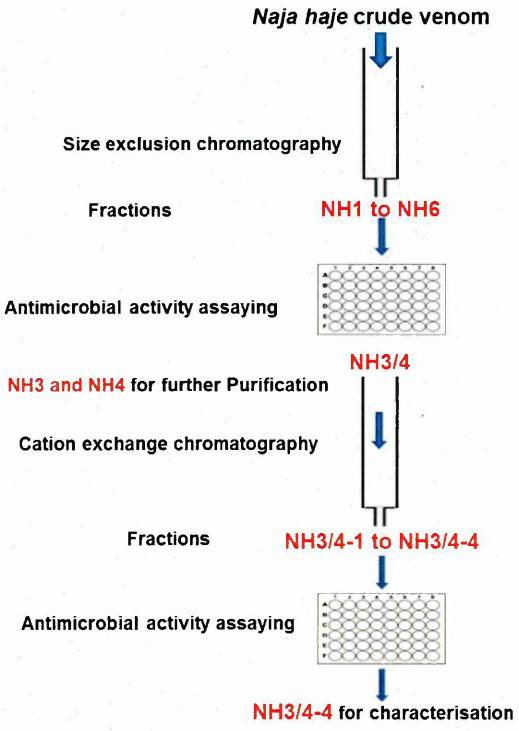

3.3.5 Purification of *Naja nubiae* venom peptides by size exclusion chromatography and cation exchange chromatography

Naja nubiae (Nubian spitting cobra) crude venom (35 mg) was fractionated by gel exclusion chromatography on a HiLoad 26/600 Superdex 200 column and resolved into four protein peaks (Figure 3.10). Whole venom inhibited the growth of *E. coli*, *S. aureus*, and *B. subtilis.* When individual peaks were screened for antibacterial activity against the same bacterial species, only peaks NN2 and NN3 showed antibacterial activity and only against *B. subtilis*. Both NN2 and NN3 were pooled, concentrated and dialysed against ultrapure water.

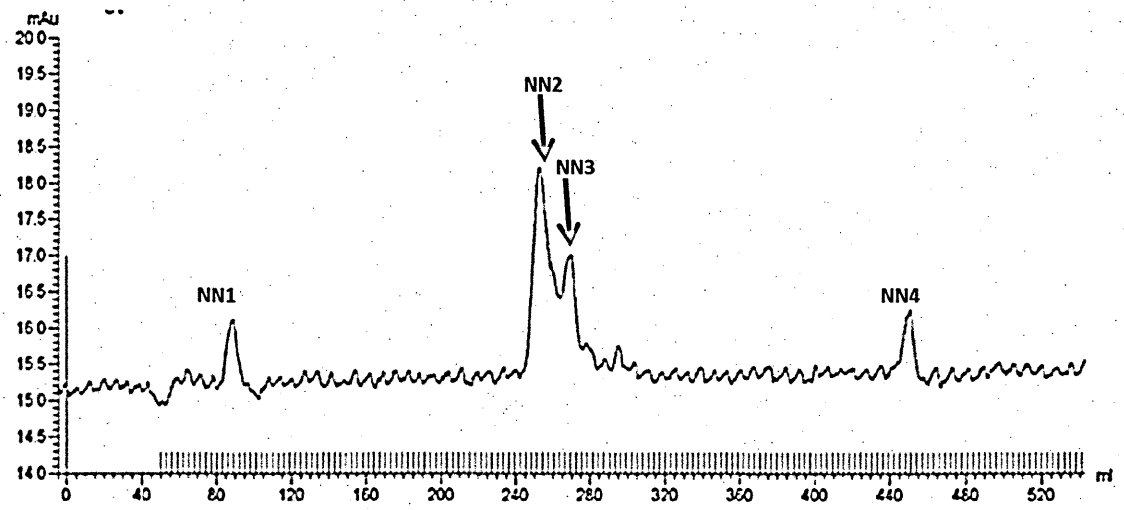

Figure 3.10 Fractionation of crude *Naja nubiae* venom by size-exclusion chromatography. Four peaks were obtained from fractionating 60 mg *Naja nubiae* crude venom on a HiLoad 26/600 (60 x2.6 cm diameter) Superdex 200 pg column at pH 4.3. The column was eluted at 0.5 ml/min flow rate via 1.5 column volume of buffer A. Protein concentration was monitored at 280 nm and the collected fractions (3 mL/tube) were numbered from NN1 to NN4. Peaks 2 and 3 were pooled together (NN2/3). Peaks labelled with red arrow have an inhibitory activity against *Bacillus subtilis.*

The pooled fractions (NN2/3) were further resolved into five peaks on a SP Sepharose cation exchange column 16X100 column by applying NaCl gradient (Figure **3.11**). Only peak 3 (NN2/3-3) exhibited potent antibacterial activity against *B. subtilis* (Table 3.4).

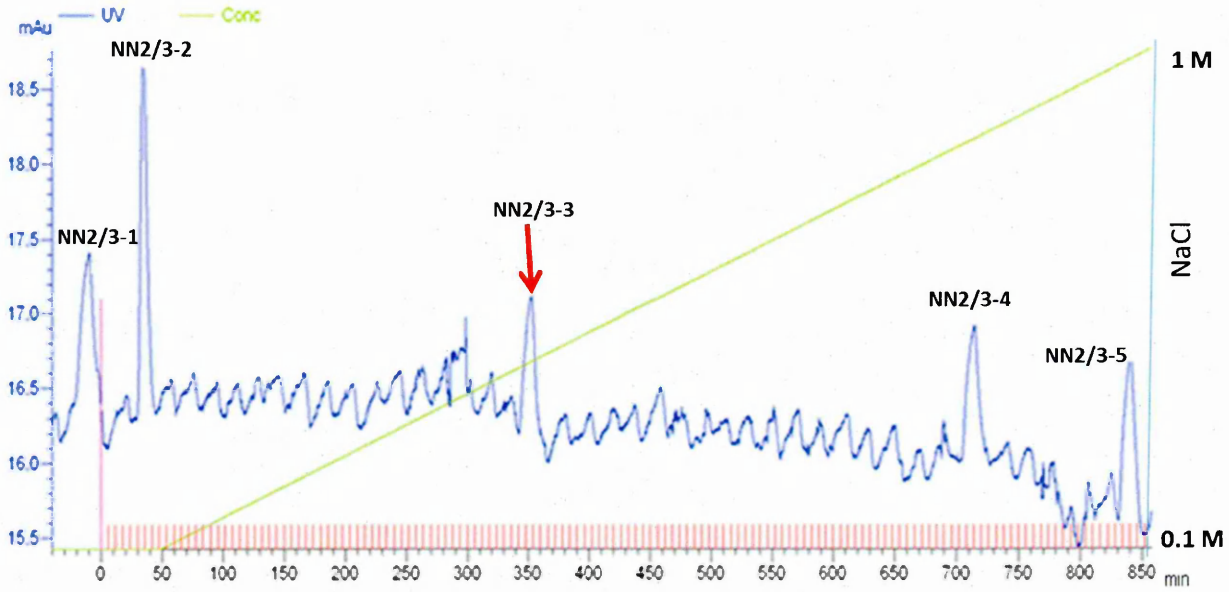

Figure 3.11 SP Sepharose cation exchange elution profile of pooled fractions NN2/3 from size exclusion fractionation *Naja nubiae* (Figure 3.10). The column (100×16 mm diameter) was washed with buffer A (50 mM Sodium acetate pH 4.3) to remove any unbound proteins, and the bound proteins were eluted with a linear gradient of 20 column volumes of NaCl (0.1–1 M) in the same buffer. Sample was eluted at 0.5 ml/min flow rate. Protein concentration was monitored at 280 nm and the collected fractions (3 mL/tube) were numbered from NN2/3-1 to NN2/3-5. The peak labelled with a red arrow fully inhibited the growth of *Bacillus subtilis*. NaCl gradient is shown by green line.

Table 3.4 Antimicrobial activity of *Naja nubiae* crude venom and fractions

Naja nubiae			Microorganism growth inhibition		
			E. coli	*S. aureus*	*B. subtilis*
Crude venom			++	++	++
Fractionation	Superdex 200	NN1	-	-	-
		NN2	-	-	++
		NN3	-	-	++
		NN4	-	-	-
	SP Sepharose	NN2/3-1	-	-	-
		NN2/3-2	-	-	-
		NN2/3-3	-	-	++
		NN2/3-4	-	-	-
		NN2/3-5	-	-	-

Negative control was Fresh Muller-Hinton broth without peptides. – no inhibition. ++ Full inhibition

Growth inhibition was determined using the broth microdilution method. Fractions were incubated with $1X10^6$ CFU/ml of overnight culture for 15 hours at 37°c. The optical density (OD) at a wavelength of 600 nm was read every 10 mins. Full inhibition was determined when OD =0.

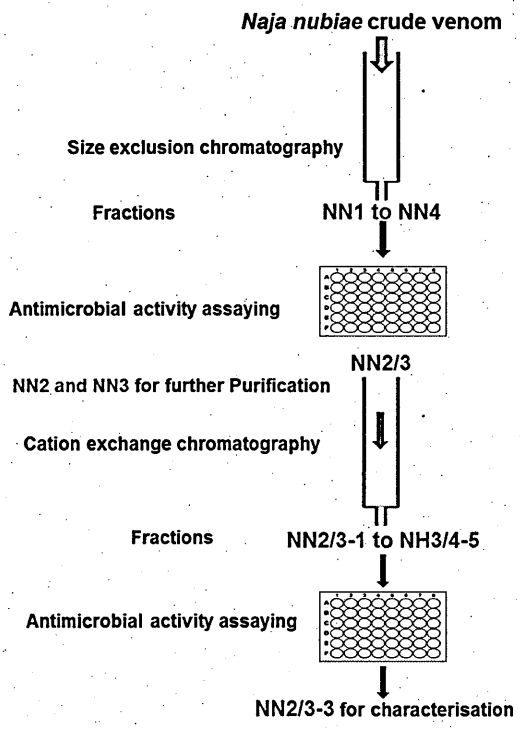

3.3.6 Purification of *Walterinnesia aegyptia* venom peptides by size exclusion chromatography and cation exchange chromatography

50 mg of the Egyptian elapid *Walterinnesia aegyptia* (Black Desert Cobra) was fractionated by gel exclusion chromatography on a HiLoad 26/600 Superdex 200 column and resolved into four protein peaks (Figure 3.12). The crude venom inhibited the growth of *E. coli*, *S. aureus*, and *B. subtilis*. However, when individual fractions were screened for antibacterial activity, only peak WG4 showed antibacterial activity and only against *B. subtilis*. WG4 was pooled, dialysed and concentrated and subsequently purified on a SP Sepharose cation column.

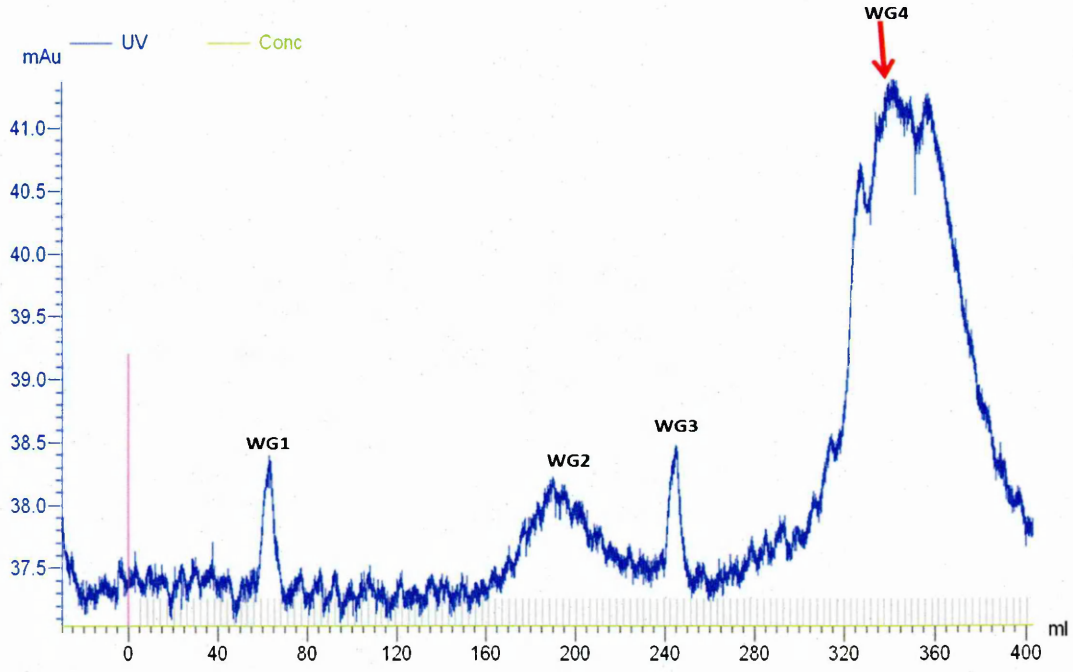

Figure 3.12 Fractionation of crude *Walterinnesia aegyptia* venom by size-exclusion chromatography. Four peaks were obtained from fractionating 50 mg *Walterinnesia aegyptia* crude venom on a HiLoad 26/600 (60 x2.6 cm diameter) Superdex 200 pg column at pH 4.3. The column was eluted at 0.5 ml/min flow rate via 1.5 column volume of buffer A. Protein concentration was monitored at 280 nm and the collected fractions (3 mL/tube) were numbered from WG1 to WG4. Peaks 4 was collected for further purification. Peak labelled with red arrow have an inhibitory activity against *Bacillus subtilis.*

Six protein peaks were obtained when WG4 (10 mg) was fractionated by SP Sepharose cation chromatography by applying NaCl gradient (Figure 3.13). Three protein peaks (WG4-2, W G4-3, and WG4-4) exhibited potent antibacterial activity exclusively against *B. subtilis*. These fractions also showed slight inhibitory activity against diluted ($1X10^6$ CFU/ml) cultures of *E. coli* ($1X10^3$ CFU/ml) (Table 3.5).

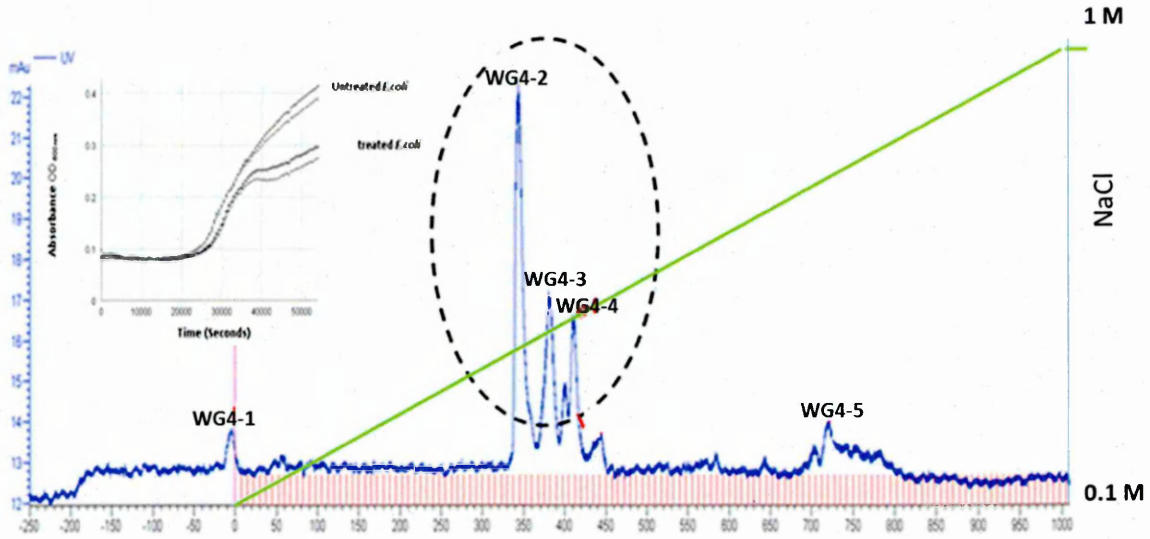

Figure 3.13 SP Sepharose cation exchange elution profile of pooled peak fractions (F4) from SEC fractionation of *Walterinnesia aegyptia* venom (Figure 3.12). The column (100×16 mm diameter) was washed with buffer A (50 mM Sodium acetate pH 4.3) to remove any unbound proteins, and the bound proteins were eluted with a linear gradient of 20 column volumes of NaCl (0.1–1 M) in the same buffer. Sample was eluted at 0.5 ml/min flow rate. Protein concentration was monitored at 280 nm and the collected fractions (3 mL/tube) were numbered from WG4-1 to WG4-5. The peaks with dotted black circle fully inhibited the growth of *Bacillus subtilis*. NaCl gradient is shown by green line. Figure 3.13 inset: Growth curve of *E. coli* ($1X10^3$ CFU/ml) culture in the absence or presence of WG4-2 (0.4 mg/ml).

Table 3.5 Antimicrobial activity of *Walterinnesia aegyptia* crude venom and fractions

Walterinnesia aegyptia			Microorganism growth inhibition		
			E. coli	*S. aureus*	*B. subtilis*
Crude venom			++	++	++
Fractionation	Superdex 200	WG1	-	-	-
		WG2	-	-	-
		WG3	-	-	-
		WG4	-	-	++
	SP Sepharose	WG4-1	-	-	-
		WG4-2	+	-	++
		WG4-3	+	-	++
		WG4-4	+	-	++
		WG4-5	-	-	-

Negative control was Fresh Muller-Hinton broth without peptides. – no inhibition, + partial inhibition and ++ Full inhibition.

Growth inhibition was determined using the broth microdilution method. Fractions were incubated with $1X10^6$ CFU/ml of overnight culture for 15 hours at 37°c. The optical density (OD) at wavelength of 600 nm was read every 10 mins. Full inhibition was determined when OD =0.

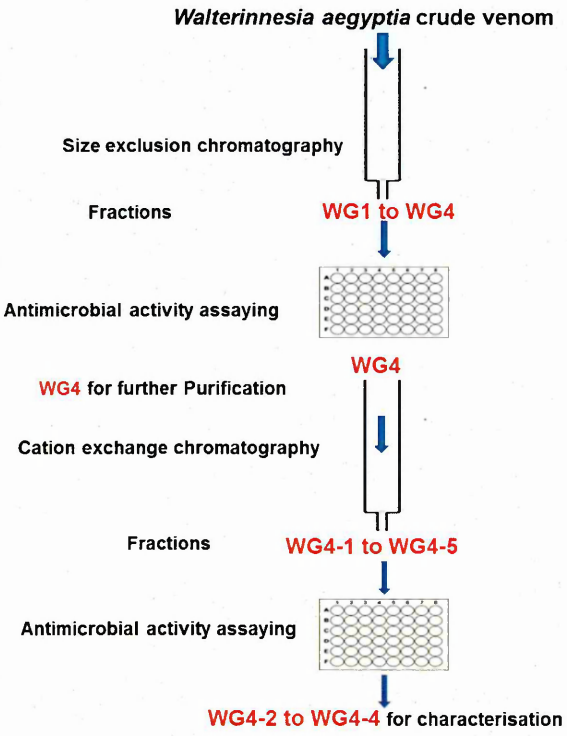

3.3.7 Purification of *Echis carinatus* venom peptides by size exclusion chromatography and cation exchange chromatography

The Size-exclusion chromatography of Egyptian viper *E. carinatus* (saw-scaled viper) venom on a HiLoad 26/600 Superdex 200 pg column resulted in obtaining four peaks (Figure 3.14). These fractions were assayed against *E. coli*, *S. aureus* and *B. subtilis.* Whole venom of *E. carinatus* inhibited the growth of *E. coli* and *S. aureus* at 500 µg/ml. Of the individual peaks, only EC3 showed slight growth inhibitory activity against *S. aureus* and *B. subtilis*. EC3 was collected, dialysed and loaded onto a SP Sepharose cation column and fractionated by applying NaCl gradient for further purification.

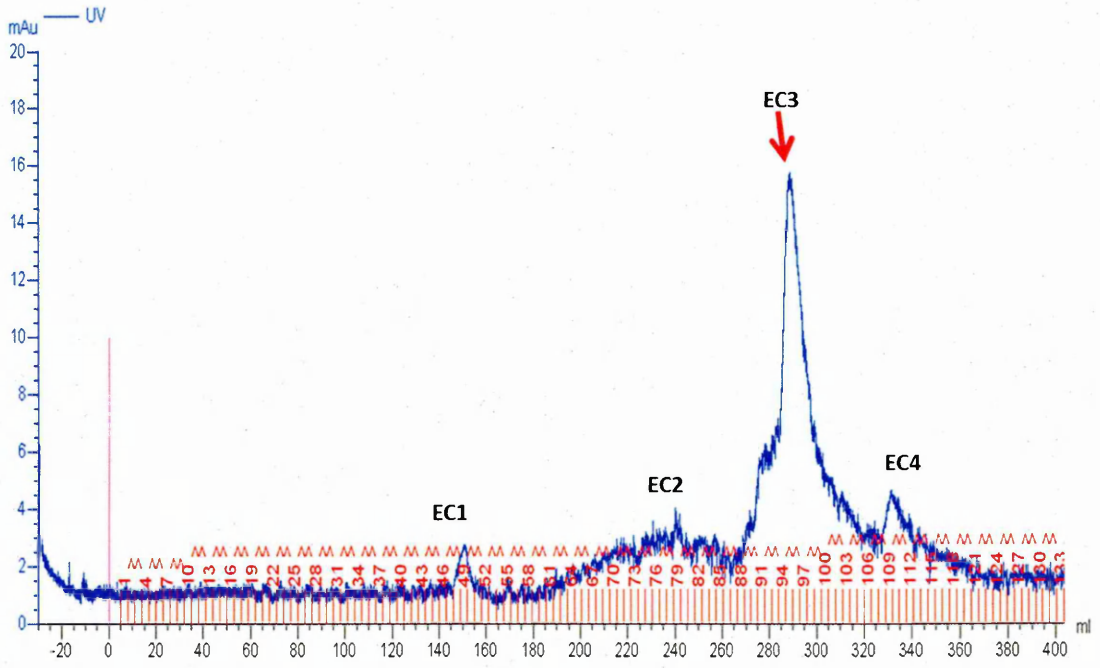

Figure 3.14 Fractionation of crude *Echis carinatus* venom by size-exclusion chromatography. Four peaks were obtained from fractionating 35 mg *Naja nubiae* crude venom on o HiLoad 26/600 (60 x2.6 cm diameter) Superdex 200 pg column at pH 4.3. The column was eluted at 0.5 ml/min flow rate via 1.5 column volume of buffer A. Protein concentration was monitored at 280 nm and the collected fractions (3 mL/tube) were numbered from EC1 to EC4. Peak labelled with red arrow have an inhibitory antibacterial activity against *B. subtilis and S. aureus*.

Ten eluted peaks resulted from SP Sepharose chromatography of EC3 (Figure 3.15). No fractions showed any activity against *E. coli*, *S. aureus* or *B. subtilis*.

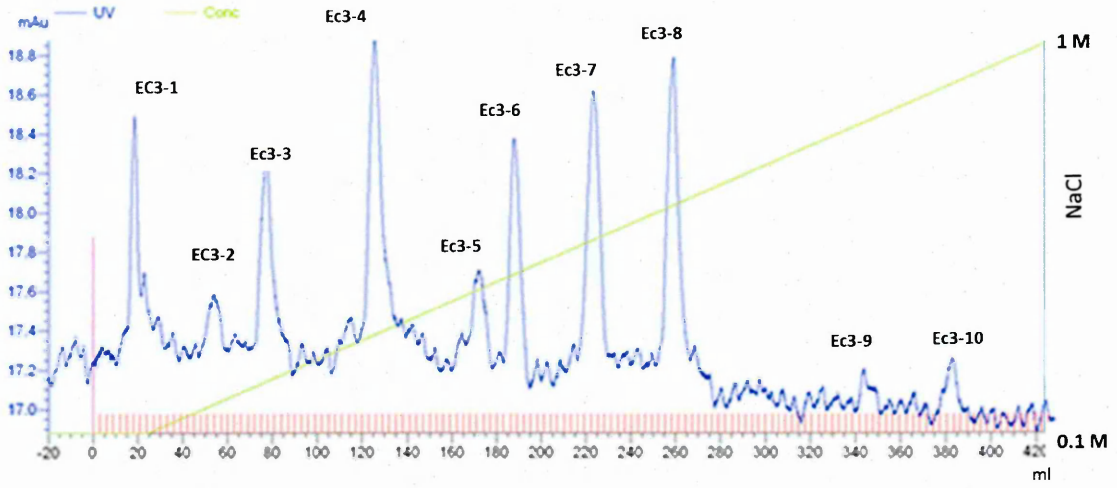

Figure 3.15 SP Sepharose cation exchange elution profile of EC3 from SEC fractionation of *Echis carinatus* (Fig.3.14). The column (100×16 mm diameter) was washed with buffer A (50 mM Sodium acetate pH 4.3) to remove any unbound proteins, and the bound proteins were eluted with a linear gradient of 20 column volumes of NaCl (0.1–1 M) in the same buffer. Sample was eluted at 0.5 ml/min flow rate. Protein concentration was monitored at 280 nm and the collected fractions (3 mL/tube) were numbered from EC3-1 to EC3-10. NaCl gradient is shown by green line.

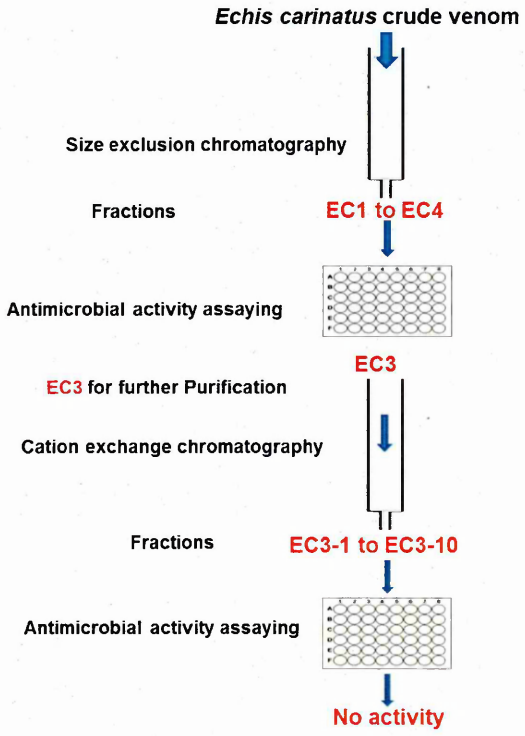

3.3.8 Haemolytic activities of snake venom peptides

NH3/4-4, WG4-2, WG4-3, WG4-4 and NN2/3-3 displayed low or no haemolytic activity on sheep erythrocytes at concentrations of 50 µg/ml (Figure 3.16).

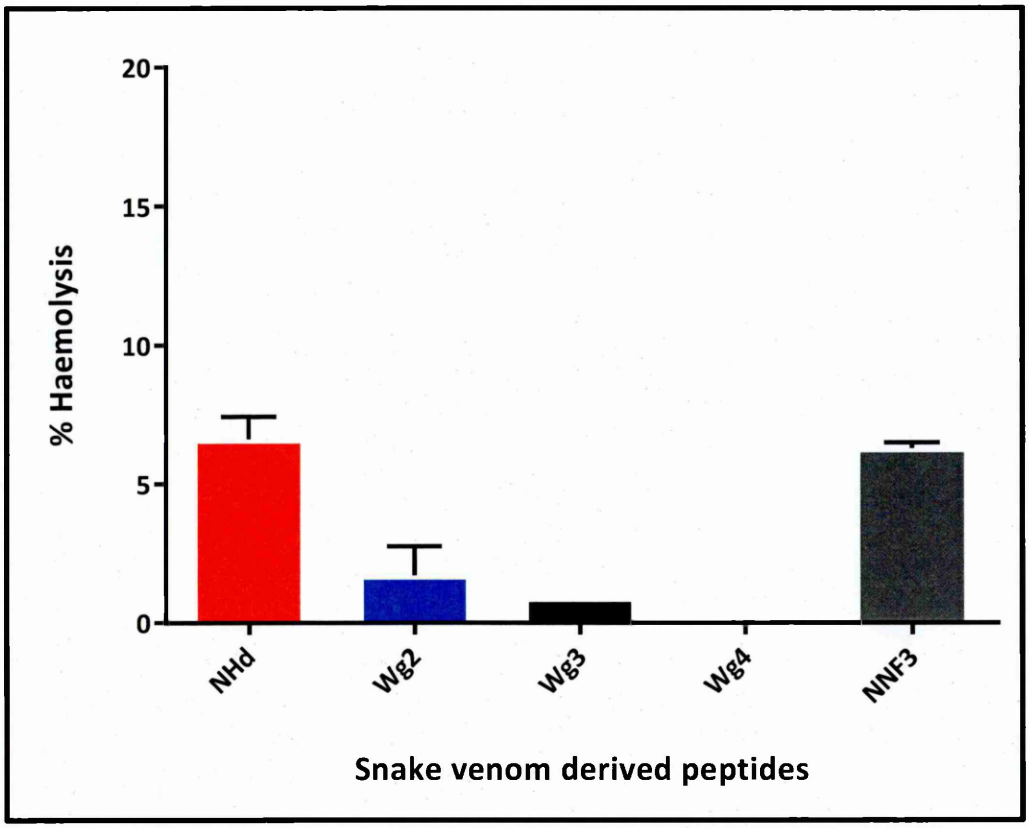

Figure 3.16 Haemolytic activities of Snake venom peptides of 50 µg/ml. A 10% (v/v) suspension of washed erythrocytes in PBS was incubated with serial dilution peptides 1 h with intermittent shaking. The absorbance in the supernatant was measured at 570 nm. PBS and 10% (v/v) Triton X-100 were used as 0 and 100% controls respectively. Error bars indicate SD.

3.3.9 Cytotoxic activities of snake venom peptides

The cytotoxic potential of snake venom purified peptides and synthetic scorpion peptides was determined using an ATP assay, to determine the ATP content of cells following incubation of HEK293 and HaCaT cells for 24 hours.

Cytotoxicities of each of snake-derived venom peptide were comparable in the two cell lines. NH3/4-4 exhibited the lowest level of cytotoxicity towards the two cell lines; the percentages of cell viability were 85 ± 1% for HEK293 cells and 77 ± 7 % for HaCaT cells at a concentration of 50 µg/ml (Figure 3.17). However, HEK293 cells were more vulnerable to WG4-2 and NN2/3-3-induced cytotoxicity in dose-dependent manner (Figure 3.18). After 24 hours of exposure to either 50 µg/ml of WG4-2 or NN2/3-3, the percentage cells viability reduced to 55 ±2% and 61.5% ±2% (HEK293), and 73 ±4.9% and 90 ±4% (HaCaT) respectively.

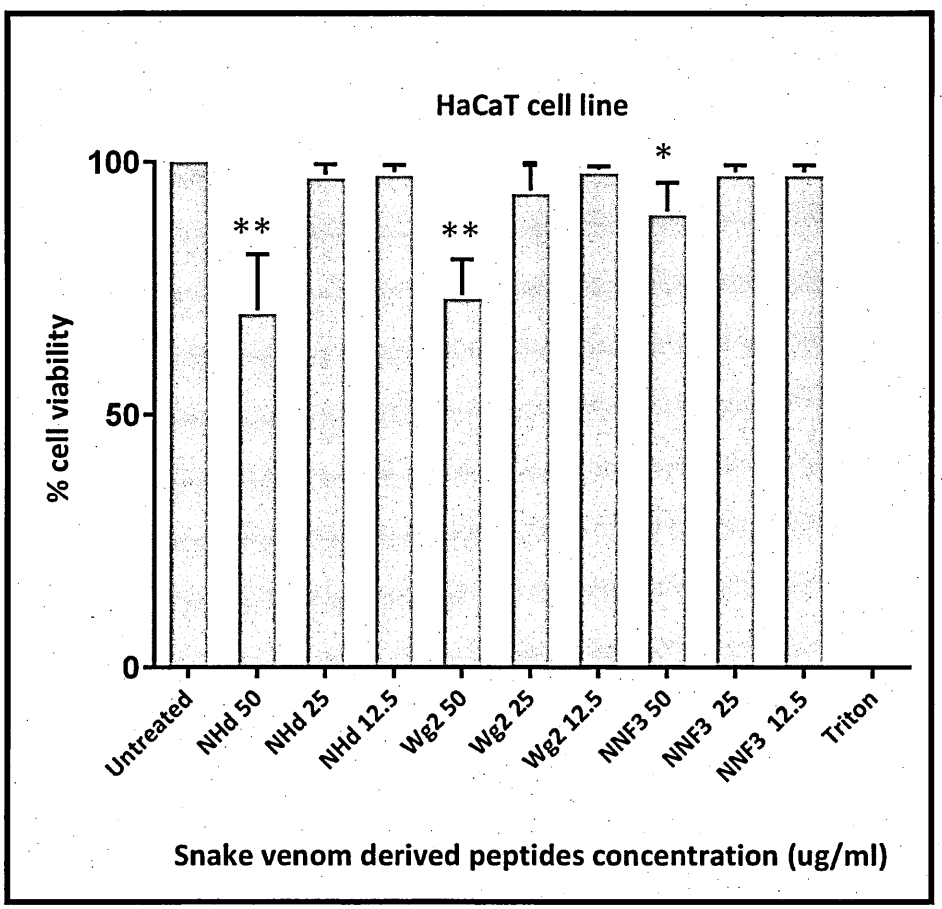

Figure 3.17 Evaluation of ATP-based cytotoxicity of human keratinocytes (HaCat) incubated with snake venom peptides at various concentrations after 24 h of incubation. Control (HaCat) cells without treatment used as a control. HaCat cells were incubated with the different concentrations (8-256 μg/ml) of Smp24 and Smp43. 10% (v/v) Triton X-100 was used as positive control. Error bars indicate SD. All treatments were performed in triplicate, in three independent experiments. Statistical analysis was performed by the Kruskal-Wallis test. *Significant P <0.05 **Significant P <0.01. ***Significant P <0.001.

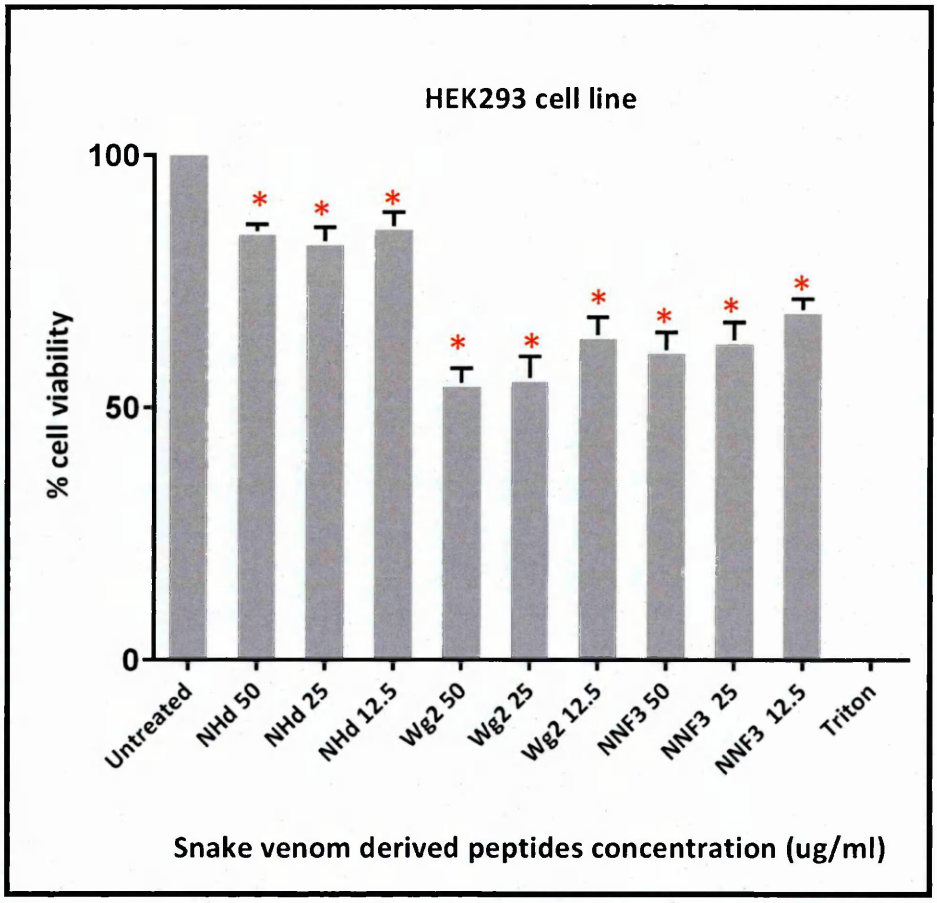

Figure 3.18 Evaluation of ATP-based cytotoxicity of human kidney cells (HEK293) incubated with snake venom peptides at various concentrations after 24 h of incubation. Control (HEK293) cells without treatment used as a control. HEK293 cells were incubated with the different concentrations (8-256 µg/ml) of Smp24 and Smp43. 10% (v/v) Triton X-100 was used as positive control. Error bars indicate SD. All treatments were performed in triplicate, in three independent experiments. The significance of differences between treated and untreated cells were statistically analysed by the two-way analysis of varience. ANOVA results were significant (P <0.05).

3.3.10 Analysis of snake venom peptides by mass spectrometry

Active fractions from *N. haje, N. nubiae,* and *W. aegyptia* venoms were analysed by MALDI-TOF-MS (Table 3.6). MALDI-TOF spectra of the purified fractions are shown in Figure 3.19 to Figure 3.22.

Table 3.6 measured mass to charge ratio (m/z) of active snake venom peptides

SP Sepharose peak	Masses m/z, Da
NH3/4-4	6870
WG4-2	6757
WG4-3	6715
NN2/3-3	6868

A single peptide with a molecular mass of 6870 Da was observed in the purified fraction from *N. haje* venom NH3/4-4, a minor peak at 2x m/z 13760 (Figure 3.19). Molecular masses of 6757 and 6715 Da were detected for *W. aegyptia* peptides WG4-2 and WG4-3 respectively (Figure 3.20 and Figure 3.21). WG4-3 was not pure with three proteins present, at 6594, 6731 and 6747 Da. WG4-4 yielded a MALDI mass spectrum with no detectable peaks when scanned up to 80KDa. The purified fraction (NN2/3-3) from the venom of *N. nubiae* venom had a calculated mass of 6868Da (Figure 3.22) with a number of minor peaks observed in the mass spectra representing m/2z, 2x m/z and 3x m/z.

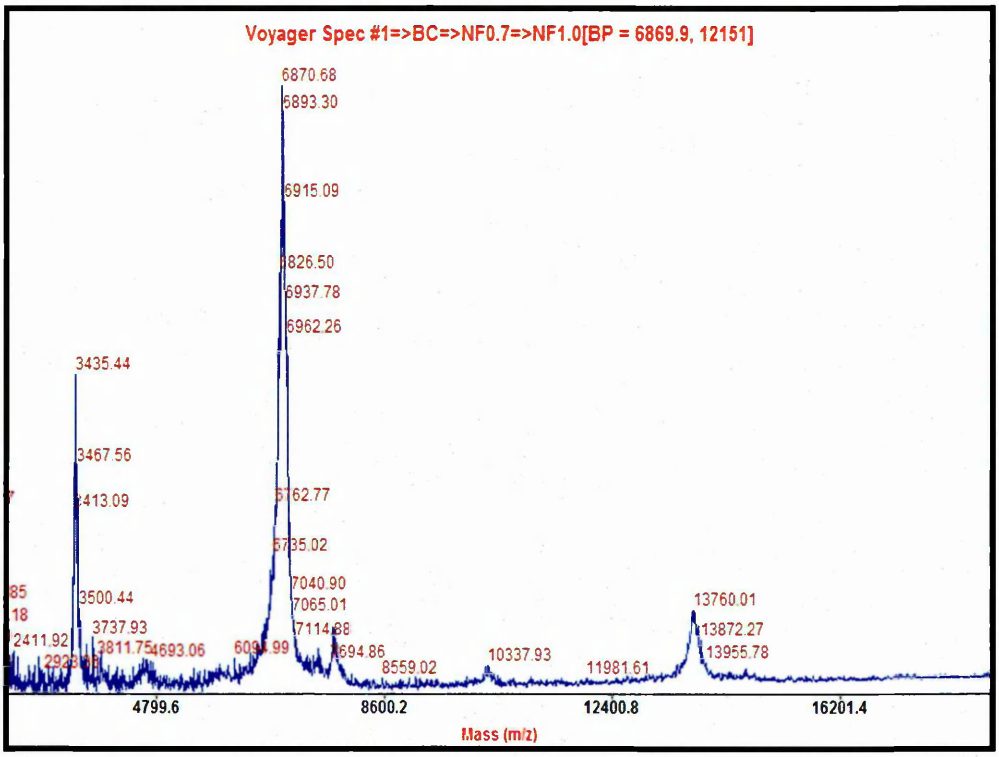

Figure 3.19 MALDI-TOF-TOF-MS spectra of purified *N. haje* venom peptide (NH3/4-4). The molecular masses of peptides were determined using MALDI-TOF mass spectrometry in positive ionization mode. α-Cyano-4-hydroxycinnamic acid was used as MALDI matrix.

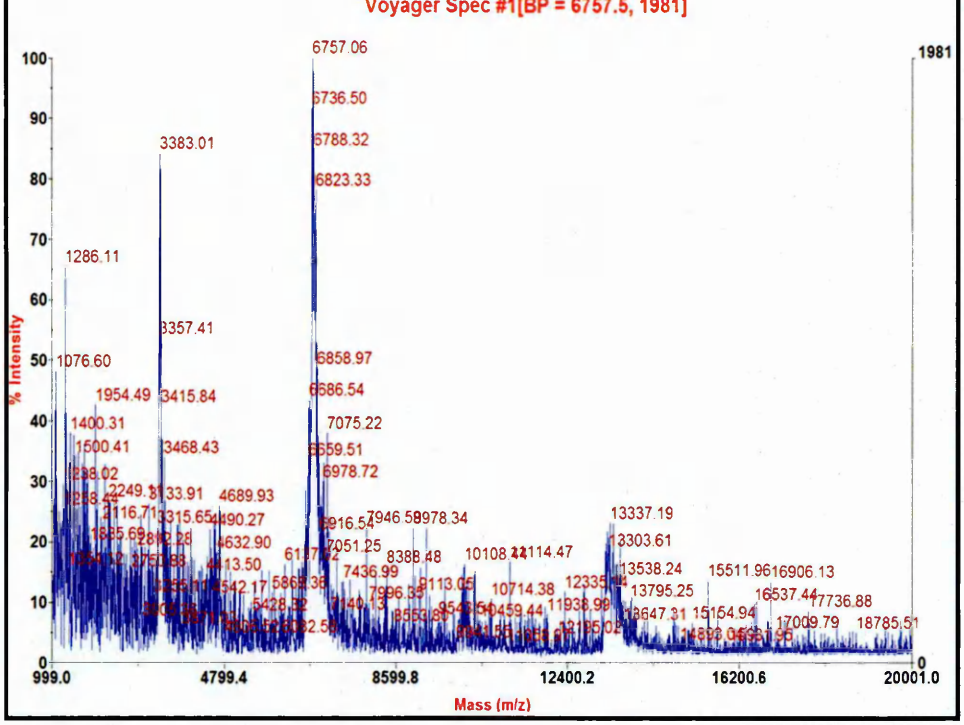

Figure 3.20 MALDI-TOF-TOF-MS spectra of purified *W. aegyptia* venom peptide (WG4-2).The molecular masses of peptides were determined using MALDI-TOF mass spectrometry in positive ionization mode.α-Cyano-4-hydroxycinnamic acid was used as MALDI matrix.

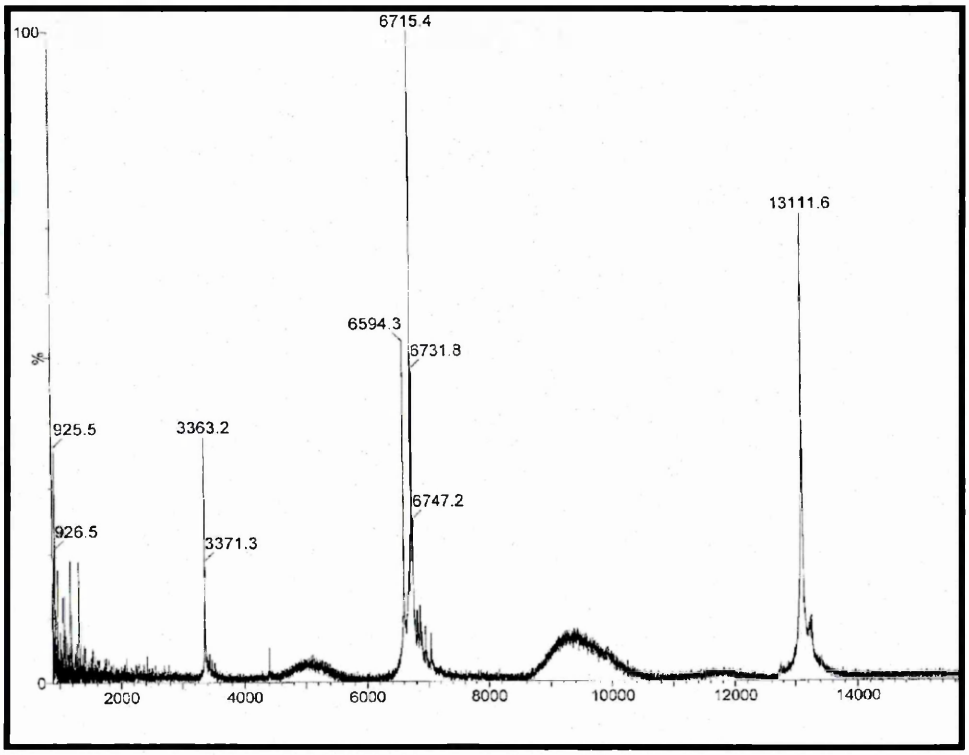

Figure 3.21 MALDI-TOF-TOF-MS spectra of purified *W. aegyptia* venom peptide (WG4-3). The molecular masses of peptides were determined using MALDI-TOF mass spectrometry in positive ionization mode.α-Cyano-4-hydroxycinnamic acid was used as MALDI matrix.

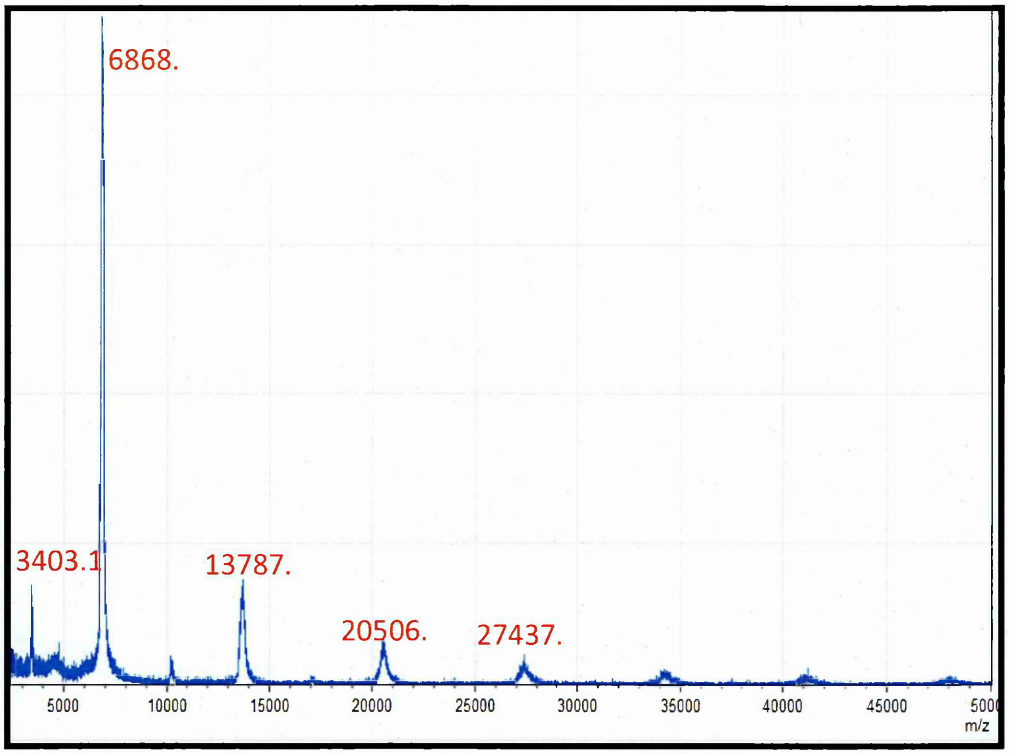

Figure 3.22 MALDI-TOF-TOF-MS spectra of purified *N. nubiae* venom peptide (NN2/3-3). The molecular masses of peptides were determined using MALDI-TOF mass spectrometry in positive ionization mode.α-Cyano-4-hydroxycinnamic acid was used as MALDI matrix.

3.3.11 Identification of N-terminal residues

The first five N-terminal amino acid residues of NH3/4-4, WG4-2, WG4-3 and NN2/3-3 were sequenced, and compared with those found in the ExPASY proteomics database using a basic local alignment search tool (BLAST). The sequence of NH3/4-4 was identical to "Short neurotoxin 2" (Joubert 1975) which has been identified as a member of the three-finger toxin superfamily. This sequence is present in a number of different *Naja* species (Figure 3.23) *Naja nivea* (Botes, 1971), *Naja haje* (Joubert 1975) and *Naja annulifera* (Joubert & Taljaard, 1978) but is unique to *Naja* genus.

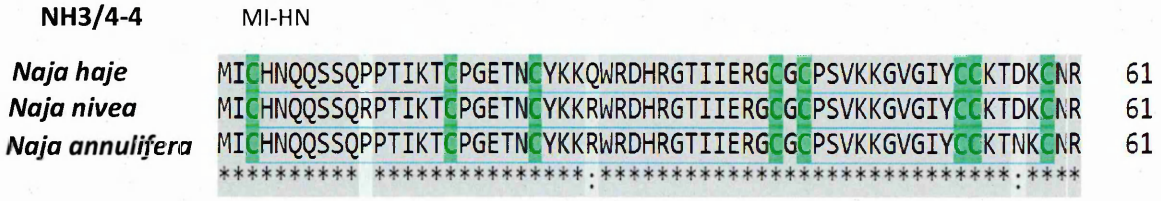

Figure 3.23 N - terminal Sequence alignment of NH3/4-4 with full sequences of short neurotoxin2 sequences (three-finger toxins) from some *Naja* genus venoms. N-terminal sequence of NH3/4-4 was obtained by automated Edman degradation. Other protein sequences were obtained from the NCBI database. Conserved cysteine residues are shown in green colour. Residue (-) at position 3 is most likely due to cysteine as it cannot be detected using N-terminal sequencing, without prior chemical modification.

N-terminal sequencing of both 6 kDa peptides WG4-2 and WG4-3 (NH_2-Leu- Lys- (Cys)-Asn- Gln) also revealed their homology with the three-finger toxins. The five amino acids residues are similar to *Naja mossambica* (Mozambique spitting cobra) cytotoxins CTX M1, M3 and M4 (Figure 3.24). No sequence data was obtained for the N-terminus of NN2/3-3, the most likely cause is that it is N-terminally blocked.

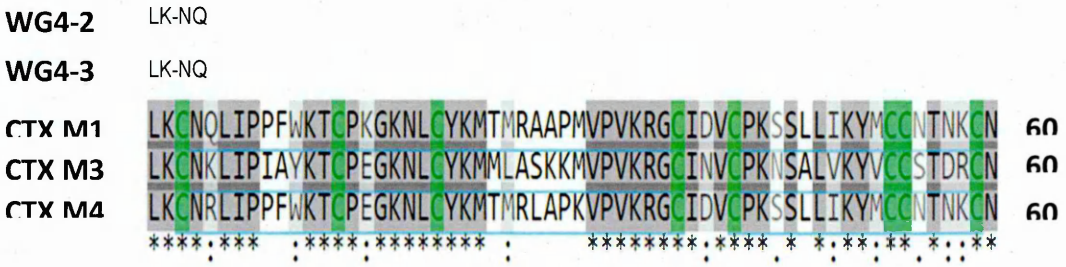

Figure 3.24 N - terminal Sequence alignment of WG4-2 and WG4-3 with full sequences of *Naja mossambica* (Mozambique spitting cobra) cytotoxins CTX M1,M3 and M4. N-terminal sequence of WG4-2 and WG4-3 was obtained by automated Edman degradation. Other protein sequences were obtained from the NCBI database. Conserved cysteine residues are shown in green colour. Residue (-) at position 3 is most likely due to cysteine as it cannot be detected using N-terminal sequencing, without prior chemical modification.

3.4 Discussion

Snake and scorpion venoms are enriched sources of some biologically active peptide with many therapeutic uses. The envenomation apparatus of snakes and scorpions which is used either for defence or to obtain food, is often contaminated with multiple pathogenic microbes (Garcia-Lima, Laure 1987, Shek, Tsui *et al.* 2009, Babalola, Balogun 2013). Since snakes and scorpions are associated with a low incidence of microbial infection (Talan, Citron *et al.* 1991), this suggests that venoms might contain potent antimicrobial agents protect against pathogens, although venoms remain largely unexamined as sources for AMPs (de Lima, Alvarez Abreu *et al.* 2005, Ferreira, Santos *et al.* 2011, Samy, Stiles *et al.* 2015).

A large number of putative AMPs have been identified from scorpion and snake venoms by proteomic or/and transcriptomic approaches from venom gland cDNA library. However, the antimicrobial and cytotoxic profiles of most of these peptides have not yet been fully investigated. The present study aimed to evaluate the potential biological activities of three such putative AMPs (Smp13, Smp24 and Smp43), which have been identified from a cDNA library of the venom gland of *S. maurus palmatus* (Abdel-Rahman, Quintero-Hernandez *et al.* 2013). Also, this study represents the first attempt to identify and characterise the peptides and proteins that having antibacterial activities from Egyptian snake venoms.

Although Smp13 shares a high level of sequence identity with some potent AMPs such as UyCT3 and IsCT derived from *Urodacus yaschenkoi* (Inland robust scorpion) and *Opisthacanthus madagascariensis* respectively, it is likely that Smp13 exhibited no

antimicrobial activity against tested bacterial strains because it has a net charge of zero. Electrostatic interactions play a crucial role in the binding of cationic AMPs to negatively charged prokaryotic membranes (Yu, Guo *et al.* 2009, Bahar, Ren 2013). The enhancement of antimicrobial potency of some AMPs is dependent on the increase in positive net charge and the number of positively charged residues which could increase the electrostatic binding of the peptide to anionic bacterial membranes (Zelezetsky, Tossi 2006, Jiang, Vasil *et al.* 2008, Phoenix, Dennison *et al.* 2012). Experimental modifications which either increase charge (e.g. to AamAP1 from *Androctonus amoerux*) (Almaaytah, Tarazi *et al.* 2014) or decrease charge (e.g. to ToAP2 from *Tityus pachyuru*) (Guilhelmelli, Vilela *et al.* 2016) support this hypothesis.

Both Smp24 and Smp43 exhibit broad-spectrum antimicrobial activity against a wide range of Gram positive and Gram negative bacteria and fungi. Smp43 (MIC 4 - 64 μg/ml) was found to have slight higher activity than Smp24 (MIC 4 - 256 μg/ml). Smp24 has a net charge of +3 with four lysine residues 4 in comparison to Smp43 which has a net charge +4 with seven lysines and greater positive. The greater positive charge on Smp43 might reflect the relative antimicrobial potency of the two peptides.

Smp24 and Smp43 both possess higher activity against Gram positive (MIC 32-256 μg /ml) than Gram negative bacteria (MIC 8-64 μg/ml). Such preferential activity has also been reported for Pin1 and Pin2 which displayed up to twenty times more potent activity against some Gram positive than Gram negative strains (Corzo, Escoubas *et al.* 2001) as well as other AMPs from *P. imperator* (Zeng, Zhou *et al.* 2013) and from *Heterometrus petersii* (Li, Xu *et al.* 2014). The bacterial selectivity of some AMPs

depends on the presence and distribution of abundant negatively charged phospholipids in the bacterial membranes where the phospholipid composition of Gram -negative membranes such *E. coli* is less anionic than Gram positive membranes *S. aureus* and *B. subtilis* which contain higher amounts of negatively charged phospholipids PG (Epand, Savage *et al*. 2007,McHenry, Sciacca *et al*. 2012, Aoki, Ueda 2013). Asymmetric lipid distribution has been reported in bacterial membranes, as neutral phospholipids as PE are located in the inner leaflet, while, PG is distributed in the outer leaflet. Whilst, CL is distributed over both leaflets in plasma membranes in Gram positive bacteria. Such membrane asymmetry is known to affect various bilayer properties, including binding affinity to AMPs (Barsukov, Kulikov *et al*. 1976, Marquardt, Geier *et al*. 2015).

Smp43 showed very low haemolytic activity at the highest concentration of 512µg/ml. While Smp24 exhibited highly haemolytic effect at the same concentration. Smp24 shares 54% homology with Pin 2, while Smp43 sharing 86% identity with Pin 1 (Harrison, Abdel-Rahman *et al*. 2016). Pin2 has high haemolytic activity is similar to that of Smp24, and Pin1 is similar to Smp43 have less or no haemolytic activity even at high concentrations (Corzo, Escoubas *et al*. 2001). The haemolytic activity of Pin1 depends on the Zwitterionic phospholipids (PC) and sphingomyelin (SM) ratio; it displayed higher haemolytic activity against guinea pig erythrocytes than sheep erythrocytes, which have less ratio of PC/SM. Therefore, Smp43 may show much higher haemolytic activity against other mammal erythrocytes such as human blood cells (rich in PC) than sheep cells (rich in SM) (Belokoneva, Villegas *et al*. 2003).

Both peptides induced cytotoxic effects on HEK293 cells in a concentration-dependent manner with a decrease in cell viability seen at 32 μg/ml with both peptides. Smp43 showed limited cytotoxic effect against keratinocyte HaCaT cell line at a highest concentration of 256 μg/ml, while, Smp24 showed significant decrease HaCaT cells viability at 128 μg/ml. Our previous work has indicated that both Smp24 and Smp43 have cytotoxic effects on HepG2 liver cells in a concentration-dependent manner (Harrison, Abdel-Rahman *et al*. 2016). These results have been attributed to the overall negative charge on extracellular face of both cancer and prokaryotic cell membranes due to the presence of negatively charged phospholipids on the outer leaflet of prokaryotic membranes and the exposure of intracellular PS on the outer leaflet of cancer cell membrane as apoptotic signal (Riedl, Rinner *et al*. 2011). However, the electrostatic affinity of AMPs to anionic membranes is less important toward neutral eukaryotic membranes (Harrison, Abdel-Rahman *et al*. 2016) Hydrophobicity of Smp peptides (more than 60%) may has a stronger influence in terms of mammalian cell toxicity. Thus, a strong correlation is reported between cytotoxicity and hydrophobicity, as hydrophobic residues of AMPs enhance their interaction with hydrophobic core of membrane (Chen, Guarnieri *et al*. 2007, Bahar, Ren 2013)

In conclusion, Smp24 and Smp43 are relatively short non-disulphide bridged peptides with a spectrum of potent activity against a wide range of Gram positive and Gram negative bacteria. There was a clear difference in the cytotoxicity of Smp43 when compared to Smp24. Smp43 showed very low haemolytic and cytotoxic activities at the maximum concentration tested against sheep red blood cells and HaCaT cells, in contrast, Smp24 caused significant erythrocyte disruption and cytotoxic effects on

HaCaT cells at the same concentration. However, both peptides were cytotoxic toward HEK293 cells.

In the current study, four proteins (NH3/4-4, WG4-2, WG4-3 and NN2/3-3) have been isolated from three Egyptian elapid venoms *Naja haje* (Egyptian cobra), *Walterinnesia aegyptia* (Black Desert Cobra) and *Naja nubiae* (nubian spitting cobra). The purified proteins displayed preferential activity against *B. subtilis.* It has been reported that *B. subtilis* exhibited high susceptibility toward crude elapid venoms such as *N. melanoleuca* (African cobra) and *N. atra* (Chinese cobra). In comparison, *E. coli* and *S. aureus* are much more resistant to these venoms (Dubovskii, Utkin 2014).

Our results appear consistent with the findings of Ovadia and colleagues that has demonstrated the preferential activity of a cytotoxin (CT P4) isolated from *Naja nigricollis* toward *B. subtilis* and *Micrococcus flavus* with no apparent antimicrobial activities against Gram negative bacteria and fungi (Mollmann, Gutsche *et al.* 1997). Unfortunately, the amino acid sequence of this toxin has not been reported.

B. subtilis is one of the most commonly isolated bacteria from the oral cavity, oropharynx and cloaca of diverse snakes (Shek, Tsui *et al.* 2009, Jho, Park *et al.* 2011, Babalola, Balogun 2013). In addition, *B. subtilis* has the most anionic membrane compared with *S. aureus* and *E. coli* membranes. *B. subtilis* contain higher amounts of PG distributed in the outer leaflet of their membrane (Clejan, Krulwich *et al.* 1986, Epand, Savage *et al.* 2007, Epand, Epand 2009). This suggests that the membrane-damaging activity of elapid peptides that have been purified are dependant on the presence of anionic phospholipids in the outer leaflet of the bilayer.

The cytotoxic effects of the purified proteins have been evaluated against different eukaryotic cells. All purified proteins showed no haemolytic activity at the highest concentration 50 µg/ml. Whereas, the ATP assay has demonstrated that the purified protein from *N. haje* venom (NH3/4-4) exhibited less cytotoxic effect against both tested cell lines (HaCaT and HEK293) at the highest concentration 50 µg/ml, but both WG4-2 and NN2/3-3 showed cytotoxic effect against HEK293 cell line in a concentration-dependent manner.

Few enzymatic peptides with antimicrobial activities derived from snake venoms such as cathelicidins , myotoxins and waprins (Nair, Fry *et al.* 2007, Wang, Hong *et al.* 2008, Oguiura, Boni-Mitake *et al.* 2011, Yamane, Bizerra *et al.* 2013). Other snake venom cytotoxic peptides such as three-finger toxins (3FTxs) (~60 amino acids) might contribute to the snake venom antibacterial activities profile although very few studies have explored this potential (Dubovskii, Utkin 2014).

The molecular masses of the purified proteins and N-terminal sequences suggests that they are members of the 3FTxs family. NH3/4-4 is identical to the N-terminal sequence short neurotoxin2 of *N. haje* (Joubert 1975), *N. nivea* (Botes 1971) and *N. annulifera* (Joubert, Taljaard 1978). WG4-2 and WG4-3 have the same N-terminal sequence as the cardiotoxins CTX- M1 and M2 of *N. mossambica* (OTTING, STEINMETZ *et al.* 1987, Chien, Chiang *et al.* 1994) and CTX-1 of *N. nigricollis* (Rees, Bilwes *et al.* 1990, Bilwes, Rees *et al.* 1994). Only two cytotoxins have been reported for *N. nigricollis* are toxin γ (Bilwes, Rees *et al.* 1994) and toxin α (Zinn-Justin, Roumestand *et al.* 1992). Interestingly, the first five amino acids of the N-terminal end of toxin γ were found to

share 100% identity with the N- terminal of both purified proteins from *W. aegyptia* venom WG4-2 and WG4-3 (Bilwes, Rees *et al.* 1994). Conversely, a newer study (Chen, Kao *et al.* 2011) showed that toxin γ have a prominent antibacterial activity against both *E. coli* and *S. aureus* through *a* permeabilising effect of the toxin as evidenced from fluorescent dye leakage studies (Chen, Kao *et al.* 2011). The common LCK sequence of the peptides isolated in this chapter, unique among many cardiotoxins of the *Naja* genus (Chen, Rose *et al.* 1991, Dubovskii, Lesovoy *et al.* 2003).

The most dominant protein components of elapid venoms are 3FTxs. 3FTxs constitutes half the contents of the *Naja* venoms (Dufton, Hider 1988, Chen, Rose *et al.* 1991). Only two 3FTxs proteins (Wa-III; 6852 Da and Wa-IV; 6782 Da) have been previously identified in *W. aegyptia* (Samejima, Aoki-Tomomatsu *et al.* 1997, Tsai, Wang *et al.* 2008). Both Wa-III and Wa-IV are similar in size to WG4-2 and WG4-3. However, WG4-2 and WG4-3 have completely different N-terminal sequences compared with Wa-III and Wa-IV, suggests these proteins represent novel additions to the *W. aegyptia* 3FTx family. Although abundant 3FTxs have been isolated from other Naja species like *N. naja*, the potential short chain 3FTxs (NN2/3-3) from *N. nubiae* venom may represent the first member of the 3FTxs family from this snake.

The majority of cardiotoxins have a potent haemolytic activity such as CTX1 (Gorai, Sivaraman 2016) and CTX3 (Troiano, Gould *et al.* 2006, Kao, Lin *et al.* 2010). The haemolytic activity of the snake peptides is consistent with results of various studies showing that some the cytotoxins have no haemolytic effect for example, Beta-

cardiotoxin CTX27 from *Ophiophagus hannah* (King cobra) venom (Rajagopalan, Pung *et al.* 2007).

Although no previous data have investigated the cytotoxic effect of cardiotoxins on HaCaT and HEK293 cell lines, it has been reported that only P-type cardiotoxin can bind to zwitterionic membranes (Sue, Rajan *et al.* 1997). The analysis of the structure of various 3FTxs revealed that, loop I and II of 3FTxs are rich in cationic residues while loop III is the hydrophobic surface (Girish, Kumar *et al.* 2012). Thus, P-type cardiotoxins (Pro30 residue at the tip of the second loop) have binding activity more strongly to zwitterionic membranes than S-type toxins (have serine residue) as P-type use the tips of all three loops in the penetration while S-type inserts via the tip of the loop I only (Chien, Chiang *et al.* 1994, Efremov, Volynsky *et al.* 2002).

The findings of the interactions of the purified proteins with eukaryotic cell lines suggest that both WG4-2 and NN2/3-3 appear to belong to P-type CTs as they able to induce membrane disruption of kidney cell lines. These findings are consistent with Chien *et al.*, (1994) that have demonstrated that P-type cardiotoxin s such as CTX M1, M4 and M5 which have similar N- terminal sequence to both WG4-2 and WG4-3 have higher affinity to zwitterionic membranes (Louw 1974, Chien, Chiang *et al.* 1994). The full-length sequences of purified proteins are needed in order to classify it as S-type or P-type cardiotoxins.

Our findings indicate that NH3/4-4, WG4-3, WG4-2 and NN2/3-3 proteins have antimicrobial properties with limited or no cytotoxic potential. Further studies are needed to complete sequencing of these proteins and to investigate their mode of

action with more details. These isolated 3FTxs may serve as starting templates for designing novel synthetic AMPs with enhanced antimicrobial activities and valuable therapeutic effect.

4 A morphological study of the effects of Smp24 and Smp43 on *Escherichia coli* and *Staphylococcus aureus* using scanning and transmission electron microscopes.

4.1 Introduction

Imaging the action of antimicrobial peptides on living bacterial cells can provide novel Insights in to the mechanism of AMP action. Different spectroscopic techniques such as fluorescence microscopy, AFM and electron microscopes have been used to demonstrate morphological changes of living cells treated with AMPs (Anderson, Haverkamp *et al.* 2004, Meincken, Holroyd *et al.* 2005, Torrent, Sánchez-Chardi *et al.* 2010, Scheinpflug, Krylova *et al.* 2015).

Fluorescence microscopy provides more detailed information about AMP-bacterial membrane interactions. It can analyse and determine the distribution and target of AMPs intracellularly or extracellularly by detecting and localising attached fluorescent probes (Scheinpflug, Krylova *et al.* 2015). The interaction of fluorescently labelled melittin K14 with PC vesicle and with *E. coli* revealed insignificant pore formation in live bacteria, compared with the artificial membrane system. According to (Gee, Burton *et al.* 2013) a new model is needed to explain peptide-membrane interactions in live bacterial cells, as they discovered the complexity of lipid-peptide interactions in living cells when compared with simple artificial systems.

Scanning and transmission electron microscopes were applied in several studies to visualise the ultrastructural damage and morphological changes to the bacterial cell envelope induced by AMPs. SEM and TEM are can be used as complementary techniques to gain insights into AMP mechanism of action when combined with other findings (Matsuzaki, Sugishita *et al.* 1997, Matsuzaki, Sugishita *et al.* 1999, Avitabile, D'Andrea *et al.* 2014).

Blebs or blister formation on microbial surfaces are a common effect for AMPs. Blister-like formations in the outer membrane of Gram negative bacteria might be attributed to the electrostatic interaction of cationic AMPs with LPS by displacing cations from their binding sites on LPS promoting the uptake of peptides across the outer membrane (Zhang, Dhillon *et al.* 2000, Grubor, Meyerholz *et al.* 2006). The appearance of abundant blebs has been previously reported on the surface of *Pseudomonas aeruginosa* strains treated with cathelicidin peptide SMAP29 as examined by SEM (Saiman, Tabibi *et al.* 2001a). LPS-binding studies of full-length and truncated SMAP-29 molecules revealed that presence of multiple binding sites in the peptide allow binding LPS with high affinity (Tack, Sawai *et al.* 2002). This affinity to LPS has been confirmed by assessing the ability of SMAP29 to displace the fluorescent dansyl polymyxin B (DPX) bound to LPS (Anderson, Yu 2005a).

The surface roughening and corrugating of cell membrane have also been identified following exposure to several AMPs of a wide range of bacterial cells examined by EM techniques. These observations demonstrated loss of membrane integrity and the release of cellular contents following treatment with the peptides leading to cell lysis and death (Lv *et al.*, 2014, Wang *et al.*, 2015).

EM also has been used successfully to monitor the action of some labelled AMPs on live bacteria in order to clarify their antimicrobial action. Nanogold-labelled sushi peptide has been tracked on *E. coli*. Gold particles were found on the inner and outer membranes, as well as in the periplasmic space and cytoplasm, while no particles were observed bound to the bacteria for controls with nanogold alone. The distribution of these particles has been quantified, the majority of nanogold (77%) was found attached to the exterior leaflet of the outer membrane. These results suggest that the

local environment at the bacterial outer surface is necessary for sushi peptide attachment to penetrate the membrane and enter the cell (Leptihn, Har *et al.* 2009). These observations were consistent with imaging of sushi peptide-treated *E. coli* and *P. aeruginosa* with AFM (Li, Lee *et al.* 2007).

Understanding the mode of action of broad spectrum Smp peptides against live bacterial cells will help to increase their potency and minimise their cytotoxic effects. Previously, AFM and quartz crystal microbalance-dissipation (QCM-D) have been used to study Smp peptides mechanisms on synthetic prototypical prokaryotic membranes. The results indicated that these peptides caused pore formation and induced the formation of non-lamellar lipid structures (Harrison, Heath *et al.* 2016). The interactions of AMPs against living cell membranes might be different and more complicated compared with simple artificial membranes (Gee, Burton *et al.* 2013). The interactions of Smp peptides with the membranes of live bacteria have not been clearly investigated. Therefore, one the goals of this current study is to examine concentration- and time-dependent effects of Smp peptides on intact *E. coli* and *S. aureus* cells using SEM and TEM.

4.2 Method Summary

Both SEM and TEM were employed to examine morphological changes and membrane damage in *E. coli* and *S. aureus* strains in response to different concentrations of Smp peptides treatment across arange of time intervals. The overnight cultures of *E. coli* JM109 and *S. aureus* SH1000 were diluted in fresh MH Broth to a cell density $1x10^6$ CFU/ml then incubated at 37°C to grow to OD_{600}=0.3 (mid-exponential growth phase). Bacterial cells were treated with different concentrations of either Smp24 or Smp43 for different time intervals (10 minutes, 1 hour, and 24 hours) at 37°C. Then samples were prepared for SEM and TEM as described in sections 2.12 and 2.13 and then visualised.

4.3 Results

4.3.1 Determination of Smp peptides concentrations used for SEM sample preparation

Since a high cell density is needed to observe EM images. *E. coli* JM109 and *S. aureus* SH1000 were grown to mid-exponential phase then treated with Smp peptides at different concentrations for three time intervals (10 minutes, 1 hour, and 24 hours) to examine concentration- and time-dependent effects of Smp peptides on intact *E. coli* and *S. aureus* cells using SEM.

The inintial peptide concentration range that was used to evaluate inhibitory concentrations in the conditions required for SEM imaging was based on those found in section 2.4. Due to differences in volume and cell densities in these experiments, new inhibitory concentrations were defined (Figure 4.1 and Figure 4.2).

Therefore, three concentrations of each peptide; sub-MIC (one-quarter), MIC and supra-MIC (4x) against *E. coli* and *S. aureus* were selected for growth curves comparing Smp peptide exposed cultures with untreated cells (Table 4.1).

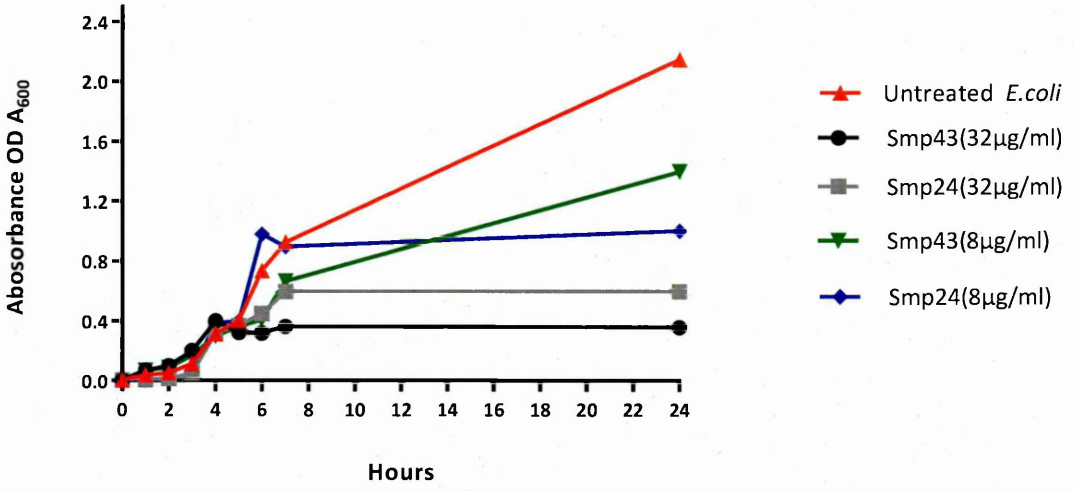

Figure 4.1 Growth of *E. coli*. Treatment with Smp24 and Smp43, at the MIC (32 µg/ml) and one -quarter (8 µg/ml) of the MIC concentrations.

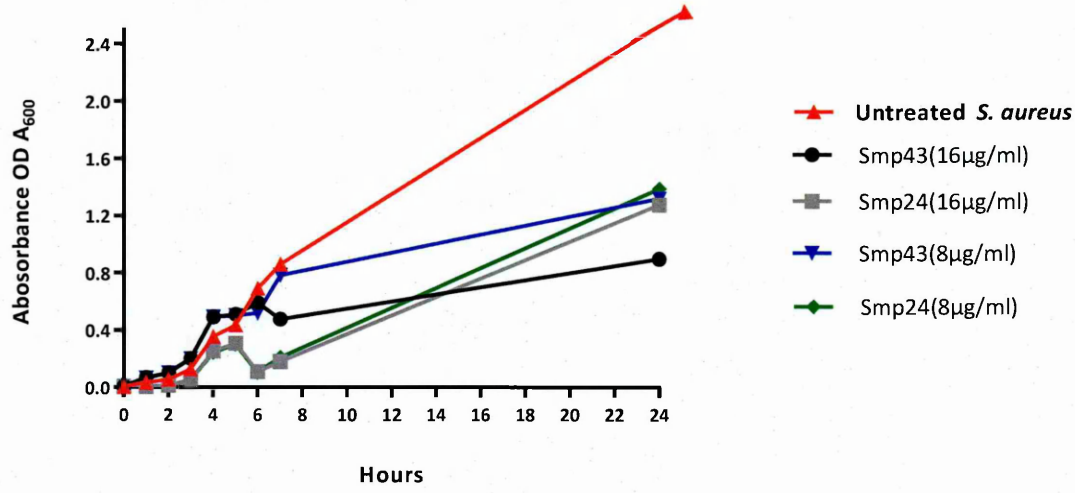

Figure 4.2 Growth of *S.aureus*. Treatment with Smp24 and Smp43 at the MIC (16 µg/ml) and one -quarter (4 µg/ml) of the MIC concentrations.

Table 4.1 Peptide concentrations used for SEM sample preparation

Bacteria	Concentrations (µg/ml)		
	Sub- MIC (1/4x)	MIC	Supra -MIC (4x)
E. coli	8	32	128
S. aureus	4	16	64

4.3.2 SEM of *E. coli* and *S. aureus* incubated with Smp peptides for 10 minutes

Untreated *E. coli and S. aureus* cells showed normal bright smooth intact surfaces (Figure 4.3A and Figure 4.4 A). *E. coli* cells developed surface protrusions of numerous small nubs and blister like structures (indicated with red arrows) after incubation with concentration of Smp24 below the MIC and at the MIC concentrations for 10 minutes (Figure 4.3B and D). In comparison, *E. coli* cells appeared very rough, corrugated (marked by orange arrow) and shrunken when treated by equivalent concentrations of Smp43 (Figure 4.3C and E).

Distortions of the morphology of *E. coli* were observed in many treated cells at greater than MIC concentrations of both peptides with depressions and fractures on their surfaces. Numerous cells look corrugated as indicated by the orange arrows (Figure 4.3F and G).

Following exposure for the same period of time, the sub-MIC concentrations of either peptide resulted in the appearance of bacterial membrane blebs in *S. aureus* cells (Figure 4.4 B and C). MIC and supra-MIC concentrations induced little cell membrane damage with accumulation of cell debris at this period of time (Figure 4.4 D- G).

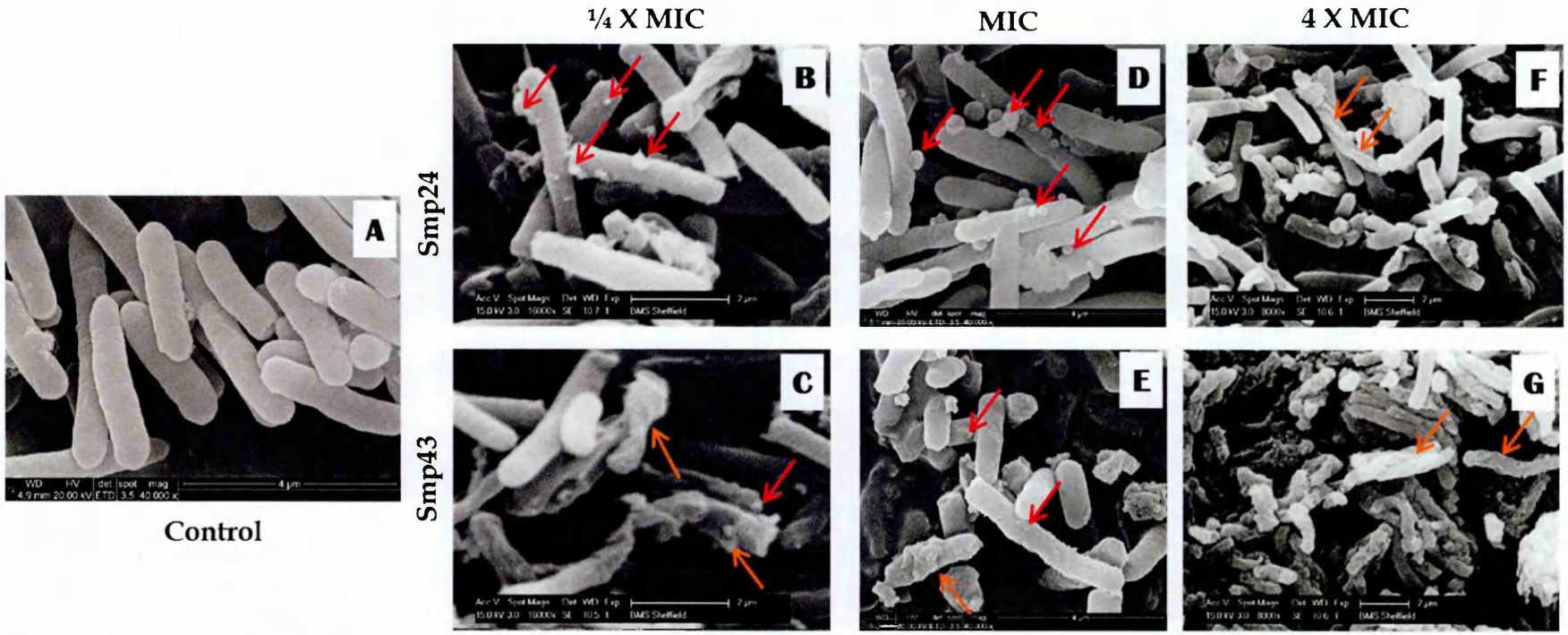

Figure 4.3 Scanning electron microscope images taken of *E. coli* cells treated with Smp24 and Smp43 for 10 minutes. (A) control, (B) at a sub-MIC of Smp24, (C) at a sub-MIC of Smp43, (D) at a MIC of Smp24, (E) at a MIC of Smp43, (F) at a supra- MIC of Smp24 and (G) at a supea-MIC of Smp43. The red arrows point to blebbings and blisterike structures or protrusions on the cell surfaces. The orange arrows indicate cells with corrugated surfaces. Images shown are representative of twenty images from three replicates.

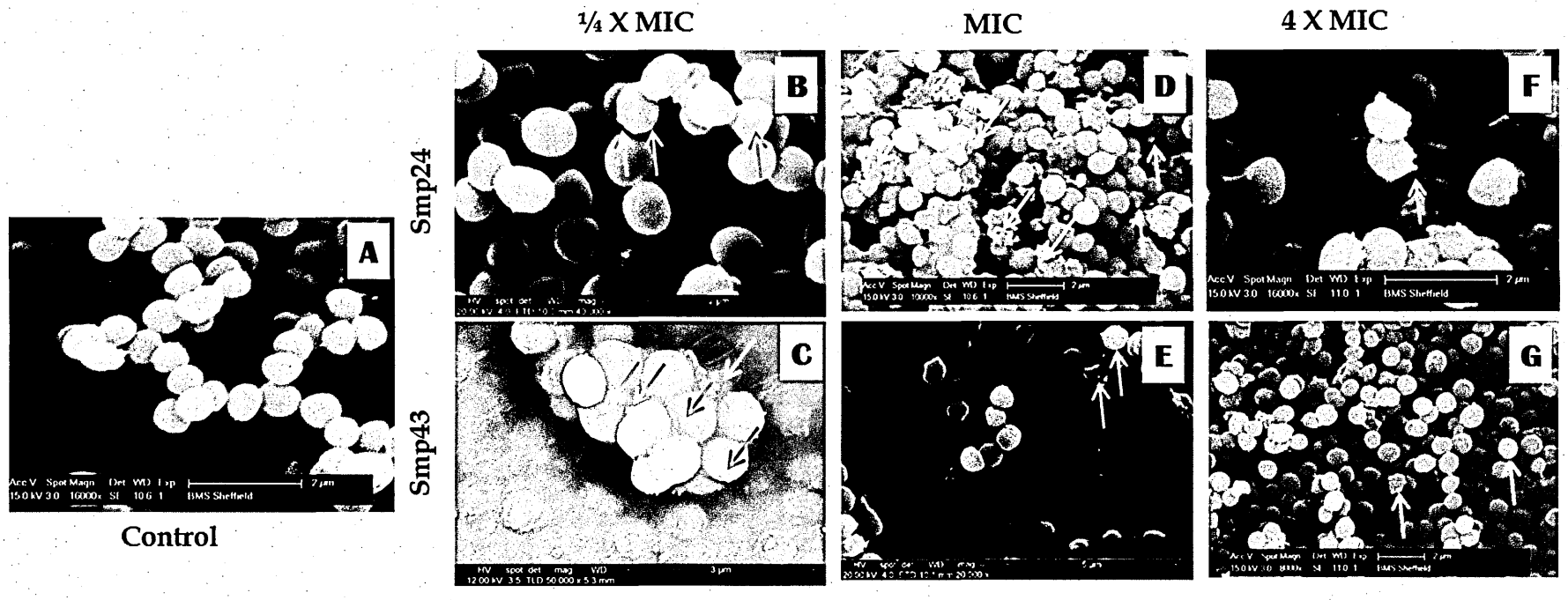

Figure 4.4 Scanning electron microscope images taken of *S. aureus* cells treated with Smp24 and Smp43 for 10 minutes. (A) control, (B) at a sub-MIC of Smp24, (C) at a sub-MIC of Smp43, (D) at a MIC of Smp24, (E) at a MIC of Smp43, (F) at a supra-MIC of Smp24 and (G) at a supra-MIC of Smp43. The red arrows point to blebbings and blisterike structures or protrusions on the cell surfaces. The yellow arrows indicate completely lysed cells. Images shown are representative of twenty images from three replicates.

4.3.3 SEM of *E. coli* and *S. aureus* incubated with Smp peptides for 1 hour

After 1 of hour incubation, most *E. coli* cells treated with sub-MIC concentrations of Smp24 showed obvious consistent with roughening and corrugating membrane damage, it also revealed few ruptured cells (Figure 4.5B). In comparison, damage of Smp43 treated cells at the same concentration was less evident; although most cells maintained intact cell structures, a few showed surface corrugated patterns and ruptured membranes (Figure 4.5C).

Many damaged *E. coli* cells were seen with more blebbing and corrugated surfaces following treatment of either peptide at MIC concentrations (Figure 4.5D and E). Panels F and G in Figure 4.5 showed many distinguishable lysed *E. coli* cells treated with supra-MIC concentrations of either Smp24 or Smp43.

After treatment of *S. aureus* with either Smp24 or Smp43 for 1 hour, completely lysed cells accompanied with the intracellular material extrusion were observed in a concentration dependent manner, as nearly no intact cells were seen in *S. aureus* cells exposed to Supra-MICs of both peptides (Figure 4.6F and G). The damage is indicated by yellow arrows showed the complete loss of membrane integrity.

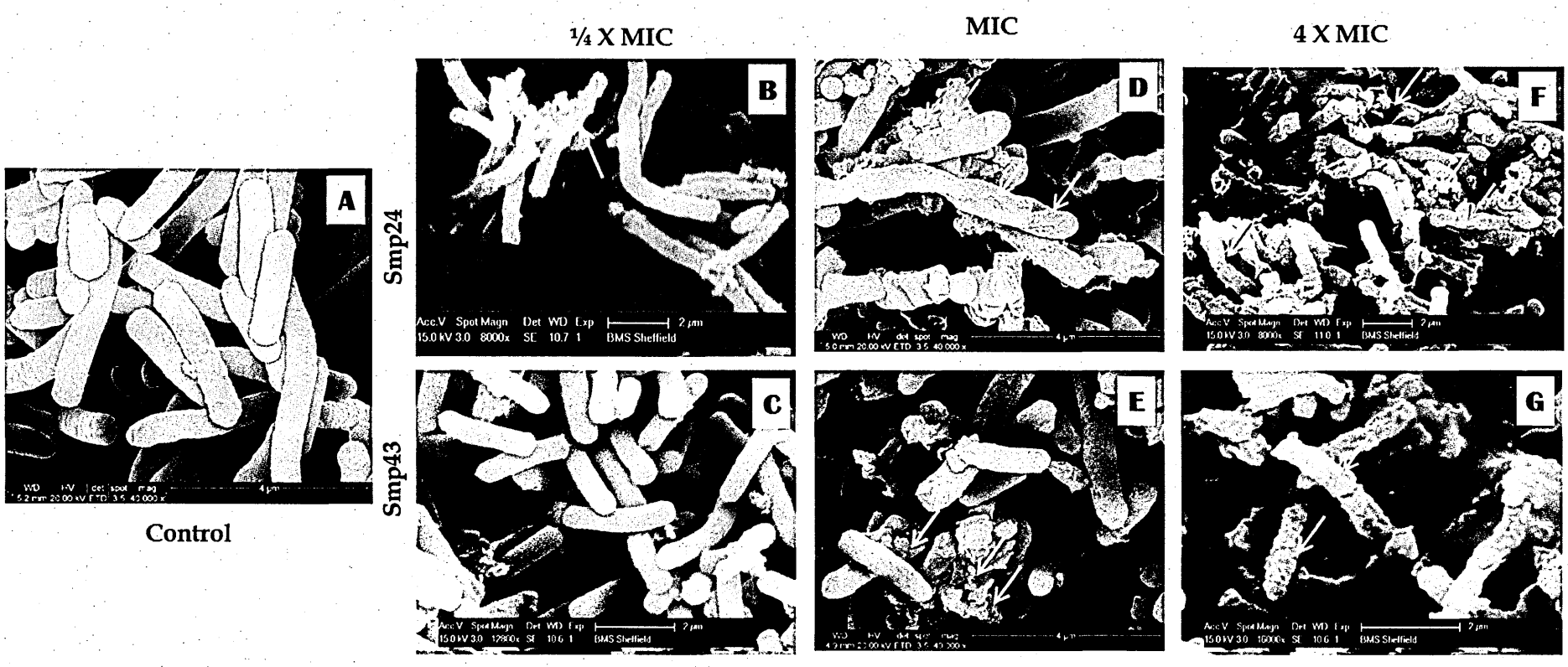

Figure 4.5 Scanning electron microscope images taken of *E. coli* cells treated with Smp24 and Smp43 for 1 hour. (A) control, (B) at a sub-MIC of Smp24, (C) at a sub-MIC of Smp43, (D) at a MIC of Smp24, (E) at a MIC of Smp43, (F) at a supra-MIC of Smp24 and (G) at a supra-MIC of Smp43. The red arrows point to blebbings and blisterike structures or protrusions on the cell surfaces. The orange arrows indicate cells with corrugated surfaces. The yellow arrows indicate ruptured and completely lysed cells. Images shown are representative of twenty images from three replicates.

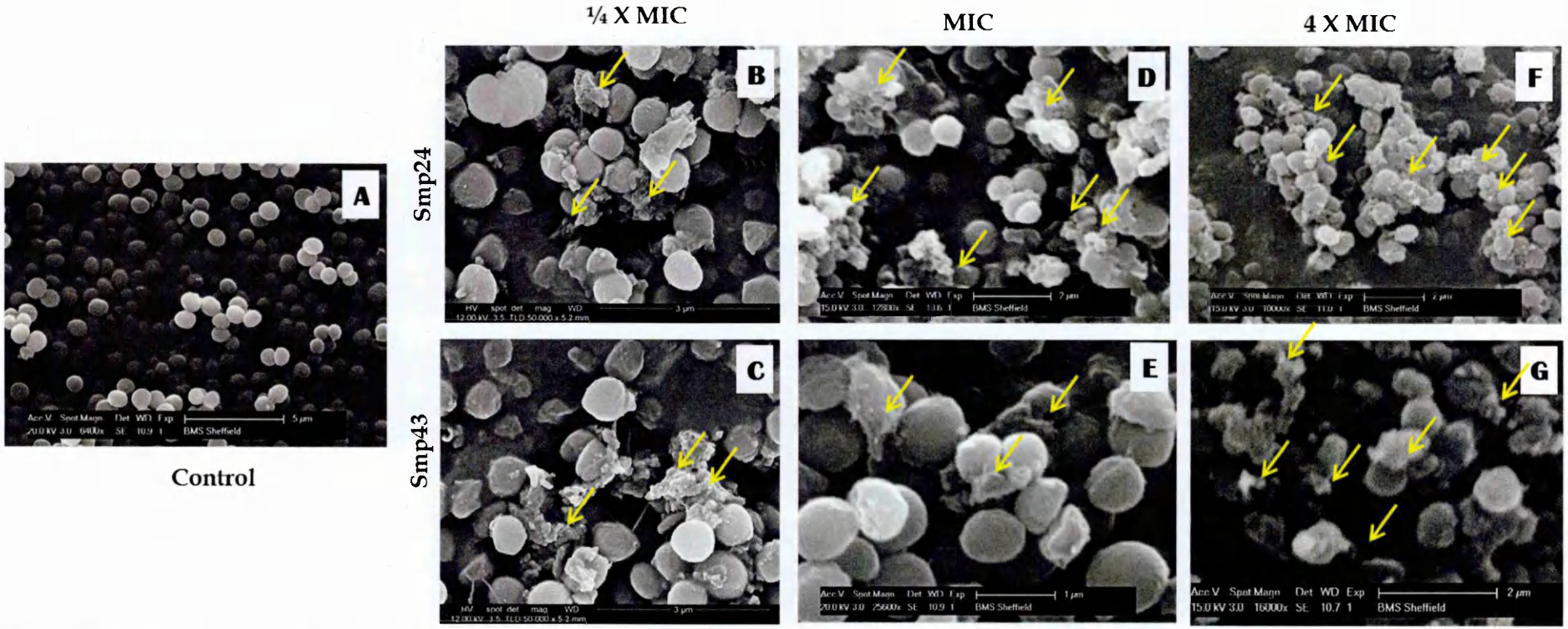

Figure 4.6 Scanning electron microscope images taken of *S. aureus* cells treated with Smp24 and Smp43 for 1 hour. (A) control, (B) at a sub-MIC of Smp24, (C) at a sub-MIC of Smp43, (D) at a MIC of Smp24, (E) at a MIC of Smp43, (F) at a supra-MIC of Smp24 and (G) at a supra-MIC of Smp43. The yellow arrows indicate the ruptured and completely lysed cells. Images shown are representative of twenty images from three replicates.

4.3.4 SEM of *E. coli* and *S. aureus* incubated with Smp peptides for 24 hours

After 24 hours of incubation with concentrations of Smp peptides below the MIC and at the MIC, a small number of *E. coli* cells were shrunken and have corrugated surfaces (Figure 4.7B - E). Also, some blebs were seen on the surface of a few *S. aureus* treated cells at the same concentrations (Figure 4.8E). No cells were harvested after 24 hours of Smp peptides treatments at supra-MIC concentrations which induce cell death and led to cell lysis.

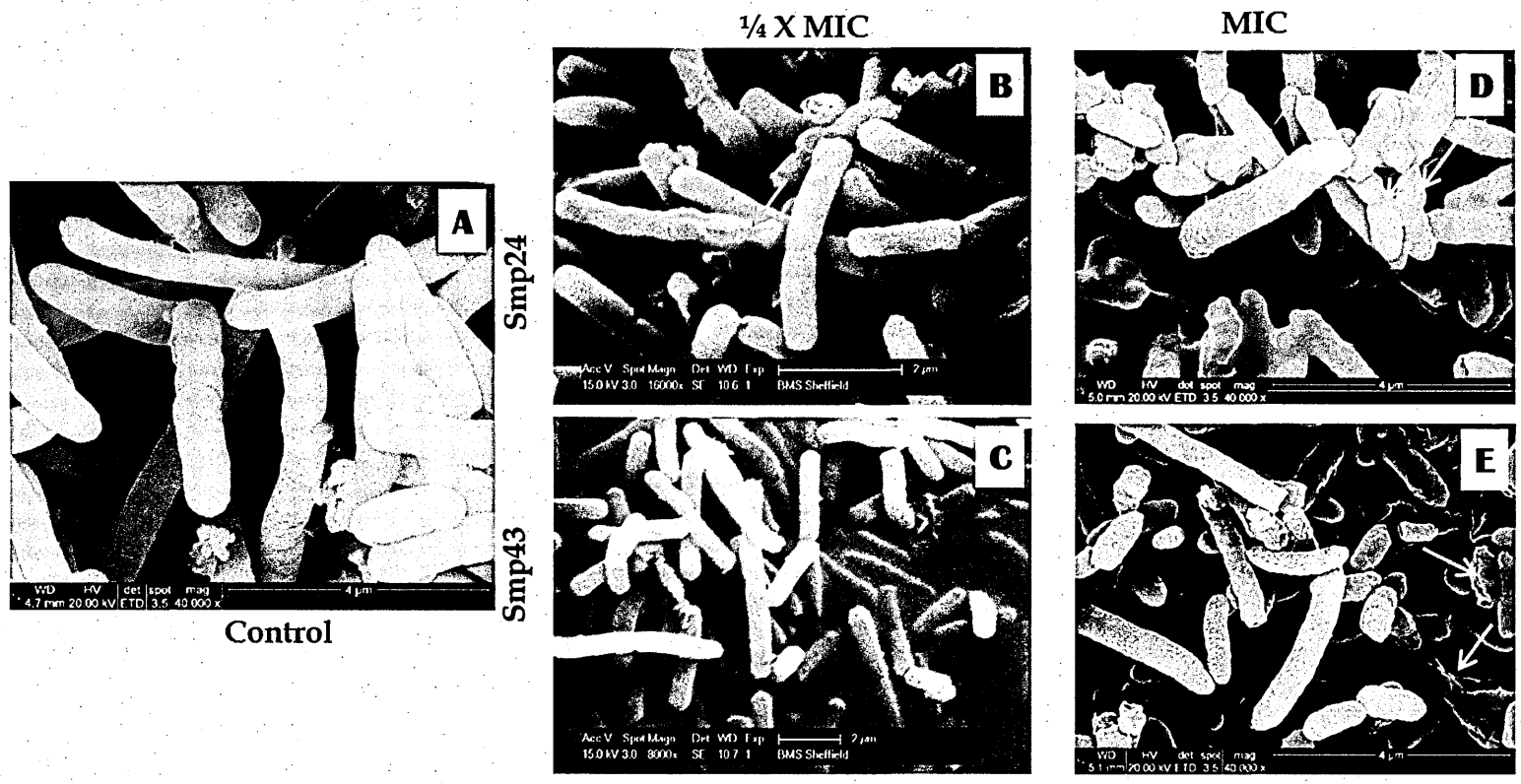

Figure 4.7 Scanning electron microscope images taken of *E. coli* cells treated with Smp24 and Smp43 for 24 hours. (A) control, (B) at a sub-MIC of Smp24, (C) at a sub-MIC of Smp43, (D) at a MIC of Smp24 and (E) at a MIC of Smp43. The orange arrows indicate cells with corrugated surfaces. Images shown are representative of twenty images from three replicates.

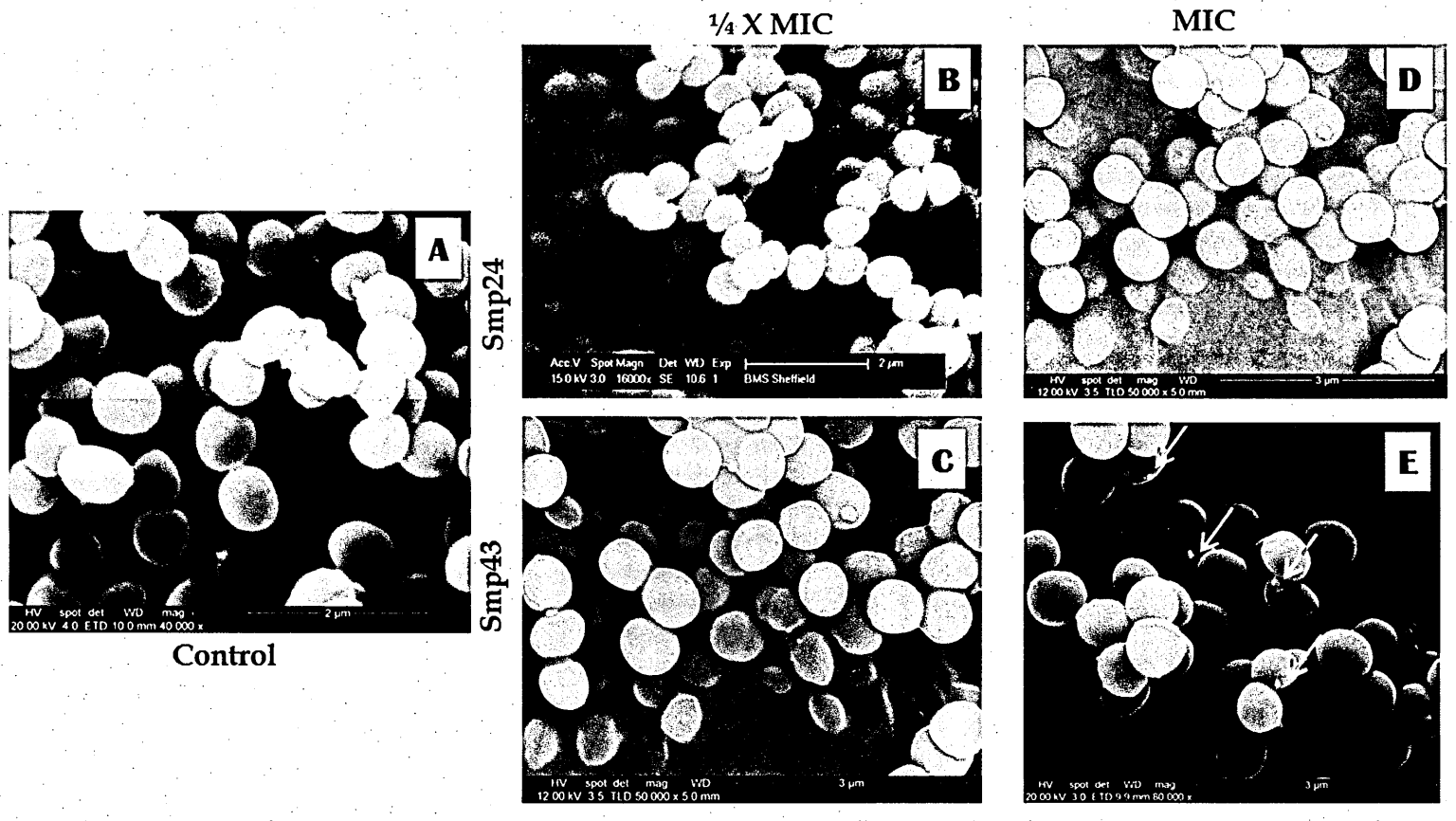

Figure 4.8 Scanning electron microscope images taken of *S. aureus* cells treated with Smp24 and Smp43 for 24 hours. (A) control, (B) at a sub-MIC of Smp24, (C) at a sub-MIC of Smp43, (D) at a MIC of Smp24 and (E) at a MIC of Smp43. The red arrows point to blebbings and blisterike structures or protrusions on the cell surfaces. Images shown are representative of twenty images from three replicates.

4.3.5 TEM images of *E. coli* and *S. aureus* incubated with sub- MICs of Smp24 and Smp43

To investigate the morphological changes of bacterial cells, TEM was employed to study the membrane integrity of bacterial cells before and after treatment with Smp peptides. *E .coli* and *S. aureus* cells were treated with sub-MICs of Smp24 or Smp43 for 10 minutes, 1 hour, and 24 hours. The samples were fixed and cut into thin sections. For each treatment duplicate samples were prepared and numerous sections were cut from each.

As shown in Figure 4.9 (panels A and B) and Figure 4.10 (panels A and B), the untreated *E.coli and S. aureus* cells were all uniformly shaped, with an undamaged structure and intact cell envelops. While after 10 minutes of incubation with both peptides, many treated *E. coli* cells showed morphological changes as cells without cell envelops and cells with separated cell surface components. In some cases the cytoplasmic contents had leaked out of the cells and exhibited obvious cytoplasmic clear zones as indicated by blue arrows in panels C and D. Some leakage of cellular material was seen after the exposure of *S. aureus* cells to Smp peptides for 10 minutes of incubation as shown in Figure 4.10 C and D

The majority of the treated cells appeared severely morphologically affected after 1 hour of incubation. They exhibited completely damaged membranes and cellular content spillage. Disrupted membranes were observed for *E. coli* cells being treated with Smp24 for 1 hour (Figure 4.9 E and F). Formation of ghost cells which have intact cell envelopes without cellular contents were visualised after 10 minutes and 1 hour and indicated by green arrows. It was obvious that *S. aureus* cells underwent lysis after

1 hour of incubation with SMP peptides as they exhibited damaged and ruptured envelops with released cellular contents (Figure 4.10 E and F).

After 24 hours of incubation, a regular cell shape was seen. A small number of *E. coli* cells showed morphological changes such as roughened membranes, zones of translucent cytoplasm and separation of outer membrane and cytoplasmic membrane (Figure 4.9 G and H). Also, the majority of the cells were indistinguishable from untreated cells. However, some zones of transparent cytoplasm were evident as seen in Figure 4.10 (panels G and H).

In conclusion, TEM images showed significant morphology changes as result of the exposure of bacterial cells to Smp peptides at sub-MICS up to 1 hour of incubation.

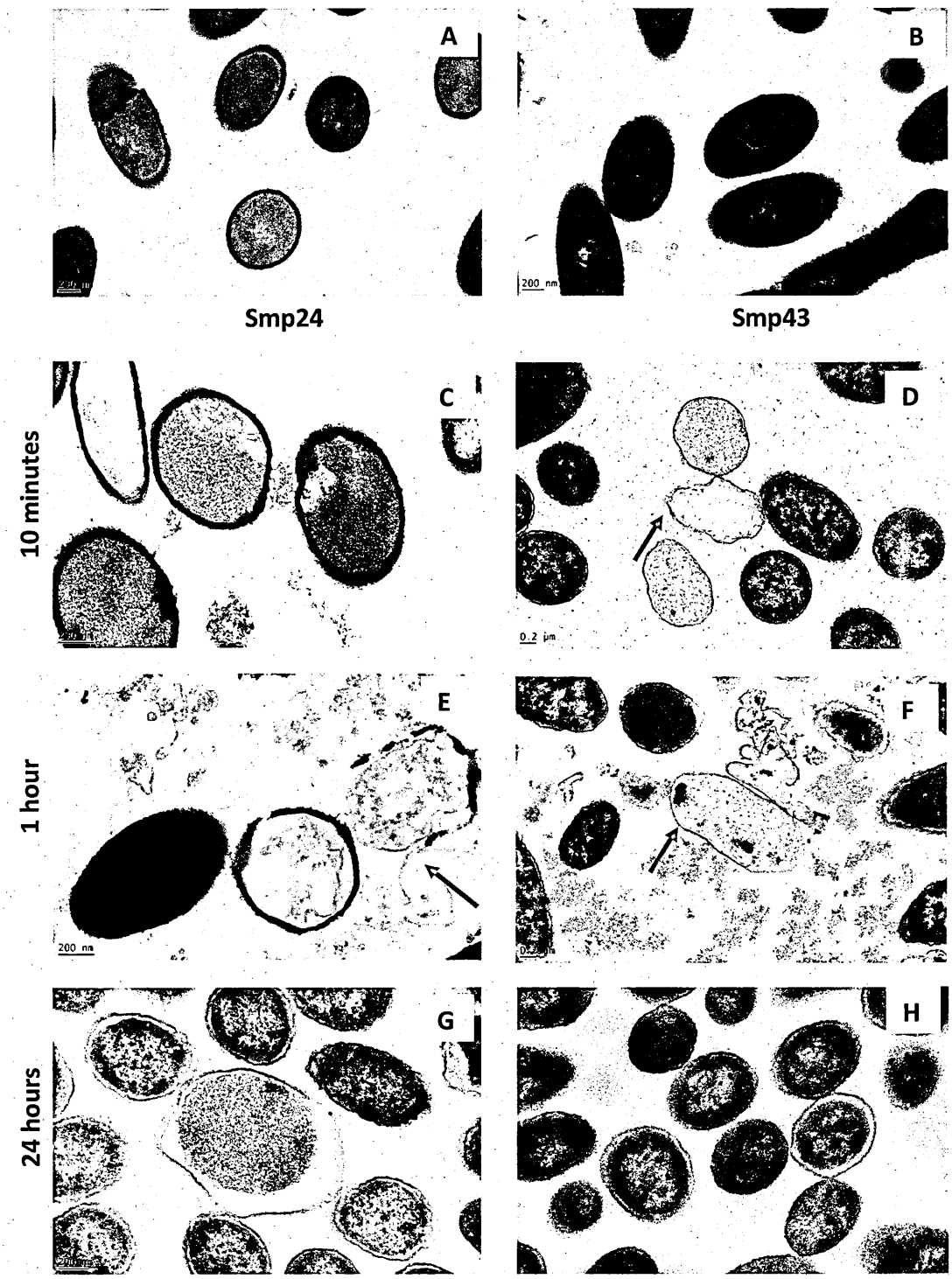

Figure 4.9 Transmission electron microscope images taken of *E. coli* JM109 cells incubated with Smp peptides at sub-MIC for different time intervals. Cells were cultured at 37 °C to mid-log phase before treatment. (A) Untreated cells after 10 minutes; (B) Untreated cells after 1 hour; (C) Smp24-treated cells for 10 minutes; (D) Smp43-treated cells for 10 minutes; (E) Smp24-treated cells for 1 hour; (F) Smp43-treated cells for 1 hour; (G) Smp24-treated cells for 24 hours; (H) Smp43-treated cells 24 hours. The green arrows point to ghost cells that are not surrounded by a cell wall. Images shown are representative of twenty images from three replicates.

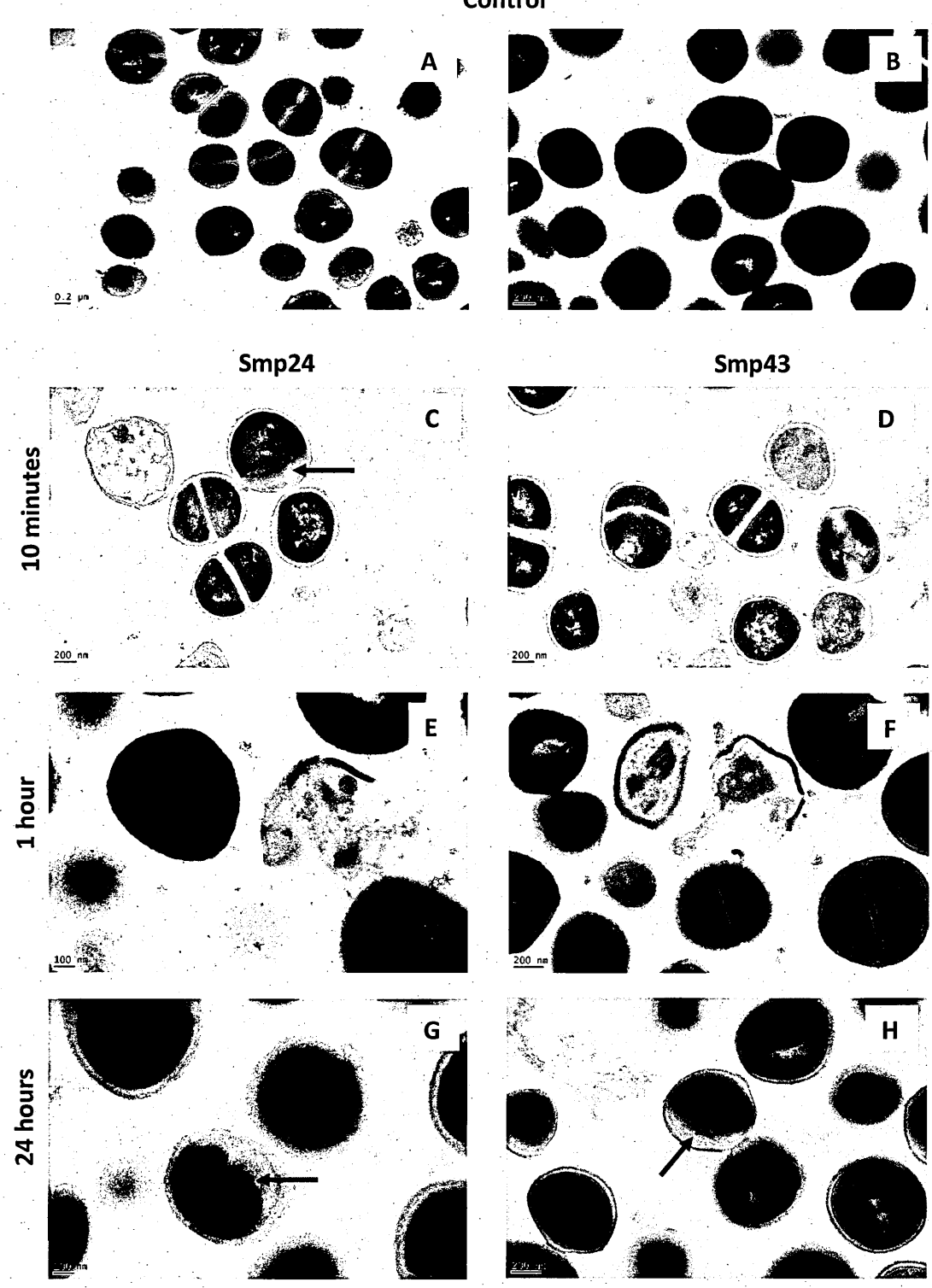

Figure 4.10 Transmission electron microscope images taken of *S. aureus* SH1000 cells incubated with Smp peptides at sub-MIC for different time intervals. Cells were cultured at 37 °C to mid-log phase before treatment: (A) Untreated cells after 10 minutes; (B) Untreated cells after 1 hour; (C) Smp24-treated cells for 10 minutes; (D) Smp43-treated cells for 10 minutes; (E) Smp24-treated cells for 1 hour; (F) Smp43-treated cells for 1 hour; (G) Smp24-treated cells for 24 hours; (H) Smp43-treated cells 24 hours. The blue arrows indicate the cytoplasmic clear zones. Images shown are representative of twenty images from three replicates.

4.4 Discussion

Interactions between Smp peptides and synthetic prokaryotic membrane models have been previously investigated using liposome leakage assays, AFM and QCM-D. These data suggested that the bactericidal mechanism of Smp peptides against prokaryotic like membranes is toroidal pore formation (Harrison, Heath *et al.* 2016). While in the current study, we investigated interaction of Smp peptides with live bacterial cells to support our understanding of the antibacterial mechanism of these molecules in order to develop their therapeutic potential as novel antimicrobial agents.

In the current study, SEM was performed on two species of bacteria *E. coli* and *S. aureus,* as representatives of Gram positive and Gram negative bacteria to visualise morphological changes following exposure to Smp peptides at different concentrations and intervals of time to investigate the dose-dependent and time-dependent interactions of Smp peptides against *E. coli* and *S. aureus.*

Formation of blebs was evident for the two species of bacteria at sub-MIC and MIC concentrations after 10 minutes of incubation. Our SEM observations provide morphological evidence of the potent permeabilising activity of Smp peptides at MIC and supra-MIC concentrations after 1 hour of treatment. The treated cells were obviously roughened and disrupted when treated with the peptide. Also, they exhibited changes to their morphology such as shortening and membrane corrugating.

In addition to SEM, TEM was employed to study the morphological and intracellular changes of *E. coli* and *S. aureus* following treatment with Smp peptides at sub-MIC concentrations after 10 minutes, 1 hour and 24 hours of incubations. Sub-inhibitory concentrations of numerous antimicrobial agents were commonly used to evaluate

the morphological and ultrastructural changes following antimicrobials challenge using TEM (Haukland, Ulvatne *et al*. 2001, Chen, Zhan *et al*. 2009, Wenzel, Chiriac *et al*. 2014). Our TEM images of these cells treated with sub-MICs concentrations of both Smp peptides confirm the interaction of the peptides with the bacterial membranes causing significant rupture and leakage of cytoplasm contents which lead to cell death. Apparent morphological changes were seen in the Smp treated cells such as cytoplasmic clear cells with intact cell membranes forming ghost cells compared with the control sample which showed regular shapes with homogenous electron density.

Similarly, other cationic AMPs e.g. melittin, magainin, moricin and King cobra venom AMP(OH-CATH) have induced the appearance of blebs and blisters like protusions after a few minutes of treatment at the Sub-MICs concentrations (Skerlavaj, Benincasa *et al*. 1999, Saiman, Tabibi *et al*. 2001b, Mangoni, Papo *et al*. 2004, Chen, Zhan *et al*. 2009, Hu, Wang *et al*. 2013). Blebbing appears on the bacterial cell surface as a result of expansion of the outer membrane due to the antibacterial activity of AMP peptides (Hancock, Rozek 2002). Moreover, formation of blebs and blisters may be indicative of the electrostatic interactions of Smp or other cationic AMPs such as LfcinB (bovine AMP) with the anionic bacterial cell membrane. It has been suggested that interactions include displacement of divalent cations (Ca^{2+}, Mg^{2+}) of the outer bacterial membrane by the large peptides and that this results in blebs formation (Hancock, Rozek 2002, Grubor, Meyerholz *et al*. 2006). Blebbing formation has also been attributed to detachment of cytoskeleton from the cell membrane causing the latter to swell (Omardien, Brul *et al*. 2016).

When the attached AMP aggregated on the bacterial surface at a high enough concentration, permeabilisation of the cell membrane is induced leading to cell death

(Chan, Prenner *et al.* 2006b). The permeabilisation effect of AMPs may also be confirmed by the electrostatic interactions between basic residues of the AMP and the negatively charged phospholipids of the bacteria membranes (Matsuzaki, Sugishita *et al.* 1997). The 24-residue AMP GI24; a derivative of PMAP-36, interacts with anionic phospholipids to induce membrane permeabilisiation. Also, the bee venom AMP melittin destabilise bacterial cell membranes by binding the anionic phospholipids inducing cell lysis (Oren, Shai 1997). The SEM examination of Melittin- and GI24 treated *E. coli* revealed the roughening and corrugating of the membrane surface at the MIC after 1 hour of incubation which is similar to Smp peptide effect against *E. coli* at the MIC after the same period of time (Lv, Wang *et al.* 2014, Wang, Chou *et al.* 2015).

The attraction to phospholipids is one of the most frequently proposed mechanisms for α-helical peptides, permeablisation of the bacterial membrane causing cell death (Shai 1999). Both Smp peptides are positively charged; net charge of Smp24 is +3 and Smp43 is +4. The positive net charge of the AMPs enhances their attraction to phospholipids.

These findings are consistent with the previous AFM micrographs of Smp peptides against synthetic prokaryotic membrane models which identified the importance of the electrostatic attraction of Smp peptides to negatively charged bilayers for induction of membrane damage (Harrison, Heath *et al.* 2016). The same topography of permeabilisation has been reported in several AFM and SEM studies of different species of bacteria treated by AMPs. For instance, the AFM and EM analyses of the 21 residue lugworm AMP arenicin interacts with *E .coli* revealed a similar effect on

bacterial membranes as we have observed with Smp peptides (Andra, Jakovkin *et al.* 2008).

Smp peptides have more than 60% hydrophobic residues in their amino acids sequences. The hydrophobic interactions of AMPs and the lipid constituents of the bacterial membranes have been proposed to lead to membrane destabilization. This interpretation is in full agreement of the proposed mechanism of several AMPs such as the 26-residue amphipathic α-helical AMP $V13K_L$ (Chen, Guarnieri *et al.* 2007). Interestingly, in the latter study they found that there is an optimum hydrophobicity in which maximum antibacterial activity of $V13K_L$. Any alteration of this hydrophobicity decreases its antimicrobial effect (Chen, Guarnieri *et al.* 2007).

Both hydrostatic and hydrophobic interactions of AMPs with the bacterial membranes are necessary for the antibacterial action of AMPs (Shai 1999). Similarly, the mechanism of action of magainins on bacterial cells determined against Gram negative bacteria can be summarised in two main steps; interaction with anionic lipopolysaccharides and then aggregation to form pores (Hancock, Rozek 2002, Grubor, Meyerholz *et al.* 2006). According to (Saiman, Tabibi *et al.* 2001b), bacteria are unlikely to develop a resistance for peptides with this mode of action. AMPs act non-specifically on the entire bacterial membrane (Park, Park *et al.* 2011). Development of microbial resistance by changing conserved targets such as the cell membrane or by gene mutation to such mechanism of action is difficult requiring significant alteration to the physiology of the cell (Zasloff 2002, Matsuzaki 2009, Aoki, Ueda 2013).

Similar micrographs of ghost cells formation have been reported in TEM studies of bacterial cells treated with some cationic AMPs such as TEM studies of *E. coli* treated with a variety of AMPs (Chapple, Mason *et al.* 1998, Anderson, Haverkamp *et al.* 2004,

Chen, Zhan *et al.* 2009, Makobongo, Gancz *et al.* 2012) . The formation of ghost cells suggest that cationic AMPs induce the formation of pores which were more evident at the 1-hour time point of Smp24 treated *E. coli*. It seems to be a general mechanism for cationic AMPs which form transmembrane pores when the peptides inserted into the lipid constituents of the bacterial membranes (Sengupta, Leontiadou *et al.* 2008, Makobongo, Gancz *et al.* 2012, Bahar, Ren 2013, Chen, Jia *et al.* 2013).

In addition, some extracellular electron-dense materials and sloughing of cell walls from some cells have been visualised using TEM following the exposure to sub-MIC concentrations of Smp peptides after 10 and 60 minutes. Similarly, the TEM micrographs of AMPs such as RRIKA, NK-2 against different species of bacteria revealed the same observations (Hammer, Brauser *et al.* 2010, Mohamed, Hammac *et al.* 2014). These findings support the permeabilisation effect of cationic AMPs against bacterial cells (Hartmann, Berditsch *et al.* 2010).

The highly disintegrated membranes of Smp peptide treated bacteria may increase the influx of water into the cytoplasm which induces cytoplasmic membrane rupture leading to a discharge of cytoplasmic materials. The cytolysis effect of Smp peptides was seen for supra-MICs concentrations as many *E. coli* lysed cells with cytoplasmic contents release and debris have been observed even after 10 minutes of incubation. Similarly, the high concentrations of other cationic AMPs; GS and PGLa lead to membrane damage and cell content leakage resulting in cell death (Hartmann, Berditsch *et al.* 2010).

However, the majority of *E. coli* and *S. aureus* of the mid-exponential growth phases exposed to sub-MIC and MIC concentrations of Smp peptides showed no prominent morphological changes after 24 hours of incubation (Figure 4.7-8). They showed

normal cell shape with an undamaged structure of their membranes and homogenous electron-dense materials. Very few cells revealed morphological changes in the form of roughened membranes and blisters on their surfaces at the MIC of Smp peptides. These results revealed that sub-MIC and MIC concentrations as determined by broth microdilution of Smp peptides were insufficient for allowing the peptide binding and interaction with all of *E. coli* and *S. aureus* cells at the mid-exponential growth phase, unbound viable bacterial cells continuously grew and the peptide effect declined after longer exposure for 24 hours (Pacor, Giangaspero *et al.* 2002). These findings demonstrate the dose–dependent manner of Smp peptides against bacterial membranes.

Some Smp24 treated *E. coli* at the MIC concentration revealed electron-dense materials inside the cells when examined using TEM similar to the reported effects of waterfowl cathelicidin peptide dCATH (Gao, Xing *et al.* 2015) and $C_{12}K\text{-}2\beta_{12}$ against *E. coli* suggesting the aggregation of biological macromolecules.

In conclusion, both SEM and TEM are influential imaging techniques that allow us to gain insights into AMP action. Our findings of EM micrographs indicated that Smp peptides and bacterial interactions might take place in a stepwise fashion including peptide binding and insertion into bacterial membranes which lead to membrane permeabilisation and cytoplasmic contents leakage even at low concentrations. Firstly, the amphipathic properties of Smp peptides could help peptides to interact with the negatively charged bacterial membrane hydrostatically by binding to positively charged amino acid residues and embedded in the non-polar components of the bacterial membrane by the hydrophobic residues. Then, the embedded peptides aggregate and reach a threshold concentration which induces the membrane

permeability to from pores or rupture the bacterial membrane. Finally, the contents of the cells were released inducing cell death.

5 Transcriptomic profiling of *Escherichia coli* following exposure to Smp24 and Smp43.

5.1 Introduction

Bacteria have evolved mechanisms to recognise and respond to AMPs by differentially expressing genes as a response to stress or as a unique resistance mechanism against each AMP (Brazas, Hancock 2005, Fehri, Sirand-Pugnet *et al.* 2005, Pietiäinen, Gardemeister *et al.* 2005). The differentially expressed genes of bacteria in response to different types of stress and treatment has been widely investigated using DNA microarray in order to identify and characterise the biological processes and pathways most affected (Overhage, Bains *et al.* 2008, Monrás, Collao *et al.* 2014).

High-density gene detection techniques like DNA microarrays can facilitate the prediction of the mode of action of antibiotics. For instance, microarray analysis has been used to investigate the mechanisms of increased activity of a combination of two antibiotics; Fosfomycin and tobramycin (F:T) against *P. aeruginosa* compared with tobramycin alone under anaerobic conditions (McCaughey, McKevitt *et al.* 2012). It was found that nitrate reductase genes *narG* and *narH* were down regulated significantly in response to growth in F:T under anaerobic conditions. Interestingly, nitrate reductase mutant strains showed higher sensitivity to F:T in anaerobic conditions compared with an aerobic environment which confirm the role of *nar* genes in inducing increased activity of F:T against *P. aeruginosa* as revealed by microarray analysis (McCaughey, Gilpin *et al.* 2013).

Bacterial resistance mechanisms to antibiotics can also be investigated using microarray. Bang-Ce Ye and colleagues (Yu, Yin *et al.* 2012) have investigated and identified the differentially expressed genes and pathways induced by fusaricidin against *Bacillus subtilis* by DNA microarray technique. They revealed that the most

upregulated genes are known to be regulated by σ^{w}extracytoplasmic function sigma factor which indicate that this regulon may play an important role in *B. subtilis* resistance to fusaricidin. Also, fusaricidin addition has led to an increase in the catabolism of fatty and amino acids and the loss of some intracellular ions that induce cation transport into the cell which may point to the mode of action of fusaricidin against *B. subtilis*. These findings indicate that a microarray-based approach allows for a more comprehensive analysis of bacterial responses to antibiotics.

DNA microarray has been used to provide insights into the mode of action of AMPs and AMP-resistance mechanisms to understand how bacteria respond to AMPs. *E. coli, S. aureus*, and *B. subtilis* have often been used as models to study the mechanism of action of AMPs as the complete genome of these bacteria have been sequenced (Yu, Yin *et al.* 2012, Suzuki, Horinouchi *et al.* 2014, Kramer, van Hijum *et al.* 2006, Li, Lai *et al.* 2007). For instance, the responses of *S. aureus*, following exposure to some linear cationic AMPs, such as temporin L, dermaseptin K4-S4 (1-16) and ovispirin-1 were analysed by DNA microarray. These AMPs share some upregulated genes with cells treated by cell wall-inhibition antibiotics such as vancomycin. The functional clustering analysis of gene groups induced by these peptides displayed some specific pathways implicated in the resistance mechanism of *S. aureus.* In particular, an ABC transporter encoded by the *vraDE* regulon was induced strongly by ovispirin-1 and dermaseptin K4-S4 (1-16) (Pietiäinen, François *et al.* 2009). Gene expression patterns of *E. coli* were analysed using DNA microarray in response to different antimicrobial peptides derived from human and animal resources (Audrain, Ferrieres *et al.* 2013). This study concluded that the sublethal doses an AMP derived from human apolipoprotein E

induced some distinct pathways that contribute to cell wall stress resistance (Audrain, Ferrieres *et al*. 2013).

Smp peptides offer a promising starting point for the development of new antimicrobial agents and transcriptomic analysis can help identify metabolic processes affected by AMPs which may be beneficial in understanding their mechanism of action. The main objective of this chapter is to identify differentially expressed genes following exposure of *E. coli* to Smp24 and Smp43 as a model for pathogenic Gram negative bacteria. A genome-wide phenotypic profiling of Smp peptide sensitivity in the KEIO collection strains of *E. coli* single gene knockout mutants was carried out to address the effect of deletion of some highly differentially expressed genes identified by microarray.

5.2 Method Summary

Bacteria were cultured overnight at 37˚C in Muller Hinton broth, MICs and subinhibitory concentrations were determined by serial microdilution methods. Total RNA was extracted, then assessed for its concentration, purity and integrity. RNA was labelled with Cyanine 3-CTP (Cy3) dye and the complimentary RNA (cRNA) was amplified and Cy3 specific activity was quantified. The labelled cRNA was loaded onto a gasket slide and assembled on the microarray slide, which contains 8 x 15K whole *E. coli K12* oligo arrays. After hybridization, slides were disassembled, and then scanned using an Agilent C Microarray Scanner (Agilent, Wokingham, UK). All samples were tested in duplicate on each of two separate arrays We analysed the changes in gene expression of *E. coli* to sub-inhibitory doses of the Smp24 and Smp43 peptides and polymyxin B as a positive control using Agilent GeneSpring GX software (version 13.1). In order to identify genes that affect the susceptibility of *E. coli* to Smp peptides, the Keio collection of knockout mutants of differentially regulated genes were screened against Smp24 and Smp43. TaqMan RT-PCR primers were used as a reference to evaluate the accuracy of expression from microarray in three experiments for four genes identified through keio collection screening (two upregulated genes, *fepA* and *fiu* and two down regulated genes, *fdnG* and *proB).*

5.3 Results

5.3.1 Determination of subinhibitory concentrations

In order to study gene expression patterns in response to Smp peptides, *E. coli* cells were exposed to subinhibitory concentrations of tested peptides. Subinhibitory concentrations stimulate bacterial adaptation to different stresses, including antimicrobial effects. These concentrations affect cellular physiology and genetic expression profiles which can assist in the identification of the mode of action of Smp peptides.

Killing curves were performed to identify subinhibitory concentrations of Smp24, Smp43 and Polymyxin B against *E. coli.* Subinhibitory concentrations were determined as concentrations that induce a measurable stress response without totally inhibiting the growth of *E. coli* over four to five hour time periods when compared with untreated cells. Subinhibitory Smp peptide concentrations ranged from a concentration of zero to the MIC. It was observed that the growth of *E. coli* was reduced at Smp24, Smp43, and Polymyxin B concentrations of 12, 7 and 0.18 µg/ml respectively (Figure 5.1).

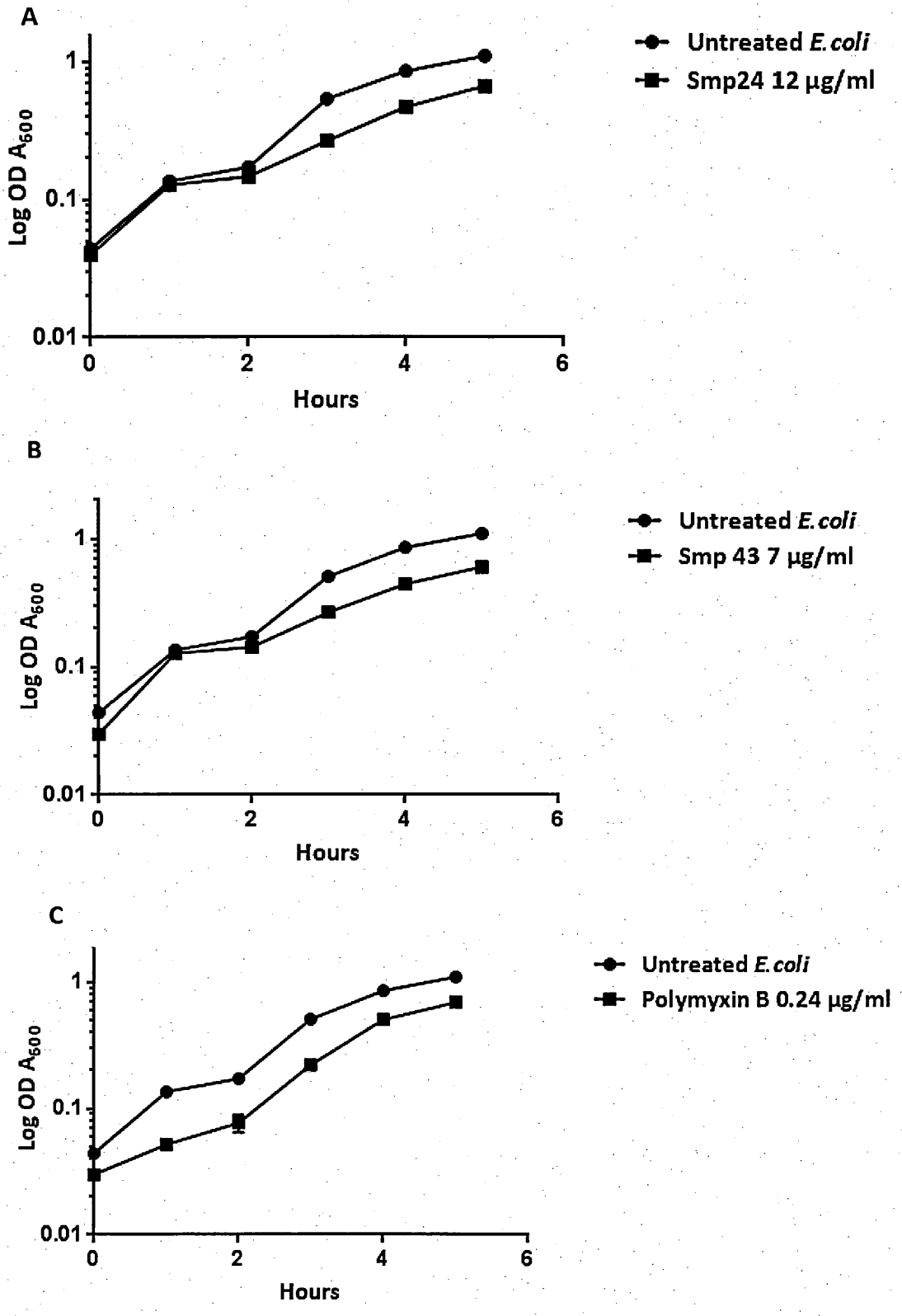

Figure 5.1 Growth of *E. coli* K12. Treatment with Smp24 at concentration of 12 µg/ml (A), Smp43 7 µg/ml (B) and Polymyxyin B 0.24 µg/ml (C).

5.3.2 Pre-microarray analysis quality control

Before carrying out the microarray experiment, the quality and purity of the extracted RNA samples were assessed by the NanoDrop spectrophotometer (Figure 5.2) then confirmed by the Agilent 2100 Bioanalyzer (Figure **5.3**). All the tested samples were of a highly pure and un-degraded RNA. The QC reports of the Agilent Feature Extraction Software showed a good quality hybridisation represented by the level and distribution of the detected signals (Figure **5.4**), and the Spike-In Linearity Plot reflects the accuracy and reproducibility of the probes signals (Figure 5.5).

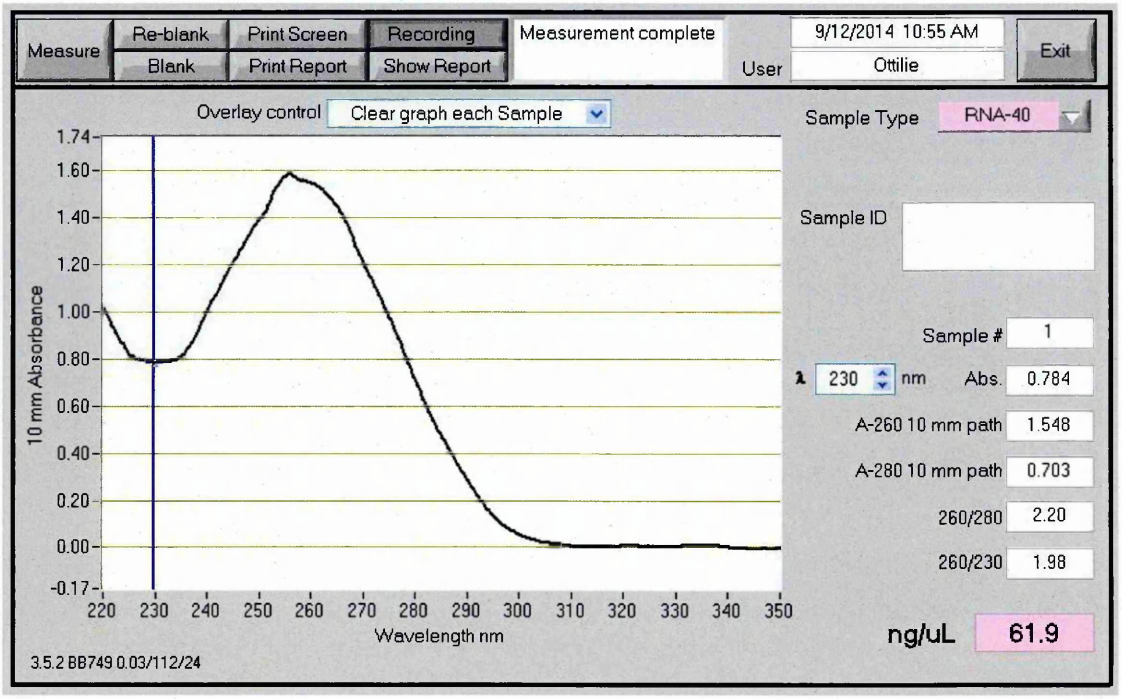

Figure 5.2 Nanodrop spectrophotometer analysis for RNA extracted from *E. coli* untreated at 260 nm. The concentration is shown is 61.9 ng/µl. 260/280 ratio is 2.2 and 260/230 ratio is 1.98.

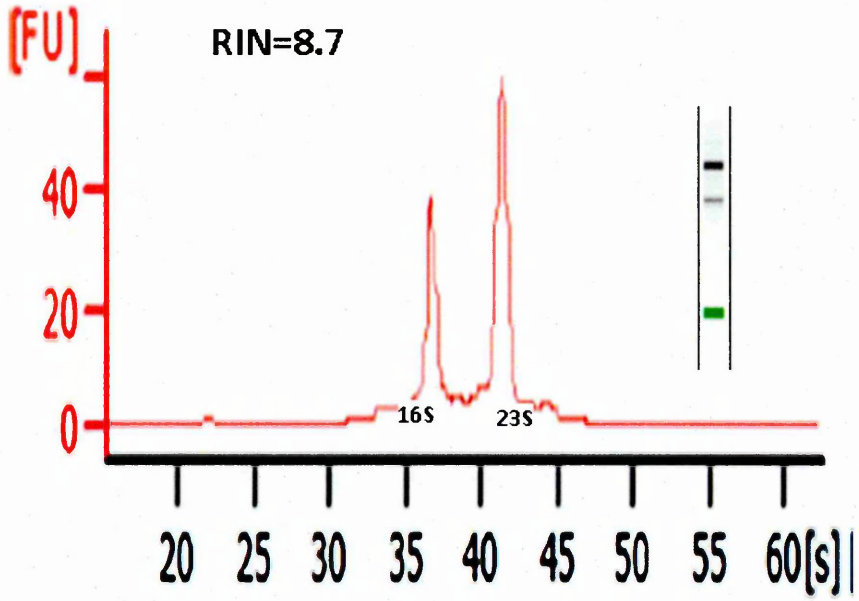

Figure 5.3 Representative electropherogram for total RNA sample using the Agilent Bioanalyzer of *E. coli* untreated. The electropherogram peaks include 16S rRNA (16S), and 23S rRNA (23S). Peak intensities are shown as fluorescence units (FU). (Inset: Instrument software generated 'virtual gel 'pattern). The RIN value is indicated.

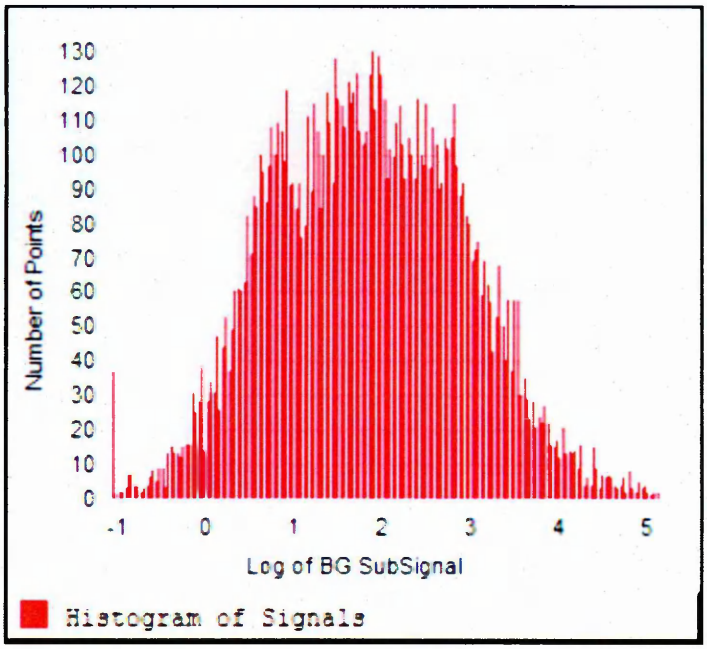

Figure 5.4 Representative histogram of microarray signal plot of *E. coli* treated with a sub lethal dose of Smp43. Following subtraction of the background intensity, FE software plots the number of spots against the log of the processed signal to create a Histogram of Signals Plot. A bell-shape confirms a normal distribution of the (Cy3) signals intensity across the array.

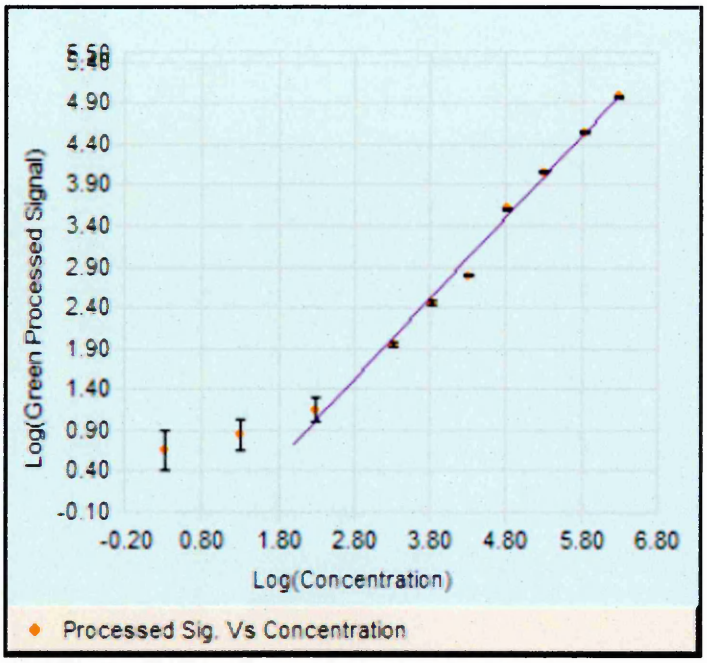

Figure 5.5 Representative Agilent Spike-In QC Report of *E.coli* treated by sub lethal dose of Smp43. Log (Signal) versus Log (Relative Concentration) Plot. Spike-in Linearity Plot shows the linear increase in the detection level from the lowest detection limit up to the optimal saturation point using the detection levels of the serially diluted spike-in internal positive controls. Small error bars occurs when the signal level is close to the saturation point, while more visible error bars indicate that the signal is close to the background noise. FE extracted data are considered reliable when falling within the signal range, while the signal increases linearly with the concentration of the target.

5.3.3 Microarray gene expression analysis

Analysis of raw data started with importing "txt" data files generated by the Feature Extraction software into Agilent GeneSpring software followed by an automatic computing of the 75th percentile-shift normalisation. In order to identify genes that were differentially expressed due to the presence of Smp peptides in *E. coli* three different peptides were used for the transcriptome analysis: Smp24, Smp43 and polymyxin B. Polymyxin B was chosen as a well characterised AMP positive control. Samples for transcriptome analyses were collected from bacterial cultures treated with sublethal concentrations of AMPs and were compared with control samples without peptide treatment. All genes with at least a two-fold change in expression in two independent array experiments with two replicates were recorded (Figure 5.6)

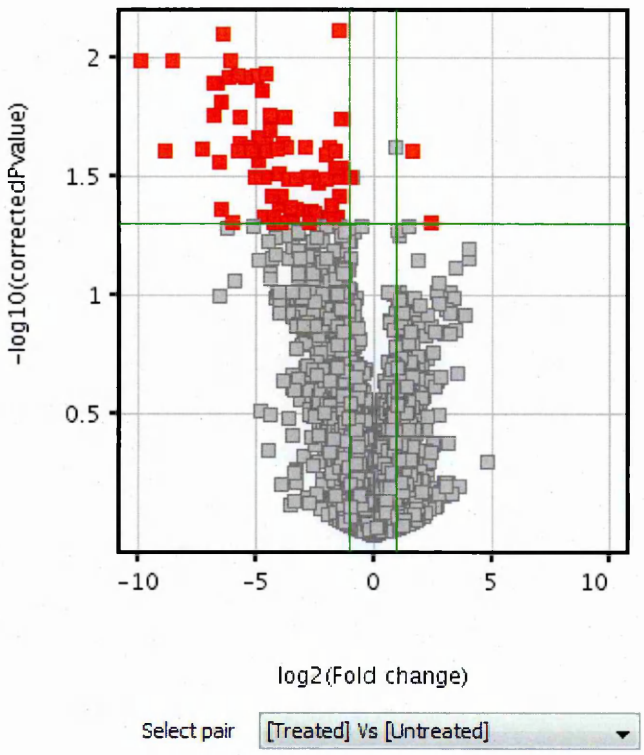

Figure 5.6 Gene expression of *E. coli* treated by a subinhibitory concentration of Smp43. Volcano plot in Genespring13.1 with P-values and intensity ratios (treated versus untreated) as log-scaled axes. Significant differences at $p < 0.05$ with >2-fold intensity ratios are shown. Red dots indicate significantly differentially expressed transcripts; upregulated (right) and down regulated (left).

In total, 313 significantly differentially expressed transcripts were identified, distributed over the three comparisons of each peptide against the inhibitor-free control. Comparing Smp24 treatment with the control revealed 130 differentially expressed transcripts (109 coding for known RefSeq genes), Smp43 induced 84 differentially expressed transcripts (68 known), and polymyxin B induced 99 differentially expressed transcripts (76 known). The 25 most differentially expressed genes for each peptide are listed in Table 5.1. We found that only 2 out of the 313 differentially expressed genes were common among all three treatments, and only 13 genes were common between Smp24 and Smp43 (Figure 5.7). Smp24 and polymyxin B upregulated a large number of genes (48 and 18 respectively) compared with the number of upregulated genes in response to Smp43 where there were only three. Ten upregulated genes were induced commonly by Smp24 and polymyxin B and are listed in Table 5.2. Forty-eight unique upregulated transcripts were identified for Smp24 treatment. While treatments with Smp43 and polymyxin B induced 3 and 18 unique upregulated transcripts respectively (Figure 5.7).

There were also down regulated genes in the transcriptomes. Smp24, Smp43, and polymyxin B decreased the expression of 56, 71 and 81 genes, respectively. There were only two genes down-regulated commonly by all peptides. 13 of 153 genes were commonly down regulated by Smp24 and Smp43 treatment as shown in Table 5.3 Also, Smp43 and polymyxin B share 38 out of 152 down regulated expressed transcripts (25%) are listed in Table 5.4.

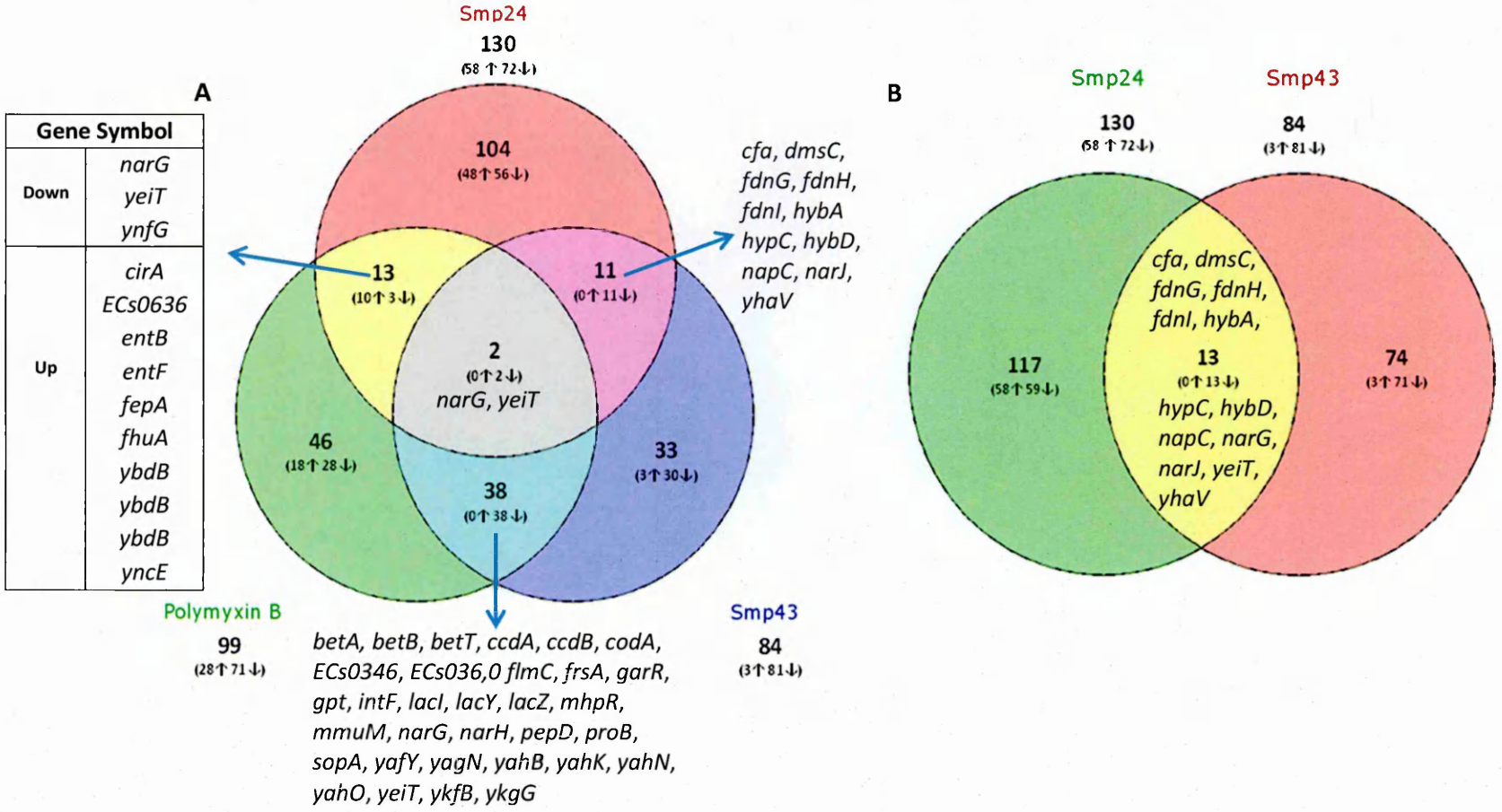

Figure 5.7 The distribution of significantly differentially expressed transcripts. A. The three different treatments, Smp24, Smp43 and Polymyxin B, were assigned and analysed according to untreated *E. coli*. B. The distribution of significantly differentially expressed transcripts between Smp24 and Smp43.

Table 5.1 The most differentially expressed gene lists following exposure to Smp24, Smp43 and Polymyxin

		Gene Symbol	Fold Change	Gene description
Smp24	Upregulated	*cirA*	56	outer membrane receptor for iron-regulated colicin I receptor
		fepA	40	Ferrienterobactin receptor precursor
		fiu	39	putative outer membrane receptor for iron transport3
		fepA	35	outer membrane receptor for ferric enterobactin
		ybiL	33	Probable tonB-dependent receptor ybiL precursor
		entC	33	isochorismate hydroxymutase 2, enterochelin biosynthesis
		ybdB	26	orf, hypothetical protein
		ybdB	23	Hypothetical protein ybdB
		ECs0636	20	hypothetical protein
		entB	19	2,3-dihydro-2,3-dihydroxybenzoate synthetase
		entA	18	2,3-dihydro-2,3-dihydroxybenzoate dehydrogenase
		nrdI	19	orf, hypothetical protein
		entF	17	Enterobactinsynthetase component F
	Down regulated	*narG*	45	nitrate reductase 1, alpha subunit
		narJ	27	nitrate reductase 1, delta subunit, assembly function
		tdcF	24	orf, hypothetical protein
		fdnG	11	formate dehydrogenase-N, nitrate-inducible, alpha subunit
		ftnA	9	cytoplasmic ferritin
		fdnI	9	formate dehydrogenase-N, nitrate-inducible ,cytochrome B556
		yeiT	8	putative oxidoreductase
		fdnH	7	formate dehydrogenase-N, iron-sulfur beta subunit
		yqeC	6	orf, hypothetical protein
		yjjI	6	orf, hypothetical protein
		soxS	5	regulation of superoxide response regulon
		ECs0981	5	anaerobic dimethyl sulfoxide reductase subunit C

Continued

		Gene Symbol	Fold Change	Gene description
Smp43	Upregulated	*flgG*	3	flagellar biosynthesis, cell-distal portion of basal-body rod
		ubiH	2	2-octaprenyl-6-methoxyphenol hydroxylase
	Down regulated	*lacI*	948	transcriptional repressor of the lac operon
		pepD	372	aminoacyl-histidine dipeptidase
		betB	151	NAD+dependent betaine aldehyde dehydrogenase
		frsA	111	orf, hypothetical protein [b0239]
		gpt	109	guanine-hypoxanthine phosphoribosyltransferase
		sopA	100	plasmid partitioning protein
		yagN	92	orf, hypothetical protein
		flmC	88	hypothetical protein
		betI	87	probably transcriptional repressor of bet genes
			86	cytotoxic protein LetB
		ykgF	72	orf, hypothetical protein
			69	SopB protein
		yahK	62	putative oxidoreductase
		ykfB	54	orf, hypothetical protein
		lacZ	54	beta-D-galactosidase
		ccdB	52	plasmid maintenance protein
		gpt	50	Xanthine-guanine phosphoribosyltransferase
		narH	42	nitrate reductase 1, beta subunit
		narG	39	nitrate reductase 1, alpha subunit
		proB	37	gamma-glutamate kinase
		yahN	34	putative cytochrome subunit of dehydrogenase
		ECs0346	31	putative transporter
		intF	30	putative phage integrase
		ECs0360	30	high-affinity choline transport
		proB	29	gamma-glutamate kinase

Continued

		Gene Symbol	Fold Change	Gene description
Polymyxin B	Upregulated	*cirA*	39	outer membrane receptor for iron-regulated colicin I receptor
		fepA	23	outer membrane receptor for ferric enterobactin
		ybdB	18	Hypothetical protein ybdB
		ybdB	17	orf, hypothetical protein
		ECs0636	15	hypothetical protein
		entF	14	Enterobactinsynthetase component F
		entF	14	ATP-dependent serine activating enzyme
		entB	12	2,3-dihydro-2,3-dihydroxybenzoate synthetase,
		entE	11	2,3-dihydroxybenzoate-AMP ligase
		yncE	10	putative receptor
		ybdB	10	orf, hypothetical protein
		feoA	9	ferrous iron transport protein A
		feoC	8	orf, hypothetical protein
	Down regulated	*lacI*	226	transcriptional repressor of the lac operon
		frsA	135	orf, hypothetical protein
		betB	127	NAD+-dependent betaine aldehyde dehydrogenase
		gpt	117	guanine-hypoxanthine phosphoribosyltransferase
		crl	109	transcriptional regulator of cryptic csgA gene
		betT	107	high-affinity choline transport
		flmC	98	hypothetical protein
		pepD	94	aminoacyl-histidine dipeptidase
		yagN	94	orf, hypothetical protein
		sopA	90	plasmid partitioning protein
		sopB	80	plasmid partitioning protein
		ykfB	71	orf, hypothetical protein

Table 5.2 Upregulated transcripts induced commonly by Smp24 and Polymyxin B.

Transcript ID	Gene symbol	Peptide (FC)		Gene description
		Smp24	Polymyxin B	
A_07_P003540	*cirA*	55	39	ferric iron-catecholate outer membrane transporter
A_07_P016680	*fepA*	40	23	iron-enterobactin outer membrane transporter
A_07_P044007	*ybdB*	26	19	hypothetical protein
A_07_P031332	*ybdB*	23	18	hypothetical protein
A_07_P054207	*ECs0636*	20	15	hypothetical protein
A_07_P016731	*entB*	19	12	isochorismatase
A_07_P031313	*entF*	17	14	enterobactin synthase subunit F
A_07_P016744	*ybdB*	14	10	conserved protein
A_07_P009354	*yncE*	10	10	conserved protein
A_07_P002712	*fhuA*	5	5	ferrichrome outer membrane transporter

Table 5.3 Down regulated transcripts induced commonly by Smp24 and Smp43

Transcript ID	Gene symbol	Peptide (FC)		Gene description
		Smp24	Smp43	
A_07_P007073	*narG*	45	39	nitrate reductase 1, alpha subunit
A_07_P007083	*narJ*	27	20	molybdenum-cofactor-assembly chaperone subunit (delta subunit) of nitrate reductase 1
A_07_P009461	*fdnG*	11	8	formate dehydrogenase-N, alpha subunit, nitrate-inducible
A_07_P009475	*fdnI*	9	7	formate dehydrogenase-N, cytochrome B556 (gamma) subunit, nitrate-inducible
A_07_P003491	*yeiT*	8	6	predicted oxidoreductase
A_07_P009468	*fdnH*	7	5	formate dehydrogenase-N, Fe-S (beta) subunit, nitrate-inducible
A_07_P000799	*napC*	5	4	nitrate reductase, cytochrome c-type, periplasmic
A_07_P004926	*dmsC*	5	3	dimethyl sulfoxide reductase, anaerobic, subunit C
A_07_P036723	*hybA*	5	3	hydrogenase 2 protein HybA
A_07_P002090	*hypC*	4	4	protein required for maturation of hydrogenases 1 and 3
A_07_P012100	*hybD*	3	3	predicted maturation element for hydrogenase 2
A_07_P018368	*cfa*	2	3	cyclopropane fatty acyl phospholipid synthase (unsaturated-phospholipid methyltransferase)
A_07_P041771	*yhaV*	2	3	Hypothetical protein yhaV

Table 5.4 Down regulated genes induced commonly by Smp43 and polymyxin B

Gene symbol	Peptide (FC)		Gene description
	Smp43	polymyxin	
betA	26	43	choline dehydrogenase, a flavoprotein
betB	151	127	betaine aldehyde dehydrogenase
betT	24	39	high-affinity choline transport
ccdA	15	26	plasmid maintenance protein
ccdB	52	44	High-affinity choline transport protein
codA	19	9	cytosine deaminase
flmC	88	98	hypothetical protein
ECs0346	29	44	putative transporter
ECs0360	30	28	high-affinity choline transport
frsA	111	135	orf, hypothetical protein
garR	15	15	putative dehydrogenase
gpt	50	51	Xanthine-guanine phosphoribosyltransferase
intF	30	42	putative phage integrase
lacI	948	226	transcriptional repressor of the lac operon
lacY	26	41	galactoside permease
lacZ	54	67	beta-D-galactosidase
mhpR	20	21	transcriptional regulator for mhp operon
mmuM	25	40	putative enzyme
narG	39	9	nitrate reductase 1, alpha subunit
narH	42	12	nitrate reductase 1, beta subunit
pepD	372	94	aminoacyl-histidine dipeptidase
proB	37	38	gamma-glutamate kinase
sopA	100	90	plasmid partitioning protein
yafY	23	18	putative transcriptional regulator LYSR-type
yagN	92	94	orf, hypothetical protein
yahB	12	18	putative transcriptional regulator LYSR-type
yahK	62	54	putative oxidoreductase
yahN	34	59	putative cytochrome subunit of dehydrogenase
yahO	17	27	orf, hypothetical protein
yeiT	6	4	putative oxidoreductase
ykfB	54	71	orf, hypothetical protein
ykgG	25	44	orf Unknown function

5.3.4 Analysis of expressed gene lists using DAVID bioinformatics resources

To determine the bacterial metabolic pathways which were significantly affected by peptide exposure, the upregulated genes were submitted to the Database for Annotation, Visualisation and Integrated Discovery (DAVID) analysis tool. Functional annotation clustering (FAC) analysis of 48 upregulated genes in response to Smp24 treatment resulted in 9 enriched functional clusters under the medium stringency option.

Siderophore biosynthetic processing and di - tri valent ion binding and transport were the most biologically important gene groups with enrichment scores (ES) of 5.45 and 4.86 respectively ($P < 0.05$) for Smp24 (Figure 5.8A). FAC revealed four genes are included in siderophore biosynthesis processing and thirteen genes were counted in the second cluster of cation binding and transport functions. The remaining FAC clusters of upregulated genes were dominated by genes of amino-acid biosynthesis, magnesium ion binding, and nucleotide binding (chloride channels).

The majority (60%) of enriched clusters identified for polymyxin B upregulated genes were similar to those clustered for Smp24 upregulated genes, both treatments share clusters related to cation binding, siderophore biosynthesis and nucleotide binding (Figure 5.8A). FAC analysis clustered the ten common upregulated genes in response to Smp24 and Polymyxin B treatments in one enriched functional cluster including mainly cation binding and transport processes under the medium stringency option (ES= 3.82, $p < 0.05$).

FAC analysis of 72 down regulated genes of Smp24 generated seven enriched clusters. The highest enriched gene group was cellular respiration (ES= 10.11), followed by

cation (iron) binding and transport (ES= 5.1). Some other clusters with lower ES were mainly related to cellular respiration such as electron transport and formate dehydrogenase (NAD+) activity. All of these clusters are shown in figure 5.8B.

Smp43 down regulated genes were clustered into 14 enriched clusters, the highest two clusters were cellular respiration and cation (iron) binding, the same as identified for Smp24 and the down regulated gene clusters are cellular respiration and cation (iron) binding and transport with very close ES, 4.69 and 4.31 respectively. The next highest Smp43 down regulated gene groups according to ES values were post-segregation antitoxin *CcdA*, stress response, electron transport chain, and some other metabolic pathways. Clusters such as post-segregation antitoxin *CcdA* (ES 3.84), Arginine and proline metabolism (ES 3.59), stress response (ES 3.21), cation binding (ES 1.99) , iron - sulfur cluster binding (ES 1.4) and electron transport chain (ES 1.1) were also identified for polymyxin B down regulated genes(Figure 5.8B).

Interestingly, the biological processes of cation binding, cellular respiration, and electron transport were the most affected processes in response to both Smp24 and Smp43 treatments.

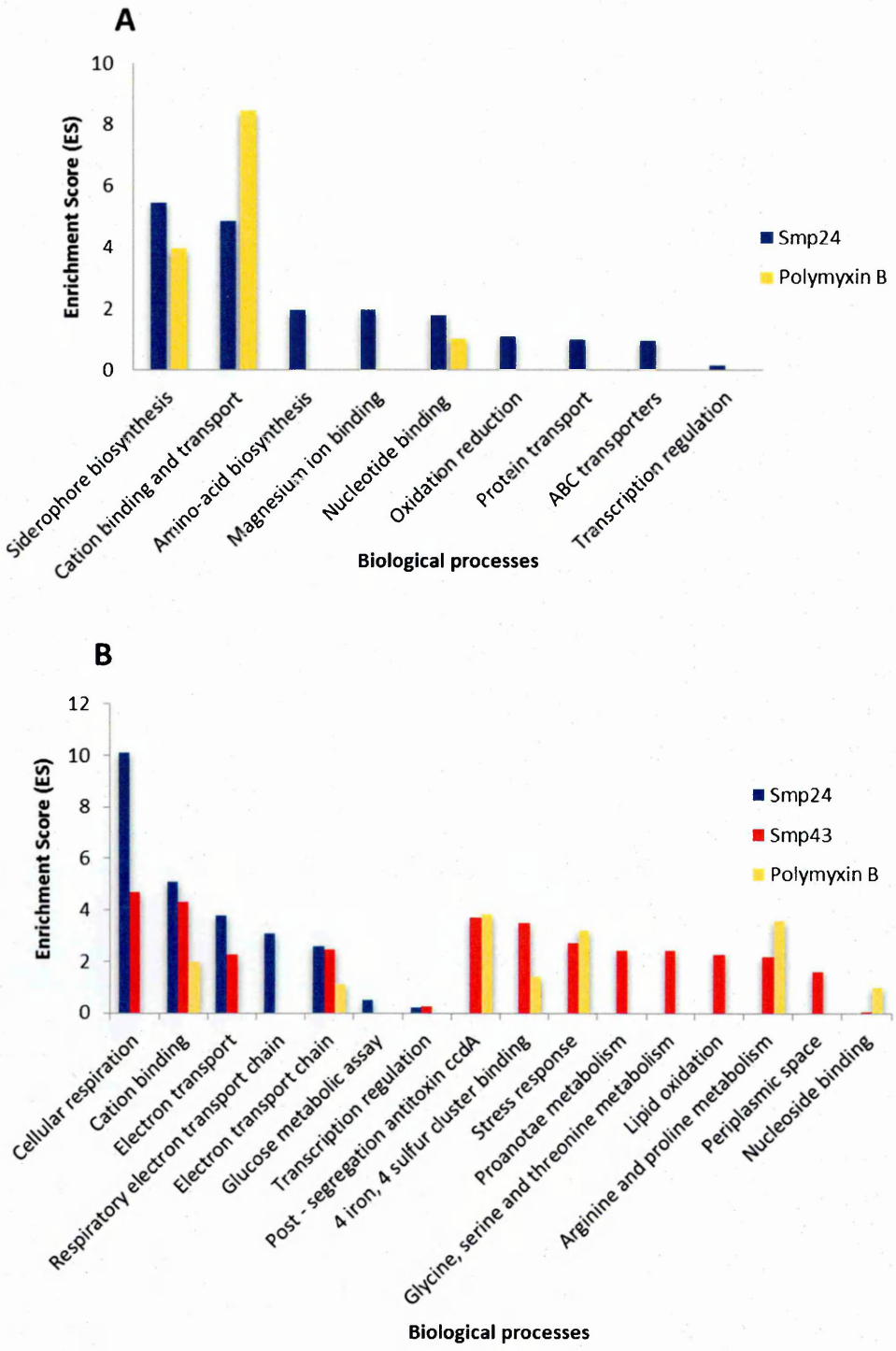

Figure 5.8 DAVID Functional Annotation Clustering (FAC) analysis of differentially expressed genes obtained by Microarray analysis of *E. coli* following exposures to subinhibitory concentrations of AMPs. A. Enriched functional gene clusters for the 58 and 28 up-regulated genes of Smp24 and Polymyxin B respectively. B. Enriched functional gene clusters for the 72, 81 and 71 down regulated genes of Smp24, Smp43 and polymyxin B respectively. Significance is determined by corresponding enrichment scores.

In conclusion, microarray analysis of the *E. coli* response to Smp peptides compared with the absence of peptides has revealed seventy two genes were down-regulated by Smp24 and eighty one genes were down-regulated by Smp43. Of these, thirteen genes were down-regulated in common and were associated with bacterial respiration. Forty eight genes were specifically up-regulated by Smp24; these genes were predominantly related to sideophores biosynthesis and transport as well as cation transport, especially iron.

These gene lists has been interpreted using DAVID, gene clusters mainly associated with siderophore biosynthesis, cation transport, electron transport chain, cellular respiration and oxidative stress responses were the most biologically important enriched gene groups.

5.3.5 Screening the Kieo collection

The Keio collection is the most used genome-wide screens of *E. coli* knockout strains. This library includes singe gene deletions for 3,985 genes representing more than 90% of the *E. coli* K-12 genome. This analysis method has successfully been used as a tool in the last decade by screening mutant cells against antimicrobial agents to identify and assess the most fundamental genetic variant or trait for antimicrobial mode of action or bacterial resistance (Liu, Tran *et al.* 2010, Audrain, Ferrieres *et al.* 2013, Stokes, Davis *et al.* 2014).

To characterise the genes that effectively contribute to the *E. coli* response to Smp peptides, a total of seventy nine strains from the Keio collection were tested for Smp24 and Smp43 susceptibility, each of which have a single deletion of highly differentially expressed genes of *E. coli* identified by microarray analysis (Table 5.5). The BW25113 parent strain of *E. coli* was assayed first against concentrations of Smp24 and Smp43 (0-512 µg/ml) to determine wild-type MIC (32 µg/ml). The sensitivity profile of Smp24 was determined against thirty-eight single-gene knockouts. Only fifteen mutants showed different MICs against Smp24 compared with the wild-type strain. Ten mutant strains were more resistant to Smp24 and had an increased MIC (64 µg/ml) with respect to the parent strain. The majority (> 75%) of these genes (*fiu*, *entC*, *entA*, *entB*, *entH*, *fepA* and *fhuA*) are involved in the biosynthesis of sideorphores and the transport of ions. Also, the deletion of the protein binding gene *fimC* increased resistance to Smp24. Moreover, the mutant cell of *tatE*, a component of TatABCE protein export complex, exhibited resistance to Smp24 (Table 5.6).

Knocking out genes *sodB*, *fdnG*, *ycgK*, *soxS* and *ccmB* resulted in cellular sensitivity to Smp24 with a one fold decrease in the MIC compared with the wild type strain. Two of these genes *sodB* and *soxS* play an important role in bacterial protection from superoxide; however *fdnG* and *ccmB* are involved in the nitrate reduction process during anaerobic respiration (Table 5.7).

Forty one strains from the Keio knockouts were tested for Smp43 susceptibility. Only nine mutants displayed different MICs against Smp43. The single deletion mutants of the genes *napC*, *garK*, *fdnG*, *dsmA*, *hypA* and *fdnH* which are involved in anaerobic respiration and oxidoreductase gene *ubiH*, implicated in response to oxidative stress, exhibited increases in susceptibility to Smp43 (16 μg/ml) (Table 5.7). Two strains showed increased resistance, one of these carried a deletion of *proB*, a gene that has a function in magnesium ion binding and kinase activity. While the other resistant strain has a deletion of *ykfB* which is an uncharacterised 'hypothetical' gene (Table 5.6).

Eight genes (*ihfB*, *uxuR*, *hcaT*, *cysG*, *ugpQ*, *idnT*, *yghB* and *pbpC*) which were not differentially expressed were randomly selected to assess single gene deletion effect on the susceptibility of *E. coli* to Smp peptides as experimental controls; all showed the same MIC for Smp peptides when compared with the wild type strain.

Table 5.5 MICs for Smp peptide aginst Keio strains compared with the wild type strain (Smp24 and Smp43 MIC= 32 μg/ml)

Smp24 (μg/ml)				**Smp43** (μg/ml)			
Strain	**MIC**	**Strain**	**MIC**	**Strain**	**MIC**	**Strain**	**MIC**
Δ*Fiu*	64	Δ*yjjV*	64	Δ*betA*	32	Δ*napC*	16
Δ*entC*	64	Δ*sodB*	16	Δ*betB*	32	Δ*narG*	32
Δ*ybdB*	64	Δ*hybA*	32	Δ*betI*	32	Δ*narH*	32
Δ*entA*	64	Δ*fdnH*	32	Δ*betT*	32	Δ*narJ*	32
Δ*entB*	64	Δ*fimC*	64	Δ*cfa*	32	Δ*pepD*	32
Δ*cirA*	32	Δ*atos*	32	Δ*codA*	32	Δ*proB*	> 32
Δ*nrdI*	32	Δ*fdnG*	16	Δ*dmsA*	16	Δ*prpB*	32
Δ*nrdE*	32	Δ*intf*	32	Δ*fdnG*	16	Δ*prpC*	32
Δ*entF*	32	Δ*ybiX*	32	Δ*fdnH*	16	Δ*prpD*	32
Δ*fepA*	64	Δ*ykgL*	32	Δ*flgG*	32	Δ*ubiH*	16
Δ*yncE*	32	Δ*ycgK*	16	Δ*frsA*	32	Δ*yafY*	32
Δ*fhuB*	32	Δ*ccmB*	16	Δ*garK*	16	Δ*yagN*	32
Δ*nrdF*	32	Δ*fldB*	32	Δ*garR*	32	Δ*yagV*	32
Δ*fhuA*	64	Δ*dmsC*	32	Δ*gpt*	32	Δ*yahJ*	32
Δ*tatE*	64	Δ*hypC*	32	Δ*hypA*	16	Δ*yahK*	32
Δ*fliI*	32	Δ*hypO*	32	Δ*intF*	32	Δ*yahO*	32
Δ*fliH*	32	Δ*nfo*	32	Δ*lacI*	32	Δ*ykfB*	> 32
Δ*bioD*	32	Δ*ynfF*	32	Δ*lacY*	32	Δ*ykfC*	32
Δ*soxS*	16	Δ*yqeC*	32	Δ*mhpR*	32	Δ*ykgF*	32
				Δ*mmuM*	32	Δ*ykgG*	32
				ΔnapB	32		

Table 5.6 Mutant strains with increased resistance to Smp24 and Smp43

Peptide	Functional Group	Gene Function	Gene knockout
Smp24	Siderophores transport and biosynthesis	Putative outer membrane receptor for iron transport	*fiu*
		Outer membrane receptor for ferric enterobactin	*fepA*
		Outer membrane ferrichrometransport system	*fhuA*
		Isochorismate synthase	*entC*
		2,3-Dihydro-2,3-dihydroxybenzoate dehydrogenase	*entA*
		2,3-dihydro-2,3-dihydroxybenzoate synthase; Asochorismatase	*entB*
		thioesterase required for efficient enterobactin production	*ybdB* (*entH*)
	Protein transporter activity	Component of TatABCE protein export complex ; Protein translocase	*tatE*
	Nuclease activity	Putative DNase (nuclease activity)	*yjjV*
	Protein binding	Periplasmic chaperone	*fimC*
Smp43	Unknown Function	Unknown Function	*ykfB*
	Magnesium ion binding	Glutamate 5-kinase, proline biosynthesis	*proB*

Table 5.7 Mutant strains with increased susceptibility to Smp24 and Smp43

Peptide	Functional Group	Gene Function	Gene knockout
Smp24	Oxidative stress response	Global transcription regulator for superoxide response	*soxS*
		Superoxide dismutase; response to oxidative stress	*sodB*
	Anaerobic respiration	Formate dehydrogenase-N	*fdnG*
		Heme exporter subunit;cytochrome c biogenesis system	*ccmB*
	Unknown Function	Unknown Function	*ycgK*
Smp43	Oxidative stress response	2-octaprenyl-6-methoxyphenol hydroxylase	*ubiH*
	Anaerobic respiration	Dimethyl sulfoxide reductase	*dmsA*
		Formate dehydrogenase-N	*fdnH*
		Metal ion binding	*hypA*
		Quinol dehydrogenase, electron source for NapAB; Cytochrome c-type protein (electron carrier)	*napC*
		Formate dehydrogenase-N	*fdnG*
		Glycerate kinase	*garK*

5.3.6 Real Time PCR

Prior to performing a RT-PCR analysis, the quality of the extracted RNA was assessed using the NanoDrop spectrophotometer. Only RNA samples with A260/280 and A260/230 ≥ 1.9 were used for DNA preparation and RT-PCR analysis. RT-PCR analysis was performed on four selected genes identified in the microarray analysis. The selected genes were differentially expressed following *E. coli* responses to either Smp24 or Smp43 as determined from Keio collection screening. Two upregulated genes selected for RT-PCR were related to siderophore transport functions; *fiu* is an outer membrane siderophore receptor for iron transport and *fepA* is an outer membrane receptor for siderophores. The two down regulated genes chosen for revalidation are *proB,* involved in magnesium ion binding in proline biosynthesis, and *fdnG,* which has metal (iron and selenium) binding functions and is involved in electron carrier activity in anaerobic respiration. Validation of the microarray data by RT-PCR analysis showed that the expression of most of the assayed genes in cells treated by Smp24 were comparable with the microarray analysis (Figure 5.9 and Figure 5.10).

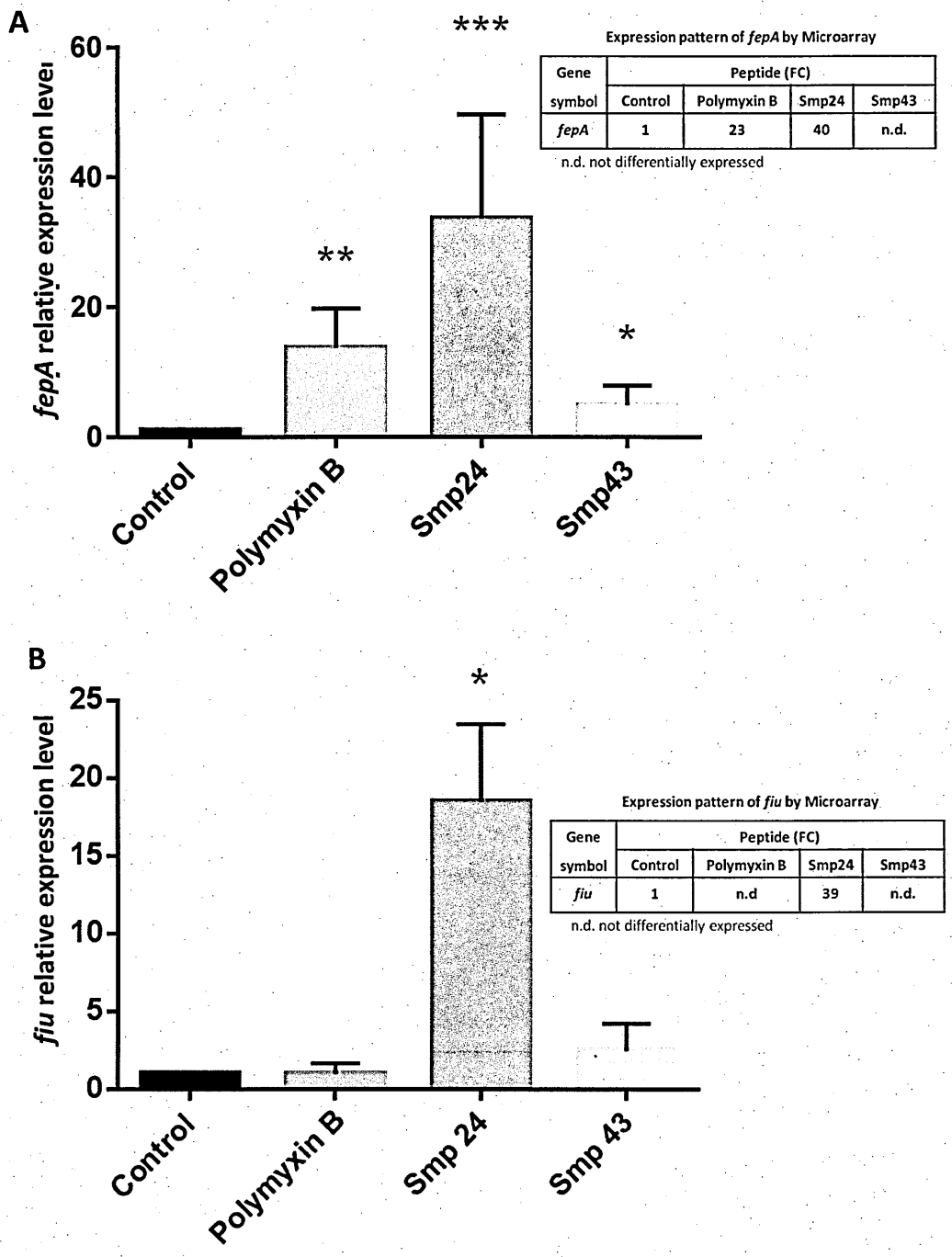

Figure 5.9 RT-PCR analysis of the relative mRNA expression levels of selected upregulated genes in polymyxin B, Smp24 and Smp43 treated *E. coli* when compared with an untreated control. A: shows relative mRNA the expression of *fepA* among the different treatments, table inset shows the expression pattern of the gene by microarray. B: represents the relative expression of *fiu* among different treatments, table inset shows the expression pattern of the gene by microarray. Data are expressed as the mean±SE. Statistical analysis was performed by the Kruskal-Wallis test. ***Significant *P* <0.05. **Significant *P* <0.01. ***Significant *P* <0.001.**

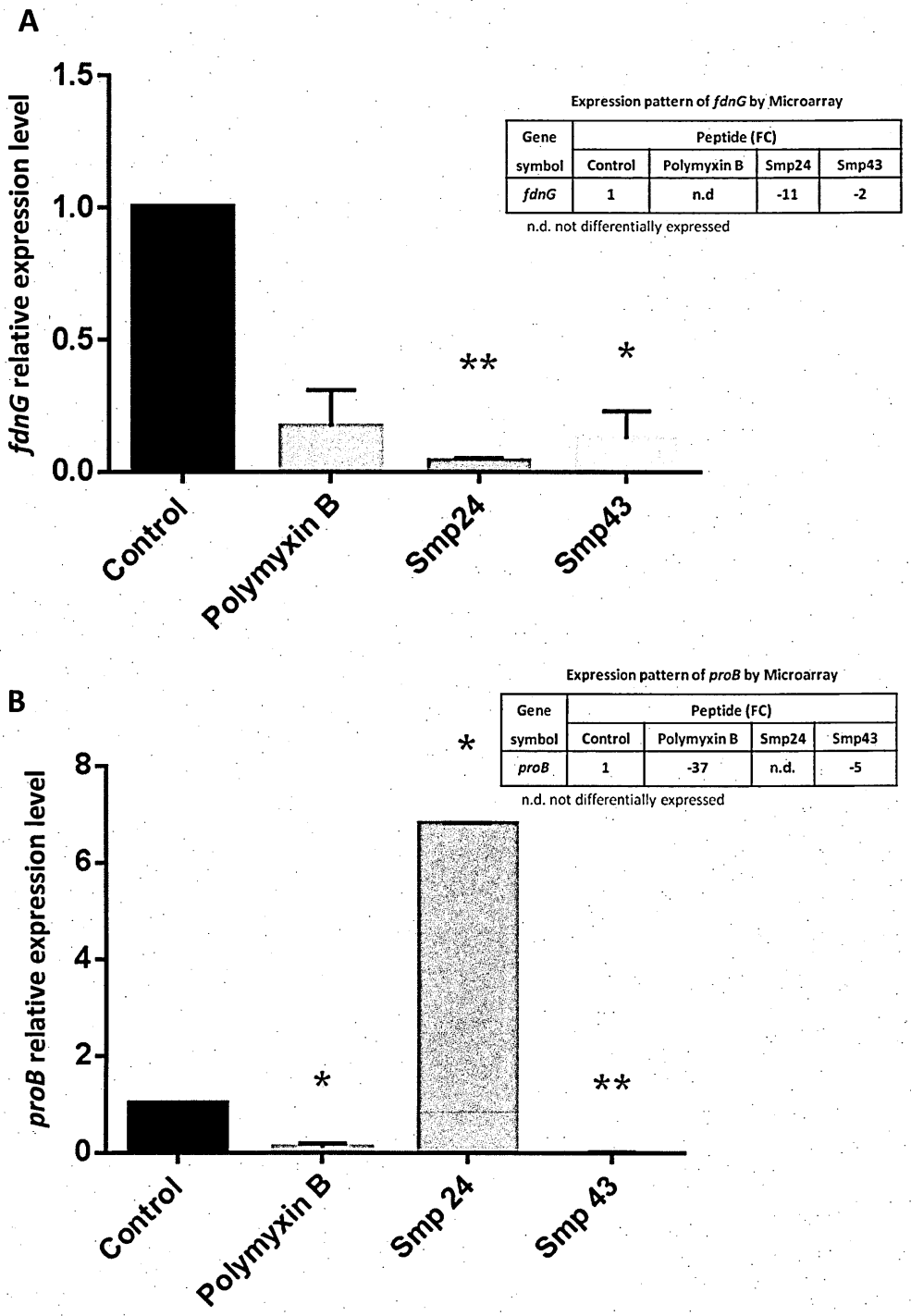

Figure 5.10 RT-PCR analysis of the relative mRNA expression levels of selected down regulated genes in polymyxin B, Smp24 and Smp43 treated *E. coli* when compared with an untreated control. A: shows the relative mRNA expression of *fdnG* among the different treatments, table inset shows the expression pattern of the gene by microarray. B: represents the relative expression of *proB* among different treatments, table inset shows the expression pattern of the gene by microarray. Data are expressed as the mean±SE * P<0.05 vs. untreated control cells. Statistical analysis was performed by the Kruskal-Wallis test. ***Significant *P* <0.05.** ****Significant *P* <0.01.** *****Significant *P* <0.001.**

5.4 Discussion

Prior to this study there was no data regarding the interaction of Smp peptides and live bacterial membranes in living cells. The mechanism of action of Smp peptides against synthetic prokaryotic membranes models have been investigated before using liposome leakage assays, AFM and QCM-D and revealed that Smp24 induced pore formation in synthetic membrane models causing lipid segregation (Harrison, Heath *et al*. 2016).

In our study, transcriptomic responses of *E. coli* to subinhibitory concentrations of Smp peptides was analysed using DNA microarray. DNA microarray has been used to provide insights into the mode of action of AMPs and AMP-resistance mechanisms to understand how bacteria respond to AMPs. Antimicrobials at subinhibitory concentrations may act as stress inducers or signalling molecules that induce the expression of specific genes that help in understanding the mechanism of action of many antimicrobial agents (Linares, Gustafsson *et al*. 2006, Bernier, Surette 2007, Fajardo, Martínez 2008, Xu 2016).

Overall, the results of our microarray analysis correlated well with RT-PCR results, indicating accurate detection of the differentially expressed genes by microarray from a total of twelve comparisons (four genes × three treatments). RT-PCR analysis showed that the selected down regulated genes in Smp43 treated cells showed a significant change in their expression as they exhibited lower expression than untreated cells. *fepA* was overexpressed in Smp24 and polymyxin B treated cells as exhibited in the microarray analysis and RT-PCR analysis. Some differences between microarray and RT-PCR have been observed, however. For example, *fepA* was significantly

overexpressed in Smp43 treated cells compared with control cells when analysed by RT-PCR, while the microarray analysis for this upregulated gene showed no significant expression in Smp43 treated cells ($p>0.05$). This type of variation is often seen between microarray and RT-PCR data. This disagreement may refer to the differences between the two methodological procedures such as the dyes or primer sets. Also, the variability of normalisation between both analyses has a great impact on this disagreement. Agilent One-Colour Microarray-based Gene Expression Analysis undergoes global normalisation which includes transforming all microarray intensity values below 1 to 1 and then dividing by the median of all intensity values. This is in contrast to RT-PCR which uses housekeeping genes as a reference point for normalisation which may contribute to the lower correlations between microarray and RT-PCR results (Etienne, Meyer *et al.* 2004, Morey, Ryan *et al.* 2006).

The data in our study clearly demonstrate that *E. coli* exhibits transcriptional differences in response to sublethal concentrations of Smp24 and Smp43. Most identified differentially expressed genes in our study responding to Smp peptides stress were genes that have been reported with increased expression during siderophore biosynthesis and cation binding and transport. Also, genes implicated in antioxidant responses and anaerobic respiration were prominent amongst the differentiated genes responding to Smp peptides.

In order to increase iron uptake, bacteria synthesise siderophores to chelate ferric iron and make complexes (Vassiliadis, Peduzzi *et al.* 2007). In the present study, *entC*, *entA*, *entB*, *entF* and *entH* were upregulated in response to Smp24 stress. The *ent* gene cluster encode proteins related to the biosynthesis of enterobactin (Fischbach, Lin *et al.* 2006, Miethke, Marahiel 2007, Salvail, Lanthier-Bourbonnais *et al.* 2010).

Siderophore ferric complexes will cross Gram negative bacteria outer membrane through specific receptors and are translocated to the cytoplasm by inner membrane transporter proteins to deliver iron (Vassiliadis, Peduzzi *et al.* 2007, Stintzi, Barnes *et al.* 2000). The microarray analysis of *E. coli* responses to a sublethal dose of Smp24 revealed that four genes encoding these types of receptors (*fiu*, *fepA*, *cirA* and *fhuA*) were found to be significantly overexpressed compared with untreated cells. Also, the siderophore transporter *fepC* was upregulated.

Siderophore biosynthesis is regulated by the ferric uptake regulator (Fur) system, as *Fur* cluster genes repress the siderophore biosynthesis according to the availability of Iron (Crosa, Walsh 2002, Dale, Doherty-Kirby *et al.* 2004). Also Fur has roles in cellular oxidative stress defence such as activation of superoxide dismutase *sodB* which is involved in oxidative stress response (Zhang, Ding *et al.* 2012, da Silva Neto, Braz *et al.* 2009). Fur is regulated by the oxidative stress response regulon *soxS* (Pomposiello, Bennik *et al.* 2001). The microarray data revealed both *soxS* and *sodB* were significantly down regulated in response to Smp24 treatment. The down regulation of these oxidative stress response genes leads directly to lower resistance to oxidative stress. Additional evidence comes from the susceptibility testing of Keio mutants which support these findings by showing that the deletion of genes *sodB* or *soxS* resulted in increased cellular sensitivity to Smp24 compared with the wild type strain. The deletion of oxidative response gene *ubiH* generated higher susceptibility than seen in the parent stain. Accordingly, Smp peptides may induce oxidative stress causing cell death.

These results are in good agreement with other recent studies which have shown the production and upregulation of siderophores in response to oxidative stress (Chen,

Yang *et al.* 2014, Ruiz, Bernar *et al.* 2015). Particularly, enterobactin plays an important role in the reduction of the oxidative stress in *E. coli*. Enterobactin is hydrolysed to release iron which is essential for the activities of antioxidants and the hydrolysed enterobactin can scavenge radicals directly (Eisendle, Schrettl *et al.* 2006, Chung 2012, Adler, Corbalan *et al.* 2014, Achard, Chen *et al.* 2013). However, both iron deficiency and excess free iron can induce oxidative stress (Fernaeus, Land 2005, Galaris, Pantopoulos 2008). Siderophores can act as a source of hydrogen atoms and efficiently terminate radical chain reactions (Povie, Guillaume, *et al.*2010). Our findings suggest that an imbalance in iron homeostasis and oxidative stress might be involved in *E. coli* response to Smp peptide treatment. These suggestions are consistent with other antimicrobial peptides in the literature which induce oxidative stress, such as microcin J25 which increase the production of reactive oxygen species and is recognised by the siderophore outer membrane receptor FhuA (Destoumieux-Garzon, Duquesne *et al.* 2005, Mathavan, Zirah *et al.* 2014). Interestingly, the microarray analysis of the transcriptomic response of *E. coli* exposed to Smp24 revealed the significant upregulation of *fhuA*. Polymyxin B can also produce reactive oxygen species (ROS) when it enters Gram negative bacterial membranes. The induced ROS by polymyxin B such as H_2O_2 affects iron homeostasis by oxidising Fe^{2+} to Fe^{3+} through the Fenton reaction (Sampson, Liu *et al.* 2012, Yu, Qin *et al.* 2015).

A recent study (Dong *et al.*, 2015) has reported that the treatment of *E. coli* with polymyxin B induce a 35-fold increase in *soxS* expression level compared with the untreated strain (Dong, Dong *et al.* 2015). Similarly, our microarray data analysis revealed that *soxS* is down regulated when *E. coli* was stressed by subinhibitory concentrations of polymyxin B. Furthermore, polymyxin B induced the upregulation of

genes that encode siderophore receptors (*fepA*, *fhuA*, and *cirA*), siderophores biosynthesis (*entF*, *entB*, and *entE*) and iron transporters proteins (*feoB*, *feoA* and *feoC*) , similar to the *E. coli* response to Smp24.These finding agree with other studies which have shown that mutants of some siderophore biosynthesis and receptor genes such as *fiu*, *fepA*, *fhuE cirA*, *fhuA*, *entA*, *entB*, *entC*, *entD*, *entE*, *feoA*, *feoC* and *feoB* have a higher resistance to polymyxin B than wild type strains (Barrios 2013, Guo, Nair *et al.* 2011).

Production of ROS leads to inactivation of Fe –S clusters which are involved in many cellular functions such as respiration (Ayala-Castro, Saini *et al.* 2008). 4Fe-4S Fes protein is required for iron release from the ferric siderophore complex, therefore Fe-S inactivation leads to a loss iron which results in ROS detoxication deficiencies (Li, Wang *et al.* 2016). Our Functional Annotation Clustering (FAC) analysis results showed that the Fe–S cluster was significantly down regulated in response to both Smp peptides treatments. These findings also support the theory that the mechanism of action of Smp peptides may involve oxidative stress. In addition, the susceptibility assay of the Keio collection against Smp peptides revealed that knockout mutants of genes related to oxidative stress response showed a marginally higher level of sensitivity to either Smp24 or Smp43 compared with the parent strain.

The oxidative stress that causes inactivation of Fe–S clusters which are important components of many proteins involved in anaerobic respirations such as DmsA, FdnH, FdnG and NapC (Jormakka, Tornroth et al. 2002, Tang, Rothery et al. 2011).These facts are amongst likely explanations of the highly significant down regulation of anaerobic related genes following exposure to sublethal doses of both Smp peptides. Also, the screening of some mutant strains from the Keio collection such as *dmsA*, *fdnH*, *fdnG*

and *napc*) against Smp peptides revealed that deletions of genes related to anaerobic respiration results in slightly decreased MIC for either Smp24 or Smp43 compared with the parent strain.

Gene clusters mainly related to the electron transport chain and cellular respiration were found to be highly significantly enriched as revealed by FAC analysis of down regulated genes in response to Smp24, Smp43 and polymyxin B treatments. Disruptions in the electron transport chain which have been reported before for polymyxin treatment in *E. coli* enhance oxidative stress by producing ROS (Sampson, Liu *et al.* 2012). In addition, polymyxin B has the ability to inhibit some respiratory enzymes such as alternative NADH dehydrogenase, quinone oxidoreductase and type II NADH-quinone oxidoreductases (NDH-2) (Deris, Akter *et al.* 2014). Consistently, other reports have found increases in the transcriptional levels of similar genes involved in envelope and oxidative stress responses for polymyxin treated bacteria (Sikora, Beyhan *et al.* 2009a, Ramos, Custódio *et al.* 2016).

The role of siderophores in enhancing the antibacterial activity of some antibiotics has been recently investigated. Some antibiotics such as albomycin and salmycin are linked naturally to siderophores to facilitate their delivery to the cell through iron uptake pathways, known as the 'Trojan Horse' strategy. These siderophore–antibiotic conjugates are called sideromycin which consists of a siderophore, a peptide linker, and an antibiotic (Braun, Pramanik *et al.* 2009, Wencewicz, Long *et al.* 2013, Ferguson, Coulton *et al.* 2000).

Siderophore uptake pathway is one of the most exploitable biological pathways in bacteria to help antibiotics reach their cytoplasmic target. This strategy has been

applied to increase susceptibility to antibiotics by avoiding or limiting the exposure of antibiotics to resistance mechanisms providing an opportunity to recycle old antibiotics rendered useless by resistance (Wencewicz, Long *et al.* 2013). The antibacterial activity of β-lactam antibiotics such as ampicillin and amoxicillin has been investigated when bound to siderophores, the conjugates exhibited high antibacterial activity compared with parent drugs (Ghosh, Ghosh *et al.* 1996, Kinzel, Tappe *et al.* 1998, Ji, Miller *et al.* 2012) (Ji, Cheng, 2012).

The potential uptake of Smp peptides by siderophores receptors has been supported by assaying the susceptibility of Smp24 against single-gene knockout mutants of *E. coli* (Keio collection). Knockout mutants of genes from the Ent gene cluster (*ΔentB*, *ΔentH*, *ΔentC* and *ΔentA*) and iron-regulated outer membrane receptors (*ΔfepA*, *Δfiu*, and *ΔfhuA*) showed a marginally higher level of resistance to Smp24 compared with the parent strain. Also, the antibacterial activity of the modified form of microcin E492, a pore-forming antimicrobial peptide, is mediated by enterobactin outer membrane receptors such as FepA, Cir and Fiu. MccE492m is an 84 amino acid long first peptide isolated from *Klebsiella pneumonaie*. It was post-translationally modified by binding the C-terminal serine residue to a siderophore molecule via an ester linkage to form conjugates with enterobactin with a broader spectrum of antibacterial activity (Thomas, Destoumieux-Garzon *et al.* 2004, Destoumieux-Garzón, Peduzzi *et al.* 2006, Nolan, Fischbach *et al.* 2007, Raines, Moroz *et al.* 2016). Microcins are rich in serine and glycine residues with a conserved serine-rich C- terminus (Vassiliadis, Destoumieux-Garzon *et al.* 2010). Both Smp24 and Smp43 have serine residues in their C-terminal tail, and are rich in serine and glycine amino acids that may enhance its binding to siderophores to form Smp24 – siderophore conjugates, that facilitate their

delivery inside the bacterial cell leading to cell death. Similarly, sideromycins such as albomycin binds to siderophores through a serine residue (Zeng, Roy *et al.* 2009, Zeng, Kulkarni *et al.* 2012). Moreover, most siderphores have a backbone based on serine and glycine residues (Zheng, Bullock *et al.* 2012). Siderophore receptors are amongst bacterial membrane targets that have been suggested to recognise AMPs (Thomas, Destoumieux-Garzon *et al.* 2004).

Despite their roles in iron transport, siderophores may act as a metallophores for a variety of other metals and play a crucial role in the protection of bacteria from oxidative stress. Some sideophores have the ability to scavenge radicals through prevention of the Fenton reaction by chelating iron (Johnstone, Nolan 2015, Peralta, Adler *et al.* 2016). AMPs promote the generation of ROS and induce plasma membrane disruption which may contribute to cell death (Oyinloye, Adenowo *et al.* 2015).

Some AMPs exert their effects through alternative modes of action and may in fact act upon multiple targets, however, the activities of AMPs are mainly dependent upon direct interaction with the bacterial cell membrane (Jenssen, Hamill *et al.* 2006).

In conclusion, the microarray analysis of Smp treated *E. coli* revealed some similar gene induction patterns with polymyxin b but also some distinctly different ones. The upregulation of siderophore biosynthesis, cation transport and oxidative stress response genes may increase sensitivity of *E. coli* to both Smp peptides, demonstrated by deletion of these upregulated genes, point to the role of oxidative stress in the inhibitory effect of Smp peptides against *E. coli.* This should be verified biochemically in future studies.

6 Influence of cations on antimicrobial activity of Smp24 against *Escherichia coli.*

6.1 Introduction

Electrostatic binding is key to AMP interaction with the negatively charged molecules of bacterial cell membrane. Such interactions between AMPs and the phospholipid headgroups and other negatively charged molecules at numerous sites covering the surface of bacteria are the initial driving force for AMPs mode of action (Berglund, Piggot *et al.* 2015). A result of the electrostatic interaction is positively charged AMPs destabilise bacterial membranes by interacting with negatively charged structures, which displace or release divalent cations from the bacterial membrane leading to its disruption (Hyldgaard, Mygind *et al.* 2014, Mojsoska, Jenssen 2015).

Cations are essential components of the bacterial cell membrane, they are also necessary for a range of metabolic processes. Divalent ions such as Mg^{2+} and Ca^{2+} electrostatically cross-link and stabilise the LPS and teichoic acids which are major anionic components of Gram negative and Gram positive bacterial cell membranes (Baddiley, Hancock *et al.* 1973, Thomas III, Rice 2014, Arunmanee, Pathania *et al.* 2016). These negatively charged molecules represent the first targets of cationic AMPs leading to their antibacterial effects (Sun, Shang 2015, Malanovic, Lohner 2016). However, the attachment of cations to LPS and teichoic acids increases the rigidity of bacterial membranes and decreases or neutralises their negative charges reducing their affinity for the cationic AMPs (Hughes, Hancock *et al.* 1973, Sahalan, Aziz *et al.* 2013). Therefore, removal of these ions or their displacement by cationic AMPs from their relative binding sites facilitates the binding of the peptide leading to permeability of the outer membrane, potentially leading to cytoplasmic access to the

AMP which is defined as the self-promoted uptake model (Giuliani, Pirri *et al.* 2007, Laverty, Gorman *et al.* 2011).

A number of studies have shown that polymyxin B is taken up by the self-promoted uptake route by displacing divalent cations from their binding sites in the LPS molecules in order to release the LPS component from the bacterial surface leading to membrane disruption and subsequent cell death (Sahalan, Aziz *et al.* 2013). The role of divalent cations in the antibacterial action of polymyxin B has been widely studied against a wide range of Gram negative bacteria. For instance, it was found that Ca^{2+} and Mg^{2+} at 20 mM protect the outer membrane of some *Pseudomonas* strains from the inhibitory damage caused by polymyxin B at 25mg/ml (Chen, Feingold 1972). Furthermore, polymyxin B-induced leakage of the outer and inner membrane enzymes (β-lactamase and β-galactosidase) from *E. coli* was significantly reduced (2 to 3 folds) in the presence of Mg^{2+} and Ca^{2+} (Sahalan, Aziz *et al.* 2013).

Increasing the concentration of divalent cations reduced or inhibited the activity of several cationic peptides against Gram negative bacteria such as Human β defensin 2 (Tomita, Hitomi *et al.* 2000), ostricacins (β-defensins AMPs) (Sugiarto, Yu 2007) and thanatin (insect defence peptide) (Wu, Ding *et al.* 2008). It is thought that basic residues of the peptides are likely to compete with the cations for the same binding sites in the lipid head group region (Kandasamy, Larson 2006). The effect of cations on MICs against *E. coli* was studied by determining MICs at increased concentrations of monovalent and divalent cations. Treatment with divalent cations (Mg^{2+} and Ca^{2+}) at 10mM inhibited the bactericidal activities of three cathelicidin peptides significantly against *E. coli*. All three of the test peptides had MICs that were higher

in presence of monovalent cations (Na^+ and K^+) than in the absence of these cations. These findings indicate that these peptides appear to be ineffective at high salt concentrations, that may limit the binding affinity of LPS to these cationic peptides which negatively affected their bactericidal activities (Anderson, Yu 2005). Bacteriocin peptide enterocin (Kumar, Srivastava 2011) and F12W-magainin 2 (Matsuzaki, Sugishita *et al.* 1999) induced no membrane permeabilisation in LPS-containing liposomes in presence of some cations such as Mg^{2+} and Ca^{2+} when evaluated using the calcein leakage assay as the rigidity of the membrane was increased which is probably due to cross-linking of adjacent LPS molecules with these cations.

The sensitivity of some AMPs to high salt concentrations may limit their application as pharmaceutical agents due to salt induced -inactivation *in vivo* (Yu, Tu *et al.* 2011). Several strategies were developed to increase the salt tolerance of AMPs such as the incorporation of arginine residues at the C-terminal end of synthetic defensins which overcame the salt-resistance effect by increasing peptide cationic net charge which improved electrostatic interaction between the peptide and the anionic bacterial membranes (Li, Saravanan *et al.* 2013). Further several short amphipathic helical peptides with potent antimicrobial activities and salt-tolerant properties have been designed more recently (Mohamed, Hammac *et al.* 2014, Mohanram, Bhattacharjya 2016).

Divalent metal cations increase the activity of anionic AMPs such as kappacin (an AMP derived from bovine milk) (Dashper, O'Brien-Simpson *et al.* 2005) and DCD-1L (an AMP derived from Human Sweat) (Paulmann, Arnold *et al.* 2012). Interestingly,

daptomycin has potent antibacterial activity against Gram positive bacteria rather than the Gram negative bacteria as the outer membrane of Gram negative bacteria act as a barrier to daptomycin. The Gram positive cytoplasmic membrane has a higher an anionic phospholipid content than that found in Gram negative membranes (Streit, Jones *et al.* 2004, Randall, Mariner *et al.* 2013). The insertion of daptomycin into the cytoplasmic membrane of Gram positive bacteria is mediated by calcium ions causing depolarisation and leakage of some ions to induce cell death (Steenbergen, Alder *et al.* 2005, Straus, Hancock 2006, Mascio, Alder *et al.* 2007).NMR analysis of daptomycin in the presence of a 1:1 molar ratio of Ca^{+2} suggested that calcium binds Trp1 and Kyn13 residues on daptomycin in order to enhance its oligomerization and amphipathicity leading to insertion into the membrane and the formation of a micellar structure (Ho, Jung *et al.* 2008). These findings were confirmed by CD spectra as the peptide showed significant conformational change in the presence of 5 mM $CaCl_2$ and PC/PG liposomes, indicating that the binding of daptomycin to the negatively charged model membrane is Ca^{2+} dependent (Jung, Rozek *et al.* 2004).

X-ray photoelectron spectroscopy (XPS) is a surface sensitive analysis technique that characterises and quantifies the elemental composition of surfaces of solid materials. XPS has been used in the last decade to provide insights about the variation of bacterial surface elemental composition at various conditions such as over a range of pH values (Leone, Loring *et al.* 2006) and following Zn^{2+} exposure (Ramstedt, Leone *et al.* 2014). XPS has been used to characterise the chemical changes within ~10 nm of the surface in different *E. coli* LPS mutants with a range

of surface compositions. The analysis is able to detect proteins/peptidoglycan, lipids, and polysaccharides which reveal the changes of LPS content between different mutants that may help in explaining changes in surface hydrophobicity which play a crucial role in protecting bacteria against antimicrobial agents (Ramstedt, Nakao *et al*. 2011). These studies provided important surface compositional biochemical information that can help in exploring molecular level processes at the bacterial surfaces in response to external stimuli which may affect metabolic activity of the cells leading to change of the composition of cell surface molecules. However, the bacterial surface characterisation of elemental composition following the exposure to AMPs has been not examined using XPS before.

The objective of this chapter is to gather information about increasing concentrations of cations that may enhance or decrease the activity of Smp24 which may explain the upregulation of cation binding genes in response to Smp24 treatment as revealed by microarray analysis. In addition, the influence of Smp24 on the elemental composition of *E. coli* surface was analysed using XPS in order to get chemical information on the outermost portion of bacterial cells when treated by Smp24 to provide other insights to help elucidate the mechanism of action of Smp24.

6.2 Method Summary

The effect of salt concentration on the antimicrobial activity of Smp24 was tested by determining the MICs against *E. coli* at various cation concentrations. The surface composition of *E. coli* has monitored using XPS after 10 minutes of incubation with Smp24 at 0 and 12 μg/ml.

6.3 Results

6.3.1 The antimicrobial activity of Smp24 against *E. coli* at different concentrations of cations.

The bactericidal activity of Smp24 against *E. coli* was compared under various concentrations of ions by determining the MIC in a variety of chloride salts. One monovalent cation, Na^+ at concentrations of 0 to 24 mM and four divalent cations Ca^{2+}, Mg^{2+}, Fe^{2+} and Mn^{2+} which were added at 0 to 3 mM. This concentration range indicates excess concentrations of cations and doesn't represent their physiological concentrations. The MIC of Smp24 increased with increasing the ionic strength of Ca^{2+} and Mg^{2+}. Smp24 had an eight-fold increase in MIC at 3 mM of $CaCl_2$ and $MgCl_2$ (p-values were less than 0.05) (Table 6.1). However, the activity of Smp24 was stable at the highest concentration used of NaCl. Also, no significant differences in the MIC of Smp24 were obtained when determined in the presence of divalent cations Fe^{2+} and Mn^{2+}. An increase in Fe^{2+} and Mn^{2+} concentrations was shown to have no effect on the growth rate or viability of *E. coli*.

Table 6.1 The effect of increased cation concentration on the minimum inhibitory concentration (MIC) of Smp24 against *E. coli*.

Cations	Concentrations (mM)	MIC (μg/ml)
No additional ions	0	32
Na^+	3	32
	6	32
	12	32
	24	32
Ca^{2+}	0.375	32
	0.75	64
	1.5	128
	3	256
Mg^{2+}	0.375	64
	0.75	64
	1.5	128
	3	256
Fe^{2+}	0.375	32
	0.75	32
	1.5	32
	3	32
Mn^{2+}	0.375	32
	0.75	32
	1.5	32
	3	32

6.3.2 XPS Analysis of Smp24- treated *E. coli.*

The ion content of Smp24- treated *E. coli* surface was characterised by XPS to determine the effect of the treatment on the chemical structure of the bacterial membrane. Survey scans were successfully collected from bacterial cells at a reduced temperature. However, these scans did not show a significant change to surface ion content as a result of treatment with the peptide in either washed and unwashed samples when compared with a peptide-free control (Figures 6.1 and 6.2). Rich oxygen content was detected in both samples. There was little variation in the C: N ratio between treated and untreated cells. Both Na^+ and Cl^- ions were largely removed by washing with water (Table 6.2 and Table 6.3).

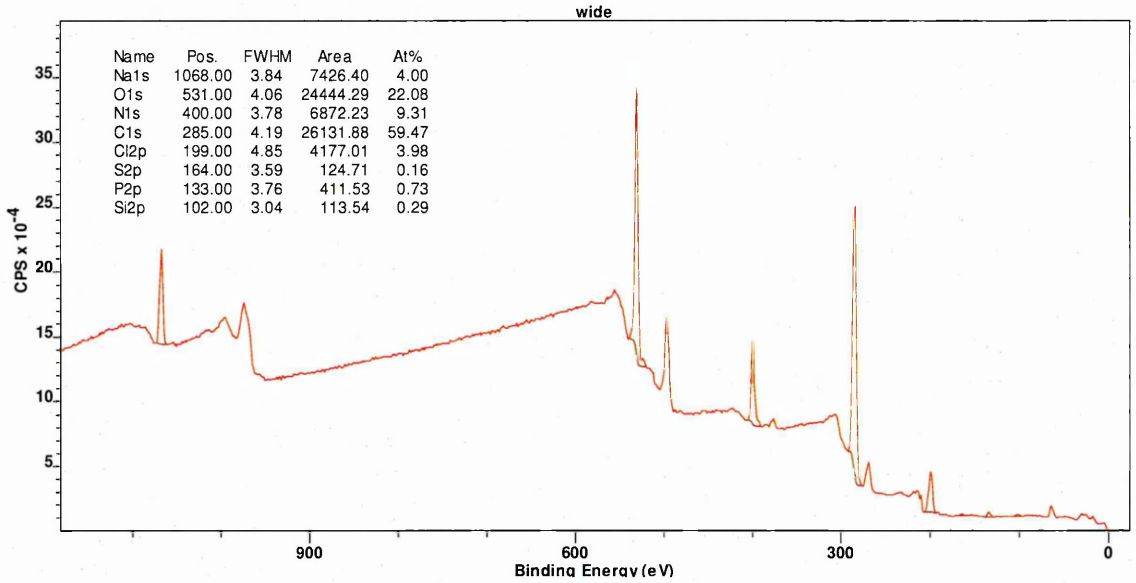

Figure 6.1 XPS survey scan from untreated *E.coli*.

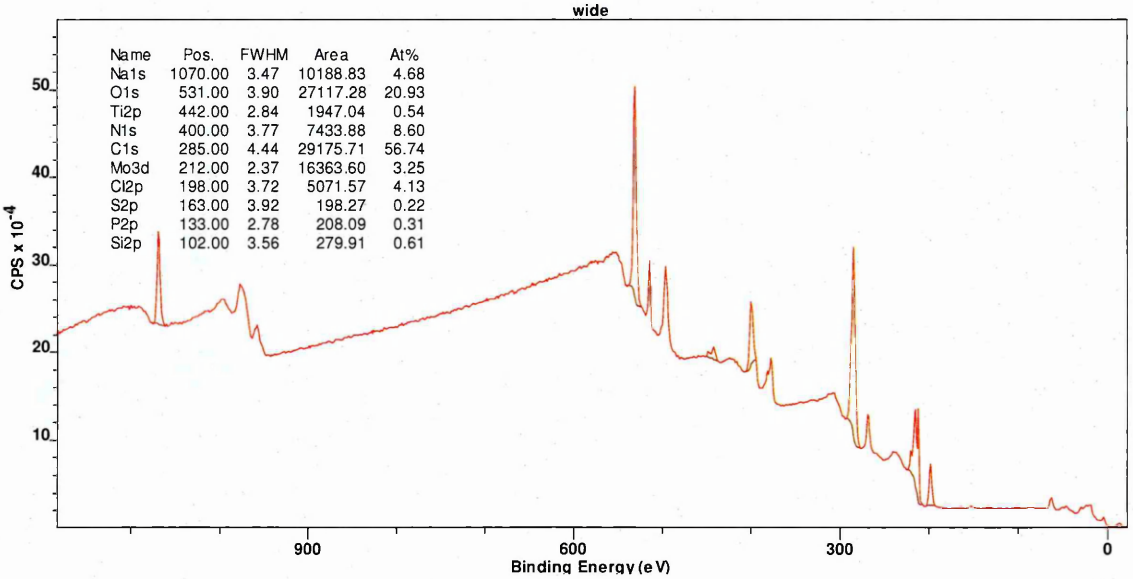

Figure 6.2 XPS survey scan from Smp24-treated *E. coli* after 10 minutes of incubation.

Table 6.2 Surface composition of unwashed samples determined by quantifying survey scans (atomic%).

Sample	Na	F	O	Ti	N	C	Mo	Cl	S	P	Si
Control	4	<0.1	22.1	<0.1	9.3	59.5	<0.1	4	0.2	0.7	0.3
Treated	4.7	<0.1	20.9	0.5	8.6	56.7	3.3	4.1	0.2	0.3	0.6

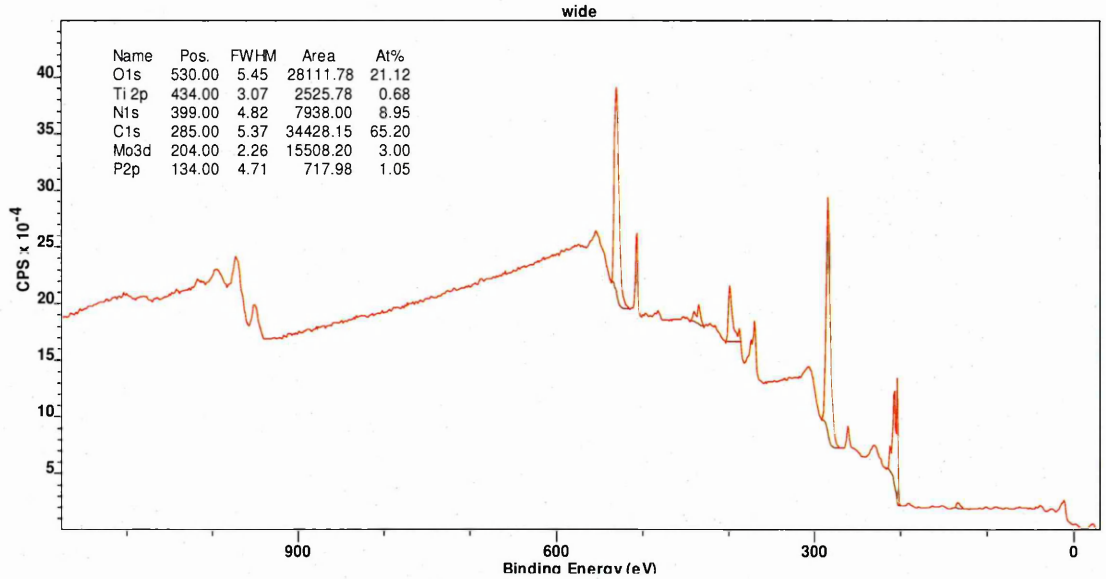

Figure 6.3 XPS survey scan from washed untreated *E.coli*

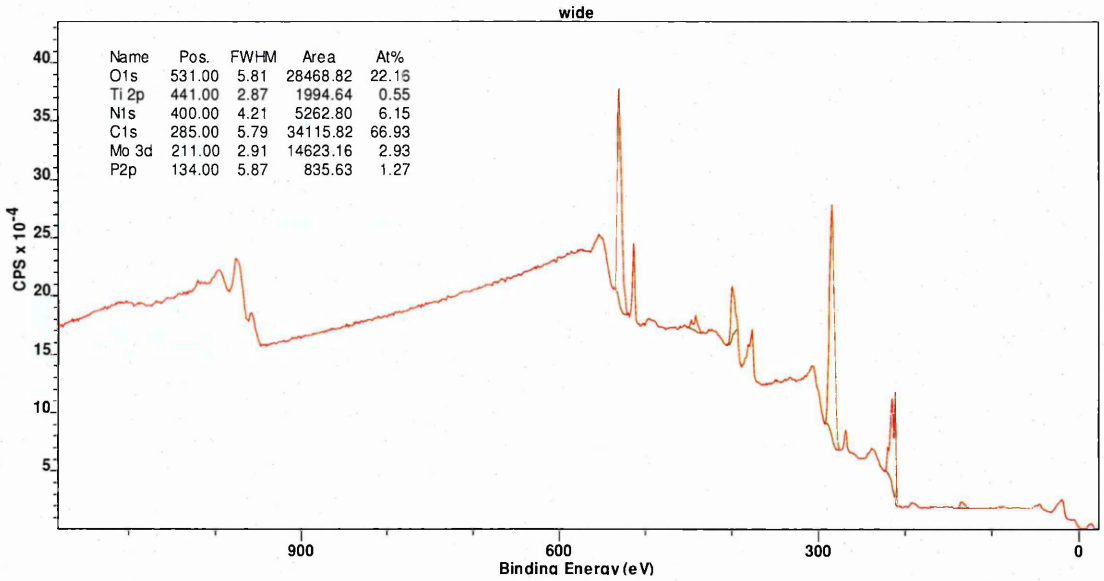

Figure 6.4 XPS survey scan from washed Smp24-treated *E. coli* after 2 hours of incubation.

Table 6.3 Surface composition of washed samples determined by quantifying survey scans (atomic%).

Sample	Na	F	O	Ti	N	C	Mo	Cl	S	P	Si
Control/ washed	<0.1	<0.1	21.1	0.7	9.0	65.2	3.0	<0.1	<0.1	1.1	<0.1
Treated/ washed	<0.1	<0.1	22.2	0.6	6.2	66.9	2.9	<0.1	<0.1	1.3	<0.1

6.4 Discussion

The functional classification of the upregulated genes of *E. coli* in response to Smp24 treatment revealed that the most abundant group of genes was predominantly related to cation binding and transport. These findings indicated that cations may play a role in the mechanism of action of Smp24 against *E. coli.*

The current study showed that the monovalent cation sodium ions Na^+ had no effect on the inhibitory activity of Smp24, while the activity of the peptide was significantly decreased in the presence of the divalent cations, Ca^{2+} and Mg^{2+} as the MIC of Smp24 was higher than in the absence of theses cations. Similar results of the effect of these cations on AMPs have been reported by other investigators. The antibacterial activity of short cationic peptide; Human Beta Defensin 2 (HBD-2) was reduced by the Ca^{2+} and Mg^{2+} ions. Whereas at higher concentration of Na^+, HBD-2 still retained its antimicrobial activity (Tomita, Hitomi *et al.* 2000).

A similar trend has also been reported with three cathelicidin peptides (SMAP29, OaBac5mini and OaBac7.5mini) as Ca^{2+} and Mg^{2+} ions had a larger effect on their antibacterial activities than the monovalent cations. Particularly, SMAP29 was completely inactive against *E. coli* in presence of Ca^{2+} and Mg^{2+} ions at 10mM (Anderson, Yu 2005). Moreover, lactoferricin B is salt sensitive, they decrease or inhibit its antibacterial activity in presence of excess of Na^+, K^+, Mg^{2+} or Ca^{2+} ions(Bellamy, Takase *et al.* 1992).

The antagonistic effect of Ca^{2+} and Mg^{2+} on Smp24 and other cationic AMPs against *E. coli* may occur through competing interactions with these antimicrobial agents.

The cationicity of AMPs is essential to enhance the electrostatic binding to the bacterial membrane, by competitive displacement of cations that are normally cross-linked to the LPS in Gram negative bacteria leading to membrane disruption (Grubor, Meyerholz *et al.* 2006, Ebenhan, Gheysens *et al.* 2014).

Polymyxin is an example of a cationic AMP which disrupts the bacterial membrane through displacing divalent cations from the LPS leading to disorganisation of the membrane (Sahalan, Aziz *et al.* 2013). Such displacement mechanisms have been proposed for cationic AMP such as bactenecin, it showed distinct ability to displace dansyl-polymyxin that were bound to LPS in the dansyl-polymyxin B displacement assay(Wu, Hancock 1999). However, bivalent ions compete with these cationic molecules for anionic binding sites on the cell surface (Tille 2013).

A similar mechanism was also identified for aminoglycoside antibiotics (Yeaman, Yount 2003). The bactericidal activity of gentamicin, streptomycin and related aminoglycoside antibiotics vary significantly in the presence and in the absence of divalent cations (Pimenta de Morais, Corrado *et al.* 1978, KUSSER, ZIMMER *et al.* 1985). The binding of labelled gentamicin to *Pseudomonas aeruginosa* increases in absence of calcium and magnesium ions (Ramirez-Ronda, Holmes *et al.* 1975).

It has been reported that replacement of arginine residues with lysine residues in human α-defensin-1 led to a decrease of its antimicrobial activity and a higher sensitivity to increasing salt concentrations suggesting that lysine is more sensitive to salt than arginine (Zou, de Leeuw *et al.* 2007, Li, Vorobyov *et al.* 2013). Many marine-derived AMPs are tolerant of high salt concentrations. Thus may be because their positive charge is based mainly on arginine rather than lysine (Falanga, Lombardi *et*

al. 2016). However, the cationicity of Smp24 is based mainly on lysine residues which may explain the salt sensitivity.

Similar concentrations of other divalent cations, Fe^{2+} and Mn^{2+}, had no effect on the antimicrobial activity of Smp24 against *E. coli.* In Gram negative bacteria, metals can diffuse across the outer membrane and are transported into the cytosol by ABC transporters (Zhen, Jacobsen *et al*. 2009). The affinity to these transporters for Fe^{2+} and Mn^{2} exceeds that for $Mg2^{+}$ and Ca^{2+}. The tendency preference follows the universal order of the Irving–Williams series ($Mg^{2+} < Ca^{2+} < Mn^{2+} < Fe^{2+}$) (Waldron, Robinson 2009). In addition, specialised chelators such as siderophores are also bind inorganic elements (notably iron) to diffuse across the outer membrane. The iron that is transported into cells by siderophores can act as a signalling agent plays an important regulatory role in iron homoeostasis (Muckenthaler, Galy *et al*. 2008).

In conclusion, calcium and magnesium reduce the activity of Smp24 against *E. coli* which might be a challenge for the application of Smp24 in vivo. Therefore, further modifications are needed for Smp24 to be salt-resistant peptide in order to develop it as novel antimicrobial therapeutic.

The XPS analysis of bacterial samples indicates that this technique is capable of probing the cell surface and collecting data regarding their ion content. However, Smp24-treated samples exhibited quite similar XPS spectra to those of untreated cells, no considerable difference were obtained from both survey scans. These results may be attributed to the depth of the XPS analysis as it was less than 10 nm, where LPS can extend up to 40 nm from the outer membrane of Gram negative cells (Beveridge 1999). Therefore, the analysis was not able to reach deeper to the cell

membrane. It is more challengeable in case of the Gram positive bacteria surface as it has a thick peptidoglycan layer (30–100 nm) containing teichoic acids, lipoteichoic acids, and proteins (Ramstedt, Leone *et al*. 2014).

Similar challenges of the analysis depth were obtained during the XPS analysis of *E. coli* LPS mutants with a varied composition of LPS (Ramstedt, Nakao *et al*. 2011) as the analysis was affected by the presence and size of surface structures and the outer membrane composition. In addition, our analysis revealed that both XPS spectra of control and treated bacterial surfaces were too rich in oxygen that may because the experiment was carried out between -70°C to -39°C, therefore any excess water present will also contribute to the oxygen content. High-resolution spectra (C 1s and O 1s) would have given more information on alterations to functional groups on the bacterial surfaces components such as polysaccharides, peptides, and lipids (Dufrene, van der Wal *et al*. 1997).

In addition, Smp24 may have no effect on the elemental composition of *E. coli*. Higher concentrations of Smp24 or extended incubation periods may affect the balance of ions of the surface of treated cells to be detected by XPS.

7 Current perspective and hypothesised mechanism of action

The progressive development of resistance to classical antimicrobial agents causes an increasing challenge to public health. It has led to an urgent need for novel antimicrobial agents with novel mechanisms of action. AMPs play an essential role in the innate immune system of the host as a first line defence in most living organisms against invaders. They are considered to be useful templates for the design of novel antibiotics (Li, Xiang *et al.* 2012, Seo, Won *et al.* 2012).

Snake and scorpion venoms are diverse sources of biologically active components and various candidate therapeutics have been characterised including AMPs (Harrison, Abdel-Rahman *et al.* 2014). However, the majority of venoms have not been fully exploited as antimicrobial molecules. Therefore, there has been considerable interest in potential novel AMPs from Egyptian snake and scorpion venoms as unexplored sources for such candidates.

Scorpion venom is composed mainly of small peptides. A variety of AMPs have been identified from scorpion venoms using proteomic and genomic techniques. Smp24 and Smp43, two novel AMPs, have been identified from a cDNA library from the venom gland of the Egyptian scorpion *Scorpio maurus palmatus* (Abdel-Rahman, Quintero-Hernandez *et al.* 2013). Both peptides have potent antimicrobial activities against a wide range of Gram positive and Gram negative bacteria and fungi. Smp43 exhibits negligible haemolytic properties, in comparison Smp24 caused significant erythrocyte disruption in a concentration dependent manner. Both peptides induced kidney cell line death in a concentration-dependent manner. However, keratinocytes were not affected by Smp43 at 4x MIC and low cytotoxic activities were detected for both peptides against both cell lines at concentrations higher than the MIC for Gram positive strains. Proteins (> 10 KDa) are the major constituents of snake venom and

include enzymes, which are the main compounds exhibiting antimicrobial activity. Few intermediate sized (3-7 KDa) non-enzymatic proteins with antimicrobial activity have been reported from snake venoms (Wang, Hong *et al.* 2008, Yamane, Bizerra *et al.* 2013, Jin, Bai *et al.* 2016). In the current study four 3FTxs-like proteins have been isolated and partially characterised from three Egyptian elapid venoms *Naja haje*, *Walterinnesia aegyptia* and *Naja nubiae*. 3FTxs have been proposed to destabilize the bilayer of anionic phospholipid-containing model membranes which is similar to the action of most cationic AMPs against bacterial mimic membranes (Dubovskii, Lesovoy *et al.* 2003, Dubovskii, Utkin 2014). The purified proteins exhibited inhibitory activity mainly against *Bacillus subtilis* in comparison with other bacteria. *B. subtilis* has an unusually enriched outer leaflet membrane in the anionic phospholipid PG (Clejan, Krulwich *et al.* 1986, Marquardt, Geier *et al.* 2015). Interestingly, *B. subtilis* is one of the most commonly isolated bacteria from the oral cavity of snakes which may point us in the direction of co-evolution of snakes and this soil bacterium (Fonseca, Moreira *et al.* 2009).

Improvement of the disadvantages that impede the development of AMPs as therapeutic agents is crucial for clinical application of AMPs (Hancock, Sahl 2006). Such limitations include low therapeutic index, high cost of production, salt resistance, gastrointestinal enzymatic degradation , short half-lives and rapid elimination and a broad spectrum of activity which may disrupt the indigenous microflora that protect the host against pathogenic organisms (Bommarius, Jenssen *et al.* 2010, Aoki, Ueda 2013, Mohanram, Bhattacharjya 2016)

High therapeutic indices of AMPs are required to avoid cytotoxic effects on host cells. Cationicity is undoubtedly crucial for the initial electrostatic binding of AMPs to

negatively charged membranes of bacteria (Yeaman, Yount 2003, Aoki, Ueda 2013). However, the electrostatic binding of AMPs is less important for mammalian membranes due to their zwitterionic nature. Although truncation of the last four C-terminal residues of Smp24 resulted in a reduction in net positive charge, it increased the therapeutic index as it displayed less haemolytic effect than that of the unmodified peptide (Harrison, Heath *et al.* 2016). Similar modifications increase the potency and specificity of some scorpion AMPs for bacterial cells and thus improves their therapeutic indices (Rodríguez, Villegas *et al.* 2014, Luna-Ramirez, Tonk *et al.* 2017).

The understanding of the fundamental mechanism of AMP action is critical to the development of AMP-based antibiotics (Nguyen, Haney *et al.* 2011, Yang, Wang *et al.* 2013). Synthetic bilayer model membranes created to mimic the properties of living cells membranes help researchers to investigate AMP-membrane interactions based on the structure and hydrophilicity/hydrophobicity of AMPs and the composition of lipid model membranes. Such biophysical interactions provide insights about AMP transport, distribution and efficacy improving our understanding of AMP mechanisms of action (Peetla, Stine *et al.* 2009). However, not surprisingly, model membrane systems do not fully explain the interaction with microbial membranes or the response of microbes to the presence of AMPs (Omardien, Brul *et al.* 2016). Previously, Smp peptides were found to cause pore formation in synthetic prototypical prokaryotic and eukaryotic membranes (Harrison, Heath *et al.* 2016). However, the mechanism of action of AMPs against the living cell membrane may include more complicated mechanistic interactions compared with simple artificial systems (Gee, Burton *et al.* 2013).

Microscopic imaging includes useful techniques that may be used to explore the antimicrobial action of AMPs against living cell membranes (Torrent, Sánchez-Chardi *et al.* 2010). Of interest are SEM and TEM which provide an overall picture of damage of the bacterial cell envelope upon AMP exposure (Hartmann, Berditsch *et al.* 2010). EM micrographs of *E. coli* and *S. aureus* treated with Smp24 and Smp43 revealed changes in cell morphology. Similar EM data have been reported for several AMPs against *E. coli* and *S. aureus* such as cathelicidin-related AMPs (Chen *et al.*, 2009), moricin (Hu *et al.*, 2013) and human lactoferrin peptide HLP2 (Chapple *et al.*, 1998). These findings indicated the permeabilisation effect of cationic AMPs against bacterial cells (Makobongo, Gancz *et al.* 2012, Verdon, Coutos-Thevenot *et al.* 2016)

However, even though SEM and TEM are complementary techniques for observing alterations in bacterial membrane integrity of cells treated with AMPs, it cannot clarify the detailed mechanisms of cell death. Therefore, a combination of different methods and techniques are needed as to gain a better understanding of the mode of action of AMPs or the response of bacteria to AMPs (Hartmann, Berditsch *et al.* 2010, Omardien, Brul *et al.* 2016).

DNA microarray has been used to analyse the transcriptomic responses of *E. coli* stressed by subinhibitory concentrations of Smp24 and Smp43 with polymyxin B as a positive control. This analysis identified approximately 2% of *E. coli* genes were significantly differentially expressed in response to each peptide treatment. Siderophore biosynthesis, cellular respiration, oxidative stress response and di - tri valent ion binding and transport were the most biologically important gene groups following exposure to Smp peptides and were similar to those clustered for polymyxin B -induced differentially expressed genes. The deletion of genes involved in the

biosynthesis of sideorphores and the transport of ions increase resistance to Smp24 compared with the parent strain. In contrast, mutants with decreased resistance to Smp24 and Smp43 were associated with oxidative stress responses and anaerobic respiration.

Beyond the known function of siderophores as an iron uptake-facilitator, several lines of evidence indicate that siderophores play an alternative role in bacteria as an antioxidant cytoprotector (Achard, Maud ES, *et al* 2013) (Johnstone, 2015). It was found that hydrolysed enterobactin in *E. coli* has exposed hydroxyl groups that can scavenge radicals and therefore reduce oxidative stress. Therefore, siderophore biosynthesis can be mediated by agents that affect oxidative stress (Adler, Corbalán *et al*. 2012, Adler, Corbalan *et al*. 2014)

Many genes of the respiratory chain were found to be downregulated following exposure to Smp peptides and polymyxin B. Downregulation of these components may contribute significantly to the change in membrane potential, and the reduced respiration may lead to a decline in energy consumption (Liu, Dong *et al*. 2013). The deletion of these genes increased susceptibility to Smp24 and Smp43.

Cell envelope perturbations following exposure to Smp peptides, as seen in EM micrographs, may induce common signalling pathways that ultimately lead to internal oxidative stress and misregulation of iron homoeostasis (Sikora, Beyhan *et al*. 2009b). AMPs disturb membrane structural integrity and function through disturbing proteins involved in energy generation and redox balancing (Hurdle, O'neill *et al*. 2011). Oxidative stress can be an important contributor to the lethal effect of these nonspecific- target agents (Guilhelmelli, Vilela *et al*. 2014). Oxidative stress results in a

more general cellular response leading to bacterial self-destruction by internal production of hydroxyl radicals (Feld, Louise,2012)

It has been proposed that positively charged AMPs similar to the Smp peptides and affect redox status or electron transfer. Cationic cathelicidin peptide LL-37 was found to influence the redox and ion status of cells. It enhanced production of reactive oxygen species causing lethal membrane depolarization (Liu, Dong *et al.* 2013). It has been reported that polymyxin can possibly induce oxidative stress by ROS through the accumulation of hydroxyl radical (•OH) which readily damages DNA, lipids, and proteins and ultimately results in cell death (Yu, Zhiliang, *et al.* 2015) (Yu, Zhiliang, *et al.* 2017).

Cation deficiency or the displacement of Mg^{2+} and Ca^{2+} may result in oxidative stress. It was found that an increase in the concentration of ions like calcium may induce oxidative defences by signalling the bacteria to upregulate antioxidant proteins (Rosch, Jason W., *et al.*2008). These findings may support the oxidative stress induced effect by Smp24 which has been found to be sensitive to the presence of Ca^{2+} and Mg^{2+}. Therefore, a quantitative study of ROS release in cells following exposure to Smp peptides is required to assess the role of oxidative stress in the antibacterial action of Smp peptides.

Data and observations obtained for the different methods in this study have resulted in a proposed transport mechanism for Smp24 across the cell envelope membranes of Gram negative bacteria (Figure 7.1). We propose that the integration of cationic peptides like Smp24 into the membrane may disturb metal cation homeostasis. The most differentially expressed genes following Smp24 exposure were cation binding

and transport. Smp24 also upregulates siderophore biosynthesis and transport genes. Siderophore receptors are multifunctional proteins that can transport the antibiotics such as albomycin and rifamycin across the outer membrane. The involvement of a siderophore receptors in susceptibility to Smp24 was supported by the observation that siderophore receptor-mutant *E. coli* strain was resistant to Smp24. Disruption of metal ions homeostasis is highly associated with oxidative stress. Therefore, increasing concentrations of cations may protect bacteria from oxidative stress induced by Smp24. Oxidative stress inactivates Fe-S dependent and leads to the release of ferrous irons (Fe2+) which is oxidized to ferric iron (Fe3+), along with the formation of •OH, which is called the Fenton reaction and may also mediate siderophore biosynthesis for the chelation Fe3+ and prevent the formation of •OH. Oxidative stress can also result from decreased protection against oxidants. Siderophore biosynthesis is regulated by the ferric uptake regulator (Fur) which is an iron protein that tends to lose activity under oxidative stress, and could potentially lead to depression of the iron acquisition system and the stimulation of iron import. The downregulation of transcriptional (bacterial Fur) regulators and iron-sulfur clusters which mediate electron transfer to the Fe-siderophore substrate results in the expression of a broad array of genes involved mainly in iron acquisition or reactive oxygen species (ROS) protection. The deletion of oxidative stress-response genes have increases the sensitivity of *E. coli* to Smp24. High levels of ROS can induce lipid peroxidation leading to disruption the membrane lipid bilayer and the integrity of cell membranes as seen even at low concentration of Smp24 against *E. coli*.

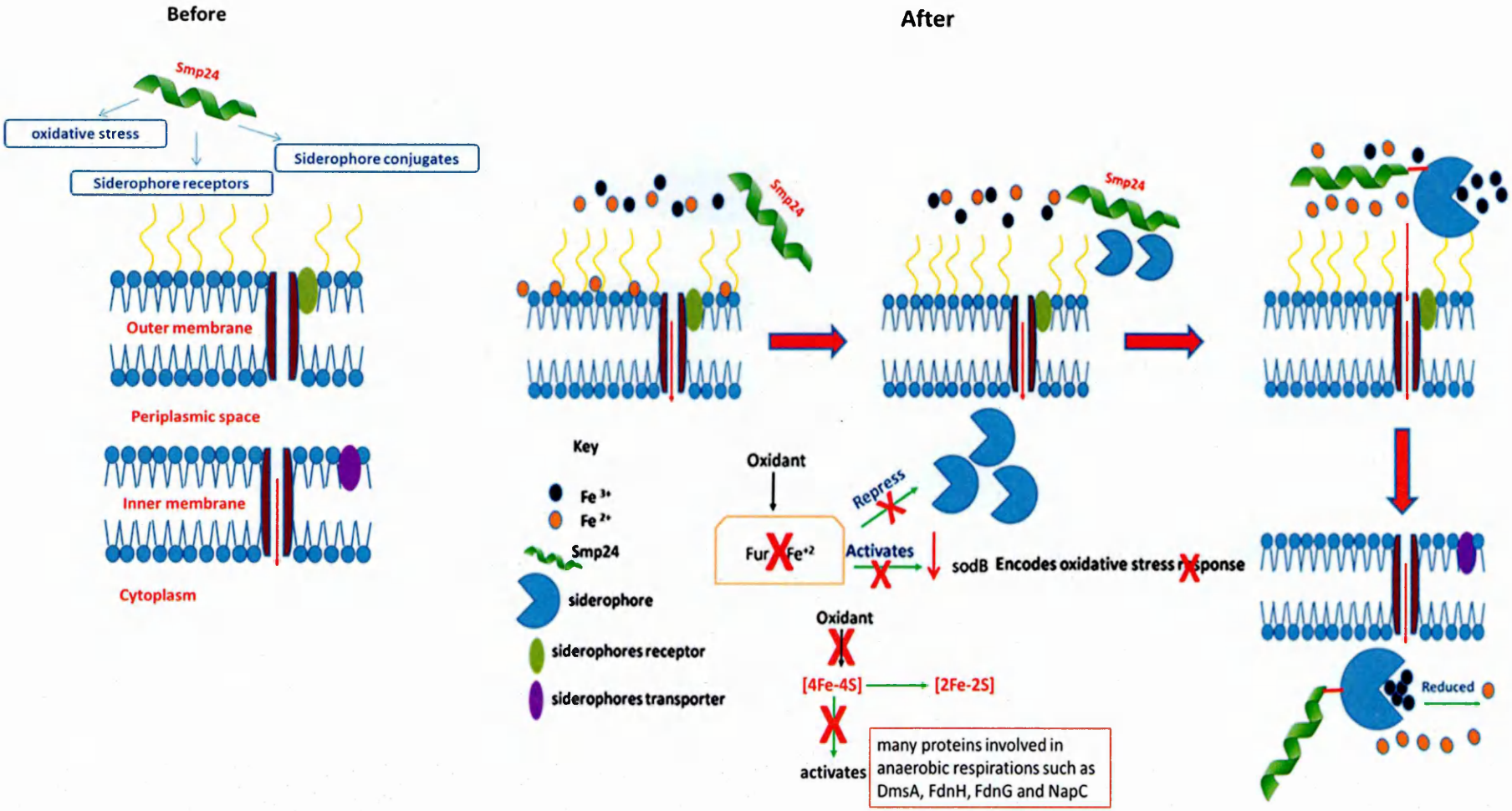

Figure 7.1 Proposed mechanism of interaction of Smp24 with the cell envelope of Gram negative bacteria.

Results obtained in this study support the idea that venoms are a viable source of AMPs and that microscopy, biochemical and transcriptomic approaches can be used in drug discovery to successfully develop new AMPs. These results indicate that the identified AMPs from both scorpion and snake venoms were found to exhibit promising antibacterial activities with favorable cytotoxic effects. Progress has been made in understanding the mode of action of AMPs and the response of bacteria to these peptides. These properties can be used as a starting point to develop AMPs as a promising template for the design of novel classes of antibacterial agents to help overcome the crisis of antimicrobial resistance.

Salt-sensitivity may limit the clinical use of Smp peptides as novel antimicrobial therapeutics. Different strategies have been employed to overcome salt resistance to some AMPs. Increasing helix stability of salt-sensitive AMPs by the introduction of helix-capping motifs at the helix termini resulted in structurally stable peptides with potent antimicrobial activities in high salt concentrations (Park, Cho *et al.* 2004). Nature produces a number of salt-resistant AMPs such as marine-derived AMPs which have evolved to adapt to the high salt concentration in sea water. Salt tolerance of marine-derived AMPs may be attributed to their cationicity being mainly based on arginine rather than lysine residues. Understanding the chemical tolerance mechanisms of marine AMPs may represent a valuable approach for the design of novel salt-resistant AMPs (Fedders, Michalek *et al.* 2008, Falanga, Lombardi *et al.* 2016). Like scorpions and snakes, marine organisms are another attractive source to isolate and characterise novel AMPs.

Although the purified snake proteins discussed in this thesis have limited cytotoxic and no haemolytic properties, much more work is required in order to evaluate their

potential as antimicrobial templates. In general, 3FTxs have limited promise in this regard due to their neurotoxic and cardiotoxic effects as well as synthesis difficulties due to their size and the presence of disulfide bonds. (Fruchart-Gaillard, Mourier *et al.* 2012, Chandrudu, Simerska *et al.* 2013). Nevertheless, investigating the structure-function relationships of these molecules using an alanine scanning method to determine the key functional residues that bind phospholipids and disturb the membrane surface may help in the synthesis of shorter peptides mimicking 3FTxs with increased antibacterial activity and better therapeutic characteristics (Iannucci, González *et al.* 2011, Cantisani, Finamore *et al.* 2014). It was found that alteration of the positive charges of Lysine residues to neutral or negative charges resulted in the loss of the lytic activity of CTX-1 from *Naja nigricollis crawshawii* venom (Kini, Evans 1989).

High production cost of AMPs presents a real obstacle to the pharmaceutical industry. Peptide synthesis costs five to twenty times as much as the synthesis of small organic molecule classical antibiotics. Expression and purification of AMPs in *E. coli* is an obvious alternative method for the production of synthetic AMPs but it is limited by the antimicrobial activity of AMPs against the host and peptide susceptibility to proteolytic degradation by the host cell (Giuliani, Pirri *et al.* 2007). The production of a fusion protein between an AMP and Small Ubiquitin-like Modifier (SUMO) protein protects the peptide from the host degradation enzymes and bacteria from the toxicity of AMP and can be scaled up for industrial-scale production for therapeutic use (Bommarius, Jenssen *et al.* 2010).

Poor stability of AMPs in serum has also limited their use as novel therapeutics. However, disulfide-bridged peptides are more resistant to protease degradation than

linear peptides, therefore joining the terminal ends of peptides by disulfide-bridges (cyclisation) constrains the peptide structure and thereby enhances antimicrobial activity (Brewer, Lajoie 2002, Rozek, Powers *et al.* 2003, Nan, Shin 2011)

The delivery of AMPs is another crucial factor limiting their clinical application. Systemic and pre-systemic enzymatic degradation and rapid hepatic and renal removal from the circulation are challenging for oral and systemic administration routes. Therefore, the most common administration route of AMPs is localised topical application (Mahlapuu, Håkansson *et al.* 2016). Several types of nanotools have been used successfully to deliver AMPs providing specificity to particular cell types or locations (Brandelli 2012, Urban, Jose Valle-Delgado *et al.* 2012). Recently Silva, Gonçalves *et al.* (2016) have succeeded in reducing proteolytic degradation of LL-37 by encapsulating the peptide with nanogels. This nanocarrier stabilises the peptide and delivers it towards the main infected sites leading to the reduction of its cytotoxic activities with increased efficacy against *Mycobacterium tuberculosis in vivo* (Silva, Gonçalves *et al.* 2016). Interestingly, some nanomaterials have antimicrobial activities independent of AMPs which can enhance the inhibitory activity of peptides and reduce any potential bacterial resistance (Malmsten 2011).

The synergistic effect of antibiotics combined with AMPs is a valuable approach to overcome the increasing recurrence and rising of antibiotic resistance rates. Such combinations enhance the potency of antibiotics making them effective against more than one target in the cell and maximises the concentration of antimicrobial agents at the site of infection. Membrane perturbation or pore formation on the bacterial surface may facilitate the uptake and access of antibiotics into the bacterial cell (Giuliani, Pirri *et al.* 2007, Nuding, Frasch *et al.* 2014). Some successful combinations of

antibiotics with AMPs has led to an increase in antibacterial activity of conventional antibiotics such as erythromycin and rifampicin (Ulvatne, Karoliussen *et al*. 2001).

Further research is needed for to better understanding of the mechanisms of action of Smp peptide to develop their potency and stability.

References

ABDEL-RAHMAN, M.A., QUINTERO-HERNANDEZ, V. and POSSANI, L.D., 2013. Venom proteomic and venomous glands transcriptomic analysis of the Egyptian scorpion *Scorpio maurus palmatus* (Arachnida: Scorpionidae). *Toxicon,* **74**, pp. 193-207.

ABDULKADIR, M. and WALIYU, S., 2012. Screening and isolation of the soil bacteria for ability to produce antibiotics. *European Journal of applied sciences,* **4**(5), pp. 211-215.

ABRAHAM, E. and CHAIN, E., 1942. Purification of penicillin. *Nature,* **149**(328), pp. 149.

ABRAHAM, T., PRENNER, E.J., LEWIS, R.N.A.H., MANT, C.T., KELLER, S., HODGES, R.S. and MCELHANEY, R.N., 2014. Structure–activity relationships of the antimicrobial peptide gramicidin S and its analogs: Aqueous solubility, self-association, conformation, antimicrobial activity and interaction with model lipid membranes. *Biochimica et Biophysica Acta (BBA) - Biomembranes,* **1838**(5), pp. 1420-1429.

ACHARD, M.E., CHEN, K.W., SWEET, M.J., WATTS, R.E., SCHRODER, K., SCHEMBRI, M.A. and MCEWAN, A.G., 2013. An antioxidant role for catecholate siderophores in Salmonella. *The Biochemical journal,* **454**(3), pp. 543-549.

ADLER, C., CORBALAN, N.S., PERALTA, D.R., POMARES, M.F., DE CRISTÓBAL, R.E. and VINCENT, P.A., 2014. The alternative role of enterobactin as an oxidative stress protector allows *Escherichia coli* colony development. *PloS one,* **9**(1), pp. e84734.

ADLER, C., CORBALÁN, N.S., SEYEDSAYAMDOST, M.R., POMARES, M.F., DE CRISTÓBAL, R.E., CLARDY, J., KOLTER, R. and VINCENT, P.A., 2012. Catecholate siderophores protect bacteria from pyochelin toxicity. *PloS one,* **7**(10), pp. e46754.

ALEWOOD, P., ALLERTON, C. and FOX, D., 2013. *Pain Therapeutics: Current and Future Treatment Paradigms.* Royal Society of Chemistry.

ALMAAYTAH, A., TARAZI, S., ABU-ALHAIJAA, A., ALTALL, Y., ALSHAR'I, N., BODOOR, K. and AL-BALAS, Q., 2014. Enhanced antimicrobial activity of AamAP1-Lysine, a novel synthetic peptide analog derived from the scorpion venom peptide AamAP1. *Pharmaceuticals,* **7**(5), pp. 502-516.

ALMEIDA, D.D., SCORTECCI, K.C., KOBASHI, L.S., AGNEZ-LIMA, L.F., MEDEIROS, S.R., SILVA-JUNIOR, A.A., DE LM JUNQUEIRA-DE-AZEVEDO, I. and DE F FERNANDES-

PEDROSA, M., 2012. Profiling the resting venom gland of the scorpion *Tityus stigmurus* through a transcriptomic survey. *BMC genomics,* **13**(1), pp. 1.

ANBAZHAGAN, V., REDDY, P.S. and YU, C., 2007. Cardiotoxin from taiwan cobra (Naja naja atra): Structure, dynamics, interaction and protein folding. *Toxin Reviews,* **26**(2), pp. 203-229.

ANDERSON, R.C. and YU, P., 2005. Factors affecting the antimicrobial activity of ovine-derived cathelicidins against *E. coli* 0157: H7. *International journal of antimicrobial agents,* **25**(3), pp. 205-210.

ANDERSON, R.C., HAVERKAMP, R.G. and YU, P.L., 2004. Investigation of morphological changes to *Staphylococcus aureus* induced by ovine-derived antimicrobial peptides using TEM and AFM. *FEMS microbiology letters,* **240**(1), pp. 105-110.

ANDRA, J., JAKOVKIN, I., GROTZINGER, J., HECHT, O., KRASNOSDEMBSKAYA, A.D., GOLDMANN, T., GUTSMANN, T. and LEIPPE, M., 2008. Structure and mode of action of the antimicrobial peptide arenicin. *The Biochemical journal,* **410**(1), pp. 113-122.

AOKI, W. and UEDA, M., 2013. Characterization of antimicrobial peptides toward the development of novel antibiotics. *Pharmaceuticals,* **6**(8), pp. 1055-1081.

ARENDT, W., HEBECKER, S., JAGER, S., NIMTZ, M. and MOSER, J., 2012. Resistance phenotypes mediated by aminoacyl-phosphatidylglycerol synthases. *Journal of Bacteriology,* **194**(6), pp. 1401-1416.

ARUNMANEE, W., PATHANIA, M., SOLOVYOVA, A.S., LE BRUN, A.P., RIDLEY, H., BASLE, A., VAN DEN BERG, B. and LAKEY, J.H., 2016. Gram-negative trimeric porins have specific LPS binding sites that are essential for porin biogenesis. *Proceedings of the National Academy of Sciences of the United States of America,* **113**(34), pp. E5034-43.

AUDRAIN, B., FERRIERES, L., ZAIRI, A., SOUBIGOU, G., DOBSON, C., COPPEE, J.Y., BELOIN, C. and GHIGO, J.M., 2013. Induction of the Cpx envelope stress pathway contributes to *Escherichia coli* tolerance to antimicrobial peptides. *Applied and Environmental Microbiology,* **79**(24), pp. 7770-7779.

AVITABILE, C., D'ANDREA, L.D. and ROMANELLI, A., 2014. Circular dichroism studies on the interactions of antimicrobial peptides with bacterial cells. *Scientific reports,* **4**, pp. 4293.

AYALA-CASTRO, C., SAINI, A. and OUTTEN, F.W., 2008. Fe-S cluster assembly pathways in bacteria. *Microbiology and molecular biology reviews : MMBR,* **72**(1), pp. 110-25, table of contents.

BABALOLA, M. and BALOGUN, J., 2013. The ecology and potential health risk of the oral microflora of *Python regius* and *Clelia scyntalina*. *International Journal of Microbiology Research,* **5**(1), pp. 349.

BADDILEY, J., HANCOCK, I. and SHERWOOD, P., 1973. X-ray photoelectron studies of magnesium ions bound to the cell walls of Gram positive bacteria. *Nature*, **243**(5401), pp.43-45.

BAHAR, A.A. and REN, D., 2013. Antimicrobial peptides. *Pharmaceuticals,* **6**(12), pp. 1543-1575.

BARBER, M., 1961. Methicillin-resistant staphylococci. *Journal of clinical pathology,* **14**, pp. 385-393.

BARNWAL, B., JOBICHEN, C., GIRISH, V.M., FOO, C.S., SIVARAMAN, J. and KINI, R.M., 2016. Ringhalexin from Hemachatus haemachatus: A novel inhibitor of extrinsic tenase complex. *Scientific reports,* **6**, pp. 25935.

BARRIOS, L.H.R., 2013. Adaptive Evolution for the Study of Complex Phenotypes in Microbial Systems (Doctoral dissertation, Texas A&M University).

BARSUKOV, L., KULIKOV, V. and BERGELSON, L., 1976. Lipid transfer proteins as a tool in the study of membrane structure. Inside-outside distribution of the phospholipids in the protoplasmic membrane of Micrococcuslysodeikticus. *Biochemical and biophysical research communications,* **71**(3), pp. 704-711.

BASTOS, H.M., 2012. *Salmonella Associated with Snakes (Suborder Serpentes).* INTECH Open Access Publisher.

BAUER, F., SCHWEIMER, K., KLÜVER, E., CONEJO-GARCIA, J., FORSSMANN, W., RÖSCH, P., ADERMANN, K. and STICHT, H., 2001. Structure determination of human and murine β-defensins reveals structural conservation in the absence of significant sequence similarity. *Protein Science,* **10**(12), pp. 2470-2479.

BAUMANN, G. and MUELLER, P., 1974. A molecular model of membrane excitability. *Journal of supramolecular structure,* **2**(5-6), pp. 538-557.

BAZZO, R., TAPPIN, M.J., PASTORE, A., HARVEY, T.S., CARVER, J.A. and CAMPBELL, I.D., 1988. The structure of melittin. *European Journal of Biochemistry,* **173**(1), pp. 139-146.

BECHINGER, B., ZASLOFF, M. and OPELLA, S.J., 1998. Structure and Dynamics of the Antibiotic Peptide PGLa in Membranes by Solution and Solid-State Nuclear Magnetic Resonance Spectroscopy. *Biophysical journal,* **74**(2), pp. 981-987.

BECHINGER, B. and LOHNER, K., 2006. Detergent-like actions of linear amphipathic cationic antimicrobial peptides. *Biochimica et Biophysica Acta (BBA) - Biomembranes,* **1758**(9), pp. 1529-1539.

BECUCCI, L., VALENSIN, D., INNOCENTI, M. and GUIDELLI, R., 2014. Dermcidin, an anionic antimicrobial peptide: influence of lipid charge, pH and Zn 2 on its interaction with a biomimetic membrane. *Soft Matter,* **10**(4), pp. 616-626.

BELLAMY, W., TAKASE, M., WAKABAYASHI, H., KAWASE, K. and TOMITA, M., 1992. Antibacterial spectrum of lactoferricin B, a potent bactericidal peptide derived from the N-terminal region of bovine lactoferrin. *Journal of Applied Bacteriology,* **73**(6), pp. 472-479.

BELOKONEVA, O.S., VILLEGAS, E., CORZO, G., DAI, L. and NAKAJIMA, T., 2003. The hemolytic activity of six arachnid cationic peptides is affected by the phosphatidylcholine-to-sphingomyelin ratio in lipid bilayers. *Biochimica et Biophysica Acta (BBA)-Biomembranes,* **1617**(1), pp. 22-30.

BÉRDY, J., 2012. Thoughts and facts about antibiotics: where we are now and where we are heading. *The Journal of antibiotics,* **65**(8), pp. 385-395.

BERGLUND, N.A., PIGGOT, T.J., JEFFERIES, D., SESSIONS, R.B., BOND, P.J. and KHALID, S., 2015. Interaction of the antimicrobial peptide polymyxin B1 with both membranes of E. coli: a molecular dynamics study. *PLoS Comput Biol,* **11**(4), pp. e1004180.

BERNIER, S.P. and SURETTE, M.G., 2007. Concentration-dependent activity of antibiotics in natural environments. *The multiple roles of antibiotics and antibiotic resistance in nature.* Frontiers in microbiology, **4**. .

BEVERIDGE, T.J., 1999. Structures of gram-negative cell walls and their derived membrane vesicles. *Journal of Bacteriology,* **181**(16), pp. 4725-4733.

BHAGWAT, A.A., YING, Z.I., KARNS, J. and SMITH, A., 2013. Determining RNA quality for NextGen sequencing: some exceptions to the gold standard rule of 23S to 16S rRNA ratio §. *Microbiology Discovery,* **1**(1), pp. 10.

BILWES, A., REES, B., MORAS, D., MENEZ, R. and MENEZ, A., 1994. X-ray Structure at 1· 55 Å of Toxin γ, a Cardiotoxin from Naja nigricollis Venom: Crystal Packing Reveals a Model for Insertion into Membranes. *Journal of Molecular Biology,* **239**(1), pp. 122-136.

BLAYLOCK, R.S.M., 2000. Antibacterial properties of KwaZulu Natal snake venoms. *Toxicon,* **38**(11), pp. 1529-1534.

BOMMARIUS, B., JENSSEN, H., ELLIOTT, M., KINDRACHUK, J., PASUPULETI, M., GIEREN, H., JAEGER, K., HANCOCK, R. and KALMAN, D., 2010. Cost-effective expression and purification of antimicrobial and host defense peptides in Escherichia coli. *Peptides,* **31**(11), pp. 1957-1965.

BOTES, D.P., 1971. Snake venom toxins. The amino acid sequences of toxins and from Naja nivea venom and the disulfide bonds of toxin. *The Journal of biological chemistry,* **246**(23), pp. 7383-7391.

BRAHMACHARY, M., KRISHNAN, S.P., KOH, J.L., KHAN, A.M., SEAH, S.H., TAN, T.W., BRUSIC, V. and BAJIC, V.B., 2004. ANTIMIC: a database of antimicrobial sequences. *Nucleic acids research,* **32**(Database issue), pp. D586-9.

BRANDELLI, A., 2012. Nanostructures as promising tools for delivery of antimicrobial peptides. *Mini reviews in medicinal chemistry,* **12**(8), pp. 731-741.

BRAUN, V., PRAMANIK, A., GWINNER, T., KÖBERLE, M. and BOHN, E., 2009. Sideromycins: tools and antibiotics. *Biometals,* **22**(1), pp. 3-13.

BRAZAS, M.D. and HANCOCK, R.E., 2005. Using microarray gene signatures to elucidate mechanisms of antibiotic action and resistance. *Drug discovery today,* **10**(18), pp. 1245-1252.

BREDESEN, J., BERG, T., FIGENSCHOU, K., FRØHOLM, L. and LALAND, S., 1968. Purification of the gramicidin S synthesizing activity in *Bacillus brevis* extracts. *European Journal of Biochemistry,* **5**(3), pp. 433-436.

BRENDER, J.R., MCHENRY, A.J. and RAMAMOORTHY, A., 2012. Does cholesterol play a role in the bacterial selectivity of antimicrobial peptides? *Antimicrobial Peptides: Utility Players in Innate Immunity,* , pp. 27.

BREUKINK, E. and DE KRUIJFF, B., 2006. Lipid II as a target for antibiotics. *Nature reviews Drug discovery,* **5**(4), pp. 321-323.

BREWER, D. and LAJOIE, G., 2002. Structure-based design of potent histatin analogues. *Biochemistry,* **41**(17), pp. 5526-5536.

BURDON-SANDERSON, J., 1871. Memoirs: The origin and distribution of microzymes (bacteria) in water, and the circumstances which determine their existence in the tissues and liquids of the living body. *Quarterly J Microscop Sci,* **11**, pp. 323-352.

BUSTILLO, S., LEIVA, L.C., MERINO, L., ACOSTA, O., BAL DE KIER JOFFÉ, E and GORODNER, J.O., 2008. Antimicrobial activity of *Bothrops alternatus* venom from the Northeast of Argentine. *Rev Latinoam Microbiol,* **50**(3-4), pp. 79-82.

BUTLER, M.S., BLASKOVICH, M.A. and COOPER, M.A., 2016. Antibiotics in the clinical pipeline at the end of 2015. *The Journal of antibiotics,* .

CALVETE, J.J., MARCINKIEWICZ, C., MONLEÓN, D., ESTEVE, V., CELDA, B., JUÁREZ, P. and SANZ, L., 2005. Snake venom disintegrins: evolution of structure and function. *Toxicon,* **45**(8), pp. 1063-1074.

CANTISANI, M., FINAMORE, E., MIGNOGNA, E., FALANGA, A., NICOLETTI, G.F., PEDONE, C., MORELLI, G., LEONE, M., GALDIERO, M. and GALDIERO, S., 2014. Structural insights into and activity analysis of the antimicrobial peptide myxinidin. *Antimicrobial Agents and Chemotherapy,* **58**(9), pp. 5280-5290.

CARBONE, M.A. and MACDONALD, P.M., 1996. Cardiotoxin II segregates phosphatidylglycerol from mixtures with phosphatidylcholine: 31P and 2H NMR spectroscopic evidence. *Biochemistry,* **35**(11), pp. 3368-3378.

CARNICELLI, V., LIZZI, A., PONZI, A., AMICOSANTE, G., BOZZI, A. and DI GIULIO, A., 2013. Interaction between antimicrobial peptides (AMPs) and their primary target, the biomembranes. *Microbial Pathogens and Strategies for Combating Them: Science, Technology and Education,* **2**, pp. 1123-1134.

CASTILLO, J.C., REYNOLDS, S.E. and ELEFTHERIANOS, I., 2011. Insect immune responses to nematode parasites. *Trends in parasitology,* **27**(12), pp. 537-547.

CENDRON, L.H., BERTOL, C.D., FUENTEFRIA, D.B., CALEGARI, E.M., DALLEGRAVE, E., MOURA, D.J., MOURA, K., DA GRAÇA MARQUES, M. and ROSSATO, L.G., 2014. Broad Antibacterial Activity of *Bothrops jararaca* Venom against Bacterial Clinical Isolates. *Advances in Microbiology,* **4**(16), pp. 1174.

CHAN, D.I., PRENNER, E.J. and VOGEL, H.J., 2006a. Tryptophan-and arginine-rich antimicrobial peptides: structures and mechanisms of action. *Biochimica et Biophysica Acta (BBA)-Biomembranes,* **1758**(9), pp. 1184-1202.

CHAN, P.F., MACARRON, R., PAYNE, D.J., ZALACAIN, M. and HOLMES, D.J., 2002. Novel antibacterials: a genomics approach to drug discovery. *Current Drug Targets-Infectious Disorders,* **2**(4), pp. 291-308.

CHAN, D.I., PRENNER, E.J. and VOGEL, H.J., 2006b. Tryptophan- and arginine-rich antimicrobial peptides: Structures and mechanisms of action. *Biochimica et Biophysica Acta (BBA) - Biomembranes,* **1758**(9), pp. 1184-1202.

CHANDA, C., SARKAR, A., SISTLA, S. and CHAKRABARTY, D., 2013. Anti-platelet activity of a three-finger toxin (3FTx) from Indian monocled cobra (*Naja kaouthia*) venom. *Biochemical and biophysical research communications,* **441**(3), pp. 550-554.

CHANDRUDU, S., SIMERSKA, P. and TOTH, I., 2013. Chemical methods for peptide and protein production. *Molecules,* **18**(4), pp. 4373-4388.

CHAPPLE, D.S., MASON, D.J., JOANNOU, C.L., ODELL, E.W., GANT, V. and EVANS, R.W., 1998. Structure-function relationship of antibacterial synthetic peptides homologous to a helical surface region on human lactoferrin against *Escherichia coli* serotype O111. *Infection and immunity,* **66**(6), pp. 2434-2440.

CHEN, C., ROSE, J., HSIAO, C., LEE, T., WU, W. and WANG, B., 1991. Preliminary crystallographic analysis of cardiotoxin V with major fusion activity from Taiwan cobra (*Naja naja atra*) venom. *Journal of Molecular Biology,* **219**(4), pp. 591-592.

CHEN, L., JIA, N., GAO, L., FANG, W. and GOLUBOVIC, L., 2013. Effects of antimicrobial peptide revealed by simulations: translocation, pore formation, membrane corrugation and Euler buckling. *International journal of molecular sciences,* **14**(4), pp. 7932-7958.

CHEN, L., YANG, S.L. and CHUNG, K., 2014. Resistance to oxidative stress via regulating siderophore-mediated iron acquisition by the citrus fungal pathogen *Alternaria alternata*. *Microbiology,* **160**(5), pp. 970-979.

CHEN, L., KAO, P., FU, Y., HU, W. and CHANG, L., 2011. Bactericidal effect of *Naja nigricollis* toxin γ is related to its membrane-damaging activity. *Peptides,* **32**(8), pp. 1755-1763.

CHEN, R. and MARK, A.E., 2011. The effect of membrane curvature on the conformation of antimicrobial peptides: implications for binding and the mechanism of action. *European Biophysics Journal,* **40**(4), pp. 545-553.

CHEN, X., ZHAN, Y., ZHANG, Y., SHEN, J. and LEE, W., 2009. Effects of the antimicrobial peptide OH-CATH on Escherichia coli. *Zoological Research*, **30**(2), pp.171-177

CHEN, C.C. and FEINGOLD, D.S., 1972. Locus of divalent cation inhibition of the bactericidal action of polymyxin B. *Antimicrobial Agents and Chemotherapy,* **2**(5), pp. 331-335.

CHEN, Y., GUARNIERI, M.T., VASIL, A.I., VASIL, M.L., MANT, C.T. and HODGES, R.S., 2007. Role of peptide hydrophobicity in the mechanism of action of alpha-helical antimicrobial peptides. *Antimicrobial Agents and Chemotherapy,* **51**(4), pp. 1398-1406.

CHEN, Y., MANT, C.T., FARMER, S.W., HANCOCK, R.E., VASIL, M.L. and HODGES, R.S., 2005. Rational design of alpha-helical antimicrobial peptides with enhanced activities and specificity/therapeutic index. *The Journal of biological chemistry,* **280**(13), pp. 12316-12329.

CHIEN, K.Y., CHIANG, C.M., HSEU, Y.C., VYAS, A.A., RULE, G.S. and WU, W., 1994. Two distinct types of cardiotoxin as revealed by the structure and activity relationship of their interaction with zwitterionic phospholipid dispersions. *The Journal of biological chemistry,* **269**(20), pp. 14473-14483.

CHUNG, K.R., 2012. Stress Response and Pathogenicity of the Necrotrophic Fungal Pathogen *Alternaria alternata*. *Scientifica,* **2012**, pp. 635431.

CIORNEI, C.D., SIGURDARDOTTIR, T., SCHMIDTCHEN, A. and BODELSSON, M., 2005. Antimicrobial and chemoattractant activity, lipopolysaccharide neutralization, cytotoxicity, and inhibition by serum of analogs of human cathelicidin LL-37. *Antimicrobial Agents and Chemotherapy,* **49**(7), pp. 2845-2850.

CLEJAN, S., KRULWICH, T.A., MONDRUS, K.R. and SETO-YOUNG, D., 1986. Membrane lipid composition of obligately and facultatively alkalophilic strains of Bacillus spp. *Journal of Bacteriology,* **168**(1), pp. 334-340.

COATES, A.R., HALLS, G. and HU, Y., 2011a. Novel classes of antibiotics or more of the same? *British journal of pharmacology,* **163**(1), pp. 184-194.

CONLY, J. and JOHNSTON, B., 2005. Where are all the new antibiotics? The new antibiotic paradox. *Canadian Journal of Infectious Diseases and Medical Microbiology,* **16**(3), pp. 159-160.

CONSTANTIN, D., BROTONS, G., JARRE, A., LI, C. and SALDITT, T., 2007. Interaction of alamethicin pores in DMPC bilayers. *Biophysical journal,* **92**(11), pp. 3978-3987.

CORZO, G., ESCOUBAS, P., VILLEGAS, E., BARNHAM, K.J., HE, W., NORTON, R.S. and NAKAJIMA, T., 2001. Characterization of unique amphipathic antimicrobial peptides from venom of the scorpion *Pandinus imperator*. *The Biochemical journal,* **359**(Pt 1), pp. 35-45.

COSTA, A., HENRIQUES, M., OLIVEIRA, R. and AZEREDO, J., 2009. The role of polysaccharide intercellular adhesin (PIA) in *Staphylococcus epidermidis* adhesion to host tissues and subsequent antibiotic tolerance. *European journal of clinical microbiology & infectious diseases,* **28**(6), pp. 623-629.

CROSA, J.H. and WALSH, C.T., 2002. Genetics and assembly line enzymology of siderophore biosynthesis in bacteria. *Microbiology and molecular biology reviews: MMBR,* **66**(2), pp. 223-249.

DA SILVA NETO, J.F., BRAZ, V.S., ITALIANI, V.C. and MARQUES, M.V., 2009. Fur controls iron homeostasis and oxidative stress defense in the oligotrophic alpha-proteobacterium *Caulobacter crescentus*. *Nucleic acids research,* **37**(14), pp. 4812-4825.

DAI, L., YASUDA, A., NAOKI, H., CORZO, G., ANDRIANTSIFERANA, M. and NAKAJIMA, T., 2001. IsCT, a novel cytotoxic linear peptide from scorpion *Opisthacanthus madagascariensis*. *Biochemical and biophysical research communications,* **286**(4), pp. 820-825.

DALE, S.E., DOHERTY-KIRBY, A., LAJOIE, G. and HEINRICHS, D.E., 2004. Role of siderophore biosynthesis in virulence of *Staphylococcus aureus*: identification and characterization of genes involved in production of a siderophore. *Infection and immunity,* **72**(1), pp. 29-37.

DAMROSCH, D.S., 1946. Chemoprophylaxis and sulfonamide resistant streptococci. *Journal of the American Medical Association,* **130**(3), pp. 124-128.

DASHPER, S.G., O'BRIEN-SIMPSON, N.M., CROSS, K.J., PAOLINI, R.A., HOFFMANN, B., CATMULL, D.V., MALKOSKI, M. and REYNOLDS, E.C., 2005. Divalent metal cations increase the activity of the antimicrobial Peptide kappacin. *Antimicrobial Agents and Chemotherapy,* **49**(6), pp. 2322-2328.

DE LIMA, D.C., ALVAREZ ABREU, P., DE FREITAS, C.C., SANTOS, D.O., BORGES, R.O., DOS SANTOS, T.C., MENDES CABRAL, L., RODRIGUES, C.R. and CASTRO, H.C., 2005. Snake Venom: Any Clue for Antibiotics and CAM? *Evidence-based complementary and alternative medicine : eCAM,* **2**(1), pp. 39-47.

DE OLIVEIRA CARVALHO, A. and MOREIRA GOMES, V., 2011. Plant defensins and defensin-like peptides-biological activities and biotechnological applications. *Current pharmaceutical design,* **17**(38), pp. 4270-4293.

DERIS, Z.Z., AKTER, J., SIVANESAN, S., ROBERTS, K.D., THOMPSON, P.E., NATION, R.L., LI, J. and VELKOV, T., 2014. A secondary mode of action of polymyxins against Gram-negative bacteria involves the inhibition of NADH-quinone oxidoreductase activity. *The Journal of antibiotics,* **67**(2), pp. 147-151.

DESTOUMIEUX-GARZÓN, D., PEDUZZI, J., THOMAS, X., DJEDIAT, C. and REBUFFAT, S., 2006. Parasitism of iron-siderophore receptors of *Escherichia coli* by the siderophore-peptide microcin E492m and its unmodified counterpart. *Biometals,* **19**(2), pp. 181-191.

DESTOUMIEUX-GARZON, D., DUQUESNE, S., PEDUZZI, J., GOULARD, C., DESMADRIL, M., LETELLIER, L., REBUFFAT, S. and BOULANGER, P., 2005. The iron-siderophore transporter FhuA is the receptor for the antimicrobial peptide microcin J25: role of the microcin Val11-Pro16 beta-hairpin region in the recognition mechanism. *The Biochemical journal,* **389**(Pt 3), pp. 869-876.

DIAMOND, G., BECKLOFF, N., WEINBERG, A. and KISICH, K.O., 2009. The roles of antimicrobial peptides in innate host defense. *Current pharmaceutical design,* **15**(21), pp. 2377-2392.

DÍAZ-GARCÍA, A., RUIZ-FUENTES, J.L., YGLESIAS-RIVERA, A., RODRÍGUEZ-SÁNCHEZ, H., GARLOBO, Y.R., MARTINEZ, O.F. and CASTRO, J.A.F., 2015. Enzymatic analysis of venom from Cuban scorpion *Rhopalurus junceus*. *Journal of venom research,* **6**, pp. 11.

DIEGO-GARCÍA, E., SCHWARTZ, E.F., D'SUZE, G., GONZÁLEZ, S.A.R., BATISTA, C.V., GARCÍA, B.I., DE LA VEGA, RICARDO C RODRÍGUEZ and POSSANI, L.D., 2007. Wide phylogenetic distribution of scorpine and long-chain β-KTx-like peptides in scorpion venoms: identification of "orphan" components. *Peptides,* **28**(1), pp. 31-37.

DOMAGK, G., 1935. Ein beitrag zur chemotherapie der bakteriellen infektionen. *DMW-Deutsche Medizinische Wochenschrift,* **61**(07), pp. 250-253.

DONG, T.G., DONG, S., CATALANO, C., MOORE, R., LIANG, X. and MEKALANOS, J.J., 2015. Generation of reactive oxygen species by lethal attacks from competing microbes. *Proceedings of the National Academy of Sciences of the United States of America,* **112**(7), pp. 2181-2186.

DONG, W., LI, H., ZHANG, Y., YANG, H., GUO, M., LI, L. and LIU, T., 2011. Matrix metalloproteinase 2 promotes cell growth and invasion in colorectal cancer. *Acta biochimica et biophysica Sinica,* **43**(11), pp. 840-848.

DOROSZ, J., GOFMAN, Y., KOLUSHEVA, S., OTZEN, D., BEN-TAL, N., NIELSEN, N.C. and JELINEK, R., 2010. Membrane interactions of novicidin, a novel antimicrobial peptide: phosphatidylglycerol promotes bilayer insertion. *The Journal of Physical Chemistry B,* **114**(34), pp. 11053-11060.

DOUGHERTY, T.J., BARRETT, J.F. and PUCCI, M.J., 2002. Microbial genomics and novel antibiotic discovery: new technology to search for new drugs. *Current pharmaceutical design,* **8**(13), pp. 1119-1135.

DOWLING, A., O'DWYER, J. and ADLEY, C., 2013. Alternatives to antibiotics: future trends. *Microbial Pathogens and Strategies for Combating Them: Science, Technology and Education,* , pp. 978-984.

DUBOVSKII, P.V., LESOVOY, D.M., DUBINNYI, M.A., UTKIN, Y.N. and ARSENIEV, A.S., 2003. Interaction of the P-type cardiotoxin with phospholipid membranes. *European Journal of Biochemistry,* **270**(9), pp. 2038-2046.

DUBOVSKII, P. and UTKIN, Y., 2014. Cobra cytotoxins: structural organization and antibacterial activity. *Acta Naturae (англоязычная версия),* **6**(3 (22)),.

DUFRENE, Y.F., VAN DER WAL, A., NORDE, W. and ROUXHET, P.G., 1997. X-ray photoelectron spectroscopy analysis of whole cells and isolated cell walls of gram-positive bacteria: comparison with biochemical analysis. *Journal of Bacteriology,* **179**(4), pp. 1023-1028.

DUFTON, M. and HIDER, R., 1988. Structure and pharmacology of elapid cytotoxins. *Pharmacology & therapeutics,* **36**(1), pp. 1-40.

EBENHAN, T., GHEYSENS, O., KRUGER, H.G., ZEEVAART, J.R. and SATHEKGE, M.M., 2014. Antimicrobial peptides: their role as infection-selective tracers for molecular imaging. *BioMed research international,* **2014**, pp. 867381.

EFREMOV, R.G., VOLYNSKY, P.E., NOLDE, D.E., DUBOVSKII, P.V. and ARSENIEV, A.S., 2002. Interaction of cardiotoxins with membranes: a molecular modeling study. *Biophysical journal,* **83**(1), pp. 144-153.

EISENDLE, M., SCHRETTL, M., KRAGL, C., MULLER, D., ILLMER, P. and HAAS, H., 2006. The intracellular siderophore ferricrocin is involved in iron storage, oxidative-stress resistance, germination, and sexual development in *Aspergillus nidulans*. *Eukaryotic cell,* **5**(10), pp. 1596-1603.

ELANDER, R., 2003. Industrial production of β-lactam antibiotics. *Applied Microbiology and Biotechnology,* **61**(5-6), pp. 385-392.

EL-BITAR, A.M., SARHAN, M.M., AOKI, C., TAKAHARA, Y., KOMOTO, M., DENG, L., MOUSTAFA, M.A. and HOTTA, H., 2015. Virocidal activity of Egyptian scorpion venoms against hepatitis C virus. *Virology journal,* **12**(1), pp. 1.

ENRIGHT, M.C., ROBINSON, D.A., RANDLE, G., FEIL, E.J., GRUNDMANN, H. and SPRATT, B.G., 2002. The evolutionary history of methicillin-resistant *Staphylococcus aureus*

(MRSA). *Proceedings of the National Academy of Sciences of the United States of America,* **99**(11), pp. 7687-7692.

EPAND, R.M. and EPAND, R.F., 2009a. Lipid domains in bacterial membranes and the action of antimicrobial agents. *Biochimica et Biophysica Acta (BBA)-Biomembranes,* **1788**(1), pp. 289-294.

EPAND, R.M. and VOGEL, H.J., 1999. Diversity of antimicrobial peptides and their mechanisms of action. *Biochimica et Biophysica Acta (BBA)-Biomembranes,* **1462**(1), pp. 11-28.

EPAND, R.F., SAVAGE, P.B. and EPAND, R.M., 2007. Bacterial lipid composition and the antimicrobial efficacy of cationic steroid compounds (Ceragenins). *Biochimica et Biophysica Acta (BBA) - Biomembranes,* **1768**(10), pp. 2500-2509.

EPAND, R.M. and EPAND, R.F., 2009. Lipid domains in bacterial membranes and the action of antimicrobial agents. *Biochimica et Biophysica Acta (BBA) - Biomembranes,* **1788**(1), pp. 289-294.

ERDEŞ, E., DOĞAN, T.S., COŞAR, İ, DANIŞMAN, T., KUNT, K.B., ŞEKER, T., YÜCEL, M. and ÖZEN, C., 2014. Characterization of *Leiurus abdullahbayrami* (Scorpiones: Buthidae) venom: peptide profile, cytotoxicity and antimicrobial activity. *Journal of Venomous Animals and Toxins including Tropical Diseases,* **20**(1), pp. 1.

ETIENNE, W., MEYER, M.H., PEPPERS, J. and MEYER, R.A., 2004. Comparison of mRNA gene expression by RT-PCR and DNA microarray. *BioTechniques,* **36**(4), pp. 618-627.

FAJARDO, A. and MARTÍNEZ, J.L., 2008. Antibiotics as signals that trigger specific bacterial responses. *Current opinion in microbiology,* **11**(2), pp. 161-167.

FALANGA, A., LOMBARDI, L., FRANCI, G., VITIELLO, M., IOVENE, M.R., MORELLI, G., GALDIERO, M. and GALDIERO, S., 2016. Marine Antimicrobial Peptides: Nature Provides Templates for the Design of Novel Compounds against Pathogenic Bacteria. *International journal of molecular sciences,* **17**(5), pp. 785.

FALES-WILLIAMS, A.J., BROGDEN, K.A., HUFFMAN, E., GALLUP, J.M. and ACKERMANN, M.R., 2002. Cellular distribution of anionic antimicrobial peptide in normal lung and during acute pulmonary inflammation. *Veterinary pathology,* **39**(6), pp. 706-711.

FATHI, B., JAMSHIDI, A., ZOLFAGHARIAN, H. and ZARE MIRAKABBADI, A., 2011. Investigation of the Antibacterial Effect of Venom of the Iranian Snake Echis carinatus. *The Iranian Journal of Veterinary Science and Technology,* **2**(2), pp. 93-99.

FEDDERS, H., MICHALEK, M., GROTZINGER, J. and LEIPPE, M., 2008. An exceptional salt-tolerant antimicrobial peptide derived from a novel gene family of haemocytes of the marine invertebrate Ciona intestinalis. *The Biochemical journal,* **416**(1), pp. 65-75.

FEHRI, L.F., SIRAND-PUGNET, P., GOURGUES, G., JAN, G., WROBLEWSKI, H. and BLANCHARD, A., 2005. Resistance to antimicrobial peptides and stress response in Mycoplasma pulmonis. *Antimicrobial Agents and Chemotherapy,* **49**(10), pp. 4154-4165.

FERGUSON, A.D., COULTON, J.W., DIEDERICHS, K., WELTE, W., BRAUN, V. and FIEDLER, H., 2000. Crystal structure of the antibiotic albomycin in complex with the outer membrane transporter FhuA. *Protein Science,* **9**(5), pp. 956-963.

FERNAEUS, S. and LAND, T., 2005. Increased iron-induced oxidative stress and toxicity in scrapie-infected neuroblastoma cells. *Neuroscience letters,* **382**(3), pp. 217-220.

FERNANDES, P. and MARTENS, E., 2016. Antibiotics in late clinical development. *Biochemical pharmacology,* **133**, pp.152-163.

FERNANDEZ, D.I., LE BRUN, A.P., WHITWELL, T.C., SANI, M., JAMES, M. and SEPAROVIC, F., 2012. The antimicrobial peptide aurein 1.2 disrupts model membranes via the carpet mechanism. *Physical Chemistry Chemical Physics,* **14**(45), pp. 15739-15751.

FERNANDEZ, D.I., SANI, M., MILES, A.J., WALLACE, B.A. and SEPAROVIC, F., 2013. Membrane defects enhance the interaction of antimicrobial peptides, aurein 1.2 versus caerin 1.1. *Biochimica et Biophysica Acta (BBA) - Biomembranes,* **1828**(8), pp. 1863-1872.

FERREIRA, L., ALVES, E. and HENRIQUES, O., 1993. Peptide T, a novel bradykinin potentiator isolated from Tityus serrulatus scorpion venom. *Toxicon,* **31**(8), pp. 941-947.

FERREIRA, B.L., SANTOS, D.O., DOS SANTOS, A.L., RODRIGUES, C.R., DE FREITAS, C.C., CABRAL, L.M. and CASTRO, H.C., 2011. Comparative analysis of viperidae venoms antibacterial profile: a short communication for proteomics. *Evidence-based complementary and alternative medicine : eCAM,* **2011**, pp. 960267.

FISCHBACH, M.A., LIN, H., LIU, D.R. and WALSH, C.T., 2006. How pathogenic bacteria evade mammalian sabotage in the battle for iron. *Nature chemical biology,* **2**(3), pp. 132-138.

FLEMING, A., 1922. On a remarkable bacteriolytic element found in tissues and secretions. *Proceedings of the Royal Society of London B: Biological Sciences,* **93**(653), pp. 306-317.

FLOREA, G., ANDREI, Ş, CIURCA, D., MARE, A., MAN, A., CORDOŞ, B., GRAMA, A. and MUNTEAN, D., 2016. New RP-HPLC Method for Separation of Naja haje haje Venom and Studies of its Bactericidal Effect. *Acta Medica Marisiensis,* **62**(1), pp. 90-94.

FONKWO, P.N., 2008. Pricing infectious disease. The economic and health implications of infectious diseases. *EMBO reports,* **9 Suppl 1**, pp. S13-7.

FONSECA, M.G., MOREIRA, W., CUNHA, K., RIBEIRO, A. and ALMEIDA, M., 2009. Oral microbiota of Brazilian captive snakes. *Journal of Venomous Animals and Toxins including Tropical Diseases,* **15**(1), pp. 54-60.

FOSGERAU, K. and HOFFMANN, T., 2015. Peptide therapeutics: current status and future directions. *Drug discovery today,* **20**(1), pp. 122-128.

FOX, J.L., 2013. Antimicrobial peptides stage a comeback. *Nature biotechnology,* **31**(5), pp. 379-382.

FRIEDRICH, C.L., ROZEK, A., PATRZYKAT, A. and HANCOCK, R.E., 2001. Structure and mechanism of action of an indolicidin peptide derivative with improved activity against gram-positive bacteria. *The Journal of biological chemistry,* **276**(26), pp. 24015-24022.

FRUCHART-GAILLARD, C., MOURIER, G., BLANCHET, G., VERA, L., GILLES, N., MÉNEZ, R., MARCON, E., STURA, E.A. and SERVENT, D., 2012. Engineering of three-finger fold toxins creates ligands with original pharmacological profiles for muscarinic and adrenergic receptors. *PloS one,* **7**(6), pp. e39166.

GALARIS, D. and PANTOPOULOS, K., 2008. Oxidative stress and iron homeostasis: mechanistic and health aspects. *Critical reviews in clinical laboratory sciences,* **45**(1), pp. 1-23.

GANZ, T., 2003. Defensins: antimicrobial peptides of innate immunity. *Nature Reviews Immunology,* **3**(9), pp. 710-720.

GAO, B., TIAN, C. and ZHU, S., 2007. Inducible antibacterial response of scorpion venom gland. *Peptides,* **28**(12), pp. 2299-2305.

GAO, W., XING, L., QU, P., TAN, T., YANG, N., LI, D., CHEN, H. and FENG, X., 2015. Identification of a novel cathelicidin antimicrobial peptide from ducks and determination of its functional activity and antibacterial mechanism. *Scientific reports,* **5**, pp. 17260.

GARCIA-LIMA, E. and LAURE, C., 1987. A study of bacterial contamination of rattlesnake venom. *Revista da Sociedade Brasileira de Medicina Tropical,* **20**(1), pp. 19-21.

GAZIT, E., MILLER, I.R., BIGGIN, P.C., SANSOM, M.S. and SHAI, Y., 1996. Structure and orientation of the mammalian antibacterial peptide cecropin P1 within phospholipid membranes. *Journal of Molecular Biology,* **258**(5), pp. 860-870.

GEBHARD, S., 2012. ABC transporters of antimicrobial peptides in Firmicutes bacteria–phylogeny, function and regulation. *Molecular microbiology,* **86**(6), pp. 1295-1317.

GEE, M.L., BURTON, M., GREVIS-JAMES, A., HOSSAIN, M.A., MCARTHUR, S., PALOMBO, E.A., WADE, J.D. and CLAYTON, A.H., 2013. Imaging the action of antimicrobial peptides on living bacterial cells. *Scientific reports,* **3**, pp. 1557.

GESELL, J., ZASLOFF, M. and OPELLA, S.J., 1997. Two-dimensional 1H NMR experiments show that the 23-residue magainin antibiotic peptide is an α-helix in

dodecylphosphocholine micelles, sodium dodecylsulfate micelles, and trifluoroethanol/water solution. *Journal of Biomolecular NMR,* **9**(2), pp. 127-135.

GHOSH, A., GHOSH, M., NIU, C., MALOUIN, F., MOELLMANN, U. and MILLER, M.J., 1996. Iron transport-mediated drug delivery using mixed-ligand siderophore-β-lactam conjugates. *Chemistry & biology,* **3**(12), pp. 1011-1019.

GILBERT, R.J., DALLA SERRA, M., FROELICH, C.J., WALLACE, M.I. and ANDERLUH, G., 2014. Membrane pore formation at protein–lipid interfaces. *Trends in biochemical sciences,* **39**(11), pp. 510-516.

GIRISH, V.M., KUMAR, S., JOSEPH, L., JOBICHEN, C., KINI, R.M. and SIVARAMAN, J., 2012. Identification and structural characterization of a new three-finger toxin hemachatoxin from Hemachatus haemachatus venom. *PloS one,* **7**(10), pp. e48112.

GIULIANI, A., PIRRI, G. and NICOLETTO, S., 2007. Antimicrobial peptides: an overview of a promising class of therapeutics. *Open Life Sciences,* **2**(1), pp. 1-33.

GLASER, R.W., SACHSE, C., DÜRR, U.H., WADHWANI, P., AFONIN, S., STRANDBERG, E. and ULRICH, A.S., 2005. Concentration-dependent realignment of the antimicrobial peptide PGLa in lipid membranes observed by solid-state 19 F-NMR. *Biophysical journal,* **88**(5), pp. 3392-3397.

GORAI, B. and SIVARAMAN, T., 2016. Delineating residues for haemolytic activities of snake venom cardiotoxin 1 from Naja naja as probed by molecular dynamics simulations and in vitro validations. *International journal of biological macromolecules* **95**, pp.1022-1036, .

GORDON, Y.J., ROMANOWSKI, E.G. and MCDERMOTT, A.M., 2005. A review of antimicrobial peptides and their therapeutic potential as anti-infective drugs. *Current eye research,* **30**(7), pp. 505-515.

GOSTELOW, M., GONZALEZ, D., SMITH, P.B. and COHEN-WOLKOWIEZ, M., 2014. Pharmacokinetics and safety of recently approved drugs used to treat methicillin-

resistant Staphylococcus aureus infections in infants, children and adults. *Expert review of clinical pharmacology,* **7**(3), pp. 327-340.

GREBER, K.E. and DAWGUL, M., 2017. Antimicrobial Peptides Under Clinical Trials. *Current topics in medicinal chemistry,* **17**(5), pp. 620-628.

GRÖNBERG, A., MAHLAPUU, M., STÅHLE, M., WHATELY-SMITH, C. and ROLLMAN, O., 2014. Treatment with LL-37 is safe and effective in enhancing healing of hard-to-heal venous leg ulcers: a randomized, placebo-controlled clinical trial. *Wound Repair and Regeneration,* **22**(5), pp. 613-621.

GRUBOR, B., MEYERHOLZ, D.K. and ACKERMANN, M.R., 2006a. Collectins and cationic antimicrobial peptides of the respiratory epithelia. *Veterinary Pathology Online,* **43**(5), pp. 595-612.

GRUENHEID, S. and LE MOUAL, H., 2012. Resistance to antimicrobial peptides in Gram-negative bacteria. *FEMS microbiology letters,* **330**(2), pp. 81-89.

GUAN, R., WANG, C., WANG, M. and WANG, D., 2001. A depressant insect toxin with a novel analgesic effect from scorpion Buthus martensii Karsch. *Biochimica et Biophysica Acta (BBA)-Protein Structure and Molecular Enzymology,* **1549**(1), pp. 9-18.

GUILHELMELLI, F.F., VILELA, N.N., SIMON, K.S., DE OLIVEIRA, M.A., ÁLVARES, A., AA, C., RIGONATTO, M.C.L., COSTA, P.H.S., TAVARES, A.H. and FREITA, S.M., 2016. Activity of scorpion venom-derived antifungal peptides against planktonic cells of Candida spp and Cryptococcus neoformans and Candida albicans biofilms. *Frontiers in Microbiology,* **7**, pp. 1844.

GUILHELMELLI, F., VILELA, N., ALBUQUERQUE, P., DERENGOWSKI, L.D.S., SILVA-PEREIRA, I. and KYAW, C.M., 2014. Antibiotic development challenges: the various mechanisms of action of antimicrobial peptides and of bacterial resistance. *New edge of antibiotic development: antimicrobial peptides and corresponding resistance,* **4**, pp. 63.

GUO, J., NAIR, M.K., GALVÁN, E.M., LIU, S. and SCHIFFERLI, D.M., 2011. Tn5AraOut mutagenesis for the identification of Yersinia pestis genes involved in resistance towards cationic antimicrobial peptides. *Microbial pathogenesis,* **51**(3), pp. 121-132.

GUTSMANN, T., HAGGE, S.O., DAVID, A., ROES, S., BOHLING, A., HAMMER, M.U. and SEYDEL, U., 2005. Lipid-mediated resistance of Gram-negative bacteria against various pore-forming antimicrobial peptides. *Journal of endotoxin research,* **11**(3), pp. 167-173.

HALLOCK, K.J., LEE, D. and RAMAMOORTHY, A., 2003. MSI-78, an analogue of the magainin antimicrobial peptides, disrupts lipid bilayer structure via positive curvature strain. *Biophysical journal,* **84**(5), pp. 3052-3060.

HAMMER, M.U., BRAUSER, A., OLAK, C., BREZESINSKI, G., GOLDMANN, T., GUTSMANN, T. and ANDRA, J., 2010. Lipopolysaccharide interaction is decisive for the activity of the antimicrobial peptide NK-2 against Escherichia coli and Proteus mirabilis. *The Biochemical journal,* **427**(3), pp. 477-488.

HANCOCK, R.E., 2001. Cationic peptides: effectors in innate immunity and novel antimicrobials. *The Lancet infectious diseases,* **1**(3), pp. 156-164.

HANCOCK, R.E. and SAHL, H., 2006. Antimicrobial and host-defense peptides as new anti-infective therapeutic strategies. *Nature biotechnology,* **24**(12), pp. 1551-1557.

HANCOCK, R.E. and ROZEK, A., 2002. Role of membranes in the activities of antimicrobial cationic peptides. *FEMS microbiology letters,* **206**(2), pp. 143-149.

HARRIS, F., DENNISON, S.R. and PHOENIX, D.A., 2009. Anionic antimicrobial peptides from eukaryotic organisms. *Current Protein and Peptide Science,* **10**(6), pp. 585-606.

HARRISON, P.L., ABDEL-RAHMAN, M.A., MILLER, K. and STRONG, P.N., 2014. Antimicrobial peptides from scorpion venoms. *Toxicon,* **88**, pp. 115-137.

HARRISON, P.L., ABDEL-RAHMAN, M.A., STRONG, P.N., TAWFIK, M.M. and MILLER, K., 2016. Characterisation of three alpha-helical antimicrobial peptides from the venom of Scorpio maurus palmatus. *Toxicon,* **117**, pp. 30-36.

HARRISON, P.L., HEATH, G.R., JOHNSON, B.R., ABDEL-RAHMAN, M.A., STRONG, P.N., EVANS, S.D. and MILLER, K., 2016. Phospholipid dependent mechanism of smp24, an α-helical antimicrobial peptide from scorpion venom. *Biochimica et Biophysica Acta (BBA)-Biomembranes,* **1858**(11), pp. 2737-2744.

HARTMANN, M., BERDITSCH, M., HAWECKER, J., ARDAKANI, M.F., GERTHSEN, D. and ULRICH, A.S., 2010. Damage of the bacterial cell envelope by antimicrobial peptides gramicidin S and PGLa as revealed by transmission and scanning electron microscopy. *Antimicrobial Agents and Chemotherapy,* **54**(8), pp. 3132-3142.

HAUKLAND, H.H., ULVATNE, H., SANDVIK, K. and VORLAND, L.H., 2001. The antimicrobial peptides lactoferricin B and magainin 2 cross over the bacterial cytoplasmic membrane and reside in the cytoplasm. *FEBS letters,* **508**(3), pp. 389-393.

HENZLER WILDMAN, K.A., LEE, D. and RAMAMOORTHY, A., 2003. Mechanism of lipid bilayer disruption by the human antimicrobial peptide, LL-37. *Biochemistry,* **42**(21), pp. 6545-6558.

HINTZ, T., MATTHEWS, K.K. and DI, R., 2015. The use of plant antimicrobial compounds for food preservation. *BioMed research international,* **2015**.

HMED, B., SERRIA, H.T. and MOUNIR, Z.K., 2013. Scorpion peptides: potential use for new drug development. *Journal of toxicology,* **2013**, pp. 958797.

HO, S.W., JUNG, D., CALHOUN, J.R., LEAR, J.D., OKON, M., SCOTT, W.R., HANCOCK, R.E. and STRAUS, S.K., 2008. Effect of divalent cations on the structure of the antibiotic daptomycin. *European biophysics journal,* **37**(4), pp. 421-433.

HOPKINS, S., 2016. UK initiatives to reduce antimicrobial resistant infections, 2013-2018. *International Journal of Health Governance,* **21**(3), pp. 131-138.

HOSKIN, D.W. and RAMAMOORTHY, A., 2008. Studies on anticancer activities of antimicrobial peptides. *Biochimica et Biophysica Acta (BBA)-Biomembranes,* **1778**(2), pp. 357-375.

HSU, C.H., CHEN, C., JOU, M.L., LEE, A.Y., LIN, Y.C., YU, Y.P., HUANG, W.T. and WU, S.H., 2005. Structural and DNA-binding studies on the bovine antimicrobial peptide,

indolicidin: evidence for multiple conformations involved in binding to membranes and DNA. *Nucleic acids research,* **33**(13), pp. 4053-4064.

HU, H., WANG, C., GUO, X., LI, W., WANG, Y. and HE, Q., 2013. Broad activity against porcine bacterial pathogens displayed by two insect antimicrobial peptides moricin and cecropin B. *Molecules and cells,* **35**(2), pp. 106-114.

HUANG, Y., HE, L., LI, G., ZHAI, N., JIANG, H. and CHEN, Y., 2014. Role of helicity of α-helical antimicrobial peptides to improve specificity. *Protein & cell,* **5**(8), pp. 631-642.

HUGHES, A.H., HANCOCK, I.C. and BADDILEY, J., 1973. The function of teichoic acids in cation control in bacterial membranes. *The Biochemical journal,* **132**(1), pp. 83-93.

HULTMARK, D., ENGSTRÖM, Å, BENNICH, H., KAPUR, R. and BOMAN, H.G., 1982. Insect immunity: isolation and structure of cecropin D and four minor antibacterial components from Cecropia pupae. *The FEBS Journal,* **127**(1), pp. 207-217.

HUMPHRIES, R.M., POLLETT, S. and SAKOULAS, G., 2013. A current perspective on daptomycin for the clinical microbiologist. *Clinical microbiology reviews,* **26**(4), pp. 759-780.

HURDLE, J.G., O'NEILL, A.J., CHOPRA, I. and LEE, R.E., 2011. Targeting bacterial membrane function: an underexploited mechanism for treating persistent infections. *Nature Reviews Microbiology,* **9**(1), pp. 62-75.

HWANG, J.S., LEE, J., KIM, Y.J., BANG, H.S., YUN, E.Y., KIM, S.R., SUH, H.J., KANG, B.R., NAM, S.H., JEON, J.P., KIM, I. and LEE, D.G., 2009. Isolation and Characterization of a Defensin-Like Peptide (Coprisin) from the Dung Beetle, Copris tripartitus. *International journal of peptides,* **2009**, pp. 10.1155/2009/136284. Epub 2009 Oct 22.

HYLDGAARD, M., MYGIND, T., VAD, B.S., STENVANG, M., OTZEN, D.E. and MEYER, R.L., 2014. The antimicrobial mechanism of action of epsilon-poly-l-lysine. *Applied and Environmental Microbiology,* **80**(24), pp. 7758-7770.

IANNUCCI, N., GONZÁLEZ, R., CASCONE, O. and ALBERICIO, F., 2011. Novel strategy for designing antimicrobial peptides: an answer to the development of drug resistance.

Science Against Microbial Pathogens: Communicating Current Research and Technological Advances; , pp. 961-967.

JENSSEN, H., HAMILL, P. and HANCOCK, R.E., 2006. Peptide antimicrobial agents. *Clinical microbiology reviews,* **19**(3), pp. 491-511.

JHO, Y., PARK, D., LEE, J., CHA, S. and HAN, J.S., 2011. Identification of bacteria from the oral cavity and cloaca of snakes imported from Vietnam. *Laboratory animal research,* **27**(3), pp. 213-217.

JI, C., MILLER, P.A. and MILLER, M.J., 2012. Iron transport-mediated drug delivery: practical syntheses and in vitro antibacterial studies of tris-catecholate siderophore–aminopenicillin conjugates reveals selectively potent antipseudomonal activity. *Journal of the American Chemical Society,* **134**(24), pp. 9898-9901.

JIANG, Y., LI, Y., LEE, W., XU, X., ZHANG, Y., ZHAO, R., ZHANG, Y. and WANG, W., 2011. Venom gland transcriptomes of two elapid snakes (Bungarus multicinctus and Naja atra) and evolution of toxin genes. *BMC genomics,* **12**(1), pp. 1-13.

JIANG, Z., VASIL, A.I., HALE, J.D., HANCOCK, R.E., VASIL, M.L. and HODGES, R.S., 2008. Effects of net charge and the number of positively charged residues on the biological activity of amphipathic α-helical cationic antimicrobial peptides. *Peptide Science,* **90**(3), pp. 369-383.

JIN, L., BAI, X., LUAN, N., YAO, H., ZHANG, Z., LIU, W., CHEN, Y., YAN, X., RONG, M. and LAI, R., 2016. A Designed Tryptophan-and Lysine/Arginine-Rich Antimicrobial Peptide with Therapeutic Potential for Clinical Antibiotic-Resistant Candida albicans Vaginitis. *Journal of medicinal chemistry,* **59**(5), pp. 1791-1799.

JOHNSTONE, T.C. and NOLAN, E.M., 2015. Beyond iron: non-classical biological functions of bacterial siderophores. *Dalton Transactions,* **44**(14), pp. 6320-6339.

JOO, H.S., FU, C.I. and OTTO, M., 2016. Bacterial strategies of resistance to antimicrobial peptides. *Philosophical transactions of the Royal Society of London.Series B, Biological sciences,* **371**(1695), pp. 10.1098/rstb.2015.0292.

JORMAKKA, M., TORNROTH, S., BYRNE, B. and IWATA, S., 2002. Molecular basis of proton motive force generation: structure of formate dehydrogenase-N. *Science (New York, N.Y.),* **295**(5561), pp. 1863-1868.

JOUBERT, F.J., 1975. The amino acid sequences of three toxins (CM-10, CM-12 and CM-14) from Naja haje annulifera (Egyptian cobra) venom. *Hoppe-Seyler´ s Zeitschrift für physiologische Chemie,* **356**(1), pp. 53-72.

JOUBERT, F. and TALJAARD, N., 1978. Purification, some properties and the primary structures of three reduced and S-carboxymethylated toxins (CM-5, CM-6 and CM-10a) from Naje haje haje (Egyptian cobra) venom. *Biochimica et Biophysica Acta (BBA)-Protein Structure,* **537**(1), pp. 1-8.

JUNG, D., ROZEK, A., OKON, M. and HANCOCK, R.E., 2004. Structural transitions as determinants of the action of the calcium-dependent antibiotic daptomycin. *Chemistry & biology,* **11**(7), pp. 949-957.

KAISER, V. and DIAMOND, G., 2000. Expression of mammalian defensin genes. *Journal of leukocyte biology,* **68**(6), pp. 779-784.

KANDASAMY, S.K. and LARSON, R.G., 2006. Effect of salt on the interactions of antimicrobial peptides with zwitterionic lipid bilayers. *Biochimica et Biophysica Acta (BBA)-Biomembranes,* **1758**(9), pp. 1274-1284.

KAO, P., LIN, S. and CHANG, L., 2010. Interaction of Naja naja atra cardiotoxin 3 with H-trisaccharide modulates its hemolytic activity and membrane-damaging activity. *Toxicon,* **55**(7), pp. 1387-1395.

KELESIDIS, T., 2014. The interplay between daptomycin and the immune system. *Frontiers in immunology,* **5**, pp. 52.

KIM, H., JANG, J.H., KIM, S.C. and CHO, J.H., 2014. De novo generation of short antimicrobial peptides with enhanced stability and cell specificity. *The Journal of antimicrobial chemotherapy,* **69**(1), pp. 121-132.

KINI, R.M. and DOLEY, R., 2010. Structure, function and evolution of three-finger toxins: mini proteins with multiple targets. *Toxicon,* **56**(6), pp. 855-867.

KINI, R.M. and EVANS, H.J., 1989. Role of cationic residues in cytolytic activity: modification of lysine residues in the cardiotoxin from Naja nigricollis venom and correlation between cytolytic and antiplatelet activity. *Biochemistry,* **28**(23), pp. 9209-9215.

KINZEL, O., TAPPE, R., GERUS, I. and BUDZIKIEWICZ, H., 1998. The synthesis and antibacterial activity of two pyoverdin-ampicillin conjugates, entering Pseudomonas aeruginosa via the pyoverdin-mediated iron uptake pathway. *The Journal of antibiotics,* **51**(5), pp. 499-507.

KLEINSCHMIDT, J.H., MAHANEY, J.E., THOMAS, D.D. and MARSH, D., 1997. Interaction of bee venom melittin with zwitterionic and negatively charged phospholipid bilayers: a spin-label electron spin resonance study. *Biophysical journal,* **72**(2 Pt 1), pp. 767-778.

KOH, C.Y. and KINI, R.M., 2012. From snake venom toxins to therapeutics – Cardiovascular examples. *Toxicon,* **59**(4), pp. 497-506.

KOMAJDA, M. and WIMART, M.C., 2000. Angiotensin converting enzyme inhibition: from viper to patient. *Heart (British Cardiac Society),* **84 Suppl 1**, pp. i11-4:discussion i50.

KOVALAINEN, M., MÖNKÄRE, J., RIIKONEN, J., PESONEN, U., VLASOVA, M., SALONEN, J., LEHTO, V., JÄRVINEN, K. and HERZIG, K., 2015. Novel delivery systems for improving the clinical use of peptides. *Pharmacological reviews,* **67**(3), pp. 541-561.

KRAMER, N.E., VAN HIJUM, S.A., KNOL, J., KOK, J. and KUIPERS, O.P., 2006. Transcriptome analysis reveals mechanisms by which Lactococcus lactis acquires nisin resistance. *Antimicrobial Agents and Chemotherapy,* **50**(5), pp. 1753-1761.

KRAUS, D. and PESCHEL, A., 2006. Molecular mechanisms of bacterial resistance to antimicrobial peptides. *Antimicrobial Peptides and Human Disease.* Springer, pp. 231-250.

KUHN-NENTWIG, L., 2003. Antimicrobial and cytolytic peptides of venomous arthropods. *Cellular and Molecular Life Sciences CMLS,* **60**(12), pp. 2651-2668.

KUMAR, M. and SRIVASTAVA, S., 2011. Effect of calcium and magnesium on the antimicrobial action of enterocin LR/6 produced by Enterococcus faecium LR/6. *International journal of antimicrobial agents,* **37**(6), pp. 572-575.

KUSSER, W., ZIMMER, K. and FIEDLER, F., 1985. Characteristics of the binding of aminoglycoside antibiotics to teichoic acids. *The FEBS Journal,* **151**(3), pp. 601-605.

LAMBERT, P.A., 2005. Bacterial resistance to antibiotics: modified target sites. *Advanced Drug Delivery Reviews,* **57**(10), pp. 1471-1485.

LAVERTY, G., GORMAN, S.P. and GILMORE, B.F., 2011. The potential of antimicrobial peptides as biocides. *International journal of molecular sciences,* **12**(10), pp. 6566-6596.

LEE, D.L. and HODGES, R.S., 2003. Structure–activity relationships of de novo designed cyclic antimicrobial peptides based on gramicidin S. *Peptide Science,* **71**(1), pp. 28-48.

LEE, D.G., PARK, J., SHIN, S.Y., LEE, S.G., LEE, M.K., KIM, K.L. and HAHM, K., 1997. Design of novel analogue peptides with potent fungicidal but low hemolytic activity based on the cecropin a-melittin hybrid structure. *IUBMB life,* **43**(3), pp. 489-498.

LEE, J. and LEE, D.G., 2015. Antimicrobial peptides (AMPs) with dual mechanisms: membrane disruption and apoptosis. *J Microbiol Biotechnol,* **25**, pp. 759-764.

LEE, M.L., TAN, N.H., FUNG, S.Y. and SEKARAN, S.D., 2011. Antibacterial action of a heat-stable form of L-amino acid oxidase isolated from king cobra (Ophiophagus hannah) venom. *Comparative Biochemistry and Physiology Part C: Toxicology & Pharmacology,* **153**(2), pp. 237-242.

LEE, M.T., SUN, T.L., HUNG, W.C. and HUANG, H.W., 2013. Process of inducing pores in membranes by melittin. *Proceedings of the National Academy of Sciences of the United States of America,* **110**(35), pp. 14243-14248.

LEONE, L., LORING, J., SJÖBERG, S., PERSSON, P. and SHCHUKAREV, A., 2006. Surface characterization of the Gram-positive bacteria Bacillus subtilis-an XPS study. *Surface and Interface Analysis,* **38**(4), pp. 202-205.

LEONTIADOU, H., MARK, A.E. and MARRINK, S.J., 2006. Antimicrobial peptides in action. *Journal of the American Chemical Society,* **128**(37), pp. 12156-12161.

LEPTIHN, S., HAR, J.Y., CHEN, J., HO, B., WOHLAND, T. and DING, J.L., 2009. Single molecule resolution of the antimicrobial action of quantum dot-labeled sushi peptide on live bacteria. *BMC biology,* **7**(1), pp. 1-13.

LEWIS, K., 2013. Platforms for antibiotic discovery. *Nature reviews Drug discovery,* **12**(5), pp. 371-387.

LI, A., LEE, P., HO, B., DING, J. and LIM, C., 2007. Atomic force microscopy study of the antimicrobial action of Sushi peptides on Gram negative bacteria. *Biochimica et Biophysica Acta (BBA)-Biomembranes,* **1768**(3), pp. 411-418.

LI, L., VOROBYOV, I. and ALLEN, T.W., 2013. The different interactions of lysine and arginine side chains with lipid membranes. *The Journal of Physical Chemistry B,* **117**(40), pp. 11906-11920.

LI, X., SARAVANAN, R., KWAK, S.K. and LEONG, S.S.J., 2013. Biomolecular engineering of a human beta defensin model for increased salt resistance. *Chemical Engineering Science,* **95**, pp. 128-137.

LI, Y., WANG, Z., LIU, X., SONG, Z., LI, R., SHAO, C. and YIN, Y., 2016. Siderophore biosynthesis but not reductive iron assimilation is essential for the dimorphic fungus Nomuraea rileyi conidiation, dimorphism transition, resistance to oxidative stress, pigmented microsclerotium formation, and virulence. *Frontiers in Microbiology,* **7**, pp. 931.

LI, Y., XIANG, Q., ZHANG, Q., HUANG, Y. and SU, Z., 2012. Overview on the recent study of antimicrobial peptides: origins, functions, relative mechanisms and application. *Peptides,* **37**(2), pp. 207-215.

LI, Z., XU, X., MENG, L., ZHANG, Q., CAO, L., LI, W., WU, Y. and CAO, Z., 2014. Hp1404, a new antimicrobial peptide from the scorpion heterometrus petersii. *PLoS one,* **9**(5), pp. e97539.

LI, M., LAI, Y., VILLARUZ, A.E., CHA, D.J., STURDEVANT, D.E. and OTTO, M., 2007. Gram-positive three-component antimicrobial peptide-sensing system. *Proceedings of the National Academy of Sciences of the United States of America,* **104**(22), pp. 9469-9474.

LIM, E., AMMONS, S., MOHLER, V., KILLIAN, D., DEDRICK, R., GIKONYO, K. and LIN, J., 2001. XMP. 629, a peptide derived from functional domain II of BPI, demonstrates broad-spectrum antimicrobial and endotoxin-neutralizing properties in vitro and in vivo, *41st Interscience Conference on Antimicrobial Agents and Chemotherapy, Chicago, IL* 2001.

LINARES, J.F., GUSTAFSSON, I., BAQUERO, F. and MARTINEZ, J.L., 2006. Antibiotics as intermicrobial signaling agents instead of weapons. *Proceedings of the National Academy of Sciences of the United States of America,* **103**(51), pp. 19484-19489.

LING, L.L., SCHNEIDER, T., PEOPLES, A.J., SPOERING, A.L., ENGELS, I., CONLON, B.P., MUELLER, A., SCHÄBERLE, T.F., HUGHES, D.E. and EPSTEIN, S., 2015. A new antibiotic kills pathogens without detectable resistance. *Nature,* **517**(7535), pp. 455-459.

LISTER, J., 1875. XVI.—A Contribution to the Germ Theory of Putrefaction and other Fermentative Changes, and to the Natural History of Torulæ and Bacteria. *Transactions of the Royal Society of Edinburgh,* **27**(03), pp. 313-344.

LIU, A., TRAN, L., BECKET, E., LEE, K., CHINN, L., PARK, E., TRAN, K. and MILLER, J.H., 2010. Antibiotic sensitivity profiles determined with an Escherichia coli gene knockout collection: generating an antibiotic bar code. *Antimicrobial Agents and Chemotherapy,* **54**(4), pp. 1393-1403.

LIU, W., DONG, S.L., XU, F., WANG, X.Q., WITHERS, T.R., YU, H.D. and WANG, X., 2013. Effect of intracellular expression of antimicrobial peptide LL-37 on growth of escherichia coli strain TOP10 under aerobic and anaerobic conditions. *Antimicrobial Agents and Chemotherapy,* **57**(10), pp. 4707-4716.

LIVERMORE, D.M., 2003. Linezolid in vitro: mechanism and antibacterial spectrum. *The Journal of antimicrobial chemotherapy,* **51 Suppl 2**, pp. ii9-16.

LOUW, A.I., 1974. Snake venom toxins The purification and properties of five non-neurotoxic polypeptides from Naja mossambica mossambica venom. *Biochimica et Biophysica Acta (BBA)-Protein Structure,* **336**(2), pp. 470-480.

LUDTKE, S.J., HE, K., WU, Y. and HUANG, H.W., 1994. Cooperative membrane insertion of magainin correlated with its cytolytic activity. *Biochimica et Biophysica Acta (BBA)-Biomembranes,* **1190**(1), pp. 181-184.

LUNA-RAMÍREZ, K., JIMÉNEZ-VARGAS, J. and POSSANI, L., 2016. Scorpine-Like Peptides. *Single Cell Biol,* **5**(138), pp. 2.

LUNA-RAMIREZ, K., TONK, M., RAHNAMAEIAN, M. and VILCINSKAS, A., 2017. Bioactivity of Natural and Engineered Antimicrobial Peptides from Venom of the Scorpions Urodacus yaschenkoi and U. manicatus. *Toxins,* **9**(1), pp. 22.

LUNA-RAMÍREZ, K., QUINTERO-HERNÁNDEZ, V., VARGAS-JAIMES, L., BATISTA, C.V.F., WINKEL, K.D. and POSSANI, L.D., 2013. Characterization of the venom from the Australian scorpion Urodacus yaschenkoi: Molecular mass analysis of components, cDNA sequences and peptides with antimicrobial activity. *Toxicon,* **63**(0), pp. 44-54.

LV, Y., WANG, J., GAO, H., WANG, Z., DONG, N., MA, Q. and SHAN, A., 2014. Antimicrobial properties and membrane-active mechanism of a potential α-helical antimicrobial derived from cathelicidin PMAP-36. *PloS one,* **9**(1), pp. e86364.

MA, Y., ZHAO, R., HE, Y., LI, S., LIU, J., WU, Y., CAO, Z. and LI, W., 2009. Transcriptome analysis of the venom gland of the scorpion Scorpiops jendeki: implication for the evolution of the scorpion venom arsenal. *BMC genomics,* **10**, pp. 290-2164-10-290.

MACKESSY, S.P., 2016. *Handbook of venoms and toxins of reptiles.* CRC Press.

MAHLAPUU, M., HÅKANSSON, J., RINGSTAD, L. and BJÖRN, C., 2016. Antimicrobial Peptides: An Emerging Category of Therapeutic Agents. *Frontiers in Cellular and Infection Microbiology,* **6** (194), pp1-12..

MAKOBONGO, M.O., GANCZ, H., CARPENTER, B.M., MCDANIEL, D.P. and MERRELL, D.S., 2012. The oligo-acyl lysyl antimicrobial peptide C(1)(2)K-2beta(1)(2) exhibits a

dual mechanism of action and demonstrates strong in vivo efficacy against Helicobacter pylori. *Antimicrobial Agents and Chemotherapy,* **56**(1), pp. 378-390.

MALANOVIC, N. and LOHNER, K., 2016. Antimicrobial Peptides Targeting Gram-Positive Bacteria. *Pharmaceuticals,* **9**(3), pp. 59.

MALMSTEN, M., 2011. Antimicrobial and antiviral hydrogels. *Soft Matter,* **7**(19), pp. 8725-8736.

MANGONI, M.L., PAPO, N., BARRA, D., SIMMACO, M., BOZZI, A., DI GIULIO, A. and RINALDI, A.C., 2004. Effects of the antimicrobial peptide temporin L on cell morphology, membrane permeability and viability of Escherichia coli. *The Biochemical journal,* **380**(Pt 3), pp. 859-865.

MARCINKIEWICZ, C., 2013. Applications of snake venom components to modulate integrin activities in cell–matrix interactions. *The international journal of biochemistry & cell biology,* **45**(9), pp. 1974-1986.

MARQUARDT, D., GEIER, B. and PABST, G., 2015. Asymmetric lipid membranes: towards more realistic model systems. *Membranes,* **5**(2), pp. 180-196.

MARTÍNEZ, B., SUÁREZ, J.E. and RODRÍGUEZ, A., 1996. Lactococcin 972: a homodimeric lactococcal bacteriocin whose primary target is not the plasma membrane. *Microbiology,* **142**(9), pp. 2393-2398.

MARTINEZ, B., BOTTIGER, T., SCHNEIDER, T., RODRIGUEZ, A., SAHL, H.G. and WIEDEMANN, I., 2008. Specific interaction of the unmodified bacteriocin Lactococcin 972 with the cell wall precursor lipid II. *Applied and Environmental Microbiology,* **74**(15), pp. 4666-4670.

MASCIO, C.T., ALDER, J.D. and SILVERMAN, J.A., 2007. Bactericidal action of daptomycin against stationary-phase and nondividing Staphylococcus aureus cells. *Antimicrobial Agents and Chemotherapy,* **51**(12), pp. 4255-4260.

MATHAVAN, I., ZIRAH, S., MEHMOOD, S., CHOUDHURY, H.G., GOULARD, C., LI, Y., ROBINSON, C.V., REBUFFAT, S. and BEIS, K., 2014. Structural basis for hijacking

siderophore receptors by antimicrobial lasso peptides. *Nature chemical biology,* **10**(5), pp. 340-342.

MATSUZAKI, K., 2009. Control of cell selectivity of antimicrobial peptides. *Biochimica et Biophysica Acta (BBA)-Biomembranes,* **1788**(8), pp. 1687-1692.

MATSUZAKI, K., MURASE, O., FUJII, N. and MIYAJIMA, K., 1996. An antimicrobial peptide, magainin 2, induced rapid flip-flop of phospholipids coupled with pore formation and peptide translocation. *Biochemistry,* **35**(35), pp. 11361-11368.

MATSUZAKI, K., SUGISHITA, K. and MIYAJIMA, K., 1999. Interactions of an antimicrobial peptide, magainin 2, with lipopolysaccharide-containing liposomes as a model for outer membranes of Gram-negative bacteria. *FEBS letters,* **449**(2-3), pp. 221-224.

MATSUZAKI, K., SUGISHITA, K., HARADA, M., FUJII, N. and MIYAJIMA, K., 1997. Interactions of an antimicrobial peptide, magainin 2, with outer and inner membranes of Gram-negative bacteria. *Biochimica et Biophysica Acta (BBA) - Biomembranes,* **1327**(1), pp. 119-130.

MCCAUGHEY, G., MCKEVITT, M., ELBORN, J.S. and TUNNEY, M.M., 2012. Antimicrobial activity of fosfomycin and tobramycin in combination against cystic fibrosis pathogens under aerobic and anaerobic conditions. *Journal of Cystic Fibrosis,* **11**(3), pp. 163-172.

MCCAUGHEY, G., GILPIN, D.F., SCHNEIDERS, T., HOFFMAN, L.R., MCKEVITT, M., ELBORN, J.S. and TUNNEY, M.M., 2013. Fosfomycin and tobramycin in combination downregulate nitrate reductase genes narG and narH, resulting in increased activity against Pseudomonas aeruginosa under anaerobic conditions. *Antimicrobial Agents and Chemotherapy,* **57**(11), pp. 5406-5414.

MCHENRY, A.J., SCIACCA, M.F., BRENDER, J.R. and RAMAMOORTHY, A., 2012. Does cholesterol suppress the antimicrobial peptide induced disruption of lipid raft containing membranes? *Biochimica et Biophysica Acta (BBA)-Biomembranes,* **1818**(12), pp. 3019-3024.

MECKE, A., LEE, D., RAMAMOORTHY, A., ORR, B.G. and HOLL, M.M.B., 2005. Membrane thinning due to antimicrobial peptide binding: an atomic force microscopy study of MSI-78 in lipid bilayers. *Biophysical journal,* **89**(6), pp. 4043-4050.

MEENA, K.R. and KANWAR, S.S., 2015. Lipopeptides as the antifungal and antibacterial agents: applications in food safety and therapeutics. *BioMed research international,* **2015**.pp 1-9.

MEINCKEN, M., HOLROYD, D.L. and RAUTENBACH, M., 2005. Atomic force microscopy study of the effect of antimicrobial peptides on the cell envelope of Escherichia coli. *Antimicrobial Agents and Chemotherapy,* **49**(10), pp. 4085-4092.

MEISTER, M., LEMAITRE, B. and HOFFMANN, J.A., 1997. Antimicrobial peptide defense in Drosophila. *Bioessays,* **19**(11), pp. 1019-1026.

MELO, M.N., FERRE, R. and CASTANHO, M.A., 2009. Antimicrobial peptides: linking partition, activity and high membrane-bound concentrations. *Nature Reviews Microbiology,* **7**(3), pp. 245-250.

MENEZ, A., 2002. *Perspectives in molecular toxinology.* John Wiley & Sons.

MIDURA-NOWACZEK, K. and MARKOWSKA, A., 2014. Antimicrobial peptides and their analogs: searching for new potential therapeutics. *Perspectives in medicinal chemistry,* **6**, pp. 73-80.

MIETHKE, M. and MARAHIEL, M.A., 2007. Siderophore-based iron acquisition and pathogen control. *Microbiology and molecular biology reviews : MMBR,* **71**(3), pp. 413-451.

MOHAMED, M.F., HAMMAC, G.K., GUPTILL, L. and SELEEM, M.N., 2014. Antibacterial activity of novel cationic peptides against clinical isolates of multi-drug resistant Staphylococcus pseudintermedius from infected dogs. *PloS one,* **9**(12), pp. e116259.

MOHANRAM, H. and BHATTACHARJYA, S., 2016. Salt resistant short antimicrobial peptides. *Peptide Science,***106**(3).pp345-356

MOJSOSKA, B. and JENSSEN, H., 2015. Peptides and peptidomimetics for antimicrobial drug design. *Pharmaceuticals,* **8**(3), pp. 366-415.

MOLLMANN, U., GUTSCHE, W., MALTZ, L. and OVADIA, M., 1997. Activity of cytotoxin P4 from the venom of the cobra snake Naja nigricollis on gram-positive bacteria and eukaryotic cell lines. *Arzneimittel-Forschung,* **47**(5), pp. 671-673.

MONRÁS, J.P., COLLAO, B., MOLINA-QUIROZ, R.C., PRADENAS, G.A., SAONA, L.A., DURÁN-TORO, V., ÓRDENES-AENISHANSLINS, N., VENEGAS, F.A., LOYOLA, D.E. and BRAVO, D., 2014. Microarray analysis of the Escherichia coli response to CdTe-GSH Quantum Dots: understanding the bacterial toxicity of semiconductor nanoparticles. *BMC genomics,* **15**(1), pp. 1.

MOORE, A.J., BEAZLEY, W.D., BIBBY, M.C. and DEVINE, D.A., 1996. Antimicrobial activity of cecropins. *The Journal of antimicrobial chemotherapy,* **37**(6), pp. 1077-1089.

MOREY, J.S., RYAN, J.C. and VAN DOLAH, F.M., 2006. Microarray validation: factors influencing correlation between oligonucleotide microarrays and real-time PCR. *Biol Proced Online,* **8**(1), pp. 175-193.

MUCKENTHALER, M.U., GALY, B. and HENTZE, M.W., 2008. Systemic iron homeostasis and the iron-responsive element/iron-regulatory protein (IRE/IRP) regulatory network. *Annu.Rev.Nutr.,* **28**, pp. 197-213.

MYGIND, P.H., FISCHER, R.L., SCHNORR, K.M., HANSEN, M.T., SÖNKSEN, C.P., LUDVIGSEN, S., RAVENTÓS, D., BUSKOV, S., CHRISTENSEN, B. and DE MARIA, L., 2005. Plectasin is a peptide antibiotic with therapeutic potential from a saprophytic fungus. *Nature,* **437**(7061), pp. 975-980.

NABI, G., AHMAD, N., ULLAH, S. and KHAN, S., 2015. Therapeutic Applications of Scorpion Venom in Cancer: Mini Review. *Journal of Biology and Life Sciences,* **6**(1), pp. 57.

NAIR, D.G., FRY, B.G., ALEWOOD, P., KUMAR, P.P. and KINI, R.M., 2007. Antimicrobial activity of omwaprin, a new member of the waprin family of snake venom proteins. *The Biochemical journal,* **402**(1), pp. 93-104.

NAN, Y. and SHIN, S., 2011. Effect of disulphide bond position on salt resistance and LPS-neutralizing activity of α-helical homo-dimeric model antimicrobial peptides. *BMB reports,* **44**(11), pp. 747-752.

NAWROCKI, K.L., CRISPELL, E.K. and MCBRIDE, S.M., 2014. Antimicrobial peptide resistance mechanisms of gram-positive bacteria. *Antibiotics,* **3**(4), pp. 461-492.

NAWROT, R., BARYLSKI, J., NOWICKI, G., BRONIARCZYK, J., BUCHWALD, W. and GOŹDZICKA-JÓZEFIAK, A., 2014. Plant antimicrobial peptides. *Folia microbiologica,* **59**(3), pp. 181-196.

NEWTON, K.A., CLENCH, M.R., DESHMUKH, R., JEYASEELAN, K. and STRONG, P.N., 2007. Mass fingerprinting of toxic fractions from the venom of the Indian red scorpion, Mesobuthus tamulus: biotope-specific variation in the expression of venom peptides. *Rapid communications in mass spectrometry,* **21**(21), pp. 3467-3476.

NGUYEN, L.T., HANEY, E.F. and VOGEL, H.J., 2011. The expanding scope of antimicrobial peptide structures and their modes of action. *Trends in biotechnology,* **29**(9), pp. 464-472.

NIE, Y., ZENG, X., YANG, Y., LUO, F., LUO, X., WU, S., ZHANG, L. and ZHOU, J., 2012. A novel class of antimicrobial peptides from the scorpion Heterometrus spinifer. *Peptides,* **38**(2), pp. 389-394.

NOLAN, E.M., FISCHBACH, M.A., KOGLIN, A. and WALSH, C.T., 2007. Biosynthetic tailoring of microcin E492m: post-translational modification affords an antibacterial siderophore-peptide conjugate. *Journal of the American Chemical Society,* **129**(46), pp. 14336-14347.

NTWASA, M., 2012. Cationic peptide interactions with biological macromolecules. *Binding Protein,* , pp. 139-164.

NUDING, S., FRASCH, T., SCHALLER, M., STANGE, E.F. and ZABEL, L.T., 2014. Synergistic effects of antimicrobial peptides and antibiotics against Clostridium difficile. *Antimicrobial Agents and Chemotherapy,* **58**(10), pp. 5719-5725.

O'NEIL, J., 2014. Antimicrobial Resistance: Tackling a crisis for the health and wealth of nations, *Review on Antimicrobial Resistance.*

OGUIURA, N., BONI-MITAKE, M., AFFONSO, R. and ZHANG, G., 2011. In vitro antibacterial and hemolytic activities of crotamine, a small basic myotoxin from rattlesnake Crotalus durissus. *The Journal of antibiotics,* **64**(4), pp. 327-331.

OLIYNYK, V., KAATZE, U. and HEIMBURG, T., 2007. Defect formation of lytic peptides in lipid membranes and their influence on the thermodynamic properties of the pore environment. *Biochimica et Biophysica Acta (BBA)-Biomembranes,* **1768**(2), pp. 236-245.

OMARDIEN, S., BRUL, S. and ZAAT, S.A., 2016. Antimicrobial activity of cationic antimicrobial peptides against gram-positives: Current progress made in understanding the mode of action and the response of bacteria. *Frontiers in cell and developmental biology,* **4**.

OPPENHEIM, J.J., BIRAGYN, A., KWAK, L.W. and YANG, D., 2003. Roles of antimicrobial peptides such as defensins in innate and adaptive immunity. *Annals of the Rheumatic Diseases,* **62 Suppl 2**, pp. ii17-21.

OREN, Z. and SHAI, Y., 1997. Selective lysis of bacteria but not mammalian cells by diastereomers of melittin: structure-function study. *Biochemistry,* **36**(7), pp. 1826-1835.

OTTING, G., STEINMETZ, W.E., BOUGIS, P.E., ROCHAT, H. and WÜTHRICH, K., 1987. Sequence-specific 1H-NMR assignments and determination of the secondary structure in aqueous solution of the cardiotoxins CTXIIa and CTXIIb from Naja mossambica mossambica. *European Journal of Biochemistry,* **168**(3), pp. 609-620.

OUKKACHE, N., CHGOURY, F., LALAOUI, M., CANO, A.A. and GHALIM, N., 2013. Comparison between two methods of scorpion venom milking in Morocco. *Journal of venomous animals and toxins including tropical diseases,* **19**(1), pp. 5.

OVERHAGE, J., BAINS, M., BRAZAS, M.D. and HANCOCK, R.E., 2008. Swarming of Pseudomonas aeruginosa is a complex adaptation leading to increased production of

virulence factors and antibiotic resistance. *Journal of Bacteriology,* **190**(8), pp. 2671-2679.

OYINLOYE, B.E., ADENOWO, A.F. and KAPPO, A.P., 2015. Reactive oxygen species, apoptosis, antimicrobial peptides and human inflammatory diseases. *Pharmaceuticals,* **8**(2), pp. 151-175.

OZKAN, O. and FILAZI, A., 2004. The determination of acute lethal dose-50 (LD50) levels of venom in mice, obtained by different methods from scorpions, Androctonus crassicauda (Oliver 1807). *Acta Parasitol.Turcica,* **28**(1), pp. 50-53.

PACOR, S., GIANGASPERO, A., BACAC, M., SAVA, G. and TOSSI, A., 2002. Analysis of the cytotoxicity of synthetic antimicrobial peptides on mouse leucocytes: implications for systemic use. *The Journal of antimicrobial chemotherapy,* **50**(3), pp. 339-348.

PADILLA, E., LLOBET, E., DOMENECH-SANCHEZ, A., MARTINEZ-MARTINEZ, L., BENGOECHEA, J.A. and ALBERTI, S., 2010. Klebsiella pneumoniae AcrAB efflux pump contributes to antimicrobial resistance and virulence. *Antimicrobial Agents and Chemotherapy,* **54**(1), pp. 177-183.

PARK, C.B., KIM, H.S. and KIM, S.C., 1998. Mechanism of action of the antimicrobial peptide buforin II: buforin II kills microorganisms by penetrating the cell membrane and inhibiting cellular functions. *Biochemical and biophysical research communications,* **244**(1), pp. 253-257.

PARK, S., PARK, Y. and HAHM, K., 2011. The role of antimicrobial peptides in preventing multidrug-resistant bacterial infections and biofilm formation. *International journal of molecular sciences,* **12**(9), pp. 5971-5992.

PARK, H.J., KANG, K.M., DYBVIG, K., LEE, B.L., JUNG, Y.W. and LEE, I.H., 2013. Interaction of cationic antimicrobial peptides with Mycoplasma pulmonis. *FEBS letters,* **587**(20), pp. 3321-3326.

PARK, I.Y., CHO, J.H., KIM, K.S., KIM, Y.B., KIM, M.S. and KIM, S.C., 2004. Helix stability confers salt resistance upon helical antimicrobial peptides. *The Journal of biological chemistry,* **279**(14), pp. 13896-13901.

PAULMANN, M., ARNOLD, T., LINKE, D., OZDIREKCAN, S., KOPP, A., GUTSMANN, T., KALBACHER, H., WANKE, I., SCHUENEMANN, V.J., HABECK, M., BURCK, J., ULRICH, A.S. and SCHITTEK, B., 2012. Structure-activity analysis of the dermcidin-derived peptide DCD-1L, an anionic antimicrobial peptide present in human sweat. *The Journal of biological chemistry,* **287**(11), pp. 8434-8443.

PEETLA, C., STINE, A. and LABHASETWAR, V., 2009. Biophysical interactions with model lipid membranes: applications in drug discovery and drug delivery. *Molecular pharmaceutics,* **6**(5), pp. 1264-1276.

PELAEZ, F., 2006. The historical delivery of antibiotics from microbial natural products—can history repeat? *Biochemical pharmacology,* **71**(7), pp. 981-990.

PERALTA, D.R., ADLER, C., CORBALÁN, N.S., GARCÍA, E.C.P., POMARES, M.F. and VINCENT, P.A., 2016. Enterobactin as Part of the Oxidative Stress Response Repertoire. *PloS one,* **11**(6), pp. e0157799.

PEREIRA, A., KERKIS, A., HAYASHI, M.A., PEREIRA, A.S., SILVA, F.S., OLIVEIRA, E.B., PRIETO DA SILVA, ALVARO RB, YAMANE, T., RADIS-BAPTISTA, G. and KERKIS, I., 2011. Crotamine toxicity and efficacy in mouse models of melanoma. *Expert opinion on investigational drugs,* **20**(9), pp. 1189-1200.

PHOENIX, D.A., DENNISON, S.R. and HARRIS, F., 2013. Antimicrobial peptides: their history, evolution, and functional promiscuity. *Antimicrobial peptides,* , pp. 1-37.

PHOENIX, D.A., DENNISON, S.R. and HARRIS, F., 2012. *Antimicrobial peptides.* John Wiley & Sons.

PIETIÄINEN, M., FRANÇOIS, P., HYYRYLÄINEN, H., TANGOMO, M., SASS, V., SAHL, H., SCHRENZEL, J. and KONTINEN, V.P., 2009. Transcriptome analysis of the responses of Staphylococcus aureus to antimicrobial peptides and characterization of the roles of vraDE and vraSR in antimicrobial resistance. *BMC genomics,* **10**(1), pp. 1.

PIETIÄINEN, M., GARDEMEISTER, M., MECKLIN, M., LESKELÄ, S., SARVAS, M. and KONTINEN, V.P., 2005. Cationic antimicrobial peptides elicit a complex stress response

in Bacillus subtilis that involves ECF-type sigma factors and two-component signal transduction systems. *Microbiology,* **151**(5), pp. 1577-1592.

PILLAI, A., UENO, S., ZHANG, H., LEE, J.M. and KATO, Y., 2005. Cecropin P1 and novel nematode cecropins: a bacteria-inducible antimicrobial peptide family in the nematode Ascaris suum. *The Biochemical journal,* **390**(Pt 1), pp. 207-214.

PIMENTA DE MORAIS, I., CORRADO, A.P. and SUAREZ-KURTZ, G., 1978. Competitive antagonism between calcium and aminoglycoside antibiotics on guinea-pig intestinal smooth muscle. *Archives Internationales de Pharmacodynamie et de Therapie,* **231**(2), pp. 317-327.

PIRRI, G., GIULIANI, A., NICOLETTO, S.F., PIZZUTO, L. and RINALDI, A.C., 2009. Lipopeptides as anti-infectives: a practical perspective. *Central European journal of biology,* **4**(3), pp. 258-273.

POMPOSIELLO, P.J., BENNIK, M.H. and DEMPLE, B., 2001. Genome-wide transcriptional profiling of the Escherichia coli responses to superoxide stress and sodium salicylate. *Journal of Bacteriology,* **183**(13), pp. 3890-3902.

POOLE, K., 2005. Efflux-mediated antimicrobial resistance. *The Journal of antimicrobial chemotherapy,* **56**(1), pp. 20-51.

POSSANI, L.D., CORONA, M., ZURITA, M. and RODRÍGUEZ, M.H., 2002. From noxiustoxin to scorpine and possible transgenic mosquitoes resistant to malaria. *Archives of Medical Research,* **33**(4), pp. 398-404.

PU, X.C., WONG, P.T.H. and GOPALAKRISHNAKONE, P., 1995. A novel analgesic toxin (hannalgesin) from the venom of king cobra (Ophiophagus hannah). *Toxicon,* **33**(11), pp. 1425-1431.

QI, Z., XU, W., MENG, F., ZHANG, Q., CHEN, C. and SHAO, R., 2016. Cloning and Expression of β-Defensin from Soiny Mullet (Liza haematocheila), with Insights of its Antibacterial Mechanism. *PloS one,* **11**(6), pp. e0157544.

QIAN, S., WANG, W., YANG, L. and HUANG, H.W., 2008. Structure of the alamethicin pore reconstructed by x-ray diffraction analysis. *Biophysical journal,* **94**(9), pp. 3512-3522.

RAHAMAN, A. and LAZARIDIS, T., 2014. A thermodynamic approach to alamethicin pore formation. *Biochimica et Biophysica Acta (BBA) - Biomembranes,* **1838**(5), pp. 1440-1447.

RAINES, D.J., MOROZ, O.V., BLAGOVA, E.V., TURKENBURG, J.P., WILSON, K.S. and DUHME-KLAIR, A.K., 2016. Bacteria in an intense competition for iron: Key component of the Campylobacter jejuni iron uptake system scavenges enterobactin hydrolysis product. *Proceedings of the National Academy of Sciences of the United States of America,* **113**(21), pp. 5850-5855.

RAJAGOPALAN, N., PUNG, Y.F., ZHU, Y.Z., WONG, P.T., KUMAR, P.P. and KINI, R.M., 2007. Beta-cardiotoxin: a new three-finger toxin from Ophiophagus hannah (king cobra) venom with beta-blocker activity. *FASEB journal : official publication of the Federation of American Societies for Experimental Biology,* **21**(13), pp. 3685-3695.

RAMIREZ-RONDA, C.H., HOLMES, R.K. and SANFORD, J.P., 1975. Effects of divalent cations on binding of aminoglycoside antibiotics to human serum proteins and to bacteria. *Antimicrobial Agents and Chemotherapy,* **7**(3), pp. 239-245.

RAMMELKAMP, C.H. and MAXON, T., 1942. Resistance of Staphylococcus aureus to the Action of Penicillin. *Experimental biology and medicine,* **51**(3), pp. 386-389.

RAMOS, P.I.P., CUSTÓDIO, M.G.F., SAJI, GUADALUPE DEL ROSARIO QUISPE, CARDOSO, T., DA SILVA, G.L., BRAUN, G., MARTINS, W.M., GIRARDELLO, R., DE VASCONCELOS, ANA TEREZA RIBEIRO and FERNÁNDEZ, E., 2016. The polymyxin B-induced transcriptomic response of a clinical, multidrug-resistant Klebsiella pneumoniae involves multiple regulatory elements and intracellular targets. *BMC genomics,* **17**(8), pp. 447.

RAMSTEDT, M., LEONE, L., PERSSON, P. and SHCHUKAREV, A., 2014. Cell Wall Composition of Bacillus subtilis Changes as a Function of pH and Zn2 Exposure: Insights from Cryo-XPS Measurements. *Langmuir,* **30**(15), pp. 4367-4374.

RAMSTEDT, M., NAKAO, R., WAI, S.N., UHLIN, B.E. and BOILY, J.F., 2011. Monitoring surface chemical changes in the bacterial cell wall: multivariate analysis of cryo-x-ray photoelectron spectroscopy data. *The Journal of biological chemistry,* **286**(14), pp. 12389-12396.

RANDALL, C.P., MARINER, K.R., CHOPRA, I. and O'NEILL, A.J., 2013. The target of daptomycin is absent from Escherichia coli and other gram-negative pathogens. *Antimicrobial Agents and Chemotherapy,* **57**(1), pp. 637-639.

REES, B., BILWES, A., SAMAMA, J. and MORAS, D., 1990. CardiotoxinV 4 II fromNaja mossambica mossambica: The refined crystal structure. *Journal of Molecular Biology,* **214**(1), pp. 281-297.

RIEDL, S., RINNER, B., ASSLABER, M., SCHAIDER, H., WALZER, S., NOVAK, A., LOHNER, K. and ZWEYTICK, D., 2011. In search of a novel target—phosphatidylserine exposed by non-apoptotic tumor cells and metastases of malignancies with poor treatment efficacy. *Biochimica et Biophysica Acta (BBA)-Biomembranes,* **1808**(11), pp. 2638-2645.

RODRÍGUEZ, A., VILLEGAS, E., MONTOYA-ROSALES, A., RIVAS-SANTIAGO, B. and CORZO, G., 2014. Characterization of antibacterial and hemolytic activity of synthetic pandinin 2 variants and their inhibition against mycobacterium tuberculosis. *PloS one,* **9**(7), pp. e101742.

RODRÍGUEZ-ROJAS, A., RODRÍGUEZ-BELTRÁN, J., COUCE, A. and BLÁZQUEZ, J., 2013. Antibiotics and antibiotic resistance: A bitter fight against evolution. *International Journal of Medical Microbiology,* **303**(6–7), pp. 293-297.

ROSA, R. and BARRACCO, M., 2010. Antimicrobial peptides in crustaceans. *Inv Surv J,* **7**, pp. 262-284.

ROY, H., DARE, K. and IBBA, M., 2009. Adaptation of the bacterial membrane to changing environments using aminoacylated phospholipids. *Molecular microbiology,* **71**(3), pp. 547-550.

ROZEK, A., FRIEDRICH, C.L. and HANCOCK, R.E., 2000. Structure of the bovine antimicrobial peptide indolicidin bound to dodecylphosphocholine and sodium dodecyl sulfate micelles. *Biochemistry,* **39**(51), pp. 15765-15774.

ROZEK, A., POWERS, J.S., FRIEDRICH, C.L. and HANCOCK, R.E., 2003. Structure-Based Design of an Indolicidin Peptide Analogue with Increased Protease Stability. *Biochemistry,* **42**(48), pp. 14130-14138.

RUIMING, Z., YIBAO, M., YAWEN, H., ZHIYONG, D., YINGLIANG, W., ZHIJIAN, C. and WENXIN, L., 2010. Comparative venom gland transcriptome analysis of the scorpion Lychas mucronatus reveals intraspecific toxic gene diversity and new venomous components. *BMC genomics,* **11**(1), pp. 1.

RUIZ, J.A., BERNAR, E.M. and JUNG, K., 2015. Production of siderophores increases resistance to fusaric acid in Pseudomonas protegens Pf-5. *PloS one,* **10**(1), pp. e0117040.

SACHIDANANDA, M., MURARI, S. and CHANNE GOWDA, D., 2007. Characterization of an antibacterial peptide from Indian cobra (Naja naja) venom. *Journal of Venomous Animals and Toxins including Tropical Diseases,* **13**(2), pp. 446-461.

SADER, H.S., FEDLER, K.A., RENNIE, R.P., STEVENS, S. and JONES, R.N., 2004. Omiganan pentahydrochloride (MBI 226), a topical 12-amino-acid cationic peptide: spectrum of antimicrobial activity and measurements of bactericidal activity. *Antimicrobial Agents and Chemotherapy,* **48**(8), pp. 3112-3118.

SAHALAN, A.Z., AZIZ, A.H.A., HING, H.L. and GHANI, M.K.A., 2013. Divalent cations (Mg^{2+}, Ca^{2+}) protect bacterial outer membrane damage by polymyxin B. *Sains Malaysiana,* **42**(3), pp. 301-306.

SAIMAN, L., TABIBI, S., STARNER, T.D., SAN GABRIEL, P., WINOKUR, P.L., JIA, H.P., MCCRAY, P.B.,Jr and TACK, B.F., 2001a. Cathelicidin peptides inhibit multiply antibiotic-

resistant pathogens from patients with cystic fibrosis. *Antimicrobial Agents and Chemotherapy,* **45**(10), pp. 2838-2844.

SAIMAN, L., TABIBI, S., STARNER, T.D., SAN GABRIEL, P., WINOKUR, P.L., JIA, H.P., MCCRAY, P.B.,Jr and TACK, B.F., 2001b. Cathelicidin peptides inhibit multiply antibiotic-resistant pathogens from patients with cystic fibrosis. *Antimicrobial Agents and Chemotherapy,* **45**(10), pp. 2838-2844.

SALAMA, W. and GEASA, N., 2014. Investigation of the antimicrobial and hemolytic activity of venom of some Egyptian scorpion. *Journal of Microbiology and Antimicrobials,* **6**(1), pp. 21-28.

SALVAIL, H., LANTHIER-BOURBONNAIS, P., SOBOTA, J.M., CAZA, M., BENJAMIN, J.A., MENDIETA, M.E., LEPINE, F., DOZOIS, C.M., IMLAY, J. and MASSE, E., 2010. A small RNA promotes siderophore production through transcriptional and metabolic remodeling. *Proceedings of the National Academy of Sciences of the United States of America,* **107**(34), pp. 15223-15228.

SAMEJIMA, Y., AOKI-TOMOMATSU, Y., YANAGISAWA, M. and MEBS, D., 1997. Amino acid sequence of two neurotoxins from the venom of the Egyptian black snake (Walterinnesia aegyptia). *Toxicon,* **35**(2), pp. 151-157.

SAMPSON, T.R., LIU, X., SCHROEDER, M.R., KRAFT, C.S., BURD, E.M. and WEISS, D.S., 2012. Rapid killing of Acinetobacter baumannii by polymyxins is mediated by a hydroxyl radical death pathway. *Antimicrobial Agents and Chemotherapy,* **56**(11), pp. 5642-5649.

SAMY, R.P., PACHIAPPAN, A., GOPALAKRISHNAKONE, P., THWIN, M.M., HIAN, Y.E., CHOW, V.T., BOW, H. and WENG, J.T., 2006. In *vitro* antimicrobial activity of natural toxins and animal venoms tested against Burkholderia pseudomallei. *BMC Infectious Diseases,* **6**(1), pp. 1.

SAMY, R.P., STILES, B.G., CHINNATHAMBI, A., ZAYED, M.E., ALHARBI, S.A., FRANCO, O.L., ROWAN, E.G., KUMAR, A.P., LIM, L.H.K. and SETHI, G., 2015. Viperatoxin-II: A novel viper venom protein as an effective bactericidal agent. *FEBS Open Bio,* **5**, pp. 928-941.

SANDERSON, J.M., 2005. Peptide–lipid interactions: insights and perspectives. *Organic & biomolecular chemistry,* **3**(2), pp. 201-212.

SANI, M., GAGNE, E., GEHMAN, J.D., WHITWELL, T.C. and SEPAROVIC, F., 2014. Dye-release assay for investigation of antimicrobial peptide activity in a competitive lipid environment. *European Biophysics Journal,* **43**(8-9), pp. 445-450.

SANI, M. and SEPAROVIC, F., 2016. How Membrane-Active Peptides Get into Lipid Membranes. *Accounts of Chemical Research,* .

SATO, H. and FEIX, J.B., 2006. Peptide–membrane interactions and mechanisms of membrane destruction by amphipathic α-helical antimicrobial peptides. *Biochimica et Biophysica Acta (BBA)-Biomembranes,* **1758**(9), pp. 1245-1256.

SCANLON, T.C., DOSTAL, S.M. and GRISWOLD, K.E., 2014. A high-throughput screen for antibiotic drug discovery. *Biotechnology and bioengineering,* **111**(2), pp. 232-243.

SCHATZ, A., BUGLE, E. and WAKSMAN, S.A., 1944. Streptomycin, a Substance Exhibiting Antibiotic Activity Against Gram-Positive and Gram-Negative Bacteria.. *Proceedings of the Society for Experimental Biology and Medicine,* **55**(1), pp. 66-69.

SCHEINPFLUG, K., KRYLOVA, O., NIKOLENKO, H., THURM, C. and DATHE, M., 2015. Evidence for a novel mechanism of antimicrobial action of a cyclic R-, W-rich hexapeptide. *PloS one,* **10**(4), pp. e0125056.

SCHITTEK, B., HIPFEL, R., SAUER, B., BAUER, J., KALBACHER, H., STEVANOVIC, S., SCHIRLE, M., SCHROEDER, K., BLIN, N. and MEIER, F., 2001. Dermcidin: a novel human antibiotic peptide secreted by sweat glands. *Nature immunology,* **2**(12), pp. 1133-1137.

SCHMIDTCHEN, A., PASUPULETI, M. and MALMSTEN, M., 2014. Effect of hydrophobic modifications in antimicrobial peptides. *Advances in Colloid and Interface Science,* **205**, pp. 265-274.

SCHURR, M.J., 2013. Which bacterial biofilm exopolysaccharide is preferred, Psl or alginate? *Journal of Bacteriology,* **195**(8), pp. 1623-1626.

SCOCCHI, M., MARDIROSSIAN, M., RUNTI, G. and BENINCASA, M., 2016. Non-membrane permeabilizing modes of action of antimicrobial peptides on bacteria. *Current topics in medicinal chemistry,* **16**(1), pp. 76-88.

SENGUPTA, D., LEONTIADOU, H., MARK, A.E. and MARRINK, S., 2008. Toroidal pores formed by antimicrobial peptides show significant disorder. *Biochimica et Biophysica Acta (BBA)-Biomembranes,* **1778**(10), pp. 2308-2317.

SEO, M., WON, H., KIM, J., MISHIG-OCHIR, T. and LEE, B., 2012. Antimicrobial peptides for therapeutic applications: a review. *Molecules,* **17**(10), pp. 12276-12286.

SHAHMIRI, M., ENCISO, M. and MECHLER, A., 2015. Controls and constrains of the membrane disrupting action of Aurein 1.2. *Scientific reports,* **5**, pp. 16378.

SHAI, Y., 1999. Mechanism of the binding, insertion and destabilization of phospholipid bilayer membranes by α-helical antimicrobial and cell non-selective membrane-lytic peptides. *Biochimica et Biophysica Acta (BBA)-Biomembranes,* **1462**(1), pp. 55-70.

SHALLCROSS, L.J., HOWARD, S.J., FOWLER, T. and DAVIES, S.C., 2015. Tackling the threat of antimicrobial resistance: from policy to sustainable action. *Philosophical transactions of the Royal Society of London.Series B, Biological sciences,* **370**(1670), pp. 20140082.

SHANBHAG, V.K.L., 2015. Applications of snake venoms in treatment of cancer. *Asian Pacific Journal of Tropical Biomedicine,* **5**(4), pp. 275-276.

SHAO, J., KANG, N., LIU, Y., SONG, S., WU, C. and ZHANG, J., 2007. Purification and characterization of an analgesic peptide from Buthus martensii Karsch. *Biomedical Chromatography,* **21**(12), pp. 1266-1271.

SHAO, J., CUI, Y., ZHAO, M., WU, C., LIU, Y. and ZHANG, J., 2014. Purification, characterization, and bioactivity of a new analgesic-antitumor peptide from Chinese scorpion Buthus martensii Karsch. *Peptides,* **53**, pp. 89-96.

SHEBL, R., MOHAMED, A., ALI, A. and AMIN, M., 2012. Antimicrobial profile of selected snake venoms and their associated enzymatic activities. *British Microbiology Research Journal,* **2**(4), pp. 251.

SHEK, K., TSUI, K., LAM, K., CROW, P., NG, K., ADES, G., YIP, K., GRIONI, A., TAN, K. and LUNG, D.C., 2009. Oral bacterial flora of the Chinese cobra (Naja atra) and bamboo pit viper (Trimeresurus albolabris) in Hong Kong SAR, China. *Hong Kong Med J,* **15**(3), pp. 183-190.

SHOEMAKER, D.M., SIMOU, J. and ROLAND, W.E., 2006. A review of daptomycin for injection (Cubicin) in the treatment of complicated skin and skin structure infections. *Therapeutics and clinical risk management,* **2**(2), pp. 169-174.

SHOKRI, A. and LARSSON, G., 2004. Characterisation of the Escherichia coli membrane structure and function during fedbatch cultivation. *Microbial cell factories,* **3**(1), pp. 9.

SIKORA, A.E., BEYHAN, S., BAGDASARIAN, M., YILDIZ, F.H. and SANDKVIST, M., 2009a. Cell envelope perturbation induces oxidative stress and changes in iron homeostasis in Vibrio cholerae. *Journal of Bacteriology,* **191**(17), pp. 5398-5408.

SIKORA, A.E., BEYHAN, S., BAGDASARIAN, M., YILDIZ, F.H. and SANDKVIST, M., 2009b. Cell envelope perturbation induces oxidative stress and changes in iron homeostasis in Vibrio cholerae. *Journal of Bacteriology,* **191**(17), pp. 5398-5408.

SILVA, J.P., GONÇALVES, C., COSTA, C., SOUSA, J., SILVA-GOMES, R., CASTRO, A.G., PEDROSA, J., APPELBERG, R. and GAMA, F.M., 2016. Delivery of LLKKK18 loaded into self-assembling hyaluronic acid nanogel for tuberculosis treatment. *Journal of Controlled Release,* **235**, pp. 112-124.

SILVER, L.L., 2011. Challenges of antibacterial discovery. *Clinical microbiology reviews,* **24**(1), pp. 71-109.

SKERLAVAJ, B., GENNARO, R., BAGELLA, L., MERLUZZI, L., RISSO, A. and ZANETTI, M., 1996. Biological characterization of two novel cathelicidin-derived peptides and identification of structural requirements for their antimicrobial and cell lytic activities. *Journal of Biological Chemistry,* **271**(45), pp. 28375-28381.

SKERLAVAJ, B., BENINCASA, M., RISSO, A., ZANETTI, M. and GENNARO, R., 1999. SMAP-29: a potent antibacterial and antifungal peptide from sheep leukocytes. *FEBS letters,* **463**(1–2), pp. 58-62.

SPELLBERG, B., 2012. New antibiotic development: barriers and opportunities in 2012. *APUA Clinical Newsletter,* **30**(1), pp.8-10.

SRISAILAM, S., ARUNKUMAR, A., WANG, W., YU, C. and CHEN, H., 2000. Conformational study of a custom antibacterial peptide cecropin B1: implications of the lytic activity. *Biochimica et Biophysica Acta (BBA)-Protein Structure and Molecular Enzymology,* **1479**(1), pp. 275-285.

STÁBELI, R.G., MARCUSSI, S., CARLOS, G.B., PIETRO, R.C.L.R., SELISTRE-DE-ARAÚJO, H.S., GIGLIO, J.R., OLIVEIRA, E.B. and SOARES, A.M., 2004. Platelet aggregation and antibacterial effects of an l-amino acid oxidase purified from Bothrops alternatus snake venom. *Bioorganic & medicinal chemistry,* **12**(11), pp. 2881-2886.

STAPLETON, P.D. and TAYLOR, P.W., 2002. Methicillin resistance in Staphylococcus aureus: mechanisms and modulation. *Science progress,* **85**(1), pp. 57-72.

STEENBERGEN, J.N., ALDER, J., THORNE, G.M. and TALLY, F.P., 2005. Daptomycin: a lipopeptide antibiotic for the treatment of serious Gram-positive infections. *The Journal of antimicrobial chemotherapy,* **55**(3), pp. 283-288.

STINTZI, A., BARNES, C., XU, J. and RAYMOND, K.N., 2000. Microbial iron transport via a siderophore shuttle: a membrane ion transport paradigm. *Proceedings of the National Academy of Sciences of the United States of America,* **97**(20), pp. 10691-10696.

STOKES, J.M., DAVIS, J.H., MANGAT, C.S., WILLIAMSON, J.R. and BROWN, E.D., 2014. Discovery of a small molecule that inhibits bacterial ribosome biogenesis. *eLife,* **3**, pp. e03574.

STOTZ, H.U., THOMSON, J. and WANG, Y., 2009. Plant defensins: defense, development and application. *Plant signaling & behavior,* **4**(11), pp. 1010-1012.

STRAUS, S.K. and HANCOCK, R.E.W., 2006. Mode of action of the new antibiotic for Gram-positive pathogens daptomycin: Comparison with cationic antimicrobial peptides and lipopeptides. *Biochimica et Biophysica Acta (BBA) - Biomembranes,* **1758**(9), pp. 1215-1223.

STREIT, J.M., JONES, R.N. and SADER, H.S., 2004. Daptomycin activity and spectrum: a worldwide sample of 6737 clinical Gram-positive organisms. *The Journal of antimicrobial chemotherapy,* **53**(4), pp. 669-674.

SUDARSHAN, S. and DHANANJAYA, B., 2016. Antibacterial activity of an acidic phospholipase A 2 (NN-XIb-PLA 2) from the venom of Naja naja (Indian cobra). *SpringerPlus,* **5**(1), pp. 1.

SUDHARSHAN, S. and DHANANJAYA, B.L., 2015. Antibacterial potential of a basic phospholipase A 2 (VRV-PL-VIIIa) from Daboia russelii pulchella (Russell's viper) venom. *Journal of Venomous Animals and Toxins including Tropical Diseases,* **21**(1), pp. 1.

SUE, S., RAJAN, P., CHEN, T., HSIEH, C. and WU, W., 1997. Action of Taiwan cobra cardiotoxin on membranes: binding modes of a β-sheet polypeptide with phosphatidylcholine bilayers. *Biochemistry,* **36**(32), pp. 9826-9836.

SUGIARTO, H. and YU, P., 2007. Effects of cations on antimicrobial activity of ostricacins-1 and 2 on E. coli O157: H7 and S. aureus 1056MRSA. *Current microbiology,* **55**(1), pp. 36-41.

SUN, Y. and SHANG, D., 2015. Inhibitory Effects of Antimicrobial Peptides on Lipopolysaccharide-Induced Inflammation. *Mediators of inflammation,* **2015**. pp.1-8

SUZUKI, S., HORINOUCHI, T. and FURUSAWA, C., 2014. Prediction of antibiotic resistance by gene expression profiles. *Nature communications,* **5**. p.5792.

SYCHEV, S.V., BALANDIN, S.V., PANTELEEV, P.V., BARSUKOV, L.I. and OVCHINNIKOVA, T.V., 2015. Lipid-dependent pore formation by antimicrobial peptides arenicin-2 and melittin demonstrated by their proton transfer activity. *Journal of Peptide Science,* **21**(2), pp. 71-76.

TACK, B.F., SAWAI, M.V., KEARNEY, W.R., ROBERTSON, A.D., SHERMAN, M.A., WANG, W., HONG, T., BOO, L.M., WU, H. and WARING, A.J., 2002. SMAP-29 has two LPS-binding sites and a central hinge. *European Journal of Biochemistry,* **269**(4), pp. 1181-1189.

TALAN, D.A., CITRON, D.M., OVERTURF, G.D., SINGER, B., FROMAN, P. and GOLDSTEIN, E.J., 1991. Antibacterial activity of crotalid venoms against oral snake flora and other clinical bacteria. *The Journal of infectious diseases,* **164**(1), pp. 195-198.

TAM, J.P., WANG, S., WONG, K.H. and TAN, W.L., 2015. Antimicrobial peptides from plants. *Pharmaceuticals,* **8**(4), pp. 711-757.

TANG, H., ROTHERY, R.A., VOSS, J.E. and WEINER, J.H., 2011. Correct assembly of iron-sulfur cluster FS0 into *Escherichia coli* dimethyl sulfoxide reductase (DmsABC) is a prerequisite for molybdenum cofactor insertion. *The Journal of biological chemistry,* **286**(17), pp. 15147-15154.

TARAZI, S., 2016. Scorpion venom as antimicrobial peptides (AMPs): A review article. *The International Arabic Journal of Antimicrobial Agents,* **5**(3),pp1-9.

TEIXEIRA, V., FEIO, M.J. and BASTOS, M., 2012. Role of lipids in the interaction of antimicrobial peptides with membranes. *Progress in lipid research,* **51**(2), pp. 149-177.

THAKURIA, B. and LAHON, K., 2013. The Beta Lactam Antibiotics as an Empirical Therapy in a Developing Country: An Update on Their Current Status and Recommendations to Counter the Resistance against Them. *Journal of clinical and diagnostic research : JCDR,* **7**(6), pp. 1207-1214.

THOMAS III, K.J. and RICE, C.V., 2014. Revised model of calcium and magnesium binding to the bacterial cell wall. *BioMetals,* **27**(6), pp. 1361-1370.

THOMAS, X., DESTOUMIEUX-GARZON, D., PEDUZZI, J., AFONSO, C., BLOND, A., BIRLIRAKIS, N., GOULARD, C., DUBOST, L., THAI, R., TABET, J.C. and REBUFFAT, S., 2004. Siderophore peptide, a new type of post-translationally modified antibacterial peptide with potent activity. *The Journal of biological chemistry,* **279**(27), pp. 28233-28242.

THWAITE, J.E., HIBBS, S., TITBALL, R.W. and ATKINS, T.P., 2006. Proteolytic degradation of human antimicrobial peptide LL-37 by Bacillus anthracis may contribute to virulence. *Antimicrobial Agents and Chemotherapy,* **50**(7), pp. 2316-2322.

TILLE, P., 2013. *Bailey & Scott's diagnostic microbiology.* Elsevier Health Sciences.

TOMITA, T., HITOMI, S., NAGASE, T., MATSUI, H., MATSUSE, T., KIMURA, S. and OUCHI, Y., 2000. Effect of ions on antibacterial activity of human beta defensin 2. *Microbiology and immunology,* **44**(9), pp. 749-754.

TORRENT, M., SÁNCHEZ-CHARDI, A., NOGUÉS, M. and BOIX, E., 2010. Assessment of antimicrobial compounds by microscopy techniques. *Microscopy: Science, Technology, Applications and Education,(3), Series,* (4), pp. 1115-1126.

TORRES-LARIOS, A., GURROLA, G.B., ZAMUDIO, F.Z. and POSSANI, L.D., 2000. Hadrurin, a new antimicrobial peptide from the venom of the scorpion Hadrurus aztecus. *European Journal of Biochemistry,* **267**(16), pp. 5023-5031.

TORRES, A., DANTAS, R., MENEZES, R., TOYAMA, M., OLIVEIRA, M., NOGUEIRA, N., OLIVEIRA, M., MONTEIRO, H. and MARTINS, A., 2010. Antimicrobial activity of an L-amino acid oxidase isolated from Bothrops leucurus snake venom. *Journal of Venomous Animals and Toxins including Tropical Diseases,* **16**(4), pp. 614-622.

TOYAMA, M., RODRIGUES, S.D., TOYAMA, D.O., SOARES, V.C., AP COTRIM, C., XIMENES, R. and SANTOS, M.L., 2012. Phospholipases A2 protein structure and natural products interactions in development of new pharmaceuticals. *Protein Structure,* .

TROIANO, J., GOULD, E. and GOULD, I., 2006. Hemolitic action of Naja naja atra cardiotoxin on erythrocytes from different animals. *Journal of Venomous Animals and Toxins including Tropical Diseases,* **12**(1), pp. 44-58.

TSAI, H., WANG, Y.M. and TSAI, I., 2008. Cloning, characterization and phylogenetic analyses of members of three major venom families from a single specimen of Walterinnesia aegyptia. *Toxicon,* **51**(7), pp. 1245-1254.

TSETLIN, V., 1999. Snake venom α-neurotoxins and other 'three-finger'proteins. *European Journal of Biochemistry,* **264**(2), pp. 281-286.

TU, J., LI, D., LI, Q., ZHANG, L., ZHU, Q., GAUR, U., FAN, X., XU, H., YAO, Y., ZHAO, X. and YANG, M., 2015. Molecular Evolutionary Analysis of beta-Defensin Peptides in Vertebrates. *Evolutionary bioinformatics online,* **11**, pp. 105-114.

UAWONGGUL, N., THAMMASIRIRAK, S., CHAVEERACH, A., ARKARAVICHIEN, T., BUNYATRATCHATA, W., RUANGJIRACHUPORN, W., JEARRANAIPREPAME, P., NAKAMURA, T., MATSUDA, M. and KOBAYASHI, M., 2007. Purification and characterization of Heteroscorpine-1 (HS-1) toxin from Heterometrus laoticus scorpion venom. *Toxicon,* **49**(1), pp. 19-29.

UDO, E.E., BOSWIHI, S.S. and AL-SWEIH, N., 2016. High prevalence of toxic shock syndrome toxin–producing epidemic methicillin-resistant *Staphylococcus aureus* 15 (EMRSA-15) strains in Kuwait hospitals. *New microbes and new infections,* **12**, pp. 24-30.

ULVATNE, H., KAROLIUSSEN, S., STIBERG, T., REKDAL, O. and SVENDSEN, J.S., 2001. Short antibacterial peptides and erythromycin act synergically against Escherichia coli. *The Journal of antimicrobial chemotherapy,* **48**(2), pp. 203-208.

URBAN, P., JOSE VALLE-DELGADO, J., MOLES, E., MARQUES, J., DIEZ, C. and FERNANDEZ-BUSQUETS, X., 2012. Nanotools for the delivery of antimicrobial peptides. *Current Drug Targets,* **13**(9), pp. 1158-1172.

UTKIN, Y.N., 2015. Animal venom studies: Current benefits and future developments. *World journal of biological chemistry,* **6**(2), pp. 28-33.

VAN BOECKEL, T.P., GANDRA, S., ASHOK, A., CAUDRON, Q., GRENFELL, B.T., LEVIN, S.A. and LAXMINARAYAN, R., 2014. Global antibiotic consumption 2000 to 2010: an analysis of national pharmaceutical sales data. *The Lancet Infectious Diseases,* **14**(8), pp. 742-750.

VARGAS, L.J., LONDOÑO, M., QUINTANA, J.C., RUA, C., SEGURA, C., LOMONTE, B. and NÚÑEZ, V., 2012. An acidic phospholipase A 2 with antibacterial activity from Porthidium nasutum snake venom. *Comparative Biochemistry and Physiology Part B: Biochemistry and Molecular Biology,* **161**(4), pp. 341-347.

VASSILIADIS, G., DESTOUMIEUX-GARZON, D., LOMBARD, C., REBUFFAT, S. and PEDUZZI, J., 2010. Isolation and characterization of two members of the siderophore-microcin family, microcins M and H47. *Antimicrobial Agents and Chemotherapy,* **54**(1), pp. 288-297.

VASSILIADIS, G., PEDUZZI, J., ZIRAH, S., THOMAS, X., REBUFFAT, S. and DESTOUMIEUX-GARZON, D., 2007. Insight into siderophore-carrying peptide biosynthesis: enterobactin is a precursor for microcin E492 posttranslational modification. *Antimicrobial Agents and Chemotherapy,* **51**(10), pp. 3546-3553.

VEISEH, M., GABIKIAN, P., BAHRAMI, S.B., VEISEH, O., ZHANG, M., HACKMAN, R.C., RAVANPAY, A.C., STROUD, M.R., KUSUMA, Y., HANSEN, S.J., KWOK, D., MUNOZ, N.M., SZE, R.W., GRADY, W.M., GREENBERG, N.M., ELLENBOGEN, R.G. and OLSON, J.M., 2007. Tumor paint: a chlorotoxin:Cy5.5 bioconjugate for intraoperative visualization of cancer foci. *Cancer research,* **67**(14), pp. 6882-6888.

VENANCIO, E.J., PORTARO, F.C.V., KUNIYOSHI, A.K., CARVALHO, D.C., PIDDE-QUEIROZ, G. and TAMBOURGI, D.V., 2013. Enzymatic properties of venoms from Brazilian scorpions of Tityus genus and the neutralisation potential of therapeutical antivenoms. *Toxicon,* **69**, pp. 180-190.

VENTOLA, C.L., 2015. The antibiotic resistance crisis: part 1: causes and threats. *P & T : a peer-reviewed journal for formulary management,* **40**(4), pp. 277-283.

VERDON, J., COUTOS-THEVENOT, P., RODIER, M., LANDON, C., DEPAYRAS, S., NOEL, C., LA CAMERA, S., MOUMEN, B., GREVE, P. and BOUCHON, D., 2016. Armadillidin H, a Glycine-Rich Peptide from the Terrestrial Crustacean Armadillidium vulgare, Displays an Unexpected Wide Antimicrobial Spectrum with Membranolytic Activity. *Frontiers in Microbiology,* **7**.

VISWANATHAN, V., 2014. Off-label abuse of antibiotics by bacteria. *Gut microbes,* **5**(1), pp. 3-4.

VIZIOLI, J. and SALZET, M., 2002. Antimicrobial peptides from animals: focus on invertebrates. *Trends in pharmacological sciences,* **23**(11), pp. 494-496.

VRANAKIS, I., GONIOTAKIS, I., PSAROULAKI, A., SANDALAKIS, V., TSELENTIS, Y., GEVAERT, K. and TSIOTIS, G., 2014. Proteome studies of bacterial antibiotic resistance mechanisms. *Journal of proteomics,* **97**, pp. 88-99.

VYAS, V.K., BRAHMBHATT, K., BHATT, H. and PARMAR, U., 2013. Therapeutic potential of snake venom in cancer therapy: current perspectives. *Asian Pacific journal of tropical biomedicine,* **3**(2), pp. 156-162.

WALDRON, K.J. and ROBINSON, N.J., 2009. How do bacterial cells ensure that metalloproteins get the correct metal? *Nature Reviews Microbiology,* **7**(1), pp. 25-35.

WANG, X., WANG, X. and GUO, Z., 2015. Functionalization of platinum complexes for biomedical applications. *Accounts of Chemical Research,* **48**(9), pp. 2622-2631.

WANG, Y., HONG, J., LIU, X., YANG, H., LIU, R., WU, J., WANG, A., LIN, D. and LAI, R., 2008. Snake cathelicidin from Bungarus fasciatus is a potent peptide antibiotics. *PLoS One,* **3**(9), pp. e3217.

WANG, G., LI, X. and WANG, Z., 2016. APD3: the antimicrobial peptide database as a tool for research and education. *Nucleic acids research,* **44**(D1), pp. D1087-93.

WANG, J., CHOU, S., XU, L., ZHU, X., DONG, N., SHAN, A. and CHEN, Z., 2015. High specific selectivity and Membrane-Active Mechanism of the synthetic centrosymmetric alpha-helical peptides with Gly-Gly pairs. *Scientific reports,* **5**, pp. 15963.

WANG, Z., BIE, P., CHENG, J., LU, L., CUI, B. and WU, Q., 2016. The ABC transporter YejABEF is required for resistance to antimicrobial peptides and the virulence of Brucella melitensis. *Scientific reports,* **6**, pp. 31876.

WANG, Z. and WANG, G., 2004. APD: the Antimicrobial Peptide Database. *Nucleic acids research,* **32**(Database issue), pp. D590-2.

WARNER, D.M. and LEVY, S.B., 2010. Different effects of transcriptional regulators MarA, SoxS and Rob on susceptibility of Escherichia coli to cationic antimicrobial peptides (CAMPs): Rob-dependent CAMP induction of the marRAB operon. *Microbiology,* **156**(2), pp. 570-578.

WATANABE, H. and KAWANO, R., 2016. Channel Current Analysis for Pore-forming Properties of an Antimicrobial Peptide, Magainin 1, Using the Droplet Contact Method. *Analytical Sciences,* **32**(1), pp. 57-60.

WEI, L., GAO, J., ZHANG, S., WU, S., XIE, Z., LING, G., KUANG, Y.Q., YANG, Y., YU, H. and WANG, Y., 2015. Identification and Characterization of the First Cathelicidin from Sea Snakes with Potent Antimicrobial and Anti-inflammatory Activity and Special Mechanism. *The Journal of biological chemistry,* **290**(27), pp. 16633-16652.

WENCEWICZ, T.A., LONG, T.E., MÖLLMANN, U. and MILLER, M.J., 2013. Trihydroxamate siderophore–fluoroquinolone conjugates are selective sideromycin antibiotics that target Staphylococcus aureus. *Bioconjugate chemistry,* **24**(3), pp. 473-486.

WENZEL, M., CHIRIAC, A.I., OTTO, A., ZWEYTICK, D., MAY, C., SCHUMACHER, C., GUST, R., ALBADA, H.B., PENKOVA, M., KRAMER, U., ERDMANN, R., METZLER-NOLTE, N., STRAUS, S.K., BREMER, E., BECHER, D., BROTZ-OESTERHELT, H., SAHL, H.G. and BANDOW, J.E., 2014. Small cationic antimicrobial peptides delocalize peripheral membrane proteins. *Proceedings of the National Academy of Sciences of the United States of America,* **111**(14), pp. E1409-18.

WILCOX, M.H., 2005. Update on linezolid: the first oxazolidinone antibiotic. *Expert opinion on pharmacotherapy,* **6**(13), pp. 2315-2326.

WIMLEY, W.C., 2010. Describing the mechanism of antimicrobial peptide action with the interfacial activity model. *ACS chemical biology,* **5**(10), pp. 905-917.

WRIGHT, G.D., 2010. Q&A: Antibiotic resistance: where does it come from and what can we do about it? *BMC biology,* **8**(1), pp. 123.

WU, G., DING, J., LI, H., LI, L., ZHAO, R., SHEN, Z., FAN, X. and XI, T., 2008. Effects of cations and pH on antimicrobial activity of thanatin and s-thanatin against Escherichia coli ATCC25922 and B. subtilis ATCC 21332. *Current microbiology,* **57**(6), pp. 552-557.

WU, S., NIE, Y., ZENG, X., CAO, H., ZHANG, L., ZHOU, L., YANG, Y., LUO, X. and LIU, Y., 2014. Genomic and functional characterization of three new venom peptides from the scorpion Heterometrus spinifer. *Peptides,* **53**, pp. 30-41.

WU, M. and HANCOCK, R.E., 1999. Interaction of the cyclic antimicrobial cationic peptide bactenecin with the outer and cytoplasmic membrane. *The Journal of biological chemistry,* **274**(1), pp. 29-35.

XU, G., 2016. Relationships between the regulatory systems of quorum sensing and multidrug resistance. *Frontiers in Microbiology,* **7**, pp. 958.

YAMADA, K., SHINODA, S., OKU, H., KOMAGOE, K., KATSU, T. and KATAKAI, R., 2006. Synthesis of low-hemolytic antimicrobial dehydropeptides based on gramicidin S. *Journal of medicinal chemistry,* **49**(26), pp. 7592-7595.

YAMAGUCHI, S., HUSTER, D., WARING, A., LEHRER, R.I., KEARNEY, W., TACK, B.F. and HONG, M., 2001. Orientation and dynamics of an antimicrobial peptide in the lipid bilayer by solid-state NMR spectroscopy. *Biophysical journal,* **81**(4), pp. 2203-2214.

YAMANE, E.S., BIZERRA, F.C., OLIVEIRA, E.B., MOREIRA, J.T., RAJABI, M., NUNES, G.L.C., DE SOUZA, A.O., DA SILVA, I.D.C.G., YAMANE, T., KARPEL, R.L., SILVA JR., P.I. and HAYASHI, M.A.F., 2013. Unraveling the antifungal activity of a South American rattlesnake toxin crotamine. *Biochimie,* **95**(2), pp. 231-240.

YANG, L., HARROUN, T.A., WEISS, T.M., DING, L. and HUANG, H.W., 2001. Barrel-stave model or toroidal model? A case study on melittin pores. *Biophysical journal,* **81**(3), pp. 1475-1485.

YANG, X., WANG, Y., LEE, W. and ZHANG, Y., 2013. Antimicrobial peptides from the venom gland of the social wasp Vespa tropica. *Toxicon,* **74**(0), pp. 151-157.

YANLING, J., ZHIYUAN, L. and XIN, L., 2013. *The Antibacterial Drug Discovery.* INTECH Open Access Publisher.

YE, S., LI, H., WEI, F., JASENSKY, J., BOUGHTON, A.P., YANG, P. and CHEN, Z., 2012. Observing a model ion channel gating action in model cell membranes in real time in situ: membrane potential change induced alamethicin orientation change. *Journal of the American Chemical Society,* **134**(14), pp. 6237-6243.

YEAMAN, M.R. and YOUNT, N.Y., 2003. Mechanisms of antimicrobial peptide action and resistance. *Pharmacological reviews,* **55**(1), pp. 27-55.

YU, L., GUO, L., DING, J.L., HO, B., FENG, S., POPPLEWELL, J., SWANN, M. and WOHLAND, T., 2009. Interaction of an artificial antimicrobial peptide with lipid membranes. *Biochimica et Biophysica Acta (BBA)-Biomembranes,* **1788**(2), pp. 333-344.

YU, W., YIN, C., ZHOU, Y. and YE, B., 2012. Prediction of the mechanism of action of fusaricidin on Bacillus subtilis. *PloS one,* **7**(11), pp. e50003.

YU, Z., QIN, W., LIN, J., FANG, S. and QIU, J., 2015. Antibacterial mechanisms of polymyxin and bacterial resistance. *BioMed research international,* **2015**.

YU, H.Y., TU, C.H., YIP, B.S., CHEN, H.L., CHENG, H.T., HUANG, K.C., LO, H.J. and CHENG, J.W., 2011. Easy strategy to increase salt resistance of antimicrobial peptides. *Antimicrobial Agents and Chemotherapy,* **55**(10), pp. 4918-4921.

ZASLOFF, M., 2002. Antimicrobial peptides of multicellular organisms. *Nature,* **415**(6870), pp. 389-395.

ZASLOFF, M., 2007. Antimicrobial peptides, innate immunity, and the normally sterile urinary tract. *Journal of the American Society of Nephrology : JASN,* **18**(11), pp. 2810-2816.

ZELEZETSKY, I. and TOSSI, A., 2006. Alpha-helical antimicrobial peptides—using a sequence template to guide structure–activity relationship studies. *Biochimica et Biophysica Acta (BBA)-Biomembranes,* **1758**(9), pp. 1436-1449.

ZENG, X., CORZO, G. and HAHIN, R., 2005. Scorpion venom peptides without disulfide bridges. *IUBMB life,* **57**(1), pp. 13-21.

ZENG, Y., KULKARNI, A., YANG, Z., PATIL, P.B., ZHOU, W., CHI, X., VAN LANEN, S. and CHEN, S., 2012. Biosynthesis of albomycin δ2 provides a template for assembling siderophore and aminoacyl-tRNA synthetase inhibitor conjugates. *ACS chemical biology,* **7**(9), pp. 1565-1575.

ZENG, X., ZHOU, L., SHI, W., LUO, X., ZHANG, L., NIE, Y., WANG, J., WU, S., CAO, B. and CAO, H., 2013. Three new antimicrobial peptides from the scorpion Pandinus imperator. *Peptides,* **45**(0), pp. 28-34.

ZENG, Y., ROY, H., PATIL, P.B., IBBA, M. and CHEN, S., 2009. Characterization of two seryl-tRNA synthetases in albomycin-producing Streptomyces sp. strain ATCC 700974. *Antimicrobial Agents and Chemotherapy,* **53**(11), pp. 4619-4627.

ZHANG, L., DHILLON, P., YAN, H., FARMER, S. and HANCOCK, R.E., 2000. Interactions of Bacterial Cationic Peptide Antibiotics with Outer and Cytoplasmic Membranes ofPseudomonas aeruginosa. *Antimicrobial Agents and Chemotherapy,* **44**(12), pp. 3317-3321.

ZHANG, S., SONG, J., GONG, F., LI, S., CHANG, H., XIE, H., GAO, H., TAN, Y. and JI, S., 2016. Design of an [alpha]-helical antimicrobial peptide with improved cell-selective and potent anti-biofilm activity. *Nature Publishing Group.Scientific Reports,* **6**, pp. 27394.

ZHANG, T., DING, Y., LI, T., WAN, Y., LI, W., CHEN, H. and ZHOU, R., 2012. A Fur-like protein PerR regulates two oxidative stress response related operons dpr and metQIN in Streptococcus suis. *BMC microbiology,* **12**(1), pp. 1.

ZHANG, X., OGLĘCKA, K., SANDGREN, S., BELTING, M., ESBJÖRNER, E.K., NORDÉN, B. and GRÄSLUND, A., 2010. Dual functions of the human antimicrobial peptide LL-37—target membrane perturbation and host cell cargo delivery. *Biochimica et Biophysica Acta (BBA)-Biomembranes,* **1798**(12), pp. 2201-2208.

ZHANG, Y., ZHAO, H., YU, G., LIU, X., SHEN, J., LEE, W. and ZHANG, Y., 2010. Structure–function relationship of king cobra cathelicidin. *Peptides,* **31**(8), pp. 1488-1493.

ZHAO, H., GAN, T., LIU, X., JIN, Y., LEE, W., SHEN, J. and ZHANG, Y., 2008. Identification and characterization of novel reptile cathelicidins from elapid snakes. *Peptides,* **29**(10), pp. 1685-1691.

ZHEN, M., JACOBSEN, F. and GIEDROC, D., 2009. Metal transporters and metal sensors: how coordination chemistry controls bacterial metal homeostasis. *Chem Rev,* **109**(10), pp. 4644-4681.

ZHENG, T., BULLOCK, J.L. and NOLAN, E.M., 2012. Siderophore-Mediated Cargo Delivery to the Cytoplasm of Escherichia coli and Pseudomonas aeruginosa: Syntheses of Monofunctionalized Enterobactin Scaffolds and Evaluation of Enterobactin–Cargo Conjugate Uptake. *Journal of the American Chemical Society,* **134**(44), pp. 18388-18400.

ZHOU, K., ZHOU, L., LIM, Q., ZOU, R., STEPHANOPOULOS, G. and TOO, H., 2011. Novel reference genes for quantifying transcriptional responses of Escherichia coli to protein overexpression by quantitative PCR. *BMC molecular biology,* **12**(1), pp. 18.

ZHU, S. and TYTGAT, J., 2004. The scorpine family of defensins: gene structure, alternative polyadenylation and fold recognition. *Cellular and Molecular Life Sciences CMLS,* **61**(14), pp. 1751-1763.

ZINN-JUSTIN, S., ROUMESTAND, C., GILQUIN, B., BONTEMS, F., MENEZ, A. and TOMA, F., 1992. Three-dimensional solution structure of a curaremimetic toxin from Naja nigricollis venom: a proton NMR and molecular modeling study. *Biochemistry,* **31**(46), pp. 11335-11347.

ZOU, G., DE LEEUW, E., LI, C., PAZGIER, M., LI, C., ZENG, P., LU, W.Y., LUBKOWSKI, J. and LU, W., 2007. Toward understanding the cationicity of defensins. Arg and Lys versus their noncoded analogs. *The Journal of biological chemistry,* **282**(27), pp. 19653-19665.

Appendix

Appendix 1 List of other scorpion and snake venoms have been purified with no antibacterial activity against *E. coli*, *S. aureus* and *B. subtilis*

Venom		Chromatography
Scorpion	*Androctonus australis*	Reverse Phase Liquid Chromatography
	leiurus quinquestriatus	Reverse Phase Liquid Chromatography
		SP Sepharose cation exchange Chromatography
	Androctonus amoreuxi	Reverse Phase Liquid Chromatography
Snakes	*Cerastes cerastes*	Size exclusion Chromatography
		SP Sepharose cation exchange Chromatography

Appendix 2 Differentially expressed genes of *E. coli* following exposure to subinhibitory concentration of Smp24

ProbeName	p	FC (abs)	Regulation	GeneSymbol	Description
A_07_P018342	7.94E-04	2.6585467	down	*sodB*	superoxide dismutase, iron [b1656]
A_07_P017057	7.76E-05	2.8361964	down	*waaU*	probably hexose transferase; lipopolysaccharide core biosynthesis [b3623]
A_07_P045631	5.02E-04	3.970346	down	*ygfJ*	orf, hypothetical protein [Z4216]
A_07_P000294	2.00E-05	23.834923	down	*tdcF*	orf, hypothetical protein [b3113]
A_07_P004463	8.02E-05	3.6474128	down	*ybiJ*	orf, hypothetical protein [b0802]
A_07_P006352	5.73E-04	4.379298	down	*ygfJ*	orf, hypothetical protein [b2877]
A_07_P000799	2.07E-04	4.9206204	down	*napC*	cytochrome c-type protein [b2202]
A_07_P020576	2.21E-04	3.1021564	down	*ynfG*	putative oxidoreductase, Fe-S subunit [b1589]
A_07_P054207	3.41E-04	20.862741	up	*ECs0636*	hypothetical protein [ECs0636]
A_07_P007930	2.82E-04	3.257086	up	*proA*	gamma-glutamylphosphate reductase [b0243]
A_07_P006342	1.27E-04	3.2505372	down	*yqeB*	putative synthases [b2875]
A_07_P012100	4.96E-04	2.8970733	down	*hybD*	probable processing element for hydrogenase-2 [b2993]
A_07_P006347	5.56E-05	6.13908	down	*yqeC*	orf, hypothetical protein [b2876]
A_07_P044691	2.34E-04	2.1416142	up	*fliI*	flagellum-specific ATP synthase [Z3031]
A_07_P009475	1.14E-04	8.521537	down	*fdnI*	formate dehydrogenase-N, nitrate-inducible, cytochrome B556 [b1476]
A_07_P009703	6.02E-04	2.1436896	up	*tatE*	orf, hypothetical protein [b0627]
A_07_P020582	1.55E-04	2.3655565	down	*ynfH*	putative DMSO reductase anchor subunit [b1590]
A_07_P059115	2.73E-04	2.8450327	up		LetA protein []
A_07_P052241	7.67E-04	2.222952	up	*ilvG*	acetohydroxy acid synthase II [Z5279]
A_07_P001504	6.45E-04	4.7459626	down	*bssS*	orf, hypothetical protein [b1060]
A_07_P020735	5.49E-04	2.3644316	down	*malI*	repressor of malX and Y genes [b1620]

A_07_P017090	7.01E-04	2.0131812	down	*rfaS*	lipopolysaccharide core biosynthesis [b3629]
A_07_P008167	4.95E-04	3.6925316	up	*ykgL*	orf, hypothetical protein [b0295]
A_07_P018484	7.00E-04	2.197446	up	*ydiI*	orf, hypothetical protein [b1686]
A_07_P008446	4.06E-04	2.7807157	up	*mhpF*	acetaldehyde dehydrogenase [b0351]
A_07_P000290	7.18E-05	24.401407	down		putative L-serine dehydratase [b3112]
A_07_P008951	5.67E-04	5.0710607	down	*soxS*	regulation of superoxide response regulon [b4062]
A_07_P018587	3.61E-04	2.7388325	down	*ydiV*	orf, hypothetical protein [b1707]
A_07_P016721	4.99E-04	32.957237	up	*entC*	isochorismate hydroxymutase 2, enterochelin biosynthesis [b0593]
A_07_P031332	1.02E-04	23.797878	up	*ybdB*	Hypothetical protein ybdB [c_0684]
A_07_P007912	2.54E-04	3.5769355	up	*crl*	transcriptional regulator of cryptic csgA gene for curli surface fibers [b0240]
A_07_P002726	6.30E-04	6.54613	up	*fhuB*	hydroxamate-dependent iron uptake, cytoplasmic membrane component [b0153]
A_07_P048933	1.99E-04	3.3425627	up	*ccdB*	plasmid maintenance protein [L7063]
A_07_P003491	2.90E-04	8.2316265	down	*yeiT*	putative oxidoreductase [b2146]
A_07_P007083	1.78E-05	27.399584	down	*narJ*	nitrate reductase 1, delta subunit, assembly function [b1226]
A_07_P039303	3.97E-04	2.6372178	down		Hypothetical protein [c_4811]
A_07_P000784	5.33E-04	3.2271059	down	*ccmC*	heme exporter protein C [b2199]
A_07_P018368	9.31E-05	2.373058	down	*cfa*	cyclopropane fatty acyl phospholipid synthase [b1661]
A_07_P039736	3.00E-04	2.219555	up	*cysE*	Serine acetyltransferase [c_4429]
A_07_P009461	5.18E-04	11.0615425	down	*fdnG*	formate dehydrogenase-N, nitrate-inducible, alpha subunit [b1474]
A_07_P009468	1.44E-04	6.868572	down	*fdnH*	formate dehydrogenase-N, nitrate-inducible, iron-sulfur beta subunit [b1475]
A_07_P004109	4.53E-05	2.9977987	down	*fimC*	periplasmic chaperone, required for type 1 fimbriae [b4316]
A_07_P034425	5.69E-04	2.1597555	down		Hypothetical protein [c_4182]
A_07_P033496	2.47E-04	32.95802	up	*ybiL*	Probable tonB-dependent receptor ybiL precursor [c_0890]
A_07_P004718	2.57E-04	2.2635646	down	*ybjN*	putative sensory transduction regulator [b0853]

A_07_P019508	1.35E-04	4.0764437	down	*fsaB*	putative transaldolase [b3946]
A_07_P010075	7.67E-04	2.012151	up	*ybgJ*	putative carboxylase [b0711]
A_07_P015065	5.87E-05	2.6272912	up	*fliH*	flagellar biosynthesis; export of flagellar proteins? [b1940]
A_07_P037351	3.12E-04	2.6006153	up	*yjjV*	Putative deoxyribonuclease yjjV [c_5461]
A_07_P059118	3.49E-05	3.3008301	up		cytotoxic protein LetB []
A_07_P017585	3.88E-04	5.584463	down	*yjjI*	orf, hypothetical protein [b4380]
A_07_P003540	6.69E-05	55.67769	up	*cirA*	outer membrane receptor for iron-regulated colicin I receptor; porin; requires tonB gene product [b2155]
A_07_P019334	7.19E-04	3.202845	up	*cpxA*	probable sensor protein [b3911]
A_07_P008006	2.82E-04	3.4939718	up	*mmuM*	putative enzyme [b0261]
A_07_P007073	2.50E-04	44.50304	down	*narG*	nitrate reductase 1, alpha subunit [b1224]
A_07_P018476	6.65E-04	2.0094576	down	*ydiH*	orf, hypothetical protein [b1685]
A_07_P006442	7.26E-04	2.7418623	down	*fldB*	flavodoxin 2 [b2895]
A_07_P016731	6.15E-04	19.056982	up	*entB*	2,3-dihydro-2,3-dihydroxybenzoate synthetase, isochroismatase [b0595]
A_07_P016193	2.77E-04	9.17442	down	*ftnA*	cytoplasmic ferritin [b1905]
A_07_P016680	4.73E-05	35.840313	up	*fepA*	outer membrane receptor for ferric enterobactin [b0584]
A_07_P055794	3.65E-04	2.2381232	down		hypothetical protein [ECs2929]
A_07_P000079	5.19E-04	13.303356	up	*yqjH*	orf, hypothetical protein [b3070]
A_07_P061567	3.85E-04	4.863046	down	*ECs5104*	fumarase B [ECs5104]
A_07_P008767	1.02E-04	2.9976404	down	*pgi*	glucosephosphate isomerase [b4025]
A_07_P010538	4.86E-04	2.0785308	up	*ypjK*	orf, hypothetical protein [b2635]
A_07_P052033	5.89E-04	4.786007	down	*dmsC*	anaerobic dimethyl sulfoxide reductase subunit C [Z1242]
A_07_P033466	2.30E-04	2.9585636	up	*bioD*	Dethiobiotin synthetase [c_0858]
A_07_P016737	3.63E-04	18.788403	up	*entA*	2,3-dihydro-2,3-dihydroxybenzoate dehydrogenase, enterochelin biosynthesis [b0596]
A_07_P000282	3.07E-05	35.314857	down		putative L-serine dehydratase [b3111]

A_07_P001851	6.26E-04	11.524574	up	*nrdF*	ribonucleoside-diphosphate reductase 2, beta chain, frag [b2676]
A_07_P000787	7.92E-04	2.7334685	down	*ccmB*	heme exporter protein B, cytochrome c-type biogenesis protein [b2200]
A_07_P003556	7.91E-04	2.3581827	down	*nfo*	endonuclease IV [b2159]
A_07_P042333	2.40E-04	3.0737033	down	*sodB*	Superoxide dismutase [c_2050]
A_07_P037356	1.62E-04	2.50273	down	*yjjW*	Hypothetical protein yjjW [c_5462]
A_07_P053485	7.27E-04	2.2778623	up	*acpS*	CoA:apo- [ECs3429]
A_07_P013765	2.14E-05	2.2973614	down	*yfbV*	orf, hypothetical protein [b2295]
A_07_P014645	5.28E-04	3.5264852	down	*uspE*	orf, hypothetical protein [b1333]
A_07_P017356	1.01E-04	2.3120582	down	*yidE*	putative transport protein [b3685]
A_07_P004701	3.41E-04	2.517839	down	*ybjC*	orf, hypothetical protein [b0850]
A_07_P008033	7.30E-04	2.1188645	up	*yagB*	orf, hypothetical protein [b0266]
A_07_P048943	3.61E-04	2.3308425	up	*sopA*	plasmid partitioning protein [L7068]
A_07_P051961	4.15E-04	15.566631	up	*Z0726*	orf Unknown function [Z0726]
A_07_P007992	7.10E-04	2.1066446	up		putative transposase [b0257]
A_07_P002712	3.14E-04	4.6608768	up	*fhuA*	outer membrane protein receptor for ferrichrome, colicin M, and phages T1, T5, and phi80 [b0150]
A_07_P016698	1.30E-04	11.981037	up	*fepC*	ATP-binding component of ferric enterobactin transport [b0588]
A_07_P007896	5.51E-04	2.418435	up	*pepD*	aminoacyl-histidine dipeptidase [b0237]
A_07_P061761	2.66E-04	2.1552413	down	*ECs5289*	hypothetical protein [ECs5289]
A_07_P000199	4.31E-04	2.9333174	down	*exuR*	negative regulator of exu regulon, exuT, uxaAC, and uxuB [b3094]
A_07_P063053	1.11E-04	5.0121493	down	*ECs0981*	anaerobic dimethyl sulfoxide reductase subunit C [ECs0981]
A_07_P003848	4.43E-04	2.5118742	up	*pepA*	aminopeptidase A/I [b4260]
A_07_P004926	1.35E-04	4.949795	down	*dmsC*	anaerobic dimethyl sulfoxide reductase subunit C [b0896]
A_07_P061747	6.58E-04	2.0589156	down	*ECs5273*	major type 1 subunit fimbrin [ECs5273]
A_07_P044007	3.63E-04	26.80637	up	*ybdB*	orf, hypothetical protein [Z0739]
A_07_P042301	4.39E-04	4.151089	down	*ynfE*	Putative dimethyl sulfoxide reductase chain ynfE precursor [c_1977]

A_07_P001846	3.76E-04	15.485645	up	*nrdE*	ribonucleoside-diphosphate reductase 2, alpha subunit [b2675]
A_07_P016744	1.66E-04	13.569944	up	*ybdB*	orf, hypothetical protein [b0597]
A_07_P008258	4.52E-04	3.421977	up	*betI*	probably transcriptional repressor of bet genes [b0313]
A_07_P041771	1.35E-04	2.116988	down	*yhaV*	Hypothetical protein yhaV [c_3885]
A_07_P061991	5.43E-04	3.0946443	down	*ECs1173*	hypothetical protein [ECs1173]
A_07_P006843	3.59E-04	2.0954187	down	*ycgK*	orf, hypothetical protein [b1178]
A_07_P001841	3.22E-04	18.64555	up	*nrdI*	orf, hypothetical protein [b2674]
A_07_P011588	5.41E-04	2.1669915	up	*hflK*	protease specific for phage lambda cII repressor [b4174]
A_07_P004028	6.96E-05	2.5110965	down	*sgcR*	putative DEOR-type transcriptional regulator [b4300]
A_07_P002719	5.38E-04	3.244939	up	*fhuC*	ATP-binding component of hydroxymate-dependent iron transport [b0151]
A_07_P018406	4.77E-04	2.8189967	down	*ydhX*	putative oxidoreductase, Fe-S subunit [b1671]
A_07_P059131	2.03E-05	2.2216775	up		SopB protein []
A_07_P004476	6.43E-05	39.35273	up	*fiu*	putative outer membrane receptor for iron transport [b0805]
A_07_P031313	3.09E-04	17.249258	up	*entF*	Enterobactin synthetase component F [c_0673]
A_07_P036723	4.92E-04	4.8232346	down	*hybA*	Hydrogenase-2 operon protein hybA precursor [c_3733]
A_07_P001409	8.16E-04	2.9722588	down	*csgE*	curli production assembly/transport component, 2nd curli operon [b1039]
A_07_P018465	1.28E-04	6.016416	up	*sufC*	putative ATP-binding component of a transport system [b1682]
A_07_P009354	1.93E-04	9.675341	up	*yncE*	putative receptor [b1452]
A_07_P007962	2.23E-04	2.0447538	up	*yafY*	orf, hypothetical protein [b0251]
A_07_P003811	1.60E-04	3.5726576	down	*yjgL*	orf, hypothetical protein [b4253]
A_07_P010661	8.38E-05	3.085565	down		KpLE2 phage-like element; predicted protein, C-ter fragment (pseudogene) [b4560]
A_07_P033805	1.87E-04	5.4224195	down		Hypothetical protein [c_1020]
A_07_P059124	2.64E-05	5.6208987	up		resolvase []
A_07_P008065	2.30E-04	3.4081862	up	*yagI*	putative regulator [b0272]

A_07_P045813	2.59E-04	2.3910189	down	*hybD*	probable processing element for hydrogenase-2 [Z4347]
A_07_P020966	4.28E-04	2.0775094	down	*hemB*	5-aminolevulinate dehydratase = porphobilinogen synthase [b0369]
A_07_P035766	6.99E-04	2.7234256	down		Hypothetical protein [c_0120]
A_07_P041652	7.09E-04	3.495403	down		Putative transport protein [c_3234]
A_07_P002090	3.94E-04	3.5357177	down	*hypC*	pleiotrophic effects on 3 hydrogenase isozymes [b2728]
A_07_P016779	5.73E-04	2.0616753	up	*dsbG*	thiol:disulfide interchange protein [b0604]
A_07_P020575	4.33E-04	2.7304697	down	*ynfF*	putative oxidoreductase, major subunit [b1588]
A_07_P000883	2.75E-04	4.2284927	down	*atoS*	sensor protein AtoS for response regulator AtoC [b2219]
A_07_P004475	2.92E-04	11.958066	up	*ybiX*	putative enzyme [b0804]
A_07_P012116	6.61E-04	3.1854455	down	*hybO*	putative hydrogenase subunit [b2997]
A_07_P010704	6.09E-04	2.5386586	up	*thrA*	aspartokinase I, homoserine dehydrogenase I [b0002]
A_07_P031310	5.30E-05	40.192997	up	*fepA*	Ferrienterobactin receptor precursor [c_0669]

Appendix 3 Differentially expressed genes of *E. coli* following exposure to subinhibitory concentration of Smp43

ProbeName	p	Regulation	FC (abs)	FC	Log FC	GeneSymbol	Description
A_07_P007924	5.86E-05	down	28.99624	-28.9962	-4.85779	*proB*	gamma-glutamate kinase [b0242]
A_07_P030911	3.49E-04	down	6.469286	-6.46929	-2.69361		Putative oxidoreductase [c_0409]
A_07_P051906	4.23E-05	down	23.8158	-23.8158	-4.57385	*betT*	high-affinity choline transport [Z0401]
A_07_P008337	2.44E-04	down	16.50492	-16.5049	-4.04482	*yahO*	orf, hypothetical protein [b0329]
A_07_P062935	1.02E-04	down	28.89229	-28.8923	-4.85261	*ECs0346*	putative transporter [ECs0346]
A_07_P000799	6.10E-05	down	3.670016	-3.67002	-1.87579	*napC*	cytochrome c-type protein [b2202]
A_07_P049050	2.65E-04	down	87.80113	-87.8011	-6.45617	*flmC*	hypothetical protein [L7089]
A_07_P012100	3.72E-04	down	3.221762	-3.22176	-1.68785	*hybD*	probable processing element for hydrogenase-
A_07_P009475	1.54E-04	down	6.604	-6.604	-2.72334	*fdnI*	formate dehydrogenase-N, nitrate-inducible,
A_07_P059115	1.27E-04	down	15.93572	-15.9357	-3.99419		LetA protein []
A_07_P018685	3.24E-04	down	2.921483	-2.92148	-1.5467	*yniC*	putative phosphatase [b1727]
A_07_P031032	8.65E-05	down	473.9064	-473.906	-8.88846		LacI protein [c_0460]
A_07_P008100	1.35E-04	down	30.09372	-30.0937	-4.91139	*intF*	putative phage integrase [b0281]
A_07_P000804	9.45E-05	down	4.070909	-4.07091	-2.02535	*napB*	cytochrome c-type protein [b2203]
A_07_P008272	1.67E-04	down	12.1168	-12.1168	-3.59894	*yahB*	putative transcriptional regulator LYSR-type
A_07_P062741	7.95E-06	down	30.50335	-30.5034	-4.9309	*ECs0346*	putative transporter [ECs0346]
A_07_P008138	3.66E-04	down	18.11563	-18.1156	-4.17916	*yagV*	orf, hypothetical protein [b0289]
A_07_P041467	2.84E-05	down	50.33184	-50.3318	-5.6534	*gpt*	Xanthine-guanine phosphoribosyltransferase
A_07_P007997	2.77E-04	down	6.428937	-6.42894	-2.68458	*ykfC*	orf, hypothetical protein [b0258]
A_07_P001521	1.19E-04	down	2.63696	-2.63696	-1.39888	*grxB*	glutaredoxin 2 [b1064]
A_07_P048933	5.03E-05	down	51.81782	-51.8178	-5.69538	*ccdB*	plasmid maintenance protein [L7063]

A_07_P003491	1.39E-04	down	6.243075	-6.24308	-2.64226	*yeiT*	putative oxidoreductase [b2146]
A_07_P007083	2.59E-05	down	20.92176	-20.9218	-4.38693	*narJ*	nitrate reductase 1, delta subunit, assembly
A_07_P062936	4.43E-05	down	29.67386	-29.6739	-4.89112	*ECs0360*	high-affinity choline transport [ECs0360]
A_07_P018368	8.24E-05	down	3.057884	-3.05788	-1.61253	*cfa*	cyclopropane fatty acyl phospholipid synthase
A_07_P009461	5.94E-05	down	7.506416	-7.50642	-2.90812	*fdnG*	formate dehydrogenase-N, nitrate-inducible,
A_07_P009468	1.82E-04	down	5.14084	-5.14084	-2.362	*fdnH*	formate dehydrogenase-N, nitrate-inducible,
A_07_P054377	3.20E-04	down	3.04735	-3.04735	-1.60755	*ECs2154*	hypothetical protein [ECs2154]
A_07_P008407	7.96E-05	down	25.6842	-25.6842	-4.68281	*lacY*	galactoside permease [b0343]
A_07_P004916	2.89E-04	down	5.676513	-5.67651	-2.50501	*dmsA*	anaerobic dimethyl sulfoxide reductase
A_07_P008362	3.83E-04	down	18.93137	-18.9314	-4.24271	*prpD*	orf, hypothetical protein [b0334]
A_07_P044746	1.73E-04	down	4.089682	-4.08968	-2.03199	*Z3082*	putative tail fiber component L of prophage
A_07_P007216	3.09E-04	down	3.661903	-3.6619	-1.87259	*ompW*	putative outer membrane protein [b1256]
A_07_P059118	1.46E-06	down	86.06097	-86.061	-6.42729		cytotoxic protein LetB []
A_07_P008006	1.58E-04	down	24.50933	-24.5093	-4.61526	*mmuM*	putative enzyme [b0261]
A_07_P041901	1.55E-04	down	1.844086	-1.84409	-0.88291		Probable tRNA modification GTPase trmE
A_07_P007073	6.53E-05	down	39.49674	-39.4967	-5.30366	*narG*	nitrate reductase 1, alpha subunit [b1224]
A_07_P008356	3.70E-05	down	21.32198	-21.322	-4.41427	*prpC*	putative citrate synthase; propionate
A_07_P043676	1.65E-05	down	26.00433	-26.0043	-4.70068	*betA*	choline dehydrogenase, a flavoprotein [Z0398]
A_07_P008419	2.93E-06	down	948.348	-948.348	-9.88927	*lacI*	transcriptional repressor of the lac operon
A_07_P008412	7.94E-05	down	53.65123	-53.6512	-5.74554	*lacZ*	beta-D-galactosidase [b0344]
A_07_P008312	3.21E-04	down	10.89233	-10.8923	-3.44524	*yahJ*	putative deaminase [b0324]
A_07_P060587	1.50E-04	down	2.722197	-2.7222	-1.44477	*ECs1502*	putative excisionase [ECs1502]
A_07_P049027	1.63E-04	down	7.16535	-7.16535	-2.84104	*L7085*	hypothetical protein [L7085]
A_07_P059154	3.75E-04	down	6.547214	-6.54721	-2.71088		hemagglutinin-associated protein []

A_07_P030986	8.65E-05	down	23.73586	-23.7359	-4.569	*betT*	High-affinity choline transport protein
A_07_P008348	4.91E-05	down	14.55929	-14.5593	-3.86387	*prpB*	putative phosphonomutase 2 [b0331]
A_07_P048943	1.41E-05	down	99.87058	-99.8706	-6.64199	*sopA*	plasmid partitioning protein [L7068]
A_07_P007992	5.96E-05	down	12.93331	-12.9333	-3.69302		putative transposase [b0257]
A_07_P007896	4.72E-06	down	371.8323	-371.832	-8.53851	*pepD*	aminoacyl-histidine dipeptidase [b0237]
A_07_P004926	1.15E-04	down	3.126643	-3.12664	-1.64461	*dmsC*	anaerobic dimethyl sulfoxide reductase
A_07_P051905	1.50E-04	down	25.20401	-25.204	-4.65558	*ykgG*	orf Unknown function [Z0386]
A_07_P008258	1.99E-05	down	87.06075	-87.0608	-6.44395	*betI*	probably transcriptional repressor of bet genes
A_07_P041771	2.19E-04	down	2.695247	-2.69525	-1.43042	*yhaV*	Hypothetical protein yhaV [c_3885]
A_07_P059085	3.23E-04	down	25.22713	-25.2271	-4.6569		recombinase []
A_07_P048930	2.17E-04	down	15.02839	-15.0284	-3.90962	*ccdA*	plasmid maintenance protein [L7062]
A_07_P008226	1.12E-05	down	71.89595	-71.896	-6.16784	*ykgF*	orf, hypothetical protein [b0307]
A_07_P059091	6.98E-05	down	17.36132	-17.3613	-4.11781		RepFIB []
A_07_P059131	3.89E-06	down	69.09206	-69.0921	-6.11045		SopB protein []
A_07_P000343	1.71E-04	down	9.902689	-9.90269	-3.30782	*garK*	orf, hypothetical protein [b3124]
A_07_P008320	3.67E-04	down	62.14762	-62.1476	-5.95763	*yahK*	putative oxidoreductase [b0325]
A_07_P007907	2.44E-05	down	111.2165	-111.216	-6.79723	*frsA*	orf, hypothetical protein [b0239]
A_07_P051897	8.50E-05	down	37.10268	-37.1027	-5.21345	*proB*	gamma-glutamate kinase [Z0303]
A_07_P036723	3.30E-04	down	3.212056	-3.21206	-1.6835	*hybA*	Hydrogenase-2 operon protein hybA precursor
A_07_P057876	3.20E-05	down	2.548259	-2.54826	-1.34951	*ECs4847*	hypothetical protein [ECs4847]
A_07_P007962	6.50E-06	down	23.38725	-23.3873	-4.54765	*yafY*	orf, hypothetical protein [b0251]
A_07_P059124	2.69E-04	down	9.842866	-9.84287	-3.29908		resolvase []
A_07_P008101	2.58E-04	down	11.51565	-11.5157	-3.52552	*yagP*	putative transcriptional regulator LYSR-type
A_07_P008092	1.06E-04	down	91.92522	-91.9252	-6.52239	*yagN*	orf, hypothetical protein [b0280]

A_07_P007903	1.30E-05	down	109.1437	-109.144	-6.77008	*gpt*	guanine-hypoxanthine
A_07_P000346	3.62E-04	down	15.42673	-15.4267	-3.94736	*garR*	putative dehydrogenase [b3125]
A_07_P007077	1.07E-05	down	42.39925	-42.3992	-5.40597	*narH*	nitrate reductase 1, beta subunit [b1225]
A_07_P008423	2.17E-04	down	20.44936	-20.4494	-4.35398	*mhpR*	transcriptional regulator for mhp operon
A_07_P047106	7.03E-07	down	2.696156	-2.69616	-1.4309	*yiiS*	orf, hypothetical protein [Z5467]
A_07_P002090	2.49E-04	down	3.421651	-3.42165	-1.77469	*hypC*	pleiotrophic effects on 3 hydrogenase
A_07_P007958	8.81E-06	down	53.80759	-53.8076	-5.74974	*ykfB*	orf, hypothetical protein [b0250]
A_07_P032895	6.40E-05	up	1.934719	1.934719	0.952124	*ubiH*	2-octaprenyl-6-methoxyphenol hydroxylase
A_07_P037325	3.79E-04	up	5.320501	5.320501	2.411562		Hypothetical protein [c_5447]
A_07_P008225	2.94E-05	down	13.65407	-13.6541	-3.77126	*ykgE*	putative dehydrogenase subunit [b0306]
A_07_P017954	1.45E-04	down	2.02158	-2.02158	-1.01548	*gph*	phosphoglycolate phosphatase [b3385]
A_07_P001593	8.95E-05	up	3.157724	3.157724	1.658885	*flgG*	flagellar biosynthesis, cell-distal portion of
A_07_P008378	3.01E-04	down	18.95954	-18.9595	-4.24485	*codA*	cytosine deaminase [b0337]
A_07_P008332	1.48E-04	down	33.5664	-33.5664	-5.06895	*yahN*	putative cytochrome subunit of
A_07_P008251	7.15E-05	down	151.2337	-151.234	-7.24064	*betB*	NAD+dependent betaine aldehyde

Appendix 4 Differentially expressed genes of *E. coli* following exposure to subinhibitory concentration of polymyxin B

ProbeName	p	FC (abs)	Regulation	Gene Symbol	Description
A_07_P007924	5.12E-06	37.60891	down	*proB*	gamma-glutamate kinase [b0242]
A_07_P053270	4.58E-04	2.682118	down	*fadI*	putative acyltransferase [ECs3225]
A_07_P008071	4.61E-04	26.4882	down	*yagJ*	orf, hypothetical protein [b0276]
A_07_P051906	3.77E-06	39.20907	down	*betT*	high-affinity choline transport [Z0401]
A_07_P033781	1.17E-04	2.025941	down	*poxB*	Pyruvate dehydrogenase [c_1004]
A_07_P008337	7.22E-05	27.23424	down	*yahO*	orf, hypothetical protein [b0329]
A_07_P062935	1.51E-05	26.06304	down	*ECs0346*	putative transporter [ECs0346]
A_07_P049050	3.28E-05	97.69341	down	*flmC*	hypothetical protein [L7089]
A_07_P020576	3.90E-04	2.631867	down	*ynfG*	putative oxidoreductase, Fe-S subunit [b1589]
A_07_P007930	6.66E-06	52.8104	down	*proA*	gamma-glutamylphosphate reductase [b0243]
A_07_P008194	1.43E-04	42.86612	down	*ykgA*	putative ARAC-type regulatory protein [b0300]
A_07_P010429	3.78E-04	2.022458	down	*yncN*	predicted protein [b4532]
A_07_P020582	4.25E-05	2.003216	down	*ynfH*	putative DMSO reductase anchor subunit [b1590]
A_07_P059115	8.14E-05	30.14845	down		LetA protein []
A_07_P031032	7.49E-05	150.6207	down		LacI protein [c_0460]
A_07_P008100	3.04E-06	41.96406	down	*intF*	putative phage integrase [b0281]
A_07_P059210	3.40E-04	17.971	down		single-strand binding protein []
A_07_P051676	2.88E-05	44.01132	down	*ykgG*	orf Unknown function [Z0386]
A_07_P041475	1.75E-06	72.47141	down		Hypothetical protein yafA [c_0386]
A_07_P031027	2.90E-05	56.38164	down	*lacZ*	Beta-galactosidase [c_0459]
A_07_P008264	6.94E-06	107.0042	down	*betT*	high-affinity choline transport [b0314]

A_07_P008272	3.90E-04	18.16215	down	*yahB*	putative transcriptional regulator LYSR-type [b0316]
A_07_P062741	1.79E-05	44.35465	down	*ECs0346*	putative transporter [ECs0346]
A_07_P004806	2.02E-05	2.261527	down	*poxB*	pyruvate oxidase [b0871]
A_07_P059230	1.10E-05	96.00961	down		Stable plasmid inheritance protein (F leading maintenance
A_07_P041467	8.14E-07	51.30566	down	*gpt*	Xanthine-guanine phosphoribosyltransferase [c_0384]
A_07_P008066	1.72E-04	12.69806	down	*argF*	ornithine carbamoyltransferase 2, chain F [b0273]
A_07_P007912	1.01E-05	109.2056	down	*crl*	transcriptional regulator of cryptic csgA gene for curli surface
A_07_P045861	4.90E-04	2.618103	down	*Z4403*	putative membrane protein [Z4403]
A_07_P048933	4.24E-06	43.90928	down	*ccdB*	plasmid maintenance protein [L7063]
A_07_P003491	8.93E-05	4.222927	down	*yeiT*	putative oxidoreductase [b2146]
A_07_P062936	6.73E-06	27.99573	down	*ECs0360*	high-affinity choline transport [ECs0360]
A_07_P008407	1.43E-05	40.78909	down	*lacY*	galactoside permease [b0343]
A_07_P057011	9.44E-05	3.509125	down	*ECs0957*	pyruvate oxidase [ECs0957]
A_07_P019508	3.63E-04	2.236329	down	*fsaB*	putative transaldolase [b3946]
A_07_P059118	4.88E-05	41.25151	down		cytotoxic protein LetB []
A_07_P008205	7.30E-05	54.9409	down		orf, hypothetical protein [b0302]
A_07_P008006	1.51E-05	39.62783	down	*mmuM*	putative enzyme [b0261]
A_07_P007073	1.64E-04	8.644049	down	*narG*	nitrate reductase 1, alpha subunit [b1224]
A_07_P043676	3.39E-05	43.28736	down	*betA*	choline dehydrogenase, a flavoprotein [Z0398]
A_07_P008419	6.04E-05	225.5742	down	*lacI*	transcriptional repressor of the lac operon [b0345]
A_07_P002585	2.34E-04	2.695642	down	*gcd*	glucose dehydrogenase [b0124]
A_07_P008412	5.86E-07	66.54588	down	*lacZ*	beta-D-galactosidase [b0344]
A_07_P007967	5.04E-05	25.61864	down	*yafZ*	orf, hypothetical protein [b0252]
A_07_P008115	2.43E-04	16.28317	down	*yagR*	orf, hypothetical protein [b0284]

A_07_P030986	4.82E-06	29.7308	down	*betT*	High-affinity choline transport protein [c_0434]
A_07_P008033	3.14E-05	50.1804	down	*yagB*	orf, hypothetical protein [b0266]
A_07_P048943	2.03E-05	89.68714	down	*sopA*	plasmid partitioning protein [L7068]
A_07_P007896	7.76E-05	94.23969	down	*pepD*	aminoacyl-histidine dipeptidase [b0237]
A_07_P059085	2.22E-06	30.61239	down		recombinase []
A_07_P048930	2.19E-04	26.09194	down	*ccdA*	plasmid maintenance protein [L7062]
A_07_P059131	1.42E-06	102.2656	down		SopB protein []
A_07_P008320	8.38E-06	53.71057	down	*yahK*	putative oxidoreductase [b0325]
A_07_P007907	1.47E-05	134.8558	down	*frsA*	orf, hypothetical protein [b0239]
A_07_P051897	7.85E-06	59.81262	down	*proB*	gamma-glutamate kinase [Z0303]
A_07_P008247	1.15E-05	31.92485	down	*betA*	choline dehydrogenase, a flavoprotein [b0311]
A_07_P007962	1.42E-04	20.07489	down	*yafY*	orf, hypothetical protein [b0251]
A_07_P048890	2.65E-06	27.35426	down	*L7054*	replication protein [L7054]
A_07_P008092	1.44E-04	93.86832	down	*yagN*	orf, hypothetical protein [b0280]
A_07_P053871	9.10E-06	38.87666	down	*ECs0357*	choline dehydrogenase [ECs0357]
A_07_P007903	1.10E-05	117.3457	down	*gpt*	guanine-hypoxanthine phosphoribosyltransferase [b0238]
A_07_P000346	3.79E-04	14.72256	down	*garR*	putative dehydrogenase [b3125]
A_07_P007077	7.69E-05	11.72012	down	*narH*	nitrate reductase 1, beta subunit [b1225]
A_07_P008423	3.29E-06	21.19263	down	*mhpR*	transcriptional regulator for mhp operon [b0346]
A_07_P053944	3.12E-04	30.24936	down	*lacA*	thiogalactoside acetyltransferase [ECs0395]
A_07_P007958	5.41E-05	71.14152	down	*ykfB*	orf, hypothetical protein [b0250]
A_07_P048946	4.71E-06	79.61149	down	*sopB*	plasmid partitioning protein [L7069]
A_07_P008378	7.92E-06	9.02937	down	*codA*	cytosine deaminase [b0337]
A_07_P008332	1.18E-05	59.46668	down	*yahN*	putative cytochrome subunit of dehydrogenase [b0328]

A_07_P008251	1.60E-06	127.3622	down	*betB*	NAD+-dependent betaine aldehyde dehydrogenase [b0312]
A_07_P059278	1.16E-05	71.4843	down		fertility inhibition protein []
A_07_P054207	1.14E-04	14.72831	up	*ECs0636*	hypothetical protein [ECs0636]
A_07_P003964	8.79E-05	3.47668	up	*fecE*	ATP-binding component of citrate-dependent iron [b4287]
A_07_P031332	6.77E-06	18.22578	up	*ybdB*	Hypothetical protein ybdB [c_0684]
A_07_P018070	2.01E-04	9.317547	up	*feoA*	ferrous iron transport protein A [b3408]
A_07_P031283	1.27E-04	3.733559	up	*ompT*	Protease VII precursor [c_0652]
A_07_P008748	2.49E-04	3.603713	up	*pepE*	peptidase E, a dipeptidase where amino-terminal residue is
A_07_P013913	3.65E-04	2.066783	up	*yfcL*	orf, hypothetical protein [b2325]
A_07_P003540	3.11E-05	39.01055	up	*cirA*	outer membrane receptor for iron-regulated colicin I receptor;
A_07_P053401	4.80E-04	2.576457	up	*murQ*	putative regulator [ECs3299]
A_07_P016731	1.70E-04	12.34368	up	*entB*	2,3-dihydro-2,3-dihydroxybenzoate synthetase, isochroismatase
A_07_P016690	2.95E-04	13.96405	up	*entF*	ATP-dependent serine activating enzyme [b0586]
A_07_P016680	4.38E-06	22.57931	up	*fepA*	outer membrane receptor for ferric enterobactin [b0584]
A_07_P016729	2.17E-04	10.84259	up	*entE*	2,3-dihydroxybenzoate-AMP ligase [b0594]
A_07_P031951	3.54E-04	3.890673	up		Putative radC-like protein yeeS [c_2529]
A_07_P018073	4.15E-04	5.504057	up	*feoB*	ferrous iron transport protein B [b3409]
A_07_P001568	1.21E-04	3.048904	up	*flgB*	flagellar biosynthesis, cell-proximal portion of basal-body rod
A_07_P002712	9.91E-05	5.173827	up	*fhuA*	outer membrane protein receptor for ferrichrome, colicin M, and
A_07_P015092	3.60E-05	3.672536	up	*fliN*	flagellar biosynthesis, component of motor switch and energizing,
A_07_P044007	8.93E-05	16.67084	up	*ybdB*	orf, hypothetical protein [Z0739]
A_07_P016744	2.29E-05	9.572627	up	*ybdB*	orf, hypothetical protein [b0597]
A_07_P018077	3.34E-04	7.866618	up	*feoC*	orf, hypothetical protein [b3410]
A_07_P003504	2.54E-04	4.231078	up	*mglC*	methyl-galactoside transport and galactose taxis [b2148]

A_07_P031313	4.68E-04	13.98224	up	*entF*	Enterobactin synthetase component F [c_0673]
A_07_P009354	1.32E-05	9.598366	up	*yncE*	putative receptor [b1452]
A_07_P042816	4.85E-04	2.514803	up	*murQ*	putative regulator [Z3693]
A_07_P001583	7.16E-05	3.250831	up	*flgE*	flagellar biosynthesis, hook protein [b1076]
A_07_P016979	4.45E-04	2.367931	up	*cysE*	serine acetyltransferase [b3607]
A_07_P020811	2.97E-04	2.258504	up	*pdxY*	pyridoxal kinase 2 / pyridoxine kinase [b1636]